



International Agreement Report

TRAC-PF1/MOD1 Post-Test Calculations of the OECD Loft Experiment LP-SB-2

Prepared by
F. Pelayo

United Kingdom Atomic Energy Authority
Winfrith, Dorchester
Dorset, England

Office of Nuclear Regulatory Research
U.S. Nuclear Regulatory Commission
Washington, DC 20555

December 1990

Prepared as part of
The Agreement on Research Participation and Technical Exchange
under the International Thermal-Hydraulic Code Assessment
and Application Program (ICAP)

Published by
U.S. Nuclear Regulatory Commission

NOTICE

This report was prepared under an international cooperative agreement for the exchange of technical information.* Neither the United States Government nor any agency thereof, or any of their employees, makes any warranty, expressed or implied, or assumes any legal liability or responsibility for any third party's use, or the results of such use, of any information, apparatus product or process disclosed in this report, or represents that its use by such third party would not infringe privately owned rights.

Available from

Superintendent of Documents
U.S. Government Printing Office
P.O. Box 37082
Washington, D.C. 20013-7082

and

National Technical Information Service
Springfield, VA 22161



International Agreement Report

TRAC-PF1/MOD1 Post-Test Calculations of the OECD Loft Experiment LP-SB-2

Prepared by
F. Pelayo

United Kingdom Atomic Energy Authority
Winfrith, Dorchester
Dorset, England

Office of Nuclear Regulatory Research
U.S. Nuclear Regulatory Commission
Washington, DC 20555

December 1990

Prepared as part of
The Agreement on Research Participation and Technical Exchange
under the International Thermal-Hydraulic Code Assessment
and Application Program (ICAP)

Published by
U.S. Nuclear Regulatory Commission

NOTICE

This report is based on work performed under the sponsorship of the United Kingdom Atomic Energy Authority. The information in this report has been provided to the USNRC under the terms of the International Code Assessment and Application Program (ICAP) between the United States and the United Kingdom (Administrative Agreement - WH 36047 between the United States Nuclear Regulatory Commission and the United Kingdom Atomic Energy Authority Relating to Collaboration in the Field of Modelling of Loss of Coolant Accidents, February 1985). The United Kingdom has consented to the publication of this report as a USNRC document in order to allow the widest possible circulation among the reactor safety community. Neither the United States Government nor the United Kingdom or any agency thereof, or any of their employees, makes any warranty, expressed or implied, or assumes any legal liability of responsibility for any third party's use, or the results of such use, or any information, apparatus, product or process disclosed in this report, or represents that its use by such third party would not infringe privately owned rights.

ABSTRACT

An analysis of the OECD-LOFT-LP-SB-2 experiment making use of TRAC-PF1/MOD1 is described in the report.

LP-SB2 experiment studies the effect of a delayed pump trip in a small break LOCA scenario with a 3 inches equivalent diameter break in the hot leg of a commercial PWR operating at full power.

The experiment was performed on 14 July 1983 in the LOFT facility at the Idaho National Engineering Laboratory under the auspices of the Organisation for Economic Co-operation and Development (OECD). This analysis presents an evaluation of the code capability in reproducing the complex phenomena which determined the LP-SB-2 transient evolution. The analysis comprises the results obtained from two different runs. The first run is described in detail analysing the main variables over two time spans: short and longer term. Several conclusions are drawn and then a second run testing some of these conclusions is shown.

All of the calculations were performed at the United Kingdom Atomic Energy Establishment at Winfrith under the auspices of an agreement between the UKAEA (United Kingdom Atomic Energy Authority) and the Consejo de Seguridad Nuclear Español (CSN).

ACKNOWLEDGEMENTS

Appreciation is expressed to all the staff members of the LOCA Thermal Hydraulics Group at Winfrith Establishment with special mention to Dr C Richards and Miss E Allen for their valuable contribution to the realisation of this work.

CONTENTS

	<u>Page</u>
ABSTRACT	I
ACKNOWLEDGEMENTS	II
1 INTRODUCTION	1
2 LOFT FACILITY	1
2.1 System Description	1
3 TRAC PF1 MOD1 MODEL OF LOFT FACILITY	2
3.1 Reactor Vessel	3
3.2 Steam Generator and Steam Line	4
3.3 Intact and Broken Loops	4
4 EXPERIMENT LP-SB-2	4
4.1 Steady State Calculation	5
4.2 Transient Boundary Conditions	6
4.3 Chronology of Events for Experiment LP-SB-2	6
5 POST-TEST CALCULATIONS	7
5.1 Run A	7
5.1.1 Code Performance	7
5.1.2 Short Time Behaviour (0.0 - 850 secs)	7
5.1.2.1 Pressure Behaviour: Primary Side	8
5.1.2.2 Pressure Behaviour: Secondary Side	8
5.1.2.3 Temperatures	9
5.1.2.4 Density Distribution	9
5.1.2.5 Fluid Velocities	10

CONTENTS (Contd)

	<u>Page</u>
5.1.2.6 Transient Mass Inventory	11
5.1.3 Long Time Behaviour (850 - 3000 secs)	11
5.1.3.1 Pressure Behaviour	11
5.1.3.2 Temperatures	12
5.1.3.3 Density Distribution	13
5.1.3.4 Fluid Velocities	14
5.1.3.5 Transient Mass Inventory	15
5.1.4 Conclusions Derived from Run A	16
5.2 Run B	16
5.2.1 Results Review	17
5.2.2 Conclusions Derived from Run B	19
6 SELECTED ITEMS	20
6A LP-SB2 Pumps Modelling	20
6B Break Flow Density in Experiment LP-SB-2	22
6C Flow Regimes Prediction for LP-SB-2	24
7 SUMMARY AND FINAL CONCLUSIONS	25
REFERENCES	28
FIGURES	32
TABLES	112
APPENDIX A Run B Snapshots at Selected Times	148
APPENDIX B Modifications Implemented in TRAC-PF1/MOD1 Winfrith Versions BO2A and BO2C	149

FIGURES

NUMBER	TITLE	<u>PAGE</u>
1	LOFT FACILITY AXONOMETRIC PROJECTION	33
2	LOFT PIPING SCHEMATIC WITH INSTRUMENTATION	34
3	LOFT FACILITY NODING DIAGRAM	35
4	CORE BYPASS FLOW PATHS	36
5	ONE-DIMENSIONAL VESSEL REPRESENTATION	37
6	STEAM GENERATOR NODING	38
 <u>RUN A</u> 		
7	TOTAL TIME STEPS	39
8	TIME STEP SIZE - SHORT TERM (0.0 - 850 SECS)	40
9	INTACT LOOP HOT LEG PRESSURE	41
10	VOID FRACTION IN THE UPPER PLENUM AND BOX BEFORE HOT LEG NOZZLES	42
11	BREAK MASS FLOW RATE	43
12	PRESSURE DIFFERENCE OVER THE MAIN COOLANT PUMPS	44
13	SECONDARY SIDE PRESSURE	45
14	LIQUID TEMPERATURE IN THE HOT LEG OF THE INTACT LOOP	46
15	LIQUID TEMPERATURE IN THE COLD LEG OF THE INTACT LOOP	47
16	PRIMARY AND SECONDARY PRESSURES IN TRAC	48
17	DENSITY IN THE HOT LEG OF THE INTACT LOOP	49
18	DENSITY IN THE COLD LEG OF THE INTACT LOOP	50

FIGURES (Contd)

<u>NUMBER</u>	<u>TITLE</u>	<u>PAGE</u>
19	GAMMA DENSITOMETERS LAYOUT IN THE HOT AND COLD LEG	51
20	VOID FRACTION AT TOP OF THE U-TUBES	52
21	LOOP SEAL DENSITY	53
22	DENSITY IN THE BREAK LINE	54
23	LIQUID AND VAPOUR VELOCITY IN THE COLD LEG	55
24	LIQUID AND VAPOUR VELOCITY IN THE HOT LEG	56
25	LIQUID AND VAPOUR VELOCITY IN THE DOWNCOMER OF THE REACTOR VESSEL	57
26	LIQUID AND VAPOUR VELOCITY AT CORE INLET	58
27	LIQUID AND VAPOUR VELOCITY AT CORE OUTLET	59
28	LIQUID AND VAPOUR VELOCITY IN THE BREAK LINE	60
29	PRIMARY SYSTEM MASS INVENTORY - LONG TERM (850 - 3000 SECS)	61
30	SECONDARY PRESSURE	62
31	PRIMARY AND SECONDARY SIDE PRESSURES IN TRAC	63
32	INTACT LOOP HOT LEG PRESSURE	64
33	LIQUID TEMPERATURE IN THE HOT LEG OF THE INTACT LOOP	65
34	COLD LEG TEM SAT - TEM LIQ	66
35	CLADDING TEMPERATURE NEAR TOP OF THE CORE	67
36	DENSITY IN THE HOT LEG INTACT LOOP	68

FIGURES (Contd)

NUMBER	TITLE	<u>PAGE</u>
37	DENSITY IN THE COLD LEG OF THE INTACT LOOP	69
38	DENSITY IN THE BREAK LINE	70
39	LIQUID AND VAPOUR VELOCITY IN THE DOWNCOMER OF THE REACTOR VESSEL	71
40	LIQUID AND VAPOUR VELOCITY AT CORE INLET	72
41	PRESSURE DIFFERENCE OVER THE MAIN COOLANT PUMPS	73
42	LIQUID AND VAPOUR VELOCITY AT CORE OUTLET	74
43	LIQUID AND VAPOUR VELOCITY IN THE HOT LEG	75
44	LIQUID AND VAPOUR VELOCITY IN THE COLD LEG	76
45	LIQUID AND VAPOUR VELOCITY IN THE BREAK LINE	77
46	HOT LEG MASS FLOW RATE AT VENTURI LOCATION	78
47	BREAK MASS FLOW RATE	79
48	PRIMARY SYSTEM MASS INVENTORY	80
<u>RUN B</u>		
49	BREAK LINE DENSITY	81
50	BREAK MASS FLOW RATE	82
51	PRIMARY SYSTEM MASS INVENTORY	83
52	INTACT LOOP HOT LEG PRESSURE	84
53	SECONDARY SIDE PRESSURE	85

FIGURES (Contd)

<u>NUMBER</u>	<u>TITLE</u>	<u>PAGE</u>
54	LIQUID TEMPERATURE IN THE HOT LEG OF THE INTACT LOOP	86
55	CLADDING TEMPERATURE NEAR TOP OF THE CORE	87
56	DENSITY IN THE HOT LEG INTACT LOOP	88
57	DENSITY IN THE COLD LEG OF THE INTACT LOOP	89
58	LIQUID AND VAPOUR VELOCITY IN THE DOWNCOMER OF THE REACTOR VESSEL	90
59	VOID FRACTION TOP FUEL REGION	91
60	LIQUID AND VAPOUR VELOCITY AT CORE INLET	92
61	LIQUID AND VAPOUR VELOCITY IN THE HOT LEG	93
62	PRESSURE DIFFERENCE OVER THE MAIN COOLANT PUMPS	94
63	HOT LEG MASS FLOW RATE AT VENTURI LOCATION	95
64	LIQUID AND VAPOUR VELOCITY IN THE BREAK LINE	96

SELECTED ITEMS

<u>NUMBER</u>	<u>TITLE</u>	<u>PAGE</u>
A1	MEASURED AND ADJUSTED COLD LEG DENSITIES AT THE STEAM GENERATOR OUTLET	97
A2	PUMP HEAD AS A FUNCTION OF VOID FRACTION FOR EXPERIMENTS LP-SB-2 AND L3-6	98

FIGURES (Contd)

<u>NUMBER</u>	<u>TITLE</u>	<u>PAGE</u>
A3	PUMP HEAD AS A FUNCTION OF VOID FRACTION OBTAINED USING THE ADJUSTED DENSITY AT THE STEAM GENERATOR OUTLET FOR EXPERIMENT LP-SB-2	99
A4	PUMP HEAD VS VOID FRACTION IN RUN A	100
A5	LOOP SEAL DENSITY IN RUN A	101
A6	PUMPS PRESSURE INCREASE VS VOLUMETRIC FLOW RATE IN RUN A	102
A7	PUMPS MASS FLOW RATE IN RUN A	103
A8	PRIMARY COOLANT PUMP POWER	104
A9	PUMPS TORQUES IN RUN B	105
A10	PUMPS MASS FLOWS IN RUN B	106
B1	EXPERIMENTAL HOT LEG DENSITY AND BREAK LINE DENSITY	107
B2	NODING MODIFICATIONS IN THE BREAK LINE	108
B3	QUALITY CONTROL VALVE CONTROL LOGIC	109
C1	TRAC FLOW REGIME MAP FOR LOFT LP-SB-2 HOT LEG CONDITIONS RUN B	110
C2	TIME VS HOT LEG VOID FRACTION IN RUN B	111

TABLES

NUMBER	TITLE	<u>PAGE</u>
1	INITIAL CONDITIONS FOR EXPERIMENT LP-SB-2 - RUN A	113
2	OPERATIONAL SET POINT FOR EXPERIMENT LP-SB-2	114
3	CHRONOLOGY OF EVENTS FOR EXPERIMENT LP-SB-2 - RUN A	115
4	INSTRUMENT LOCATIONS FLOW AREAS	116
5	INITIAL CONDITIONS FOR EXPERIMENT LP-SB-2 - RUN B	117
6	CHRONOLOGY OF EVENTS FOR EXPERIMENT LP-SB-2 - RUN B	118
A1	PUMP HEAD MULTIPLIERS - RUN A	119
A2	PUMP HEAD MULTIPLIERS - RUN B	120
B1	DESIRED BRANCH QUALITY VS VOID FRACTION IN THE HOT LEG	121

MIMIC DIAGRAMS

MIMIC DIAGRAMS FOR RUN B	122
--------------------------	-----

1 INTRODUCTION

Experiment LP-SB-2 studies the effect of a delayed pumps trip in a Small Break LOCA scenario with a three inches equivalent diameter break in the hot leg of a commercial PWR operating at full power. The experiment was performed on 14 July 1983 in the LOFT facility at the Idaho National Engineering Laboratory under the auspices of the Organisation for Economic Co-operation and Development (OECD). The evolution of the experiment was determined by several features, among the most important of which were the flow patterns present in the loop, vapour pull-through and liquid entrainment observed in the break line, and pumps behaviour.

Early in the transient a density gradient developed in the vertical section of the hot leg. The break line density was sensitive to this gradient; moreover a preferential flow of steam was detected as soon as two-phase conditions occurred. Under stratified conditions and later in the transient, the break suddenly uncovered increasing the depressurisation rate; from then on some liquid entrainment was observed to occur.

The pumps behaviour was important in determining the fluid velocities and density distribution as well as changes in flow distribution and flow patterns in the loop.

Many of the features of TRAC-PF1/MOD1 were used during the analysis of the experiment, ie the flow regime dependent constitutive equation package, choked flow model, pump model under two-phase conditions, fluid transport and associated two-phase pressure losses along the whole loop, etc.

The SETS numerics were applied to all the components in the system as no three-dimensional vessel was used.

All the calculations were performed on a CRAY X-MP computer and the Code versions used were the Winfrith versions BO2A for RUN A and BO2C for RUN B. Both versions contain Los Alamos updates up to Version 12.7. A description of the difference between the Winfrith code version and Version 12.7 is given in Appendix B.

2 LOFT FACILITY

2.1 System Description

The LOFT test facility simulates a four loop PWR 1000 MW (electric) commercial plant. It has a thermal power of 50 MW produced by nuclear fission sustained in the reactor core. The system was designed to simulate the major components and system responses during LOCAs or operational transient accidents. The facility components were instrumented to record the main system variables during the experiments.

The facility consists of a reactor vessel volumetrically scaled to 1/47; an intact loop with an active steam generator, pressuriser, and two primary coolant pumps connected in parallel; a broken loop connected by recirculation lines to the intact loop to keep the fluid temperature at about the core inlet temperature prior to experiment, a reflood assist bypass valve connecting both legs of the broken loop as a safety device, and two quick opening valves (kept closed during SB-2 experiment) connecting both legs of the broken loop to the suppression tank header. During experiment LP-SB-2 the blowdown valves and isolation valves were kept closed as the break was in the hot leg of the "intact" loop. The broken loop spool pieces with orifices to simulate the steam generator and pump hydraulic resistance were not installed for this experiment, but were replaced by a straight piping spool piece.

The LOFT ECCS simulates that of a commercial PWR. It consists of two accumulators, a high pressure injection system, and a low pressure injection system. Each system is arranged to inject scaled flows of emergency core coolant directly into the primary coolant system. During experiments LP-SB-1 and 2 the accumulators and LPIS were not used and scaled HPIS flow was directed into the intact cold leg. Volume scaling of the HPIS flow was based on the assumption that only one of three charging pumps and one of three HPIS pumps in the reference plant were available.

The LOFT steam generator located in the intact loop is a vertical U-tube design steam generator. The use of auxiliary feedwater flow to the steam generator during the experiment reflected the initiation and employment of backup emergency feedwater in a commercial PWR until the simulated depletion of feedwater source (about 30 minutes).

In experiments LP-SB-1 and 2 the breakline was connected between the midplane of the hot leg and the blowdown suppression tank.

An axonometric projection of the LOFT system configuration for experiments LP-SB-1 and LP-SB-2, and a LOFT piping schematic with instrumentation are shown respectively in Figures 1 and 2. More detailed information on the LOFT system configuration is provided in Reference 1.

3 TRAC PF1/MOD1 MODEL OF LOFT FACILITY

Starting from the nodalisation used in the analyses of the experiments LP-LB-1 and LP-FP-1, an existing Atomic Energy Establishment of Winfrith (AEEW) input deck was adapted to reproduce the actual configuration of experiments LP-SB-1 and LP-SB-2 (Ref 2) these modifications were:-

Removal of the three-dimensional vessel and implementation of a one-dimensional model.

Nodalisation of the broken loop.

Addition of pump injection.

Removal of accumulator and line.

Nodalisation of the hot leg break.

The final noding diagram is shown in Figure 3. The number of components used to model the facility were 36, with 142 cells and 42 junctions.

3.1 Reactor Vessel

After the initial consideration that in LP-SB-2 the transient evolution in the vessel did not show strongly asymmetrical behaviour it was decided to take advantage of the multistep numerics of TRAC-PF1/MOD1, which are restricted to one-dimensional components, by changing to a one-dimensional vessel.

The one-dimensional vessel geometry was developed by transposing fluid volumes, flow areas and cell lengths from the three-dimensional vessel cell mesh of the LP-FP-1 deck, and the results were cross checked with the LOFT reference documentation.

The nature of the description, to TRAC, of heat structures (specification of a pipe's internal radius and thickness) prohibits the exact representation of the surface areas, and volume and thickness of the vessel metalwork. Any two parameters may be input precisely and some compromise between all three may be used. The approach adopted here was to concentrate on preserving the overall volumes and surface areas of the metalwork. No representation of two sided heat structures is available in the one or three dimensional vessel, resulting in a further substantial limitation.

On the basis of steady state mode calculations, friction factors were derived which enable reasonable agreement with the available pressure drop data to be obtained. Five of six core bypass paths were modelled (see Figure 4): Bypass Path 1 (lower core support structure bypass), Bypass Path 2 (lower end box bypass) and Bypass Path 3 (gauge hole bypass) were represented by the side arm of a TEE component (Figure 5). Bypass Path 4 (outlet nozzle gap) was modelled as a PIPE. Bypass Path 5 (core barrel alignment key) was represented by a PIPE component between the two sections of the upper plenum. It was not possible to model Bypass Path 6 (core filler block gap) because the one-dimensional core component is permitted to have only two junctions. The downcomer bypass was also modelled.

3.2 Steam Generator and Steam Line

The steam generator consisted of a boiler, a separator and a downcomer region. In order to adequately reproduce the subcooled region of the boiler, the bottom cell of the boiler was halved in length, as well as the corresponding primary side cells. The steam separator was simply modelled by imposing perfect separation at its top junction.

The overall heat losses were set to 21.4 Kw as the best fit to the available data (Ref 3).

Heat structures in the steam generator were better represented than in the vessel due to the capability of the steam generator component to cope with two-sided and multiple heat structures.

The friction loss in the junction between the downcomer and the boiler was modified to fit the reported recirculation ratio 4.8. No steam bypass valve was modelled; its function was taken over by the main steam control valve. A detailed description of the modelling can be seen in Figure 6.

3.3 Intact and Broken Loops

The loss of coolant occurred through a break in the intact loop hot leg; therefore the hot leg representation in the TRAC deck was modified to accommodate the break.

The length of the break line was 5.61 m with flow area section of $6.82 \cdot 10^{-4} \text{ m}^2$ and a nozzle of $1.2668 \cdot 10^{-4} \text{ m}^2$ that corresponds to a diameter of $1.27 \cdot 10^{-2} \text{ m}$. The length of the cell connecting to the nozzle was made equal to 0.1 m. The HPIS discharged into the cold leg at an angle of 90° to the mainline.

A characteristic of the LOFT facility is the existence of a fluid path connection between both legs of the broken loop in order to equalise the pressures between the upper core and upper downcomer, making it easy to flood the core under unexpected conditions. This bypass was supposed to be closed during the experiment but a leakage of about 5.3% of the circuit flow (480 kg/sec) passed through the reflood assist bypass valves (Reference 3). In the nodalisation the flow area of this junction was adjusted to obtain a flow rate in reasonable agreement with the data.

4 EXPERIMENT LP-SB-2

Experiment LP-SB-2 addresses the analysis of a small break loss of coolant accident with the break at the midplane of the intact loop hot leg. In contrast with LP-SB-1 the primary coolant pumps were running for most of the experiment until the trip set point on pressure was reached.

A detailed description of the experiments is found in Reference 4.

4.1 Steady State Calculations

Starting with input conditions well away from the operating steady state, 500 seconds of steady state calculations were run to achieve a reasonable degree of convergence. During this period the predominant timestep was 1 sec and the (CPU/Problem) time was 0.36. In order to obtain a final steady state a subsequent run of 70 secs with a maximum timestep of 0.1 sec was performed; the (CPU/Problem) time was 2.0. The total (CPU/Problem) time ratio was 0.56.

To establish the required steady state a control system was implemented acting on the following variables:-

Steam generator mass balance

Downcomer liquid level

Secondary pressure

Primary system pump speed

A further description of the control system may be found in References 5 and 6.

The model environmental heat losses from the primary side were 224 Kw and 21.4 Kw from the steam generator in agreement with Reference 3.

The percentage of the loop mass flow (480 Kg/s) diverted through the different bypasses was the following:-

Component

79	Core Barrel Alignment Key	0.04%
83	Outlet Nozzle Gap	2.7%
85	Downcomer Bypass	20%
89	Core Bypass	3.5%
31	Reflood Assist Bypass Valve	5.3%

The obtained primary side initial mass was 5640 Kg. The total deviation with the computed inventory for the LOFT facility of around + 7.6%. A further study on the broken loop structure allowed for a reduction of this offset up to a +3.8%.

The steam generator secondary side water mass inventory obtained for the steady state was 2089 Kg.

The steady state initial conditions obtained are shown in Table 1.

4.2 Transient Boundary Conditions

As far as possible all variables and parameters external to the LP-SB-2 calculation were modelled using the actual experimental data.

Among the most important parameters is the actual size of the break, 1.27 cm in diameter. The subcooled and two phase choked flow multipliers were 1.0 in value. The reactor power decay heat was provided by the best estimate data provided in Reference 7.

The pumps were kept on spinning at their steady state velocity, 331.3 rad/sec (~ 316 in experiment), throughout all the transient until their trip set point was reached. No heat source from pumps dissipation was provided, which is thought not to have affected the overall evolution of the calculation. The pumps injection flow was added immediately downstream, each pump assuming a constant flow of 0.0475 l/s

The secondary side steam control valve, as previously mentioned, assumed the function of the steam bypass valve. Estimated pressure setpoints deduced from direct reading of experimental data on pressure and valve movement governed its behaviour in the transient. After 80 seconds it was latched closed to a minimum flow area of 0.35% of its fully opened value, throughout the transient. This figure, derived from the LP-SB-3 EASR (Ref 8), implies a steam leakage of $\sim 0.125 \text{ Kg s}^{-1}$ at a secondary pressure of $\sim 5.5 \text{ MPa}$.

The auxiliary feedwater flow was constant and its temperature 209°C.

4.3 Chronology of Events for Experiment LP-SB-2

The experiment started with the opening of the break valve in the hot leg of the intact loop. After 1.8 secs the pressure fell below the reactor scram set point value (14.28 MPa). Simultaneously the main feedwater valve started to close and with a one second delay the main steam control valve began to close. At 4.3 seconds the main feedwater valve was isolated and the main steam control valve was fully closed at 14.8 seconds, though a small leakage was assumed. As a consequence of the subsequent pressure increase, the steam bypass valve was actuated. Meanwhile at 42.4 seconds the HPIS was initiated and at 50.2 seconds the subcooled blowdown ended. At 63.8 seconds the steam generator auxiliary feedwater was manually initiated. At 582.2 seconds the pumps degradation was observed and at around 600 seconds the onset of partial phase separation in the hot leg was detected. At around 1200 seconds the break started to uncover so increasing the depressurisation rate and after 1290 seconds the secondary pressure exceeded the primary pressure. After 1864 seconds the auxiliary feedwater was shut off and at

~ 2853 seconds both primary coolant pumps were tripped after reaching their pressure set point (3.16 MPa in primary system).

5 POST TEST CALCULATIONS

The results from two different runs are described in this Section. The first one, called Run A, was the first attempt to reproduce the experiment LP-SB-2 and no feature other than those implemented in the current standard version of the code (12.7) was used. Important conclusions were derived from this run. To confirm these results a major modification in the break line, together with a Winfrith implemented model, were used to make a second run, called Run B; at the same time other minor modifications were added to the input deck.

5.1 Run A

Operational set points and chronology of events are shown in Tables 2 and 3 respectively.

5.1.1 Code Performance

The code speed can be clearly separated in three regions (Figure 7). The first one comprises from 0.0 to 1000 seconds, the code is mostly using its maximum allowed time step of 0.5 seconds (Figure 8) and the (CPU/Problem) time is ~ 0.45. From 1000 seconds to 2650 seconds the code drops its speed and the average time step is ~ 0.08 seconds. The (CPU/Problem) time is ~ 3.1. This change of behaviour is found to be related to changes in flow directions in the broken loop and in Pump No 1 (discussed later). From ~ 2650 up to the end of the calculation the average time step recovers to ~ 0.4 and the (CPU/Problem) time is ~ 0.51. This recovery of speed in the calculation is found after the pumps trip. At 3000 secs the total number of time steps is ~ 25500 and the total (CPU/Problem) time is 1.95.

The SETS numerical method allows for the violation of the material Courant limit. A Courant value of ~ 12 is common in the cold leg during the fastest period of the transient ($\Delta t = 0.5$ sec). A Courant value of 1 would imply $\Delta t = 0.04$. This capability to violate the Courant limit allows the detailed modelling of bypass pathways in the vessel.

5.1.2 Short Time Behaviour (0.0 - 850 sec)

The evolution of the main variables: pressure, temperature and density is now described, finally the fluid velocities and transient mass inventory will be discussed.

5.1.2.1 Pressure Behaviour: Primary Side

Following the opening of the break valve a sudden decrease of the pressure (Fig 9) is observed. This period corresponding to the subcooled blowdown, is adequately predicted by the code, reaching the scram set point at 2.3 seconds. After ~ 53 seconds the fluid gets into saturated conditions; as voidage develops, the upper plenum of the vessel becomes vapour bound (Fig 10). The steam generation helps to stabilise the pressure, which is well reproduced by the code. Discrepancies in the break flow (Fig 11) may account for the slight differences obtained between experimental and calculated primary pressures.

The calculated pressure drop from the bottom of the loop seal to the pumps inlet was about 75 Kpa at time 0.0 while the experiment indicates ~ 20 Kpa. The reason for the discrepancy is the big pressure loss predicted by TRAC at the symmetrically flow dividing tee. As the overall system pressure loss is reasonably well reproduced, the actual pump pressure increase should remain unaffected. Having in mind this result the pressure increase through Pump No 2 is compared with the reading from PDE-PC-001 (Fig 12). It shows a bigger sensitivity at low void fractions than the experiment that is due to the selection of the head multipliers (Appendix A). The overall result is considered to reproduce the experimental result adequately. This indicates that the combination of mass flow, pump speed (constant), density and void fraction, together with the pump head degradation multipliers and pump homologous curves is consistent with the experiment.

5.1.2.2 Pressure Behaviour: Secondary Side

Simultaneously to the reactor scram, the main feedwater valve starts to close, followed by the closure of the steam control valve. As a consequence an increase of the secondary side pressure (Fig 13) is observed. The rate of pressurisation is overpredicted producing an early activation of the steam bypass valve. This overpressurisation was found to be dependent on steady state initial pressure, mass distribution and timing for the closure of main feedwater and steam valves. In any case the pressure rise rate was above the experimental one. Due to the secondary role played by the steam generator this problem did not affect the results seriously.

The energy removal from the steam generator was through the steam valve leakage (0.125 kg/s at 5.5 MPa) and heat losses through the shell. The combined effects of these and the introduction of subcooled water via the auxiliary feedwater dealt with the heat transferred from

the primary side and finally determined the secondary side pressure.

5.1.2.3 Temperatures

As soon as the chain reaction ceases in the core the main source of heat during the transient is the core decay heat. The early slow decrease of the hot leg liquid temperature during the subcooled blowdown (Fig 14) is associated with the rapid increase of the pressure in the steam generator. On reaching saturation the temperatures follow the same behaviour as the pressures.

The temperature in the cold leg of the intact loop (Fig 15) rises during the first ~ 20 seconds due to the decrease of ΔT through the steam generator. After the opening of the steam bypass valve and up to its final closing the temperature decreases as ΔT increases. In the experiment this behaviour is not observed. The cold leg temperature remains almost constant until the final closure of the steam bypass valve, at which time it rises and finally follows the pressure trend.

During all the period studied the steam generator behaves as a heat sink (Fig 16) due to the existence of a small positive difference in the pressures between primary and secondary side. Most of the energy however, is released through the break.

5.1.2.4 Density Distribution

In the experiment LP-SB-2 the distribution of the densities is strongly affected by the running pumps. In Figures 17 and 18 the hot leg and cold leg densities are represented. The experimental measurements are related to the absorption of three beams of gamma rays covering the top, middle and bottom cross section of the hot and cold leg specified locations (see Fig 19).

Early in the transient voidage started to develop in the upper plenum of the vessel (~ 46 sec), in the top of the steam generator U-tubes and in the loop seal (~ 60 sec), Figures 10, 20 and 21. This voidage (SG and loop seal) was strongly influenced by the secondary side behaviour in the first seconds of the transient. As soon as the heat transfer to the secondary side falls, the cold leg temperature increases, and as the loop seal is the minimum pressure location of the loop some voidage occurs there. After 80 seconds the secondary side steam bypass valve finally closes, thus increasing the secondary side pressure and enhancing the voidage generation. In the experiment this voidage is partially collapsed in the cold leg, ie the cold leg density decreases later than the density in the loop seal. This

was not observed in the calculation resulting in a lower density than the experiment for a period of about 200 seconds. In general, though, the density in the cold leg is reasonably well reproduced during this period.

The calculated density in the hot leg initially increased because the more dense fluid overrode the incipient voidage being transported from the vessel during the first 100 seconds; from then on the density decreased steadily. Early in the experiment (~ 50 secs) a more or less continuous density gradient develops in the pipe and at around 600 seconds it turns into a steep gradient indicating a probable flow transition. This complicated pattern is not observed in the cold leg as the mixing from the pumps tends to maintain an homogenous void distribution in the cross section of the pipe.

As is clear from Figure 22, a systematic overprediction of the break line density was obtained; the calculated density practically matches that of the average hot leg while the experimental is almost that of the top beam in hot leg. This vapour pull-through phenomenon is not modelled in the code.

5.1.2.5 Fluid Velocities

LP-SB-2 experiment was characterised by the long time both reactor coolant pumps were running. During the period under study no cessation of loop forced flow happened, therefore the fluid velocity in the loop was closely related to the pumps performance. The reduction in pump pressure rise implied a reduction in fluid velocity; this trend was specially well reproduced in the cold leg (Fig 23). The calculated velocity reduction in the hot leg was analogous to the one in the cold leg but it did not fit the experimental trend so well (Fig 24). The fluid velocity in the downcomer had an initial value lower than the experimental one, the flow directed through the downcomer bypass could account for most of this initial mismatch, Figure 25. The constant decrease in velocity observed in the experiment is not observed in the calculation. An asymmetrical flow distribution in the downcomer annulus could explain in some degree this discrepancy.

The calculated fluid velocities in the core inlet and outlet were multiplied by 1.3 to account for the difference in flow area in the measurements location between the experiment and the calculation (Table 4); with this correction the results obtained are shown in Figures 26 and 27 respectively. The results obtained before the pumps degraded show a better agreement than after. The pumps degradation was not reproduced with

the sharpness of the experiment, correspondingly the velocities did not fall so sharply.

The fluid velocity in the break line (Fig 28) is well reproduced, with a small underprediction in the subcooled region.

5.1.2.6 Transient Mass Inventory

To achieve a proper description of the actual mass inventory detailed calculations of the inlet and outlet flows are required. The fluid inlet sources to the primary system were the pumps cooling injection and the HPIS. During the period under study the mass loss through the break was much bigger, being well within LOCA conditions. In Figure 11 the break mass flow rate is shown. As soon as the break opened, choked flow conditions were detected. During the subcooled blowdown the code subcooled choked flow model was invoked with a multiplier factor of 1. The results show a slight underprediction. The code two-phase model was invoked with a multiplier factor of 1. For the very low quality region a slight underprediction was observed. From 600 seconds on, a permanent overestimation of the break mass flow rate is obtained. The evolution of the calculated and experimental mass (obtained from the integrated flow balance) can be seen in Figure 29.

5.1.3 Long Time Behaviour (850 - 3000 Seconds)

5.1.3.1 Pressure Behaviour

The secondary side pressure decline appears to be reasonably well reproduced indicating that leakage through the steam valve is about correct (Fig 30). After 1307 seconds the primary side pressure fell below the secondary side. Thus the steam generator no longer acted as a heat sink (Fig 31). At a 1864 seconds the auxiliary feedwater to the steam generator was suppressed and as a consequence the rate of depressurisation slowed down. Unexpectedly the experimental trend is the opposite.

In the primary side (Fig 32) a discrepancy with respect to the experimental result arises from 800 seconds onwards, the break uncover which in the experiment happened at about 1200 seconds was delayed in the calculation up to 1900 seconds. The experimental break uncover appears to happen when the hot leg collapsed level reaches the break level (Ref 9) while in the calculation transition to steam flow corresponds to a complete depletion of the hot leg. This depletion is consequence of the loss of sufficient mass inventory to eventually allow the vessel swell level to fall below the nozzles at around 1920 secs. The hot leg was

emptied and consequently only steam was released through the break with the subsequent increase in depressurisation rate. At around 2100 and 2660 seconds the primary pressure curve shows the existence of two spikes which correspond to the sudden transport of water to the break line after a momentary increase in the swell level in the core (first spike), and to the water drained from the inlet plenum of the steam generator after the pumps trip for the second one.

The time at which the pumps were tripped (3.16 MPa in primary side) was ~ 200 seconds before that in the experiment.

5.1.3.2 Temperatures

In the hot leg the fluid temperatures Figure 33 were at saturated conditions and therefore followed the trend in pressures. The situation in the cold leg was strongly dependent on the distance from the HPIS injection location. As can be seen in Figure 34 the difference from saturation temperature 1.52 m before the HPIS location was almost nil until the pumps were tripped, after which part of the HPIS subcooled water was flowing back to the loop seal. In the experiment no sudden decrease in temperature was observed because after the pump trip the cold leg was partially flooded with water coming from the vessel outweighing the cooling from the HPIS.

The subcooling at the HPIS injection location and at the cold leg nozzle (~ 1.15 m from HPIS) started to be noticeable after 1200 seconds, the inlet subcooling ($T_{sat} - T_{lig}$) to the vessel was around 5°C up to ~ 1850 seconds, when the cold leg was depleted. At this time the subcooling temperature in the cell where the HPIS was discharging jumped to ~ 120°C and the subcooling at the inlet nozzle of the vessel was around 10°C. After the pumps were tripped the non-uniformity was more pronounced with a subcooling of ~ 170°C at the injection point and a subcooling ~ 40°C at the inlet of the vessel.

The fuel cladding temperature merely followed the trend of the saturation temperature corresponding to the existing pressure. After the pumps were tripped the downcomer and core levels equalised and as a result the top of the core slightly uncovered producing a negligible excursion in the cladding temperature of about 10°K (Fig 35) until the growth of the swell level quenched the rod.

5.1.3.3 Density Distribution

The calculated hot leg density (Fig 36) shows an evolution in reasonable agreement to the experiment up to ~ 1500 seconds in which the calculated and experimental trend noticeably starts to differ. In the calculation no forced flow cessation is detected and at ~ 1800 seconds the hot leg is completely depleted while in the experiment forced flow cessation is observed which results in a fall in the hot leg level but later the level rises again. The explanation given in Reference 4 is the following: The level rise is... "due to a coolant density decrease in the core as a result of decreased fluid velocity and a liquid level drop in the downcomer because the pump operation pressurised the cold leg and upper part of the downcomer relative to the upper plenum. The downcomer liquid level also decreased due to the manometer effect between the column of liquid in the downcomer and the column of less dense coolant in the core and upper plenum". After the pumps were tripped the consequent increase in the core void fraction accounts for the observed rising in level. This late rise in level was not observed in the calculation due to the small inventory of water remaining in the system which did not allow the core swell level to reach the nozzles.

The calculated tendency in the cold leg (Fig 37) was quite similar to that of the hot leg, reproducing the phenomena observed in the hot leg. Note, though, that after the pumps were tripped an increase in the cold leg density was observed. This is due to the growth of the layer of water coming from the HPIS which at this time is no longer dragged to the vessel by the steam previously pumped from the pumps. At the same time the density in the loop seal increased as the water was running down to the bottom of the loop seal from the cold leg. The experimental trend is markedly different from that of the hot leg. First of all there was no density gradient across the pipe until ~ 1200 seconds, due to the mechanical mixing provided by the pumps. As soon as the forced flow ceased, around ~ 1500 seconds, the fluid stratified. It is thought that after ~ 1200 seconds of transient the transport of liquid in the upside of the U-tubes of the steam generator greatly worsened due to the low velocity of the steam and to the onset of clear stratification conditions throughout the hot leg. This produced a gradual depletion of the cold leg with respect to the hot leg, and as a result the level above the bottom of the pipe was considerably lower than that of the hot leg. After the pumps trip a jump in the cold leg density was observed. This was due to the level increase in the downcomer that reached the cold leg level allowing its flooding. Once the level was enough to pass over the pumps outlet lip (~ 10 cm height) part of the liquid ran down to the loop seal.

In the nodalisation used this lip was not modelled, therefore the flow to the cold leg was greatly favoured.

The break flow density (Fig 38) was systematically overpredicted until the hot leg pipe emptied. From then on the density was correctly calculated.

5.1.3.4 Fluid Velocities

The liquid and vapour velocities in the downcomer (Fig 39) followed a quite different trend with one another. To start with there is an initial slip induced by the steam buoyancy. The liquid velocity shows an increasing trend as the void fraction increases, as a result of the liquid flow area reduction. At around 2000 seconds the void fraction starts to decrease, reducing the liquid velocity until it stagnates. The steam follows the opposite trend, and after a further decrease in the pump Δp at ~ 1200 seconds and the depletion of the broken loop, it changes direction, and instead of flowing towards the core through the lower plenum it rises, going to the broken loop cold leg nozzle, towards the broken loop hot leg via RABV.

The trend observed in the measurement from the experiment is markedly different. The decrease in velocity is sharper and at around 600 seconds the velocity is extremely low. Meanwhile the velocity in the core inlet, Figure 40, does not reproduce this result, having at that time a high velocity. This points to an asymmetrical distribution of the flow in the downcomer, in which most of the flow is falling in a fairly narrow section, centred on the cold leg nozzle. This could be supported by the fact that the measurement location in the downcomer is situated at $\sim 160^\circ$ from the cold leg nozzle. This suggests that the use of a three-dimensional model of the vessel in a SBLOCA simulation could be beneficial.

In the calculated core inlet velocities there is an initial slip due to the positive effect of the buoyancy of the steam bubbles. The liquid velocity reduces at a lower rate than the experiment although the pumps Δp (Fig 41) is well reproduced; at ~ 1200 seconds the further decrease in the pumps pressure rise is followed by a sharp reduction in the liquid and steam velocities. Finally there is a residual liquid flow up to ~ 2000 seconds when the flow definitely stagnates.

The velocities in the core outlet (Fig 42) practically follow the core inlet velocities. The evolution of the liquid and steam velocities after the pumps trip reflect the level drop in the core followed by the minor core uncover.

The hot leg velocities (Fig 43) are following the same trend as the core velocities. Just after the sharp drop in velocities after ~ 1200 seconds the code detects stratified flow conditions, according to the Taitel Dukler's criterion built into the code flow regime map. From then on the liquid and steam velocity are less strongly coupled and as a result the slip ratio increases markedly. No cessation of the liquid flow is calculated, stabilising at a velocity of around 1 m/s when the bottom of the pipe fluid velocity detector indicates stagnation. Along the top of the pipe the steam is flowing toward the break and the steam generator. Once the pumps are tripped a sharp decrease in the velocities is detected and a residual steam flow is maintained feeding the break. The liquid in the upside of the steam generator is observed to begin to drain towards the inlet plenum at around ~ 2000 secs where it stagnates until the pumps are tripped. Then the liquid is drained back to the hot leg.

The experimental and calculated cold leg velocities, are very similar to those of the hot leg. The code detected stratified conditions at about the same time as in the hot leg independently of the strong mixing produced by the pumps.

An important feature observed in the calculation is the asymmetrical further pump degradation observed at around 1200 secs. A sudden instability develops in which the pump number 2 is delivering all the fluid, while through pump 1 some fluid is being recirculated. As a result the system velocities drop quite substantially. A somewhat similar behaviour is reported in Reference 4 developing at the moment of the pumps degradation in the experiment (582 secs).

The break line velocities (Fig 45) are well predicted before the break uncovers ~ 1200 secs, at that time the calculated density in the break line is much bigger than in the experiment. At around ~ 2000 secs the code detects the break uncover and then the velocities are again well predicted.

As a result of the reasonable representation of the velocities and densities in the pipework the hot leg mass flow rate (Fig 46) was in good agreement with the experimental results up to ~ 1500 seconds.

5.1.3.5 Transient Mass Inventory

The permanent overestimation of the break mass flow rate (Fig 47) produced a greater mass loss than in the experiment. At around ~ 2000 secs the calculated rate of mass loss equalised the inlet water from HPIS and pumps cooling injection. In the experiment this time is

subject to a large uncertainty. A possible time at which the LOCA was effectively terminated is ~ 2200 secs. The minimum inventory calculated was about 1100 Kg while in the experiment it was around 1800 Kg (Figure 48).

5.1.4 Conclusions Derived From Run A

- a • TRAC PF1-MOD1 (12.7) provides a reasonably good account of the evolution of the SB-2 transient.
- b • The main discrepancy between the experiment and calculation is the overprediction of mass loss from the primary system.
- c • The TRAC built-in flow regime map performs well in identifying fully stratified conditions.
- d • To improve the predictive capability of TRAC for transients where phase separation upstream of the break affects the break density, requires a model relating quality in a branch to the thermal hydraulic condition of the fluid in the main pipe as well as considering the geometric characteristics of the break line junction to the main line.
- e • Prediction of the correct break flow should reduce or remove discrepancies between the experimental and calculated:-
 - Primary Pressure
 - Hot Leg Density
 - Cold Leg Density
 - Primary Mass
 - Vessel Inventory and Subsequent Heat Up
- f • The use of a one-dimensional vessel did not allow reproduction of an asymmetrical flow distribution in the cross section of the downcomer annulus and its influence in the transient flow distribution through the bypasses, especially the RABV bypass.
- g • SETS allow timesteps ~ 0.5 seconds to be used for large parts of the calculation, and results in relatively economical computing times.

5.2 Run B

In order to test the validity of Conclusion e derived from

Run A a second run was made. The main modifications with respect to the input deck of Case A where:-

- Set up, using the TRAC control logic and two offtakes, of a system which effectively could control the quality in the break line as a function of the void fraction in the hot leg.
- Modification of pump head multipliers to force a sharp degradation at an inlet void fraction of ~ 0.35 and further modification of Pump No 1 head multipliers in order to try to reproduce the asymmetrical pump behaviour after degradation.
- Addition of a factor $\sqrt{\pi}$ missing in the determination of the critical gas velocity in the stratified model (agreed from Los Alamos Reference 16).

The steady state conditions and chronology of events can be seen in Tables 5 and 6 respectively.

5.2.1 Results Review

The control on the quality in the break line allowed the reproduction of the experimental density with adequate accuracy during all the transient (Fig 49). At the moment at which the pumps were tripped the level in the hot leg increased, allowing the discharge of a more dense mixture. This transition was slightly accentuated in the calculation although the final density at 3000 secs is correct.

The break mass flow rate (Fig 50) shows as expected a much better agreement with the experiment than in Run A. It is observed that the region from subcooled blowdown to very low quality two phase shows a tendency to underpredict the mass flow, and that at higher quantity there is a tendency to overprediction.

The primary system mass inventory (Fig 51) agrees well with the experiment, the minimum inventory is reached at around ~ 1865 secs with a mass of about ~ 2060 Kg. In the experiment the minimum inventory is reached after ~ 2200 secs with a minimum mass of about ~ 1800 Kg that agrees well with the calculation [considering the initial offset of ~ 250 kg]. The slight underprediction of the break flow in the very high quality region $x > 0.99$ implies a faster mass inventory recovery than in the experiment. The correct description of the break flow as well as the appropriate heat losses results in an excellent description of the primary pressure (Fig 52). The change in the depressurisation rate after break uncover is properly calculated. The secondary side pressure (Fig 53) has improved as well, although some discrepancies in the trend of depressurisation

appear after 1200 secs. Corresponding to the good primary pressure calculated, the fluid temperatures are very well reproduced. The liquid hot leg temperature is shown in Figure 54. Similarly the cladding temperature, Figure 55, in the core was correctly calculated; the increase in temperature after the pumps trip was due to the increase in pressure following the decrease in volumetric flux through the break after the growth of the hot leg liquid level.

The smaller amount of mass lost through the break implied in general a higher density of the fluid throughout the transient than in Run A. In Figure 56 the hot leg density is shown. The value obtained up to ~ 1400 secs is reasonable while the evolution of the density after that time, as no cessation of forced flow was obtained, differs significantly from that of the experiment and a constant value for the density, corresponding to a normalized collapsed level above the bottom of the pipe of ~ 0.3 was obtained. After the pumps were tripped an increase in the hot leg density was obtained due to the draining of water from the upside of the steam generator, and the increase in the swell level of the vessel which overrides the decrease in the collapsed level in the core. The computed cold leg density (Fig 57) shows a similar behaviour to that of the hot leg before the pumps degrade. After the subsequent sharp decrease in velocity a build up of liquid with respect to the hot leg is calculated. The failure of the code to predict the end of the forced flow in the system prevents the pumps from emptying the loop seal and cold leg, therefore the density calculated from ~ 1400 secs on is considerably higher than that of the experiment. Once the pumps are tripped the fluid in the cold leg drains partly to the vessel and partly to the loop seal producing a considerable reduction in the cold leg density.

The transient fluid velocities in the system were significantly affected by the modifications to the pumps as well as by the higher densities calculated in Run B, compared to Run A. The downcomer liquid velocity (Fig 58) is no longer steadily increasing as in Run A. At ~ 1200 secs the broken loop empties, establishing a new flow distribution in which the steam content in the downcomer rises and is diverted to the upper plenum via the RABV (vapour velocity negative in Fig 58) while practically only liquid is flowing to the core. This strongly affected the density distribution in the core, Figure 59, inducing a voidage decrease and a slight drop in the swell level. The general trend of the core inlet velocities is reasonably reproduced (Fig 60), although the rate in decrease of the velocity is always underestimated. At around 1300 secs the liquid and steam velocities became stable and no cessation of the

forced loop flow is observed. The fluid velocities calculated in the hot leg (Fig 61) did not reproduce the permanent slowing down observed in the experiment. On the contrary after the pumps degradation an almost constant velocity is obtained. The reasonable description of the pumps delta pressure (Fig 62), that after degradation shows a weak dependency on the voidage and volumetric flux, seems to eliminate its influence as a main source of the problem unless the data is significantly in error. Three factors could play an important role in the explanation of the discrepancy in the velocities. First of all there could be an underprediction of the two-phase pressure losses in the circuit. Secondly the considerable liquid mass flow transported from the hot leg, under stratified conditions, to the steam generator inlet plenum, overcoming the upside bend section of the hot leg which prevents the loop seal from being depeleted. Thirdly, the phases separate in the downcomer inlet annulus, with the steam being bypassed through the RABV line. If the RABV leakage were smaller this would present a greater resistance to the general loop circulation, in particular reducing the steam velocity. As a result of the poor prediction of the velocity the mass flow rate in the hot leg was not properly reproduced after the pumps degradation (Fig 63). The prediction for stratified flow was acceptably performed in the code; at around 700 secs (at a steam velocity slightly below the experimental value of 1.5 m/s) transition to stratified flow begins. At ~ 1150 secs the code computes pure stratified flow that is in good agreement with the experiment. (See Chapter 6).

Before the break uncover the velocities in the break line (Fig 64) showed a permanent overprediction while after the uncover, when practically only steam was flowing, the velocities were underpredicted. As the density in the break line was correctly reproduced a possible explanation would lie in the velocity predicted by the choked flow model.

5.2.2 Conclusions Derived from Run B

- a The good reproduction of the break line density notably improves the results for:-
 - Primary Pressures and Temperatures
 - Primary Mass Inventory
 - Vessel Inventory (No Core Heat Up)

- b The removal of a model deficiency in the description of break flow allows a deeper insight into the ability of TRAC-PF1/MOD1 in reproducing

phenomena which otherwise would have been masked, eg loop flow velocities.

- c Taitel and Dukler's criterion built into the code performs well in determining fully stratified conditions. The interpolating criteria used by TRAC properly identifies the transition to stratified flow, although at a lower steam velocity than in the experiment.
- d The pumps behaviour in LP-SB-2 experiment is considered to have been only partially reproduced and considerable uncertainties remain about the true pump characteristics for the LOFT configuration.
- e The loop fluid velocities never dropped to almost stagnation conditions in contrast to indications from the experiment. It is possible that a better prediction of two-phase pressure losses and liquid transport from horizontal stratified conditions in the hot leg toward the inlet plenum of the steam generator, together with an accurate RABV bypass flow may help to remove the discrepancies.

6 SELECTED ITEMS

6A LP-SB-2 Pumps Modelling

The experiment LP-SB-2 was characterised by the important role played by the primary coolant pumps. They were a main factor in explaining many of the features observed in the experiment: density distribution, RABV and vessel flows, and flow regimes.

The uncertainty involved in the description of the two-phase performance of the pumps has been regarded as a limiting factor in the capability to reproduce the experiment (Ref 9). The intact loop of the facility contains two similar pumps working in parallel. The strong coupling between both pumps constitutes a potential source of instability as soon as asymmetrical perturbations in the flow conditions affect the pumps inlet.

The assumption of similar behaviour of both pumps could not be sustained as the actual trend observed in the experiment pointed to a clearly asymmetrical one (Ref 4). Thus in order to create an adequate set of head multipliers it would have been desirable to know the individual fluid conditions and performance for each pump; unfortunately that was not the situation and the available data only provides an average description.

In experiment LP-SB-2 the density measurement in the vertical section connecting the steam generator with the bottom of the

loop seal (DE-PC-003B) was questioned in Reference 4 as unreliable, thus an adjusted density was used to derive the pump head versus pump void fraction. (Figures A1, A2 and A3 taken from Reference 4). With the adjustment it was found that the SB2 pump head closely matched that of L3-6 experiment. Under this assumption a set of two phase head multipliers was derived from Reference 11, and they are shown in Table A1; to be consistent with the procedure to obtain the head multipliers, the TRAC LOFT pump data for the first quadrant of the fully degraded characteristic curve was set equal to zero.

The head versus pump void fraction calculated in Run A for both pumps is plotted in Figure A4. It is observed that although the head multipliers derived from L3-6 have been used, the results for a void fraction below 0.4, lay between the unadjusted head for SB-2 and the L3-6 head (Fig A2). This discrepancy could be partly related to the uncertainty of the data used to derive the head multipliers for low voidage and possibly to the mass flow dependence of the head multipliers, which is not included in the TRAC model for the PUMP component. On the other hand the coincidence, between the calculated and measured density in the loop seal (Fig A5) up to 500 seconds points to a questioning of the trend for the adjusted density at low voidage, which would suggest that the unadjusted head could be correct at least up to a voidage of ~ 0.4 .

A better description of the degradation could be obtained with the available data used to derive the general set of head multipliers.

At the moment of the degradation ~ 580 secs a perturbation related to the individual behaviour of both pumps was observed in the calculation (Fig A6); after a few seconds the behaviour stabilised again until at around 900 secs ($\alpha \sim 0.55$) the behaviour of both pumps started to differ and very quickly the direction of the flow within the pumps loop was such that all the mixture was pumped by Pump 2, Figure A7. In Pump 1 the situation was very different; the void fraction at its inlet rose to practically 1 and a flow of about 5 Kg/sec was recirculated from Pump 2.

The mechanism driving this behaviour was found to be related to the slight asymmetry of the pumps layout which implied that the fluid velocities through both pumps were slightly different. This in turn implied that the void fraction at the inlet of both pumps were not the same and as a consequence the heads through the pumps were not equal. This mode of degradation was found to be strongly sensitive to variation in the pumps characteristic curves and multipliers; by varying them the time of divergence could be drastically changed, or the behaviour could be completely suppressed.

The consequences of this asymmetrical degradation were important as the fall in the pressure increase provided by the pumps implied a sudden drop in the loop velocities (Fig 43) and the onset of counter-current flow in the downcomer of the vessel (Fig 39). A somewhat similar asymmetrical degradation was reported in Reference 4 to happen in the SB-2 experiment at the moment of the pumps two-phase performance degradation. In order to try to reproduce this experimental trend in RUN B the pump head multipliers were modified as shown in Table A2; it is observed that the head multipliers differ from one pump to the other after degradation, this in fact constitutes a coarse approximation but allows us to induce the asymmetrical behaviour to happen at the moment of the degradation as it actually happened in the experiment. An indication of the ability to reproduce these results may be compared in Figures A8 and A9 (no possible quantitative comparison is available as the motor and pump efficiencies are not known for SB-2). At the moment of the degradation Pump 2 takes over the delivery of the fluid mixture, thus increasing the hydraulic torque while through Pump 1 some fluid is being recirculated from Pump 2. The mass flow for each pump are shown in Figure A10, where the sudden reduction in the loop mass flow is evident; this in fact happens to be too large at this stage if we compare with the experimental result, Figure 63, which suggests that the degradation has not been accurately reproduced and therefore a better set of head multipliers would be desirable.

6B Break Flow Density in Experiment SB-2

The ability to reproduce the flow through the break line in a small break LOCA scenario constitutes an important, if not the main, factor in performing a satisfactory best estimate calculation.

The problem of predicting the correct break flow can be divided into two parts, first obtaining the correct mixture density of the fluid convected from the main pipe to the break line and secondly predicting the liquid and steam velocities at the break nozzle under choked flow conditions. This section deals with the first of these two elements.

In experiment SB-2 the observed density in the break line strongly differed from the average of the density in the hot leg; being biased towards the density at the top of the hot leg pipe (Fig B1). The pressure drop from the hot leg to the break line was not large enough to explain the observed difference between the average density in the hot leg and the break line in terms of flashing so it should be related to the phenomenon of vapour pull-through.

To reproduce this behaviour has been a common problem for different organisations and codes including TRAC-PF1-MOD1 (see Fig 38) trying to reproduce the LP-SB-2 experiment, eg

References 9, 10, 12, and at the present time it remains as an open problem.

No information has been found covering the characteristics of the experiment SB-2, that is: liquid and steam velocities in the main pipe up to 8m/sec and flow conditions from bubbly with high density gradient in the cross section to stratified flow with steam at the top of the pipe and nonhomogenous two-phase in the bottom of the pipe. The available information covered purely stratified flow with stagnant or very small velocities in the liquid, eg References 13 and 14.

From Reference 13 a correlation of the type:-

$$X_{\text{BRANCH}} = \text{EXP} \left(C_x \left(\frac{h - h_\ell}{h_g - h_\ell} \right) \right)$$

h = collapsed liquid height in hot leg

was attempted, where the height for the onset of entrained fluid h_ℓ is obtained from:-

$$\frac{h_\ell}{D} = \frac{1}{2} - \frac{C_\ell}{D} \left(\frac{\dot{m}_g^2 \text{ Branch}}{g \rho_g (\rho_\ell - \rho_g)} \right)^{0.2}$$

and analogously the height for the onset of vapour pull through h_g :-

$$\frac{h_g}{D} = \frac{1}{2} + \frac{C_g}{D} \left(\frac{\dot{m}_\ell^2 \text{ Branch}}{g \rho_\ell (\rho_\ell - \rho_g)} \right)^{0.2}$$

where C_x , C_ℓ and C_g were constants to be obtained, \dot{m}_g and \dot{m}_ℓ are the gas and liquid mass flux respectively, D is the main pipe diameter. The results obtained were unsatisfactory due to the uncertainty in determining the mentioned constants and the inability to find a single correlation applicable to all the transient, in particular it was difficult to reproduce the transition between the steady drop in density up to 1100 seconds and the quite sharp decrease as the break uncovers (1100 - 1300 secs).

An alternative approach was finally adopted and the quality in the break line was correlated to the void fraction in the hot leg in the form of a table of pairs (α, x) , see Table B1, being used in conjunction with the Winfrith offtake model (Ref 15). This of course implied that it would be only applicable to the SB-2 experiment thus losing the generality of a proper correlation. The values for the void fraction in

the hot leg were deduced from Reference 9, although for $\alpha > 0.4$ the correlated quality had to be slightly re-adjusted in an iterative fashion to reproduce the experimental timing. To implement this correlation the hot leg nodding was modified as seen in Fig B2. An extra offtake attached to the hot leg was added and invoking a pure separator model would guarantee a source of pure steam from the hot leg which would be discharged to the break line. The flow of steam delivered to the break line was controlled by the so called "control quality valve". The scheme of the control logic is provided in Figure B.3. At the same time the original offtake from the hot leg makes use of the Winfrith offtake model for a horizontal offtake when the level of the stratified fluid drops below a determined value. This way of implementation has the advantage of allowing the testing of different correlations in a straight forward way, eliminating the problems involved in modifying the cell edge quality within the TRAC code.

The results obtained with this procedure can be seen in Figure 49.

6C Flow Regimes Prediction for LP-SB-2

From the point of view of the analysis of flow regimes, the experiment LP-SB-2 constitutes an interesting example of the important role the exact nature of the flow can play during the evolution of a transient. In LP-SB-2 the break flow was strongly determined by the flow conditions in the hot leg.

The existence of density data at different elevations in the hot and cold leg allows us to obtain at least an idea of the complexity of the flow patterns during the transient. As can be seen in Figure 56, early in the transient (~ 200 secs) the outputs from the gamma densitometers indicate the onset of a density gradient across the pipe with trailing bubbles in the upper section of the pipe. After the pumps degradation and up to ~ 1200 secs the reduction in fluid velocity allows the steam to concentrate in the upper half of the pipe and as a result the density gradient noticeably steepened. The possibility of stratification in the sense of pure steam in the very top of the pipe could be considered but the idea of a well defined level cannot be supported as the density reading in the top of the pipe indicates the presence of liquid while the other two measurements indicate the presence of steam. From 1200 seconds on, the top beam is indicating only the presence of steam; from Reference 9 and according to the trend of the collapsed and swell levels the flow was stratified up to 1400 secs, stratified with bubbles up to 2000 secs and from then on pure stratified again. In the cold leg, Figure 57, there is no detachment between the densitometer readings up to 1200 secs which is due to the transport of the mixing created by the pumps. From 1200 secs up to 1500 secs a density gradient is present in the cross section of the pipe, from 1500 secs up to 2000 secs the noisy

reading from the densitometers could indicate the presence of erratic waves probably caused by fluctuations in the flow delivered from the pumps as the loop seal is being depleted. Despite this the flow regime may be considered as stratified throughout the rest of the transient.

The recognition by TRAC of some of the flow patterns involved in the transient is difficult especially when they involve non fully developed regimes, ie partially stratified flow in which the separation of the liquid and steam phases is far from complete. The TRAC flow regime map from Reference 5 is shown in Figure C1 plotted as $\log(Froude)$ vs vapour void fraction. Included on the map is the TRAC implementation of Taitel-Dukler stratified flow criterion and the limit for interpolation for transitions into stratified flow.

The prediction for Run B can be considered satisfactory as the code is able to predict the trend of the experiment fairly well. Up to ~ 500 secs, see Figure C2, only bubbly flow is predicted. From 500 secs up to ~ 700 secs some weighting with slug is made. At 700 seconds the interpolating criterion for stratified flow is reached. Finally at around 1150 secs pure stratified flow is predicted, this being the flow regime for the rest of the transient. For the cold leg the results obtained indicated transition to fully stratified conditions at about the same time as that in the hot leg, that is ~ 1100 secs; this is not the trend of the experimental measurement which by that time indicated the onset of a vertical density gradient. This discrepancy is mainly dependent on the high degree of mechanical mixing in the fluid induced by the rotating pumps being transported along the cold leg. This effect should be taken into account as the flow through a break in the cold leg would be dependent on the fluid characteristics in the main pipe and in particular the void profile at the break line offtake location. It should also be noted that for Run B a missing factor $\sqrt{\pi}$ in the determination of gas critical velocity in the Taitel Dukler Test was implemented as agreed from Los Alamos, Reference 16.

7 SUMMARY AND FINAL CONCLUSIONS

- Two calculations of LOFT test LP-SB-2 were carried out with TRAC PF1/MOD1 (approximately Version 12.7).
- A one-dimensional description of the vessel was implemented in the input deck. Due to the relative importance of the different core bypasses, especially the RABV, it would be desirable to use a 3-D representation of the vessel in order to assess the degree the prediction of the transient evolution is affected. It would also help to evaluate the possibility of asymmetrical flow distribution in the downcomer annulus.

- The representation of the vessel, whether one- or three- dimensional, has the limitation of the poor description for heat structures. No double sided heat structure is available and thus the radial heat flux across all the vessel structures is only partially reproduced. At the present time it is an important limitation in the TRAC PF1/MOD1 modelling of the vessel and a better description would be desirable.
- The Code (CPU/Problem) time for Run A was considered good, having a value ~ 1.95 . In Run B this ratio increased to ~ 2.3 .
- The use of large timesteps was found as a possible source of running problems as the code sometimes failed when trying to reduce the timestep from big timestep values. This meant that the maximum time step had to be reduced in Run B during parts of the transient.
- The set of initial conditions obtained for the steady state in Run A and B were reasonably good. No special problem was found in obtaining these steady states.
- The chronology of events for Run A and B matched the experiment in some degree. Not surprisingly, when the break flow is well reproduced (Run B) the code overall reproduces of the experiment results better.
- Vapour pull through and liquid entrainment were observed to occur at the offtake of the break line. TRAC PF1/MOD1 was unable to recognise this phenomenon as no relevant model is actually implemented relating quality in a branch to the thermal hydraulic conditions of the fluid in the main pipe, as well as considering the geometric characteristics of the break line junction to the main line.
- The TRAC built-in flow regime map performs well in identifying fully stratified conditions in the hot leg. The introduction of a missing factor $\sqrt{\pi}$ (modification agreed by LANL) in the determination of the gas critical velocity (performed in Run B) helps to improve the results and the code is able to predict the initiation of the transition to stratified flow at about the correct time, although the steam velocity at that time is underestimated.
- The calculated flow transitions predicted for the cold leg closely match in time those of the hot leg. The experiment shows that the high mixing provoked by the pumps maintains bubbly conditions for a long period. This generation of mechanical mixing, its

transport and then its influence on the flow regime map should be considered for small breaks located in the cold leg. The break flow will still be a function of the void profile in the cold leg, but this is likely to be quite different from that in a fully developed flow.

- The reproduction of the pumps behaviour in LP-SB-2 constitutes an important problem and no satisfactory solution has been found yet. The pump model could not be appropriately validated as the set of head multipliers was not completely reliable, because it was deduced under the assumptions of pumps average behaviour and similitude to L3-6 experiment. Further uncertainties were involved in the reproduction of the asymmetrical pumps degradation, ie pumps inlet flow condition.

It seems likely that in order to reproduce the observed behaviour a priori, more sophisticated models of the pumps themselves, and of the effect of the pump inlet branching geometry on inlet conditions, would be needed than TRAC currently provides. Better data from the test, however, would probably allow an improved (a posteriori) fit within the scope of the existing models.

- The velocities predicted by the code after the pumps degradation were not entirely satisfactory and the steady fall in velocity observed in the experiment was not reproduced. Finally no liquid flow cessation was calculated. Three possible causes may be mentioned: underprediction of two-phase pressure losses, handling of the liquid convected from the hot leg towards the steam generator inlet plenum under stratified conditions, and influence of the flow through the RABV.
- The choked flow model predicted the results with reasonable accuracy and the subcooled and two-phase multipliers used for all the calculations were 1.0. Small discrepancies in the velocities were observed when the break line density was correct (RUNB).
- The mass loss predicted for Run A was large enough to provoke a mild uncovering of the top of the core after the pumps trip, contrary to experiment. In Run B the break flow was adequately predicted and the mass loss closely matched the experimental result. No core uncovering was predicted.

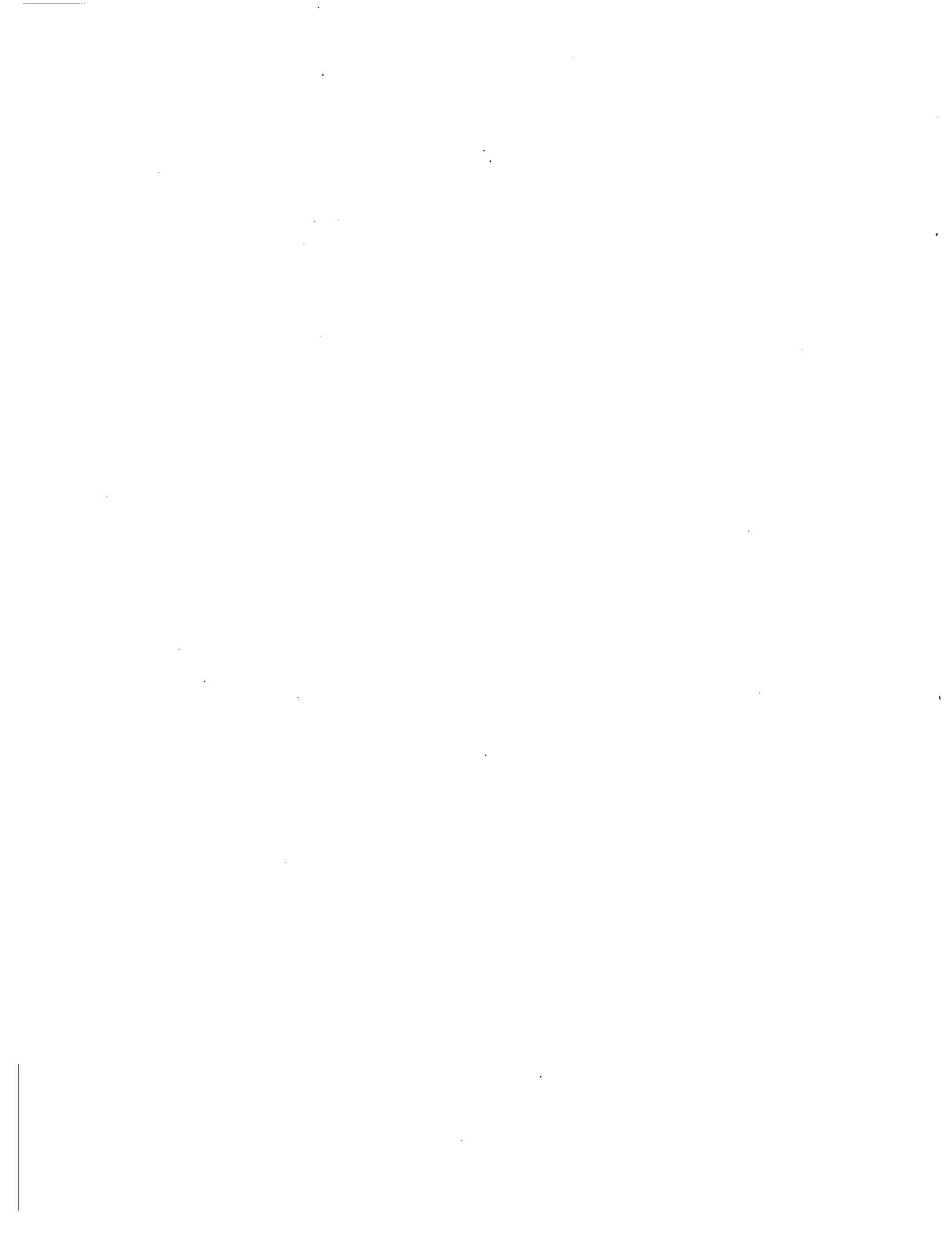
REFERENCES

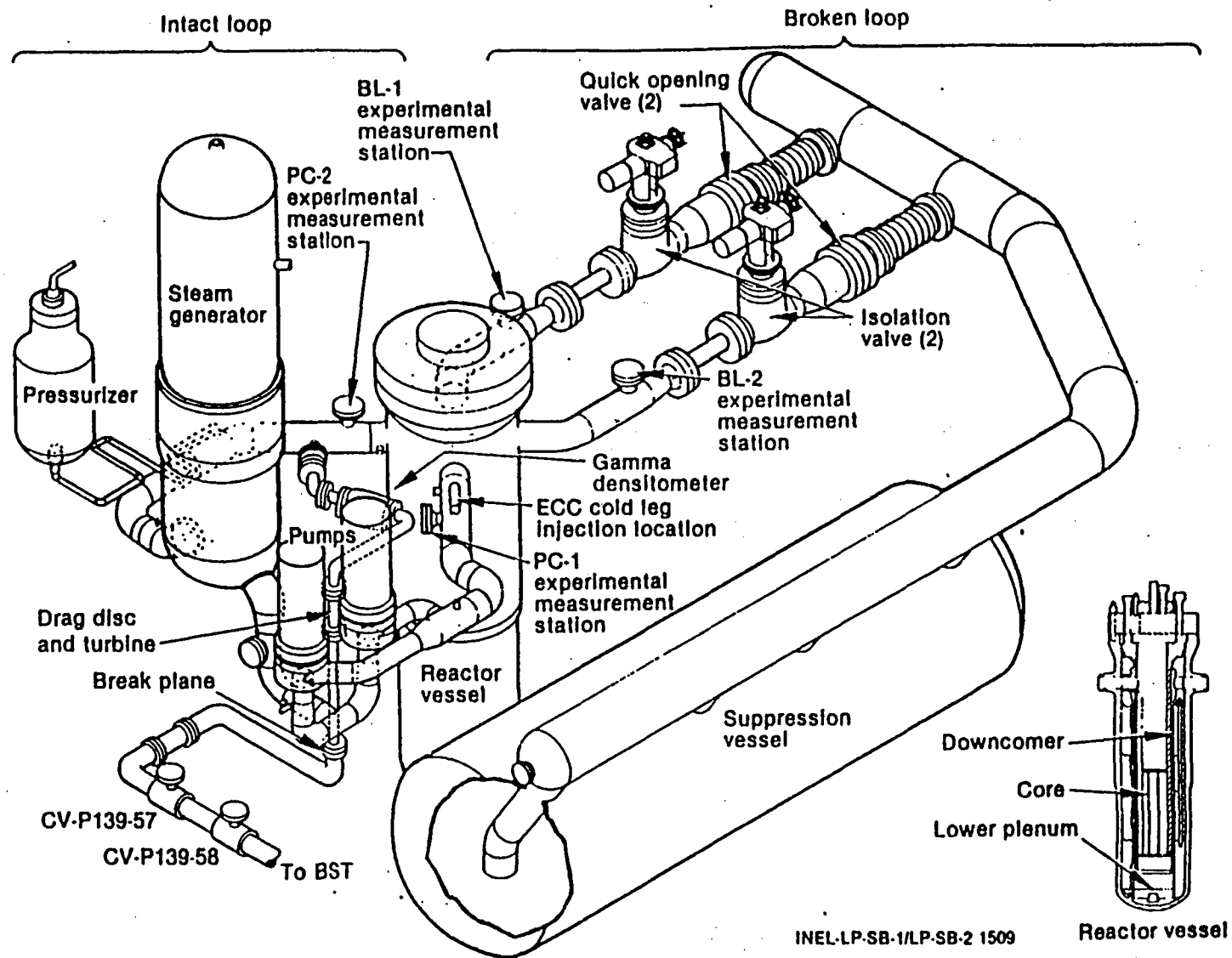
REFERENCES

- 1 READER, D L. "LOFT System and Test Description." NUREG/CR-0247, Tree-1208.
- 2 ALLEN, E J. Internal Document.
- 3 BIRCHLEY, J. Private Communication.
- 4 MODRO, S M et al. "Experiment Analysis and Summary Report on OECD LOFT Nuclear Experiments LP-SB-1 and LP-SB-2. OECD-LOFT-T-3205, May 1984.
- 5 LILES, R et al. "TRAC PF1/MOD1 and Advanced Best-Estimate Computer Program for Pressurised Water Reactor Thermal-Hydraulics Analysis". NUREG CR/3858, July 1986.
- 6 PELAYO, F. Internal Document
- 7 McPHERSON, G D. "Decay Heat Data for OECD LOFT Experiments". USDOE, October 1985.
- 8 ALEMBERTI, PROTO. "Experiment Analysis and Summary Report on OECD LOFT Nuclear Experiment LP-SB-3." December 1985, Draft (T-20000-XX-140-020).
- 9 ANODA, Y. "OECD LOFT Experiment LP-SB-1 and LP-SB-2 Calculation Comparison Report." July 1986, Draft. Japan Atomic Energy Research Institute.
- 10 POINTER, W. "Post-Test Calculation of the OECD LOFT Experiment LP-SB-2 with DRUFAN-02." OECD-LOFT-T-3307, December 1984.
- 11 TIEN-HU CHEN, SLAVOMIR, M MODRO. "Transient Two-Phase Performance of LOFT Reactor Coolant Pumps". ASME Winter Annual Meeting, 13-18 November, 1983. EGG-N1-21982,
- 12 WESTACOTT, J L, PETERSON, G E & CHEXAL, U K. "Retran 03 Analysis of LOFT Experiments LP-SB-1 and LP-SB-2." EPRI NP-4799 P Project 2420 Final Report, September 1986.
- 13 ANDERSON, J L & BENEDETTI, R L. "Critical Flow Through Small Pipe Breaks." EPRI NP-4532, Project 2299-2 Final Report, May 1986.

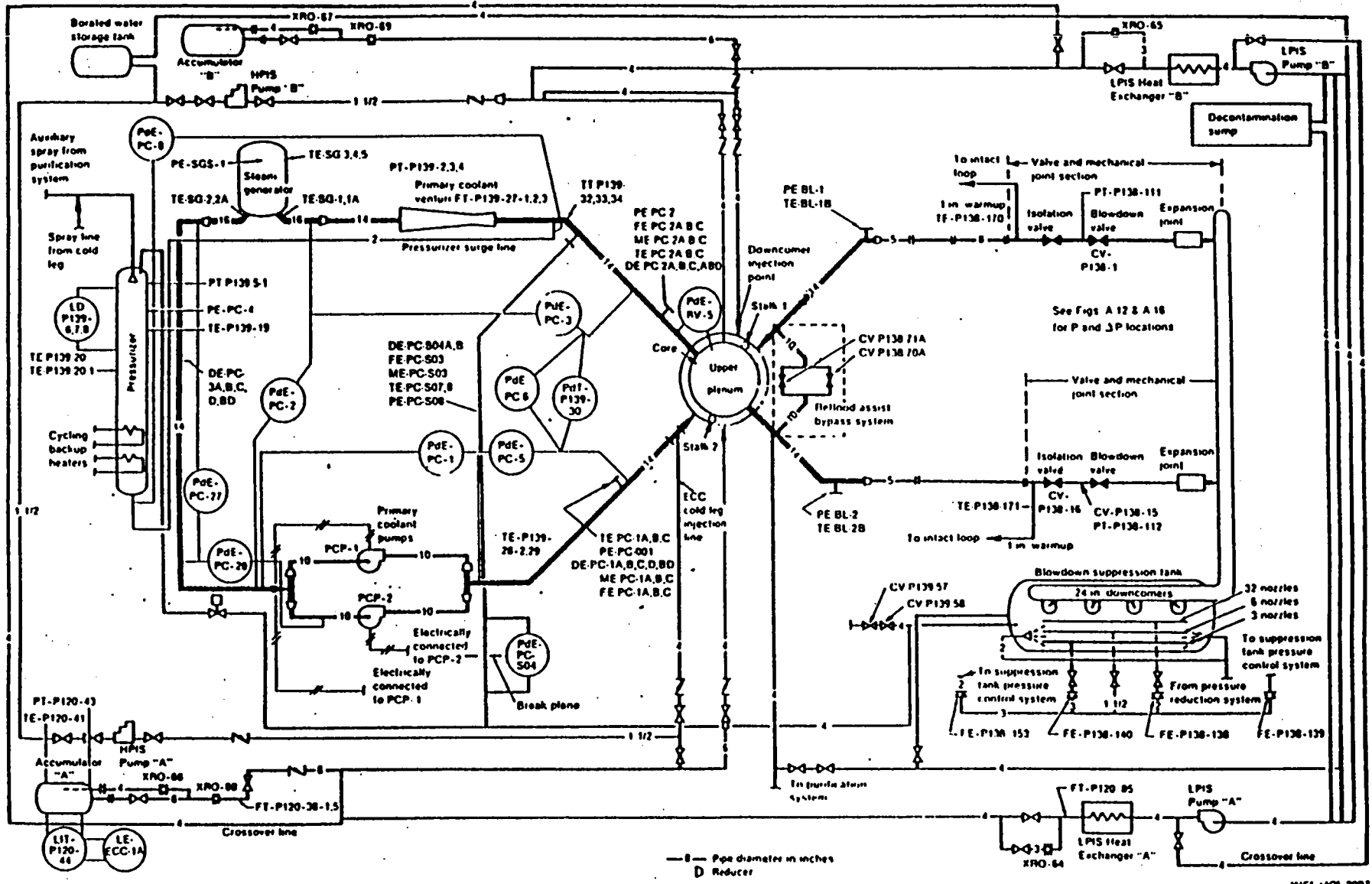
14. SCHROCK, V E. "Critical Flow Through a Small Pipe Break on a Large Pipe with Stratified Flow." Presented at the 13th Water Reactor Safety Meeting, Gaitersburg, October 1985.
- 15 RICHARDS, C. Internal Document.
- 16 Letter from Los Alamos, R Jenks to C G Richards, 14 January 1987.

FIGURES

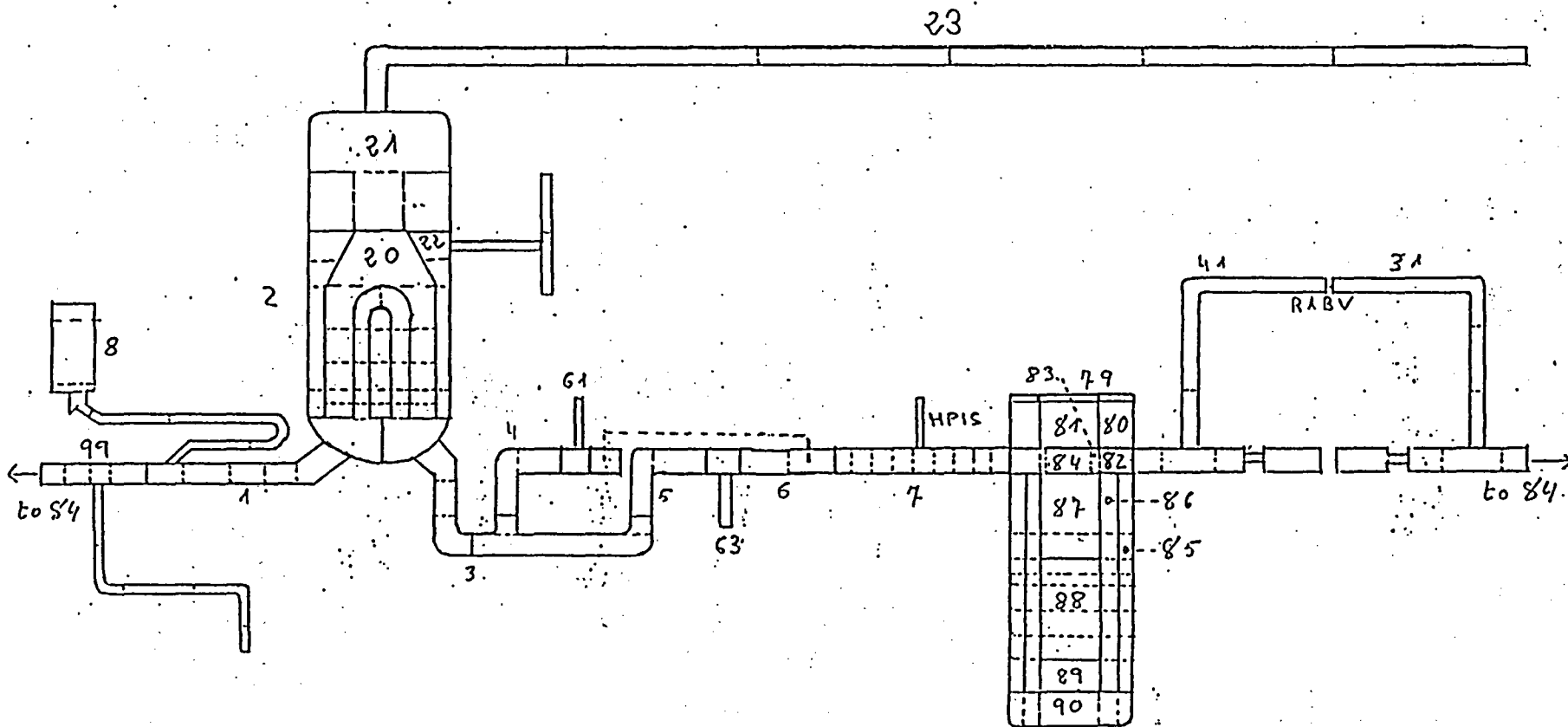




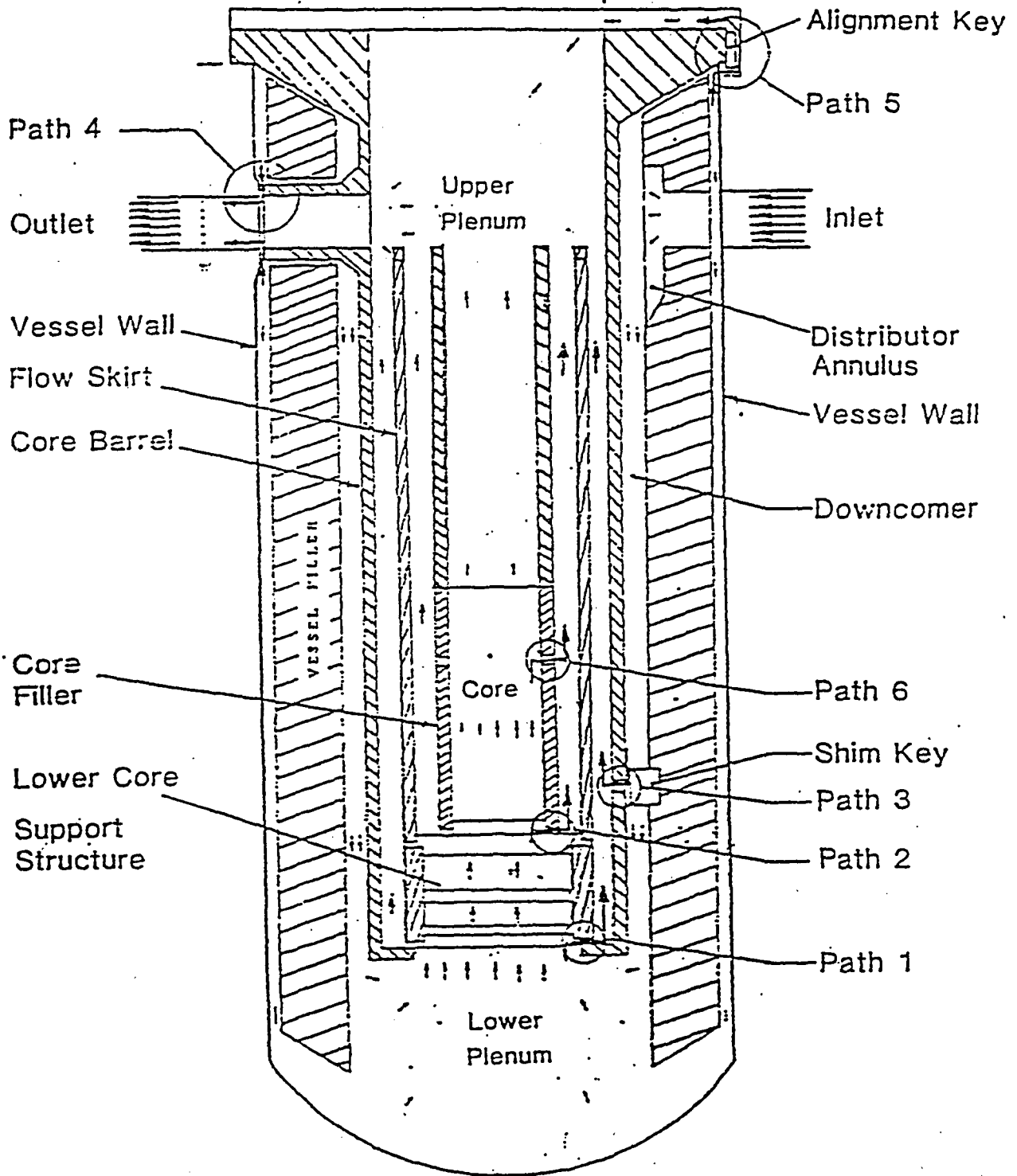
1 Axonometric projection of the LOFT system configuration for Experiments LP-SB-1 and LP-SB-2. From Reference 4

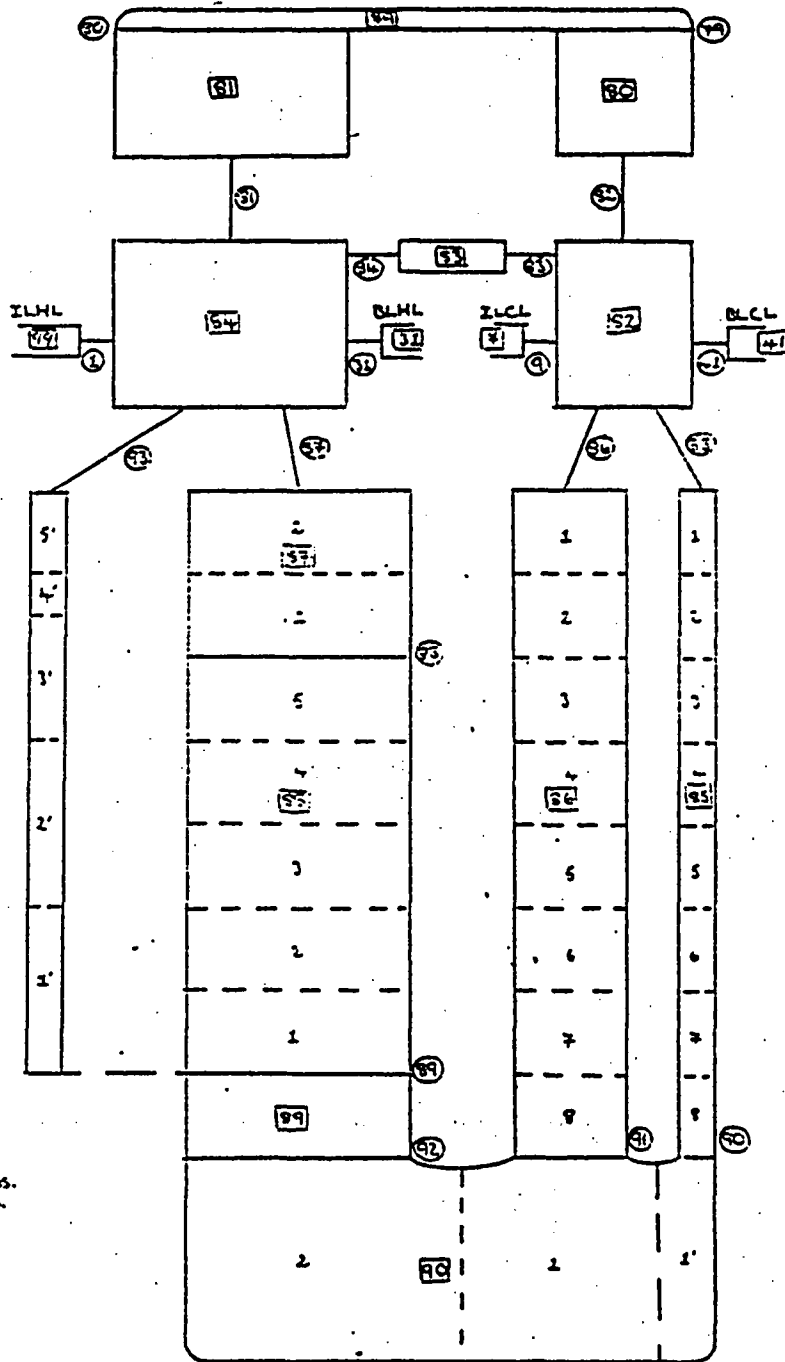


2 . LOFT piping schematic with instrumentation. From Reference 4



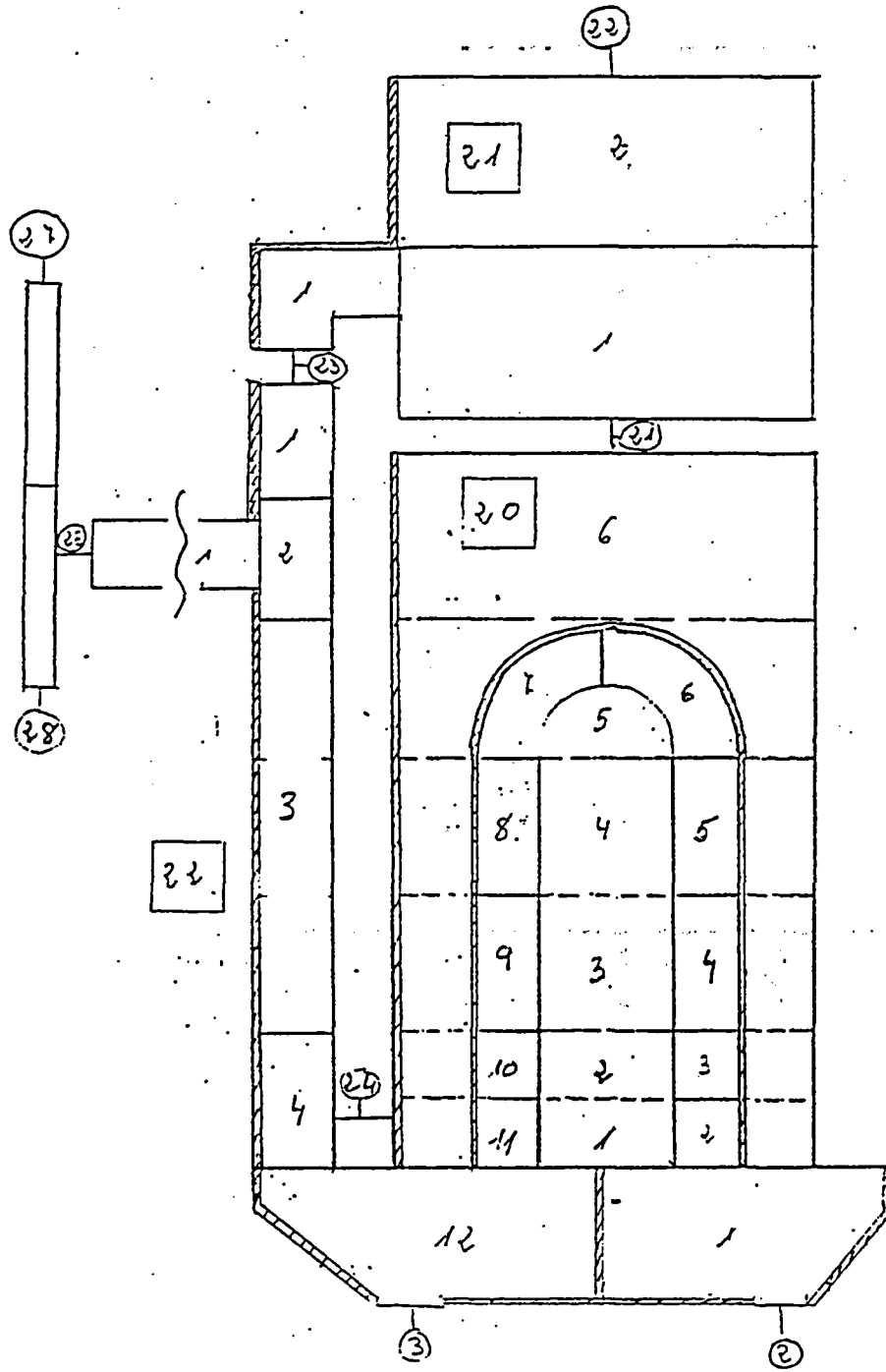
3 LOFT FACILITY NODING DIAGRAM





□ COMPONENT NOS.
○ JUNCTION NOS.

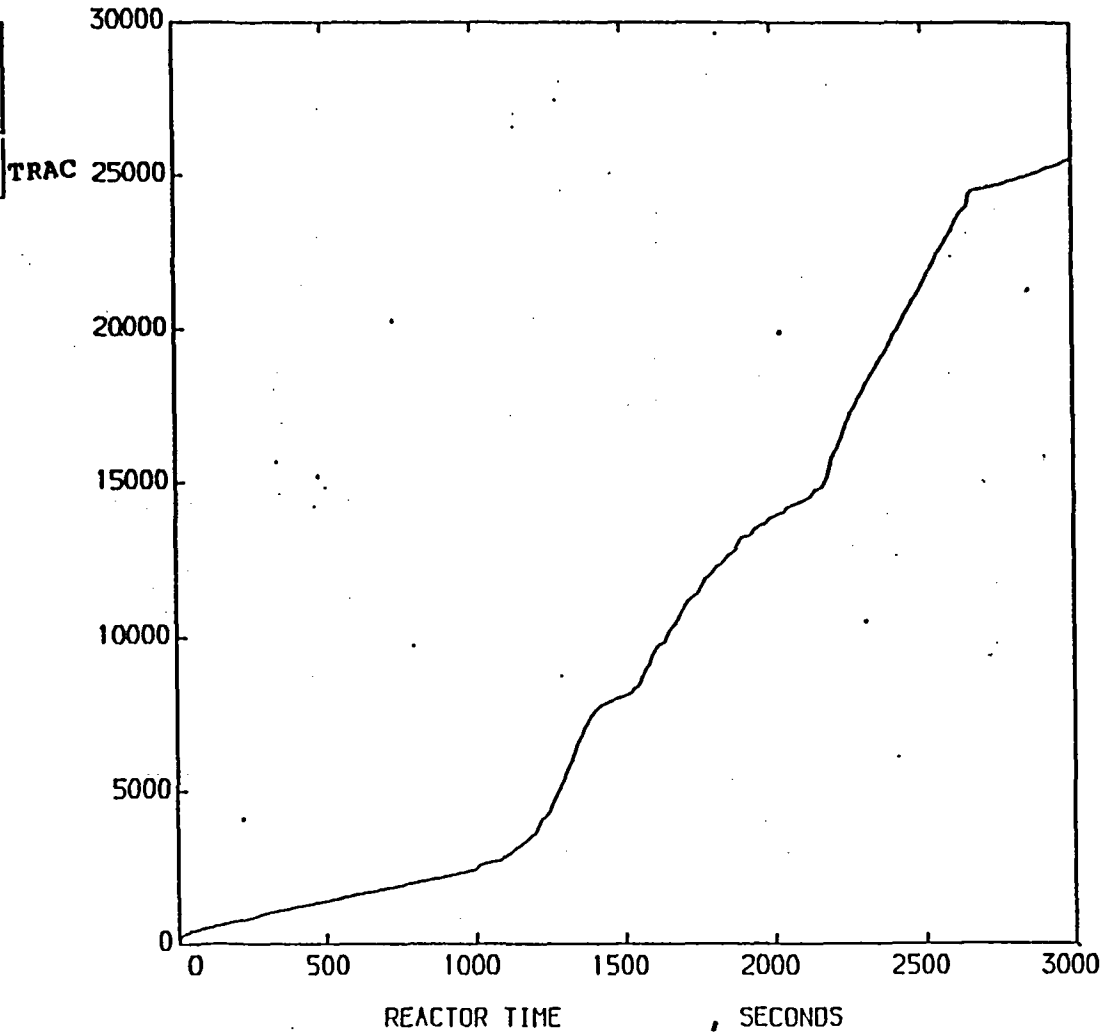
- | | | | |
|--------------|------------------------------|--------------|------------------------------|
| COMPONENT 79 | Bypass Path 5 | COMPONENT 85 | Downcomer Bypass |
| COMPONENT 80 | Upper Plenum (Downcomer) | COMPONENT 86 | Downcomer |
| COMPONENT 81 | Upper Plenum (Core) | COMPONENT 87 | Upper Stack Region |
| COMPONENT 82 | Plenum Component (Downcomer) | COMPONENT 88 | Core |
| COMPONENT 83 | Bypass Path 4 | COMPONENT 89 | Laser Plenum and Core Bypass |
| COMPONENT 84 | Plenum Component (Core) | COMPONENT 90 | Laser Plenum |



6 STEAM GENERATOR NODING

THE FOLLOWING ARE PLOTTED AGAINST REACTOR TIME
TOTAL TIME STEPS

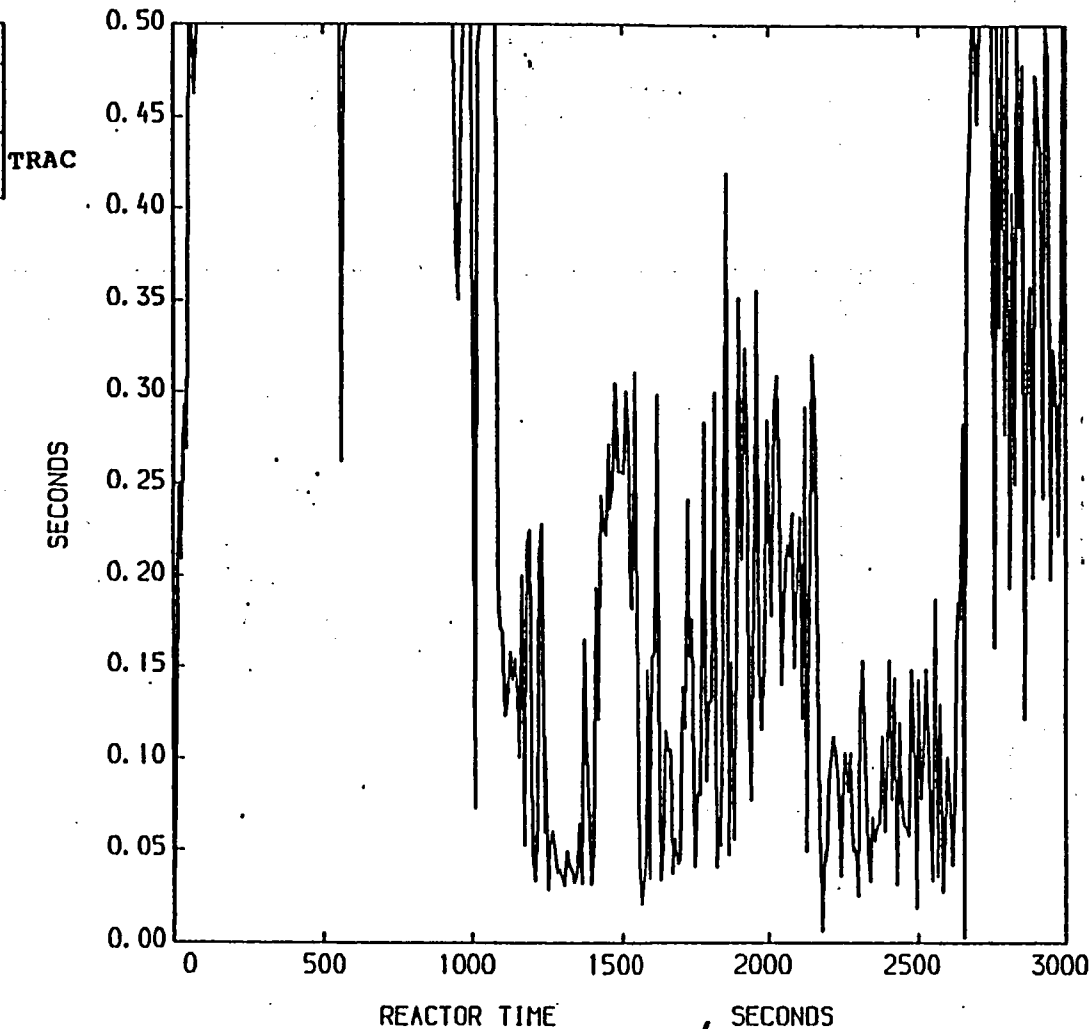
KEY		
SYM BOL	NAME	UNITS
—	TOTAL TIME STEPS	
LOC= 0/ 0/ 1	MINCH-STPT INF=1	TRAC



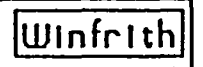
7 TOTAL TIME STEPS
LP-SB-2 - TRAC PF1-MOD1 AND EXPERIMENT COMPARISON

THE FOLLOWING ARE PLOTTED AGAINST REACTOR TIME
TIME STEP SIZE

KEY		
SYN BOL	NAME	UNITS
—	TIME STEP SIZE	SECONDS
LOC=	0/ 0/ 1	MNEM=STEP INF=1

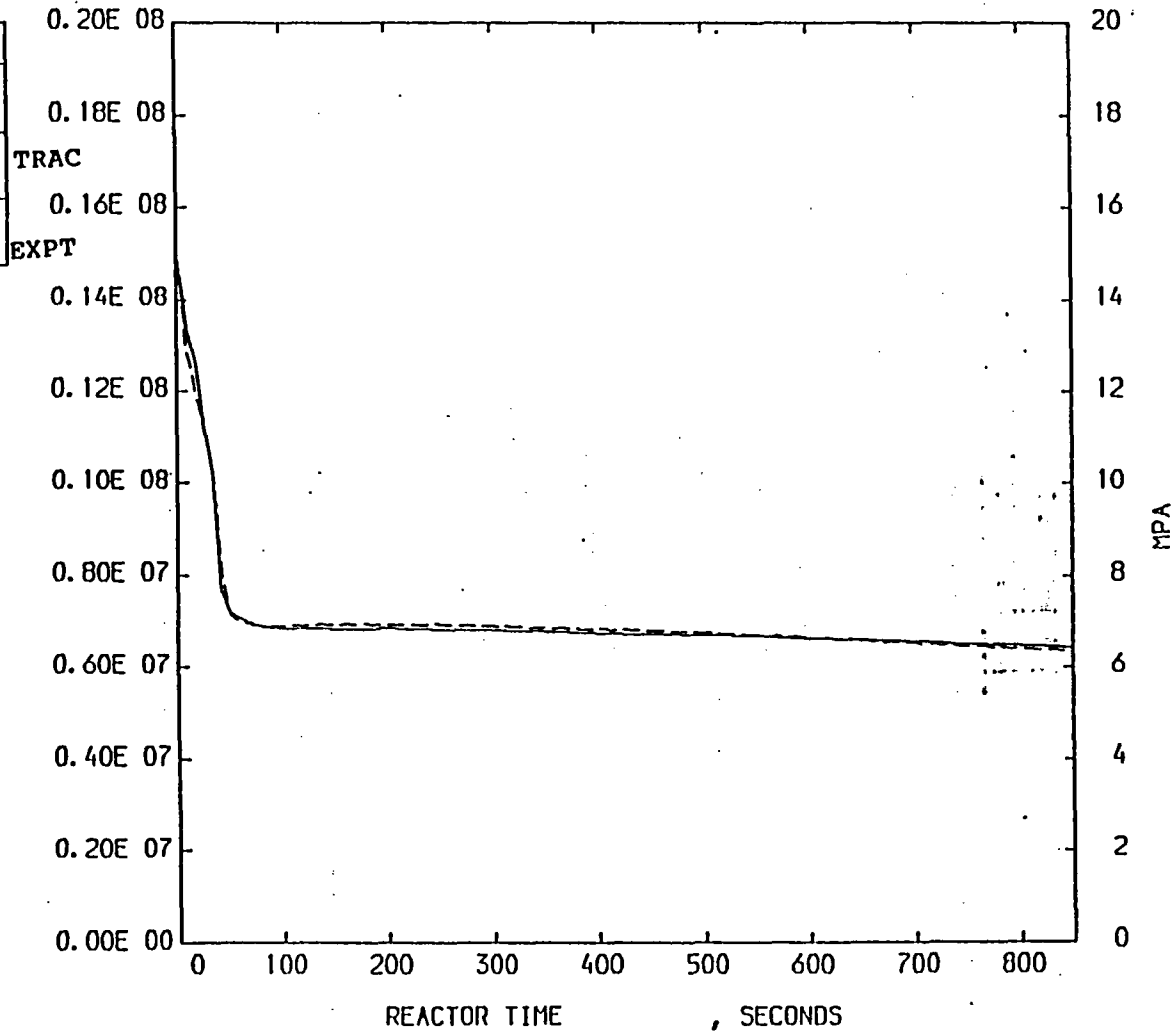


8 TIME-STEP SIZE
LP-SB-2 - TRAC PF1-MOD1 AND EXPERIMENT COMPARISON



THE FOLLOWING ARE PLOTTED AGAINST REACTOR TIME
 SIGNAL VAR. NO. 2, PE-PC-002

KEY		
SYM BOL	NAME	UNITS
—	SIGNAL VAR. NO. 2, LOC= 0/ 0/ 1 MNEM=S 2 INF=1	
---	PE-PC-002 LOC= 77/ 0/ 0 MNEM-PRES INF=2	,MPA



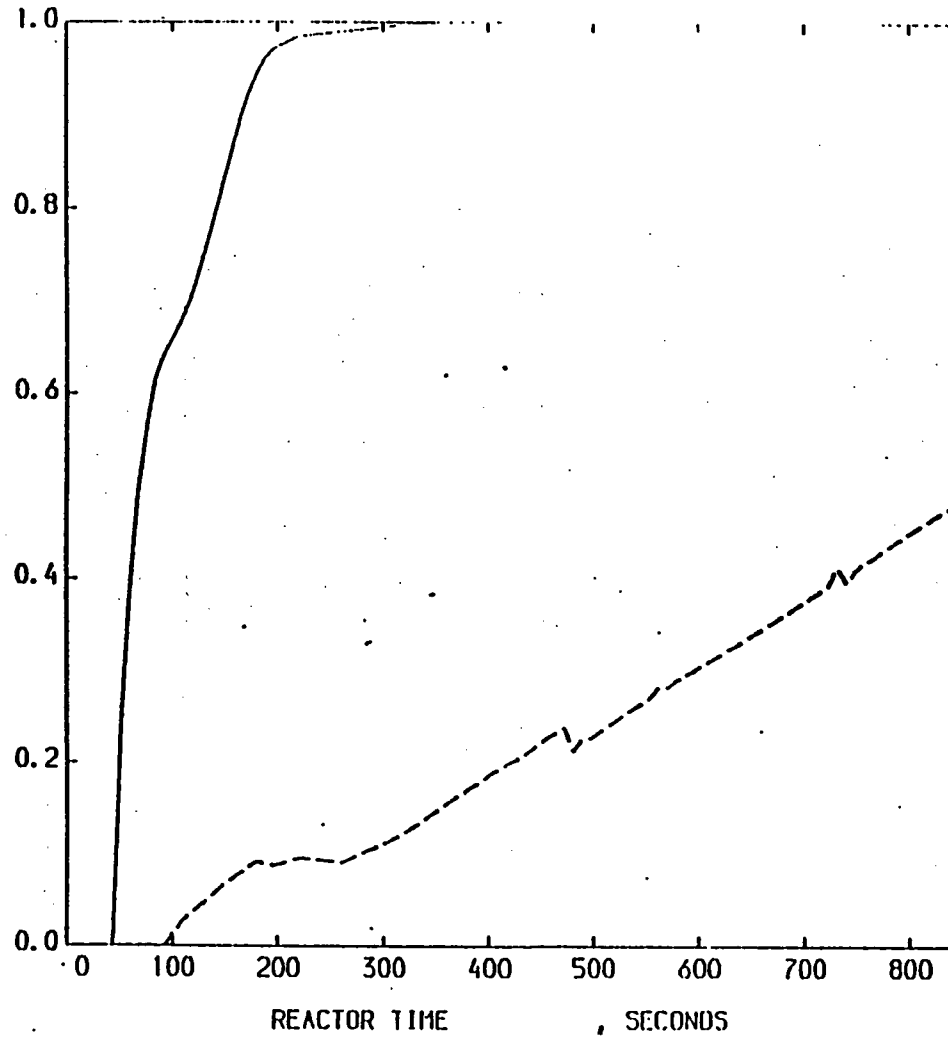
9 INTACT LOOP HOT LEG PRESSURE
 LP-SB-2 - TRAC PF1-MOD1 AND EXPERIMENT COMPARISON

Winfrith

THE FOLLOWING ARE PLOTTED AGAINST REACTOR TIME
 VAPOR FRACTION

KEY		
SYH BOX	NAME	UNITS
---	VAPOR FRACTION	
LOC= B1/ 0/ 1	HEM-VOID INF=1	TRAC
---	VAPOR FRACTION	
LOC= B4/ 0/ 1	HEM-VOID INF=1	

TRAC



Vessel upper plenum

Box before hot leg nozzles

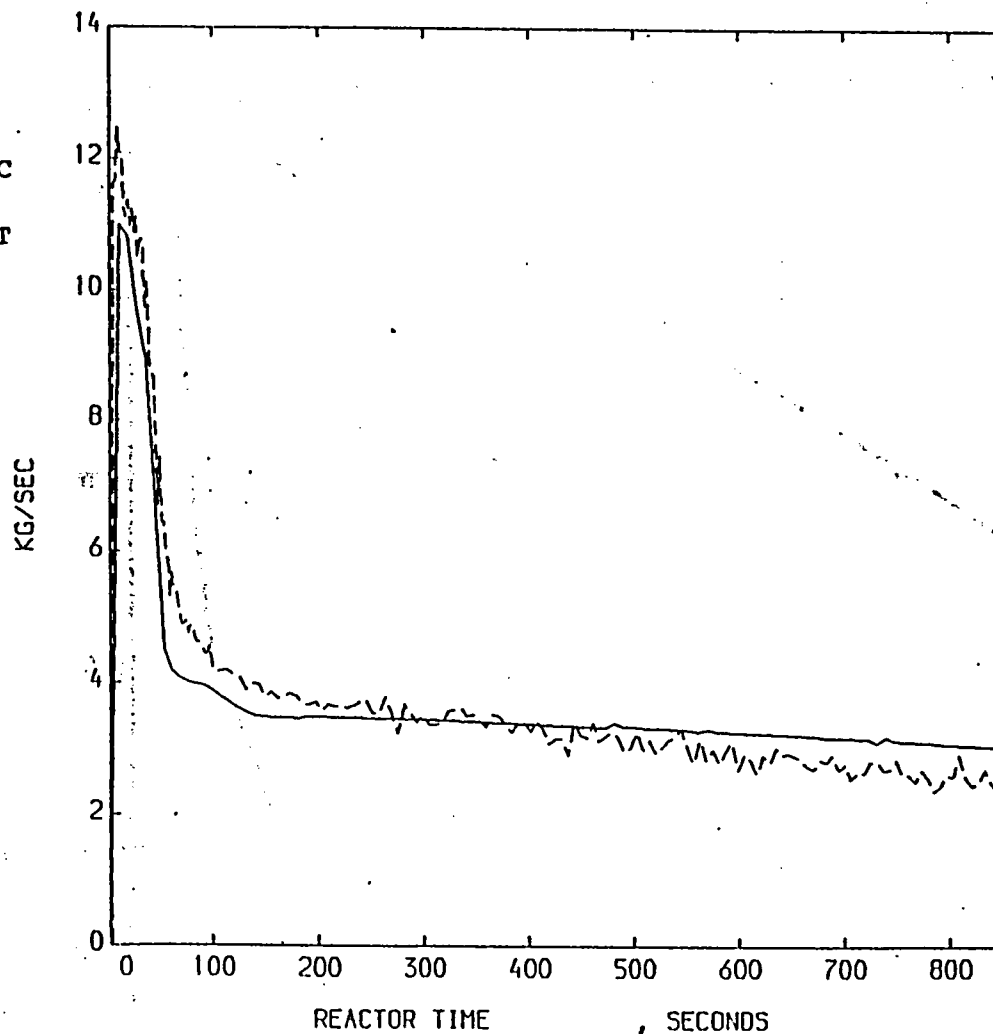
10 VOID FRACTION IN THE UPPER PLENUM AND BOX BEFORE HOT LEG NOZZLES
 LP-SB-2 - TRAC PF1-MOD1

THE FOLLOWING ARE PLOTTED AGAINST REACTOR TIME
 MASS FLOW RATE ,FR-PC-S03

KEY		
SYM BOL	NAME	UNITS
—	MASS FLOW RATE	,KG/SEC
LOC= 98/ 0/ 1	MNEM=FLOW INF=1	
---	FR-PC-S03	,KG/SEC
LOC= 23/ 0/ 0	MNEM=FLOW INF=2	

TRAC

EXPT

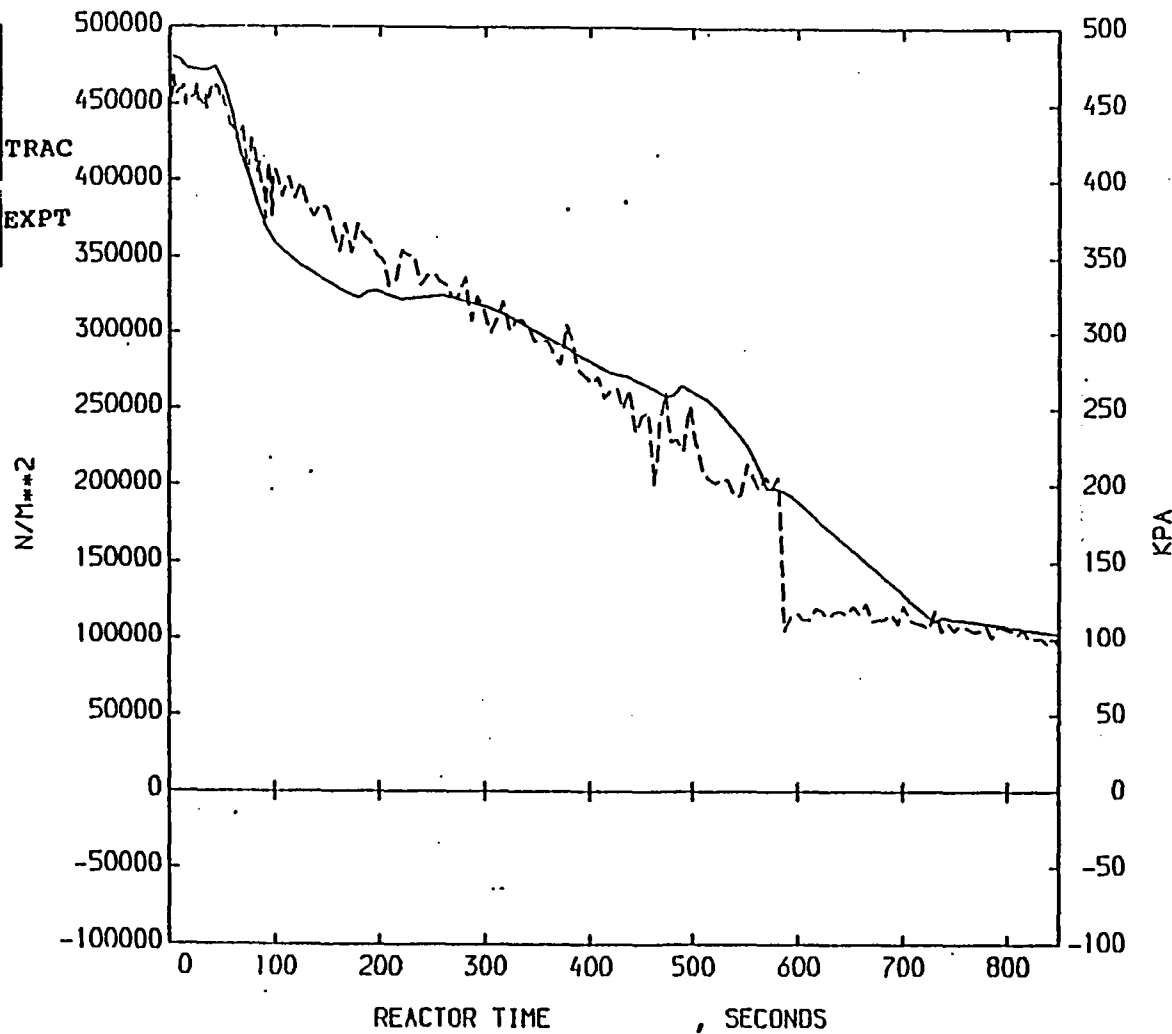


11 BREAK MASS FLOW RATE
 LP-SB-2 - TRAC PF1-MOD1 AND EXPERIMENT COMPARISON

Winfrith

THE FOLLOWING ARE PLOTTED AGAINST REACTOR TIME
 PUMP DELTA-P ,PDE-PC-001

KEY		
SYM BOL	NAME	UNITS
—	PUMP DELTA-P	N/M**2
LOC= 4/ 0/ 1	MNEM=DELP	INF=1
- - -	PDE-PC-001	KPA
LOC= 65/ 0/ 0	MNEM=PD	INF=2



12 PRESSURE DIFFERENCE OVER THE MAIN COOLANT PUMPS
 LP-SB-2 - TRAC PF1-MOD1 AND EXPERIMENT COMPARISON

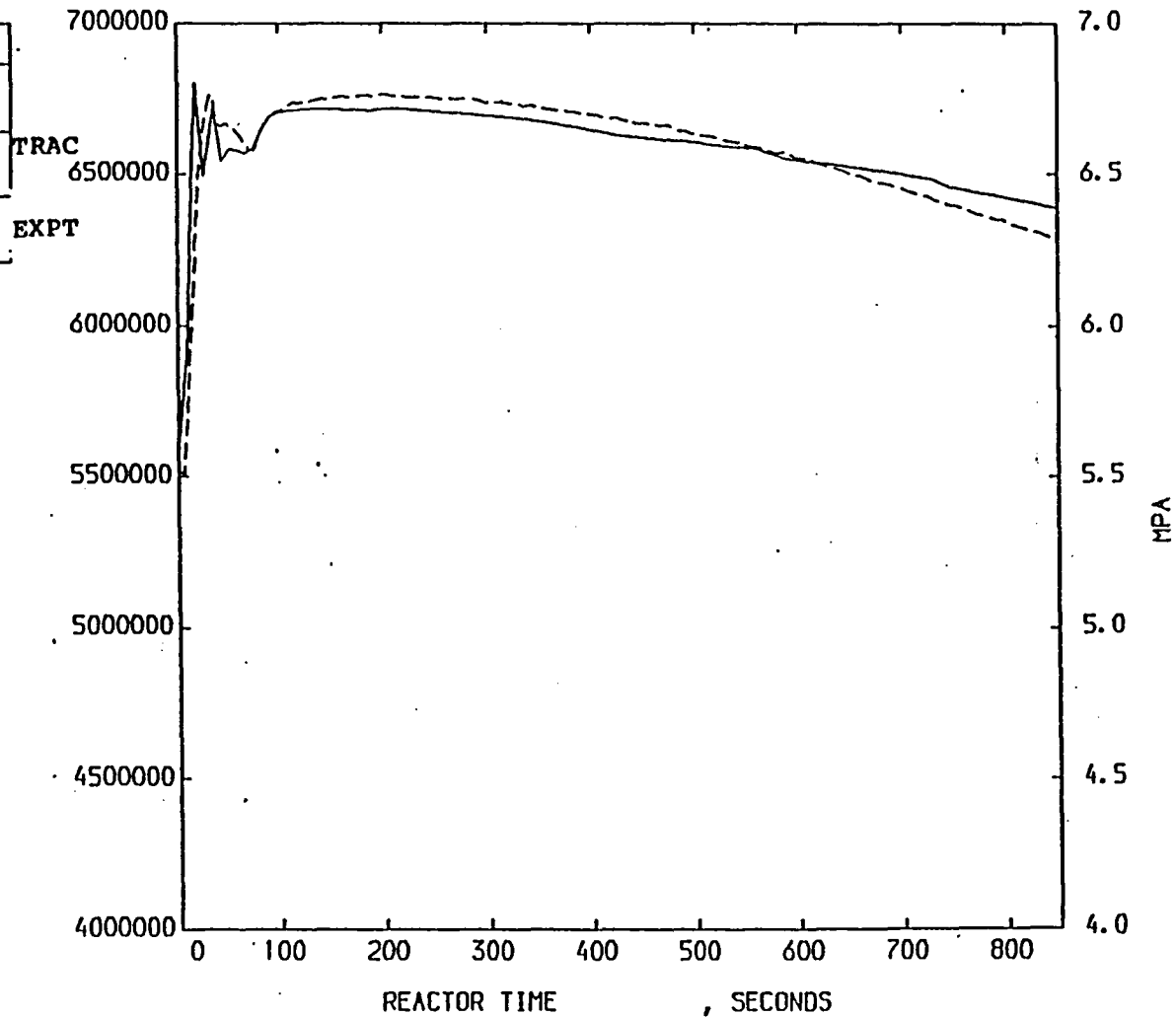
AEEW - R 2202

45

THE FOLLOWING ARE PLOTTED AGAINST REACTOR TIME
SIGNAL VAR. NO. 6, PT-P004-010A

Winfrith

KEY		
SYH BOL	NAME	UNITS
—	SIGNAL VAR. NO. 6,	
LOC= 0/ 0/ 1	MNEH=S 6 INF=1	
--	PT-P004-010A	,MPA
LOC= 86/ 0/ 0	MNEH=PRES INF=2	

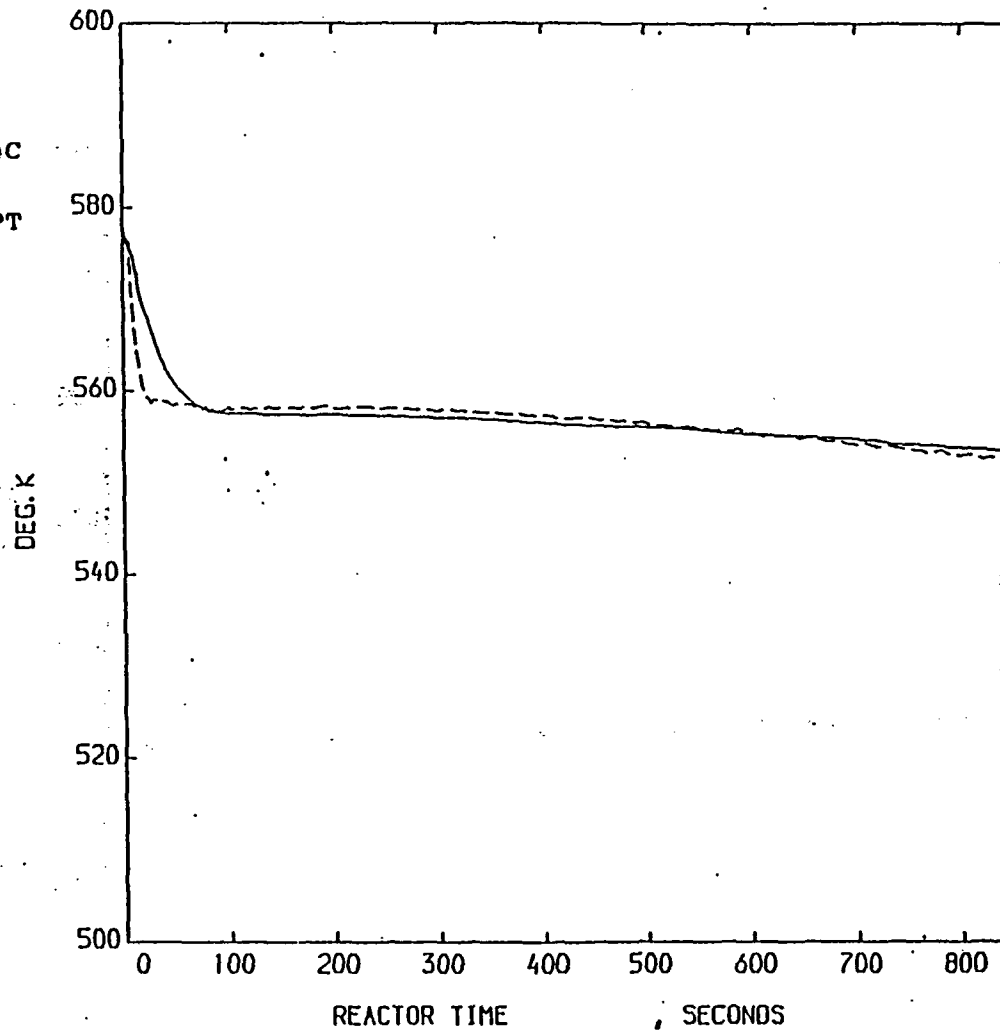


13 SECONDARY SIDE PRESSURE .
LP-SB-2 - TRAC PF1-MOD1 AND EXPERIMENT COMPARISON

THE FOLLOWING ARE PLOTTED AGAINST REACTOR TIME
LIQUID TEMPERATURE , TE-PC-002B

KEY		
SYM BOL	NAME	UNITS
—	LIQUID TEMPERATURE ,	DEG. K
LOC= 99/ 0/ 2	MNEM=TEML	INF=1
---	TE-PC-002B	, DEG. K
LOC= 130/ 0/ 0	MNEM=TMCL	INF=2

TRAC
EXPT



14

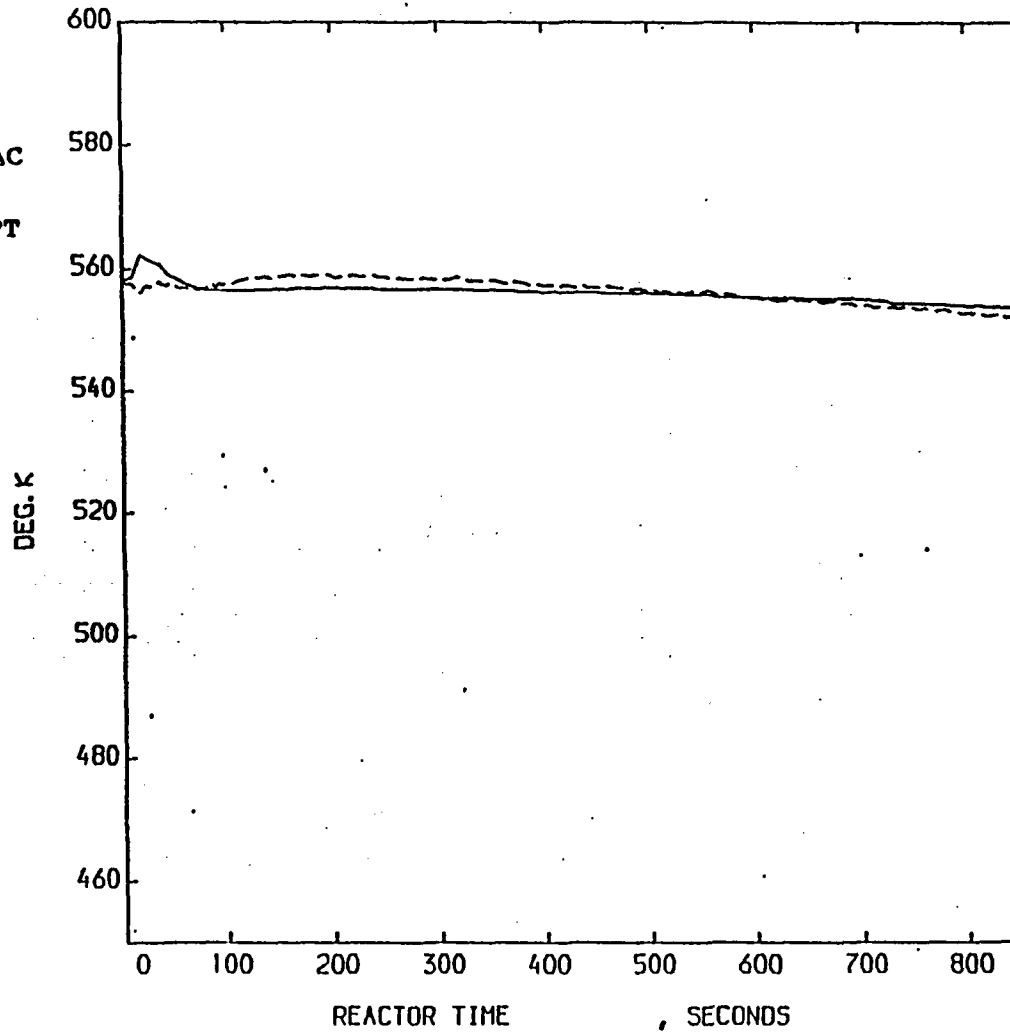
LIQ TEMPERATURE IN THE HOT LEG OF THE INTACT LOOP
LP-SB-2 - TRAC PF1-MOD1 AND EXPERIMENT COMPARISON

THE FOLLOWING ARE PLOTTED AGAINST REACTOR TIME
 LIQUID TEMPERATURE , TE-PC-001B

KEY		
SYN BOL	NAME	UNITS
---	LIQUID TEMPERATURE	, DEG. K
LOC= 7/ 0/ 4	MNEM=TEML	INF=1
---	TE-PC-001B	, DEG. K
LOC= 127/ 0/ 0	MNEM=THCL	INF=2

TRAC

EXPT

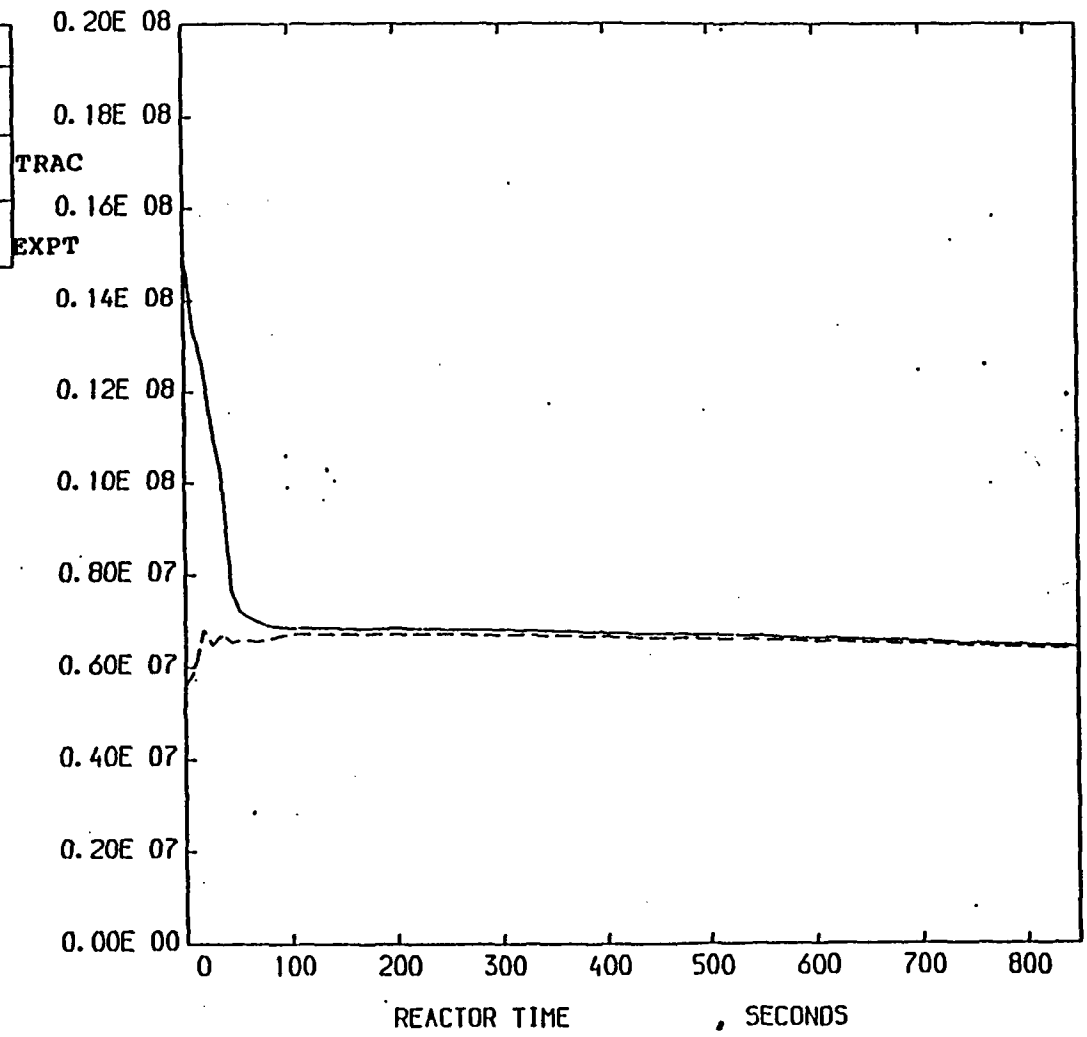


15 LIQ TEMPERATURE IN THE COLD LEG OF THE INTACT LOOP
 LP-SB-2 - TRAC PF1-MOD1 AND EXPERIMENT COMPARISON

Winfrith

THE FOLLOWING ARE PLOTTED AGAINST REACTOR TIME
 SIGNAL VAR. NO. 2, SIGNAL VAR. NO. 6

KEY		
SYMBOL	NAME	UNITS
—	SIGNAL VAR. NO. 2, LOC= 0/ 0/ 1 MNEM-S 2 INF=1	
- -	SIGNAL VAR. NO. 6, LOC= 0/ 0/ 1 MNEM-S 6 INF=1	



16 PRIMARY AND SECONDARY PRESSURES IN TRAC
 LP-SB-2 - TRAC PF1-MOD1 AND EXPERIMENT COMPARISON

Winfrith

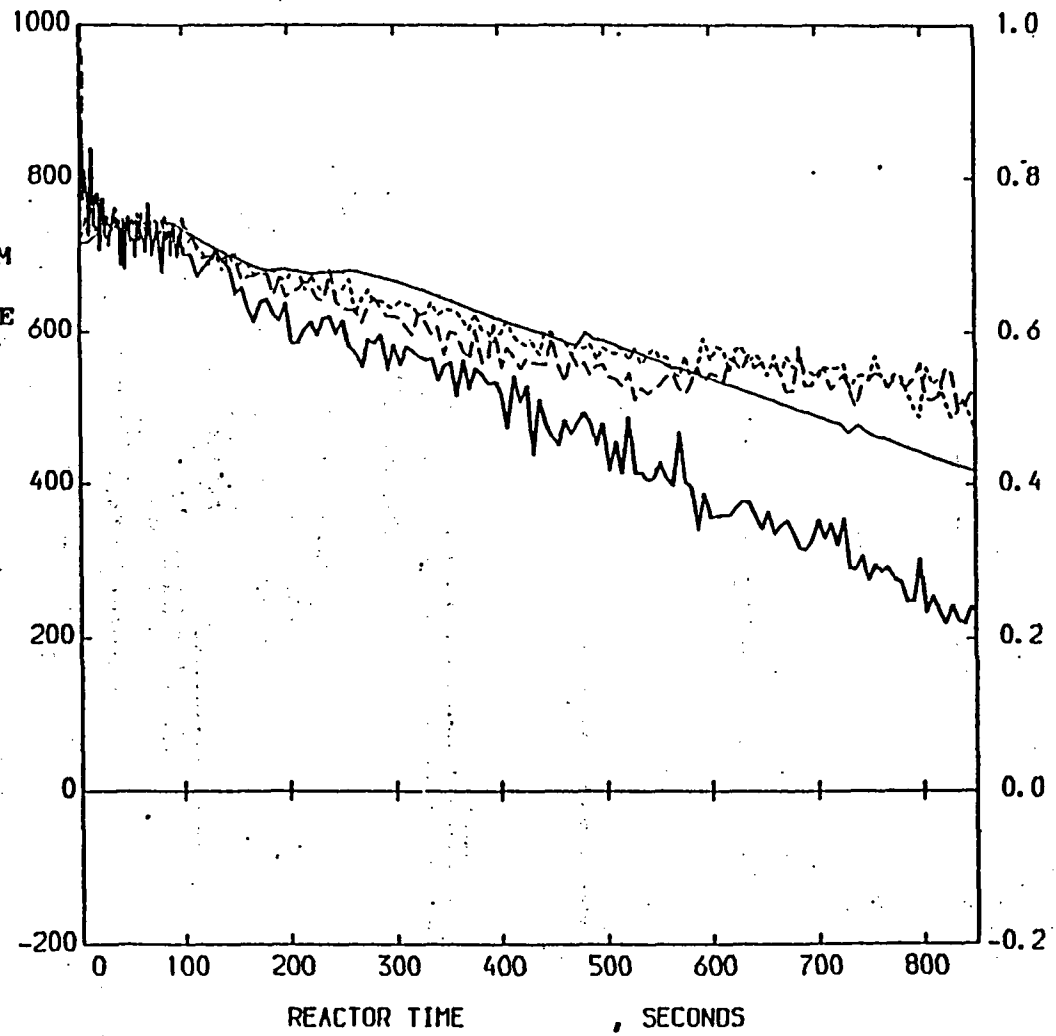
THE FOLLOWING ARE PLOTTED AGAINST REACTOR TIME

MIXTURE DENSITY , DE-PC-002A , DE-PC-002B
 DE-PC-002C

KEY		
SYM BOL	NAME	UNITS
—	MIXTURE DENSITY	,KG/M**3
LOC= 99/ 0/ 2	MNEM=DEHM INF=1	
- -	DE-PC-002A	,MG/M**3
LOC= 8/ 0/ 0	MNEM=DEHM INF=2	
- - - -	DE-PC-002B	,MG/M**3
LOC= 9/ 0/ 0	MNEM=DEHM INF=2	
—	DE-PC-002C	,MG/M**3
LOC= 10/ 0/ 0	MNEM=DEHM INF=2	

TRAC
 EXPT
 BOTTOM
 MIDDLE
 TOP

KG/M**3



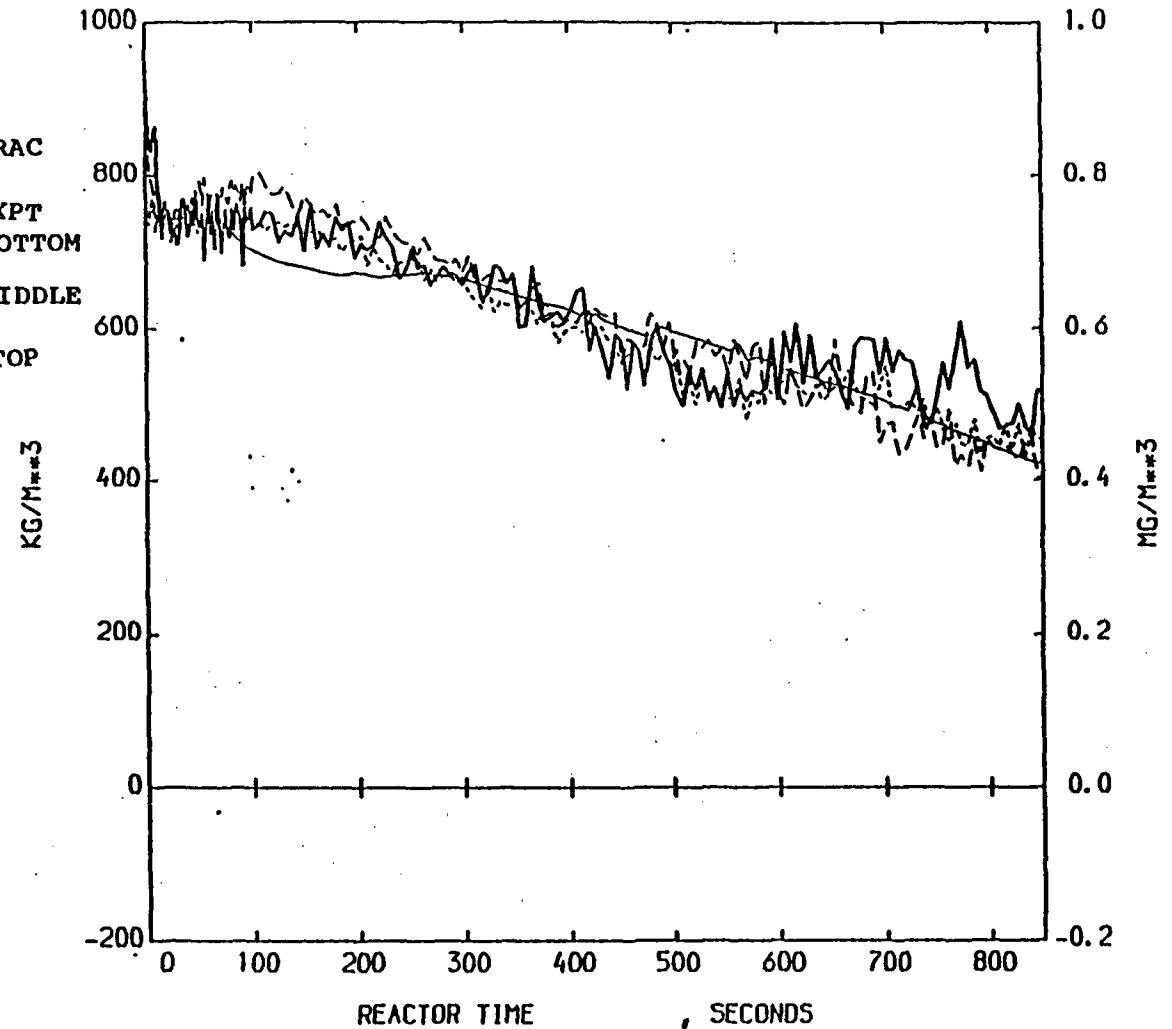
17 DENSITY IN THE HOT LEG INTACT LOOP
 LP-SB-2 - TRAC PF1-MOD1 AND EXPERIMENT COMPARISON

Winfrith

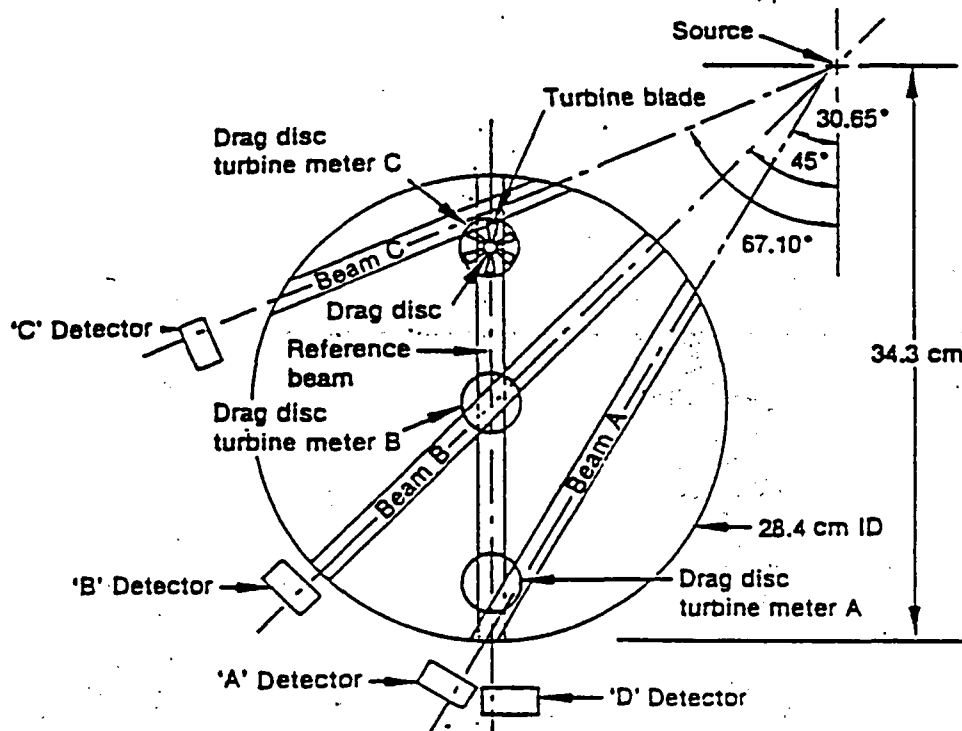
THE FOLLOWING ARE PLOTTED AGAINST REACTOR TIME
 MIXTURE DENSITY , DE-PC-001A , DE-PC-001B
 DE-PC-001C

KEY		
SYH BOL	NAME	UNITS
---	MIXTURE DENSITY	,KG/M**3
LOC= 7/ 0/ 4	MNEM=DEMI	INF=1
---	DE-PC-001A	,MG/M**3
LOC= 5/ 0/ 0	MNEM=DEMI	INF=2
----	DE-PC-001B	,MG/M**3
LOC= 6/ 0/ 0	MNEM=DEMI	INF=2
---	DE-PC-001C	,MG/M**3
LOC= 7/ 0/ 0	MNEM=DEMI	INF=2

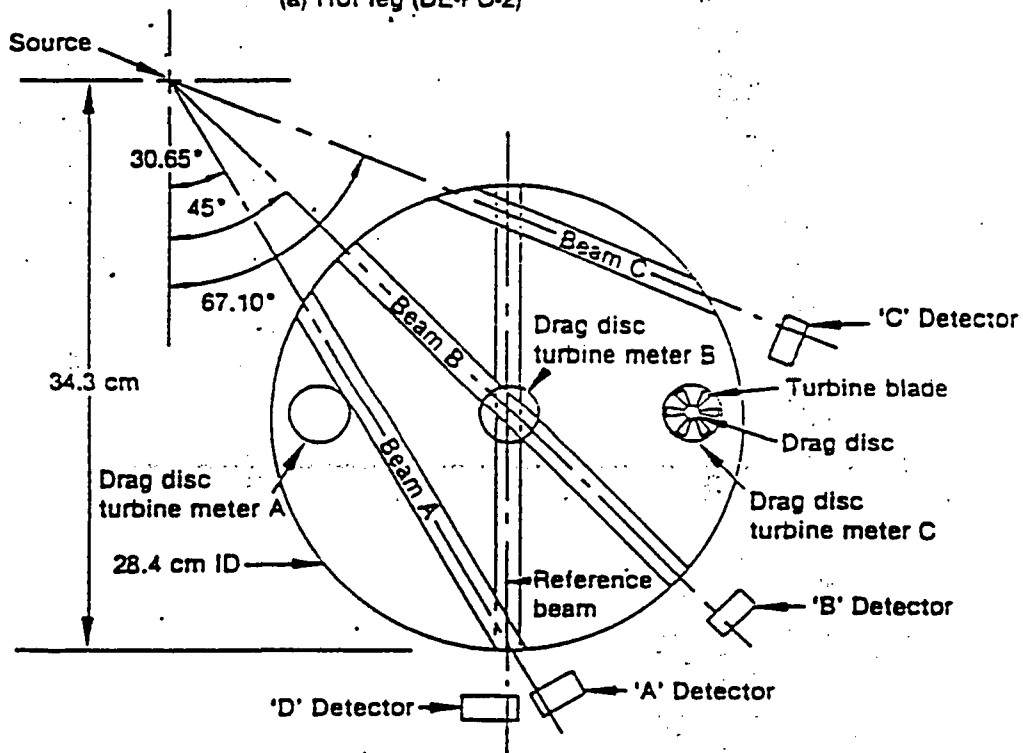
TRAC
 EXPT
 BOTTOM
 MIDDLE
 TOP



18 DENSITY IN THE COLD LEG OF THE INTACT LOOP
 LP-SB-2 - TRAC PF1-MOD1 AND EXPERIMENT COMPARISON



(a) Hot leg (DE-PC-2)



(b) Cold leg (DE-PC-1)

INEL 4 0039

19

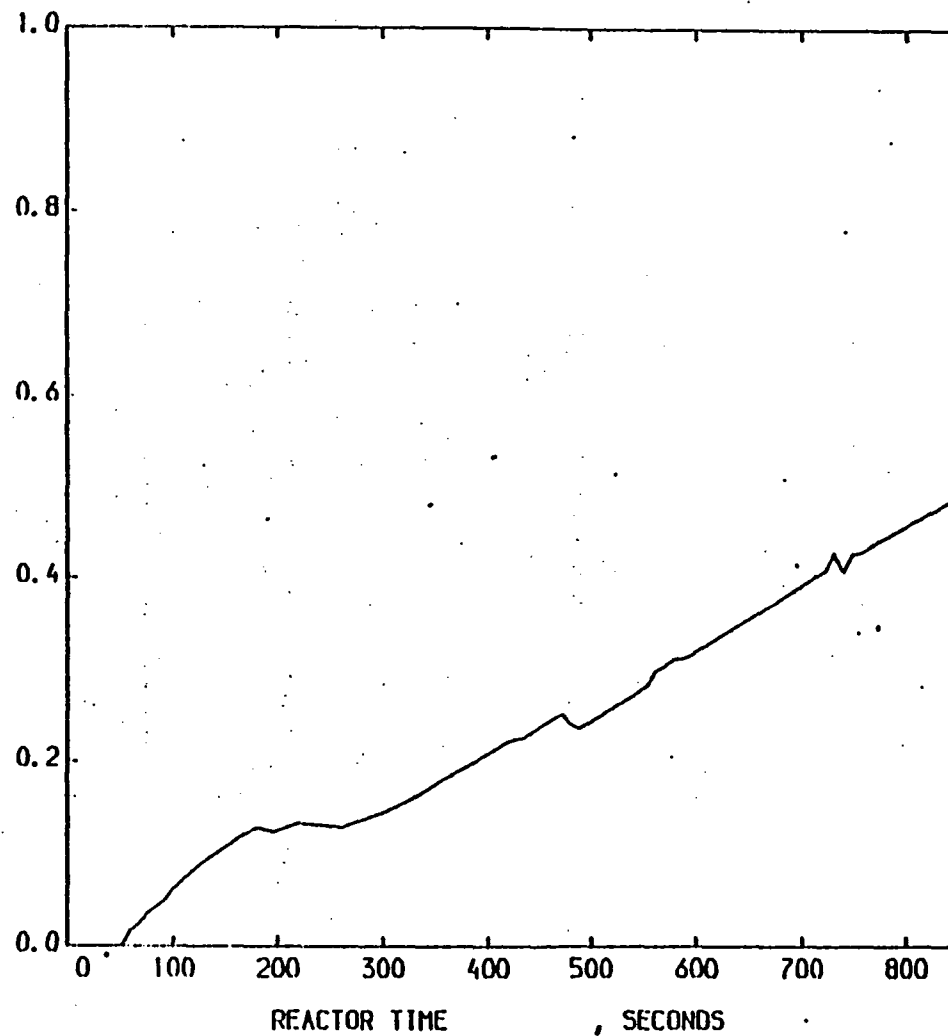
Relation of source and detectors to pipe for LOFT gamma densitometers and flowmeters in intact loop hot and cold legs. From Reference 4

Winfrith

THE FOLLOWING ARE PLOTTED AGAINST REACTOR TIME
 VAPOR FRACTION

KEY		
SYN	NAME	UNITS
60L		
— VAPOR FRACTION		
LOC= 2/ 0/ 7 INEN=VOID INF=1		

TRAC

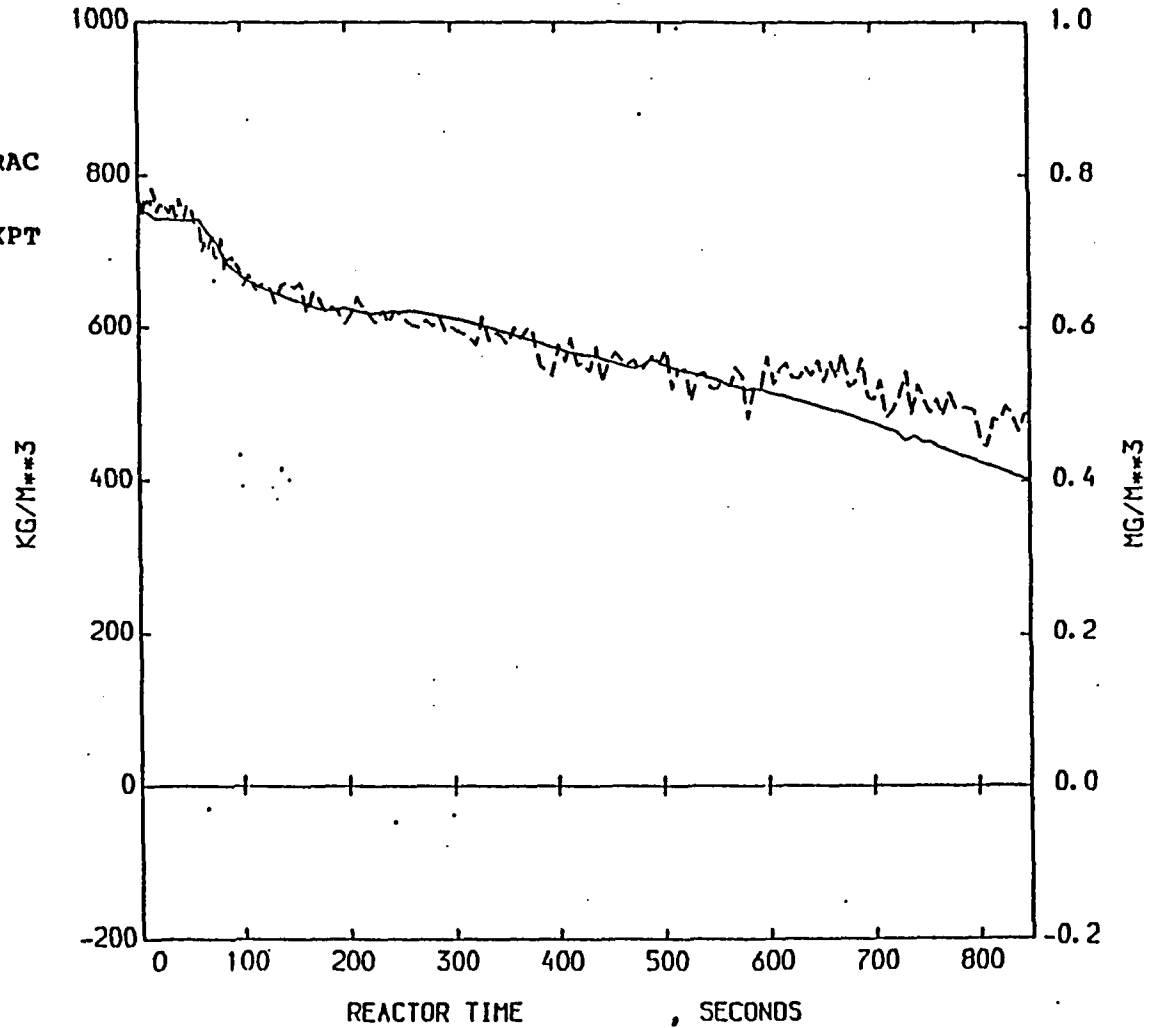


20 VOID FRACTION AT TOP OF U TUBES
 LP-SB-2 - TRAC PF1-MOD1

THE FOLLOWING ARE PLOTTED AGAINST REACTOR TIME.
 MIXTURE DENSITY , DE-PC-003B

KEY		
SYM BOL	NAME	UNITS
—	MIXTURE DENSITY	,KG/M**3
LOC= 3/ 0/ 5	MNEM=DEMI	INF=1
- - -	DE-PC-003B	,MG/M**3
LOC= 11/ 0/ 0	MNEM=DEMI	INF=2

TRAC
 EXPT



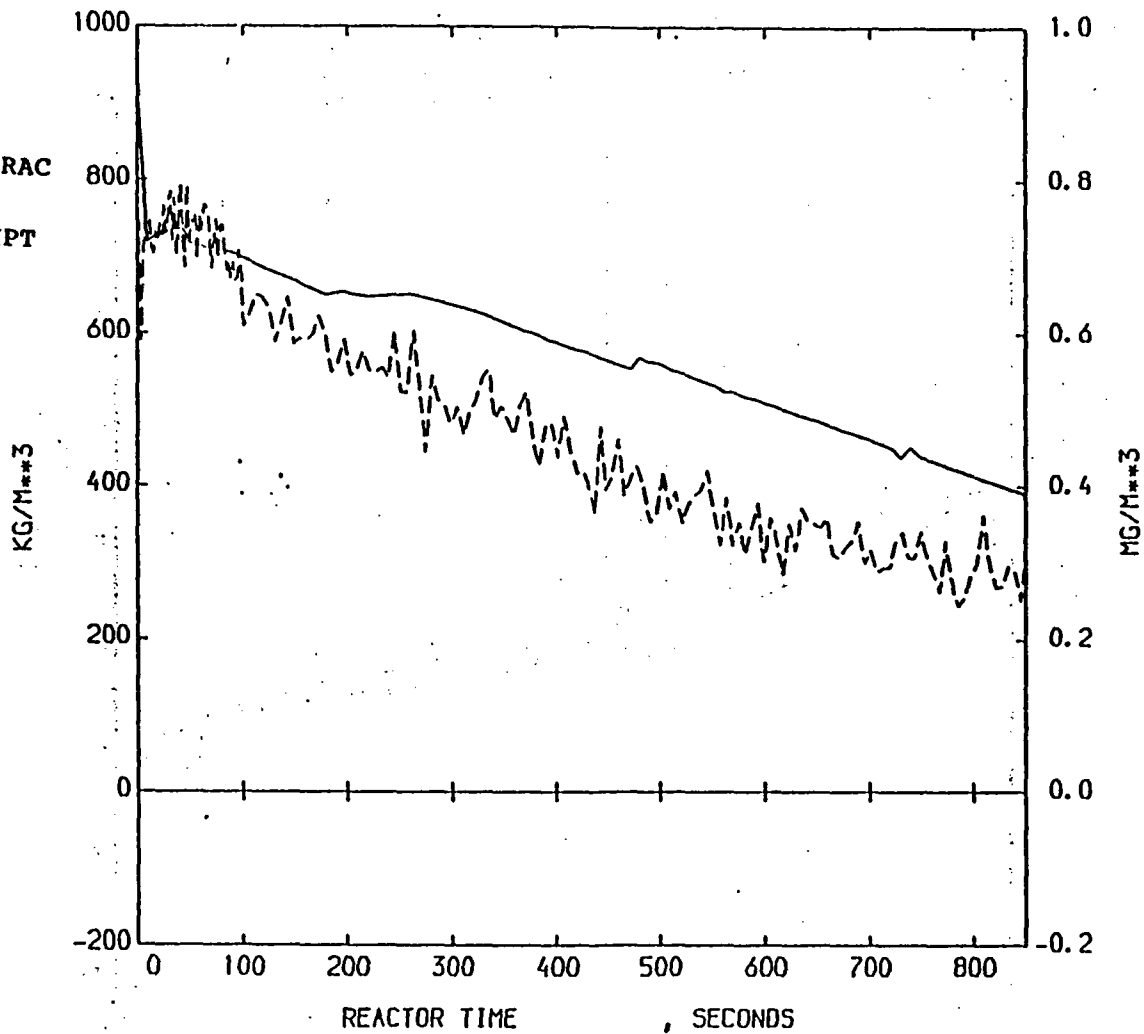
21 LOOP SEAL DENSITY
 LP-SB-2 - TRAC PF1-MOD1 AND EXPERIMENT COMPARISON

Winfrith

THE FOLLOWING ARE PLOTTED AGAINST REACTOR TIME
MIXTURE DENSITY ,DE-PC-S04B

KEY		
SYN BOL	NAME	UNITS
---	MIXTURE DENSITY	,KG/M**3
LOC= 99/ 0/ 8	HNEM-DENN INF=1	
---	DE-PC-S04B	,MG/M**3
LOC= 4/ 0/ 0	HNEM-DENN INF=2	

TRAC
EXPT

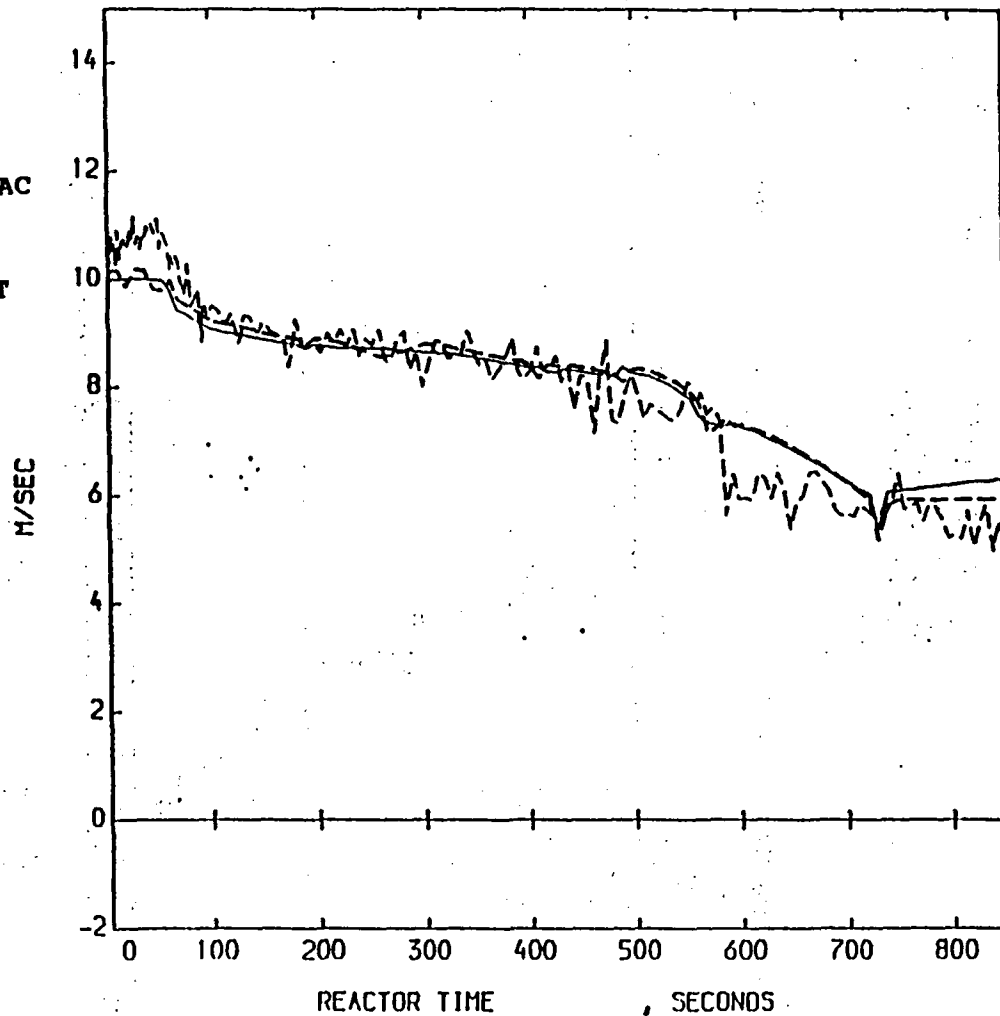


22 DENSITY IN THE BREAK LINE
LP-SB-2 - TRAC PF1-MOD1 AND EXPERIMENT COMPARISON

THE FOLLOWING ARE PLOTTED AGAINST REACTOR TIME
 LIQUID VELOCITY , VAPOR VELOCITY , FE-PC-001C

KEY		
SYN BOL	NAME	UNITS
—	LIQUID VELOCITY	,M/SEC
LOC= 7/ 0/ 4	MNEM=VLID	INF=1
- -	VAPOR VELOCITY	,M/SEC
LOC= 7/ 0/ 4	MNEM=VVAP	INF=1
- -	FE-PC-001C	,M/SEC
LOC= 15/ 0/ 0	MNEM=FE	INF=2

TRAC
 EXPT

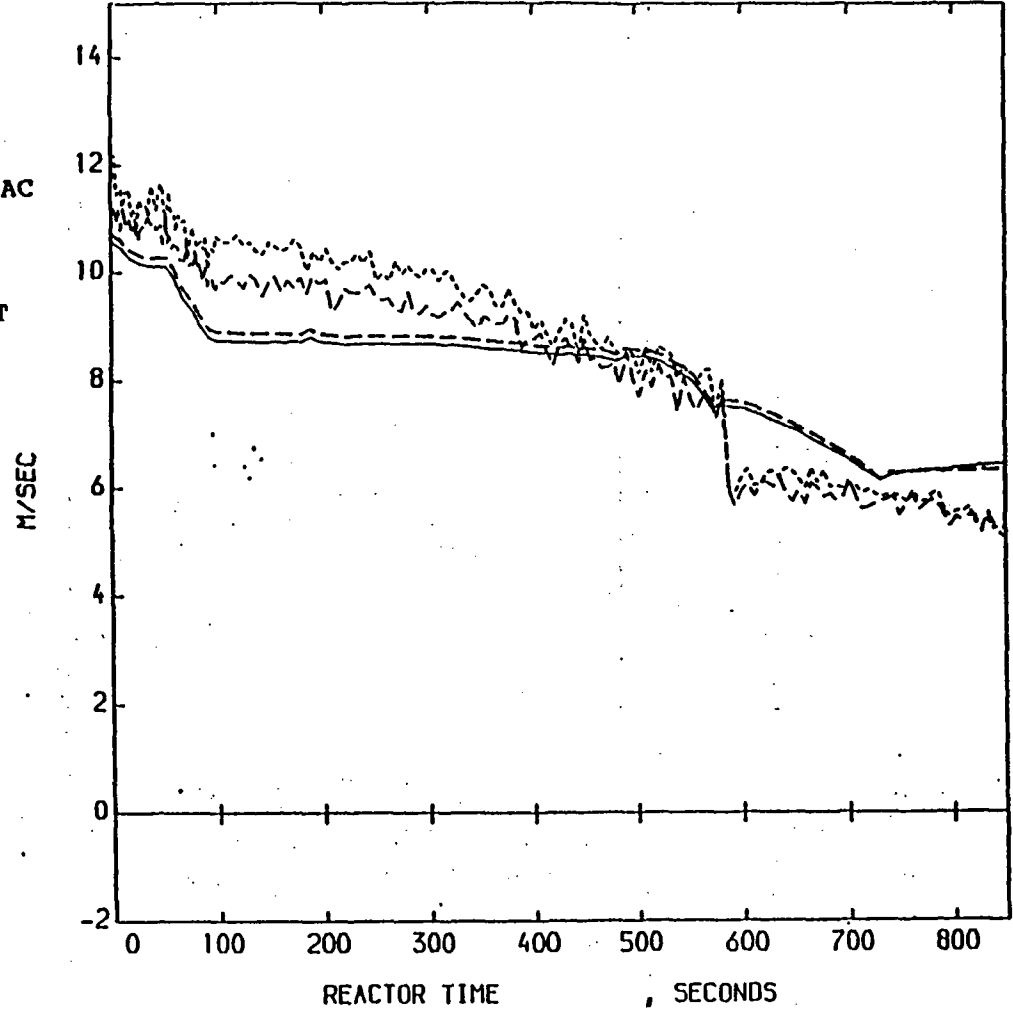


23 LIQ AND VAP VELOCITY IN THE COLD LEG
 LP-SB-2 - TRAC PF1-MOD1 AND EXPERIMENT COMPARISON

THE FOLLOWING ARE PLOTTED AGAINST REACTOR TIME
 LIQUID VELOCITY , VAPOR VELOCITY , FE-PC-002A
 FE-PC-002C

KEY		
SYN BOL	NAME	UNITS
—	LIQUID VELOCITY	,H/SEC
LOC= 99/ 0/ 2	MNEM=VLIQ	INF=1
--	VAPOR VELOCITY	,H/SEC
LOC= 99/ 0/ 2	MNEM=VAP	INF=1
---	FE-PC-002A	,H/SEC
LOC= 16/ 0/ 0	MNEM=FE	INF=2
----	FE-PC-002C	,H/SEC
LOC= 17/ 0/ 0	MNEM=FE	INF=2

TRAC
 EXPT



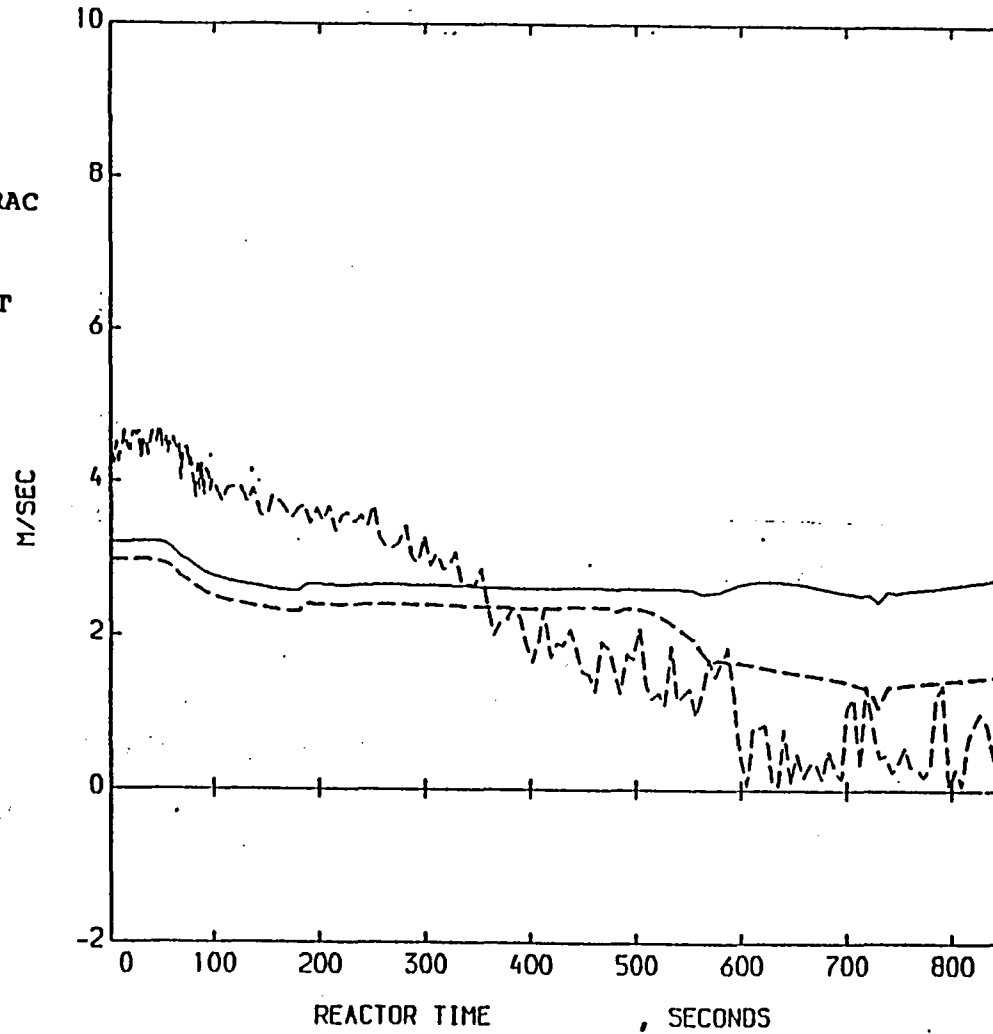
24 LIQ AND VAP VELOCITY IN THE HOT LEG
 LP-SB-2 - TRAC PF1-MOD1 AND EXPERIMENT COMPARISON

THE FOLLOWING ARE PLOTTED AGAINST REACTOR TIME
 LIQUID VELOCITY , VAPOR VELOCITY , FE-1ST-001

KEY		
SYN BOL	NAME	UNITS
—	LIQUID VELOCITY	,M/SEC
LOC= 86/ 0/ 8	MNEH=VLIO	INF=1
--	VAPOR VELOCITY	,M/SEC
LOC= 86/ 0/ 8	MNEH=VVAP	INF=1
--	FE-1ST-001	,M/SEC
LOC= 18/ 0/ 0	MNEH=FE	INF=2

TRAC

EXPT

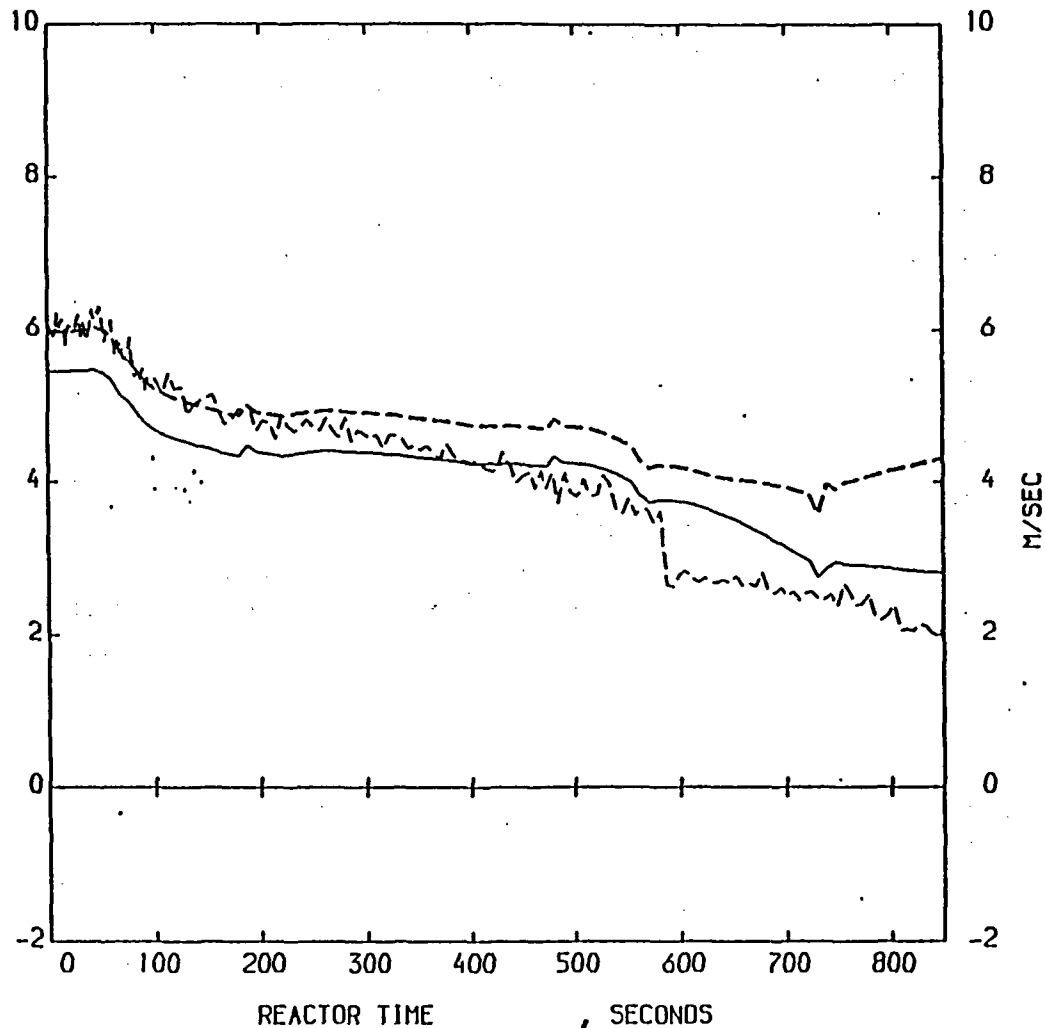


25 LIQ AND VAP VELOCITY IN THE DOWNCOMER OF THE REACTOR VESSEL
 LP-SB-2 - TRAC PF1-MOD1 AND EXPERIMENT COMPARISON

THE FOLLOWING ARE PLOTTED AGAINST REACTOR TIME
 FUNCTION FE-SLP-001

KEY		
SYMBOL	NAME	UNITS
—	FUNCTION VLIO'	
- - -	FUNCTION VVAP	
- - -	FE-SLP-001	M/SEC
LOC= 20/ 0/ 0	MNEM=FE	INF=2

TRAC
 EXPT

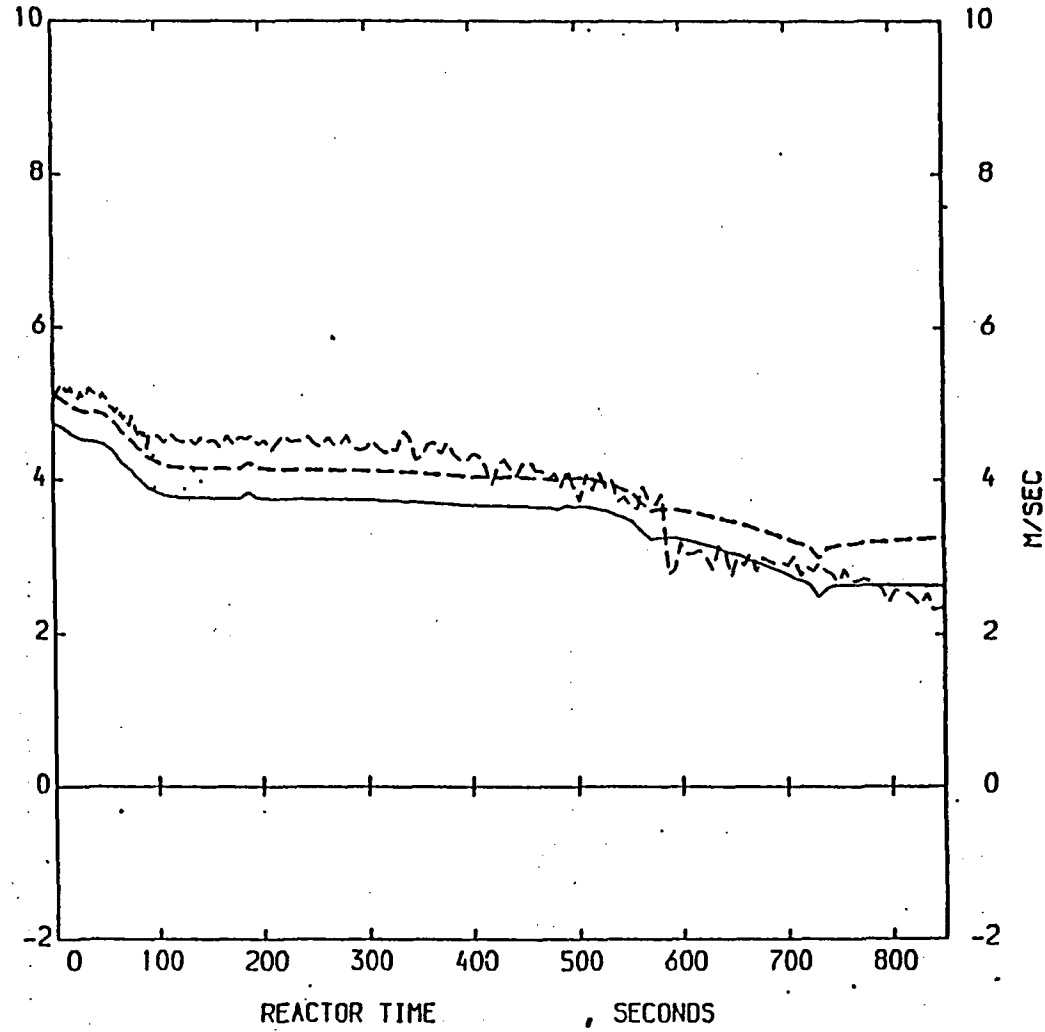


26 LIQ AND VAP VELOCITY AT CORE INLET
 LP-SB-2 - TRAC PF1-MOD1 AND EXPERIMENT COMPARISON

THE FOLLOWING ARE PLOTTED AGAINST REACTOR TIME
 FUNCTION ,FE-SUP-001

KEY		
SYN BOL	NAME	UNITS
—	FUNCTION VLIO	
- - -	FUNCTION VVAP	
- - -	FE-SUP-001	M/SEC
LOC= 22/ 0/ 0	MNEM=FE	INF=2

TRAC
 EXPT



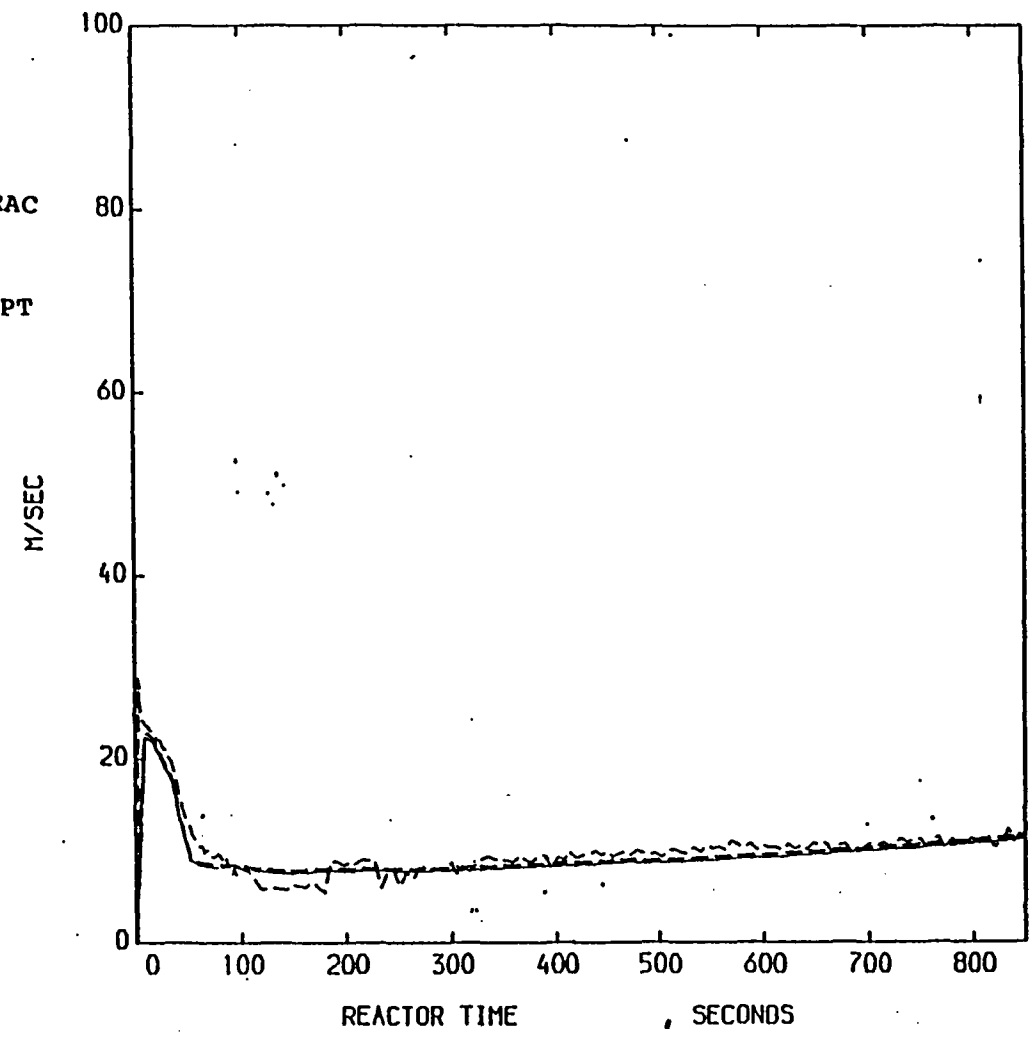
27 LIQ AND VAP VELOCITY AT CORE OUTLET
 LP-SB-2 - TRAC PF1-MOD! AND EXPERIMENT COMPARISON

Winfrith

THE FOLLOWING ARE PLOTTED AGAINST REACTOR TIME
 LIQUID VELOCITY , VAPOR VELOCITY , FE-PC-S03

KEY		
SYMBOL	NAME	UNITS
—	LIQUID VELOCITY	,M/SEC
LOC= 99/ 0/ 8	MNEM=VLIO	INF=1
--	VAPOR VELOCITY	,M/SEC
LOC= 99/ 0/ 8	MNEM=VVAP	INF=1
--	FE-PC-S03	,M/SEC
LOC= 14/ 0/ 0	MNEM=FE	INF=2

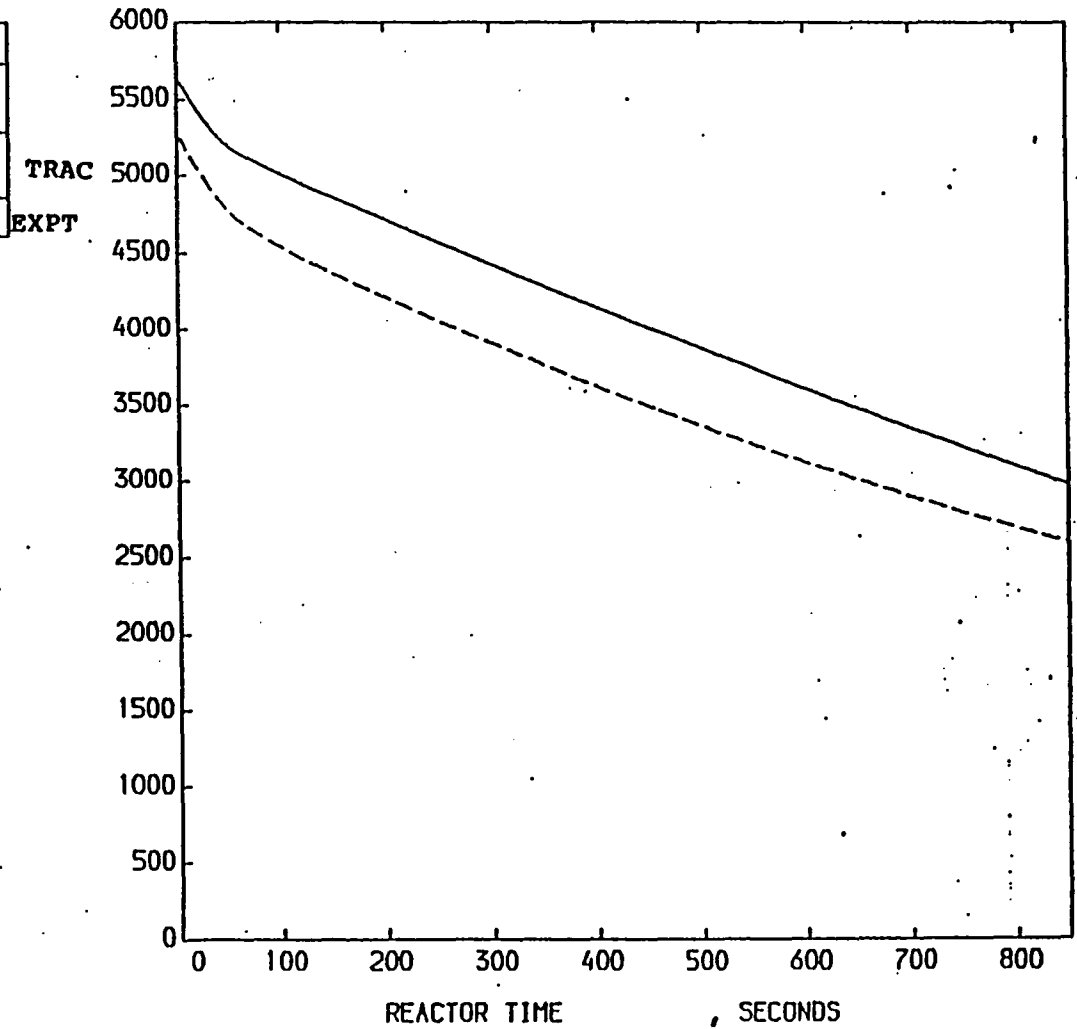
TRAC
 EXPT



28 LIQ AND VAP VELOCITY IN THE BREAK LINE
 LP-SB-2 - TRAC PF1-MOD1 AND EXPERIMENT COMPARISON

THE FOLLOWING ARE PLOTTED AGAINST REACTOR TIME
 CONTROL BLK ID -81, FUNCTION

KEY		
SYM BOL	NAME	UNITS
—	CONTROL BLK ID -81, LOC= 0/ 0/ 1 MNEM=C-81 INF=1	TRAC
--	FUNCTION	EXPT

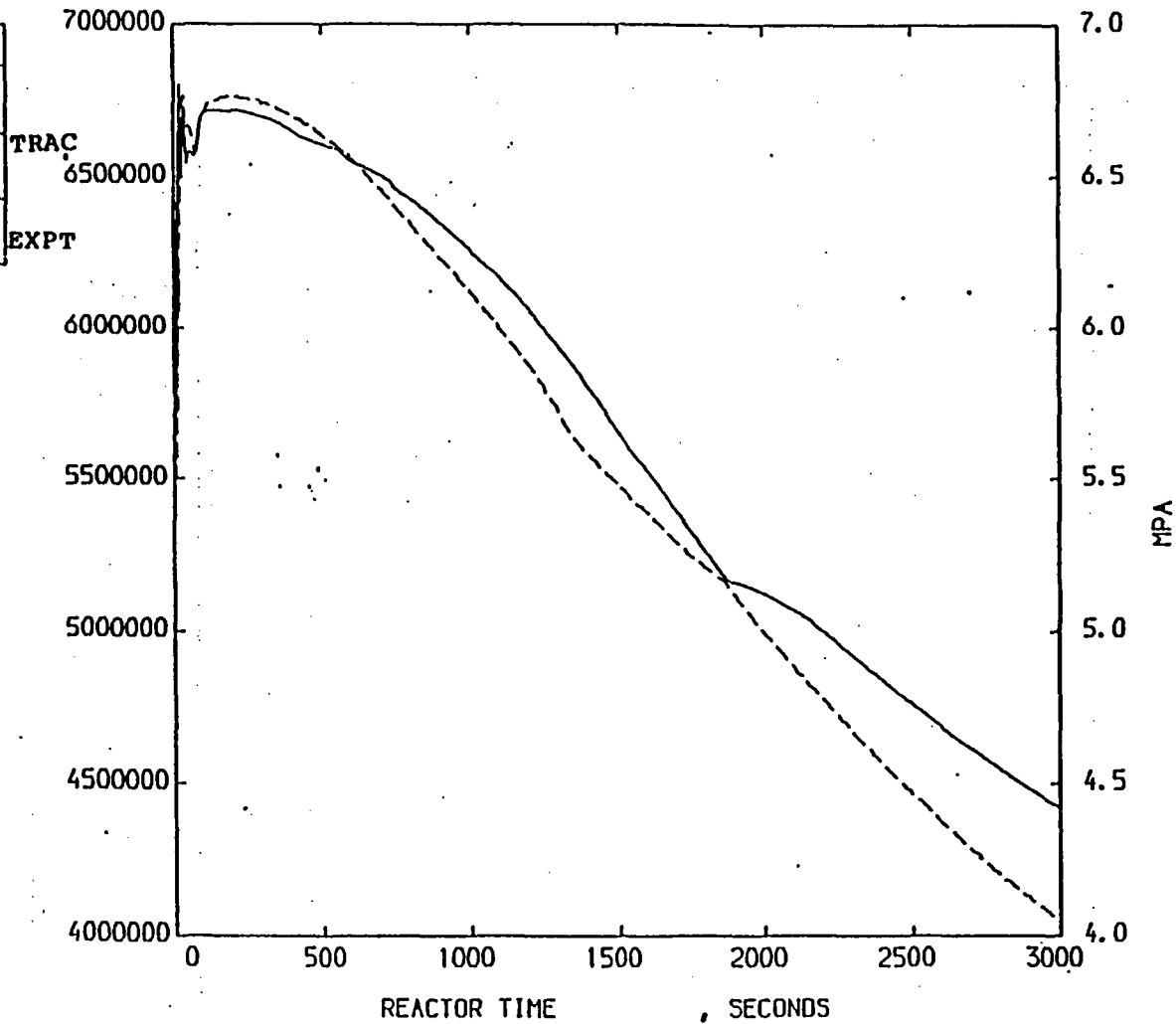


29 TRANSIENT MASS INVENTORY
 ++PLUS++ PLOTTING UTILITY SYSTEM

THE FOLLOWING ARE PLOTTED AGAINST REACTOR TIME
 SIGNAL VAR. NO. 6, PT-P004-010A

Winfrith

KEY		
SYM BOL	NAME	UNITS
—	SIGNAL VAR. NO. 6,	
LOC= 0/ 0/ 1	MHEM-S 6	INF=1
---	PT-P004-010A	,MPA
LOC= 86/ 0/ 0	MHEM-PRES	INF=2

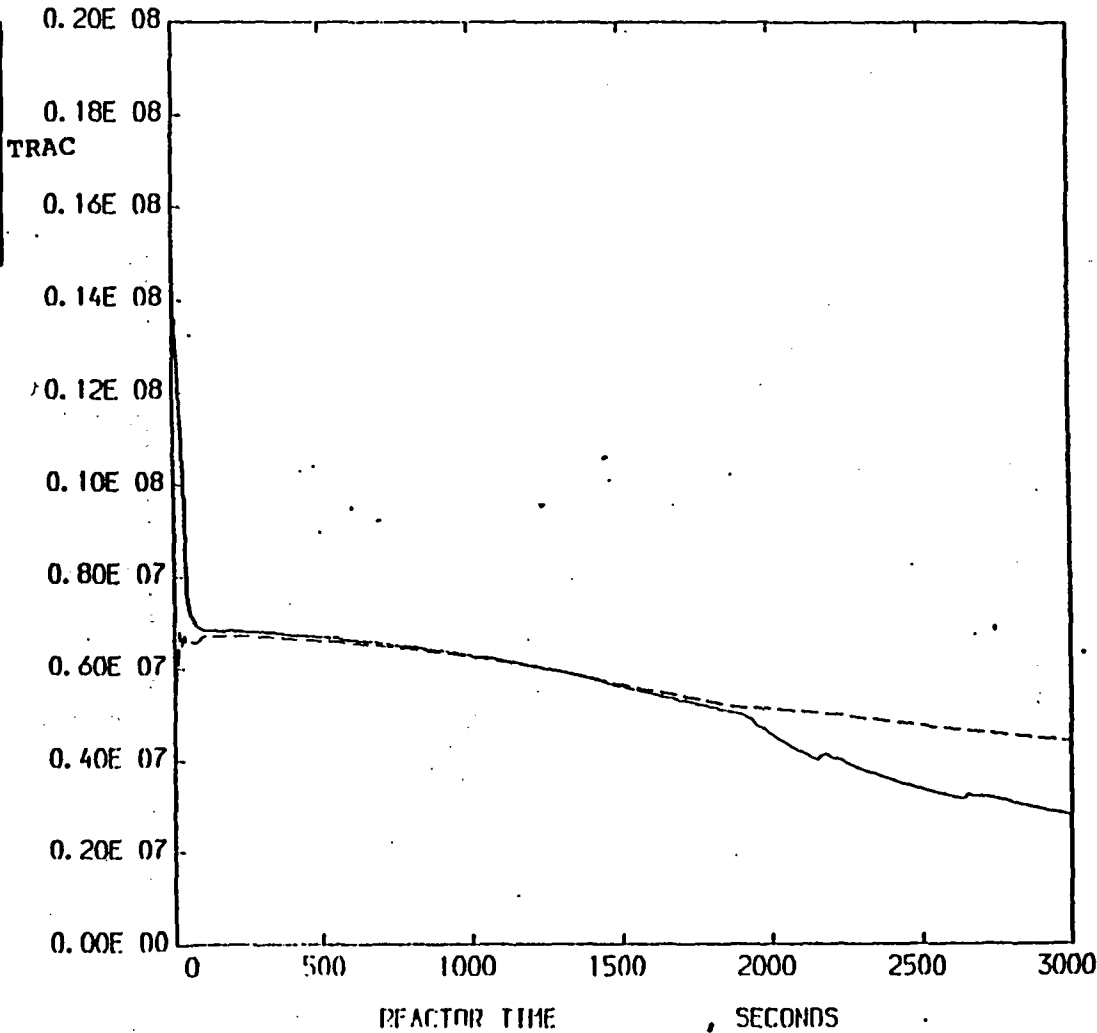


30 SECONDARY SIDE PRESSURE
 LP-SB-2 - TRAC PF1-MOD1 AND EXPERIMENT COMPARISON

THE FOLLOWING ARE PLOTTED AGAINST REACTOR TIME
 SIGNAL VAR. NO. 2, SIGNAL VAR. NO. 6

Winfrith

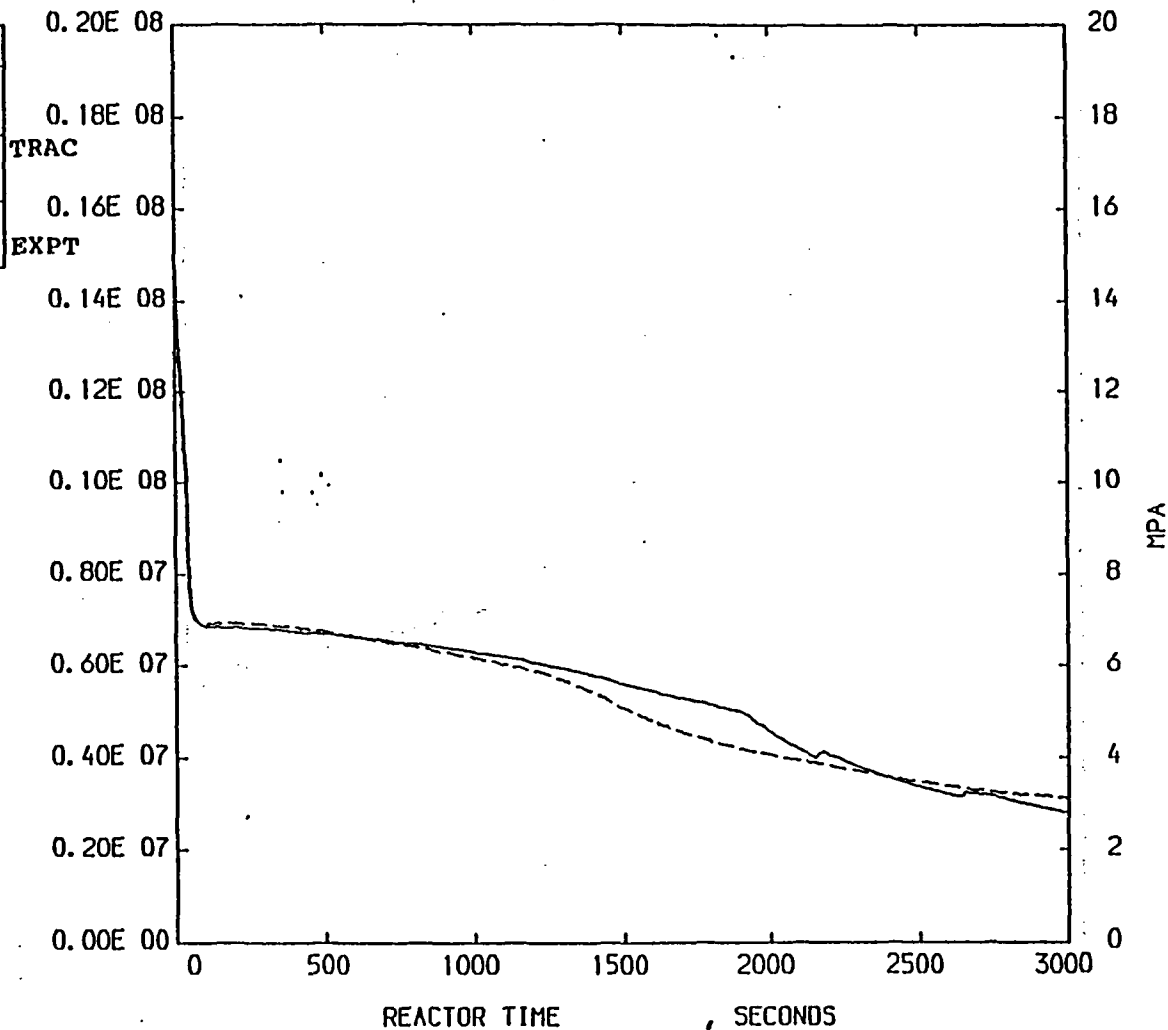
KEY		
SYMBOL	NAME	UNITS
—	SIGNAL VAR. NO. 2, LOC= 0/ 0/ 1 MNEH=5 2 INF=1	
- -	SIGNAL VAR. NO. 6, LOC= 0/ 0/ 1 MNEH=5 6 INF=1	



31 PRIMARY AND SECONDARY PRESSURES IN TRAC
 LP-SB-2 - TRAC PL-1-MOD1 AND EXPERIMENT COMPARISON

THE FOLLOWING ARE PLOTTED AGAINST REACTOR TIME
 SIGNAL VAR. NO. 2, PE-PC-002

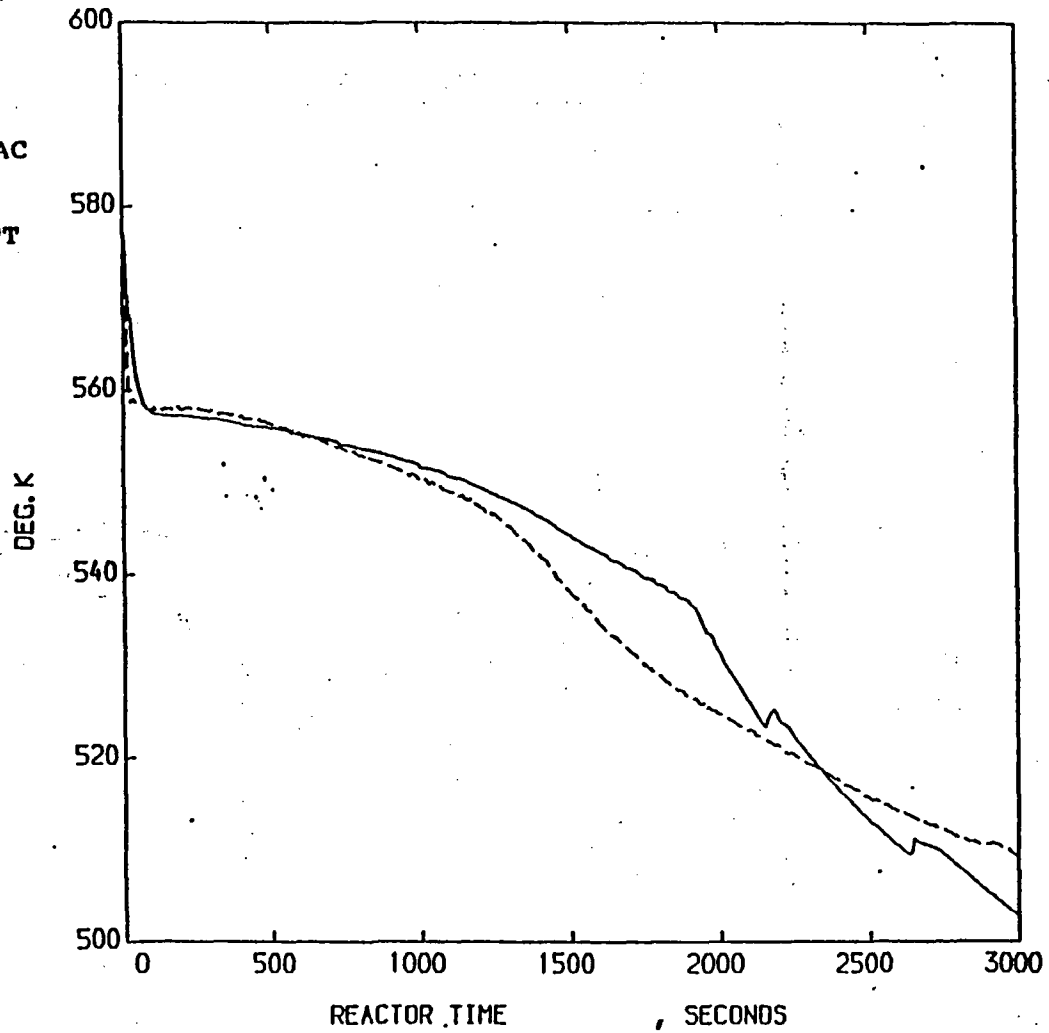
KEY		
SYMBOL	NAME	UNITS
—	SIGNAL VAR. NO. 2, LOC= 0/ 0/ 1 MNEH-S 2 INF=1	TRAC
- -	PE-PC-002 LOC= 77/ 0/ 0 MNEH-PRES INF=2	EXPT ,MPA



32 INTACT LOOP HOT LEG PRESSURE
 LP-SB-2 - TRAC PF1-MOD1 AND EXPERIMENT COMPARISON

THE FOLLOWING ARE PLOTTED AGAINST REACTOR TIME
 LIQUID TEMPERATURE , TE-PC-002B

KEY		
SYMBOL	NAME	UNITS
—	LIQUID TEMPERATURE	DEG. K
LOC= 99/ 0/ 2	MNEM=TEML	INF=1
---	TE-PC-002B	DEG. K
LOC= 130/ 0/ 0	MNEM=THCL	INF=2



33 LIO TEMPERATURE IN THE HOT LEG OF THE INTACT LOOP.
 LP-SB-2 - TRAC PF1-MOD1 AND EXPERIMENT COMPARISON

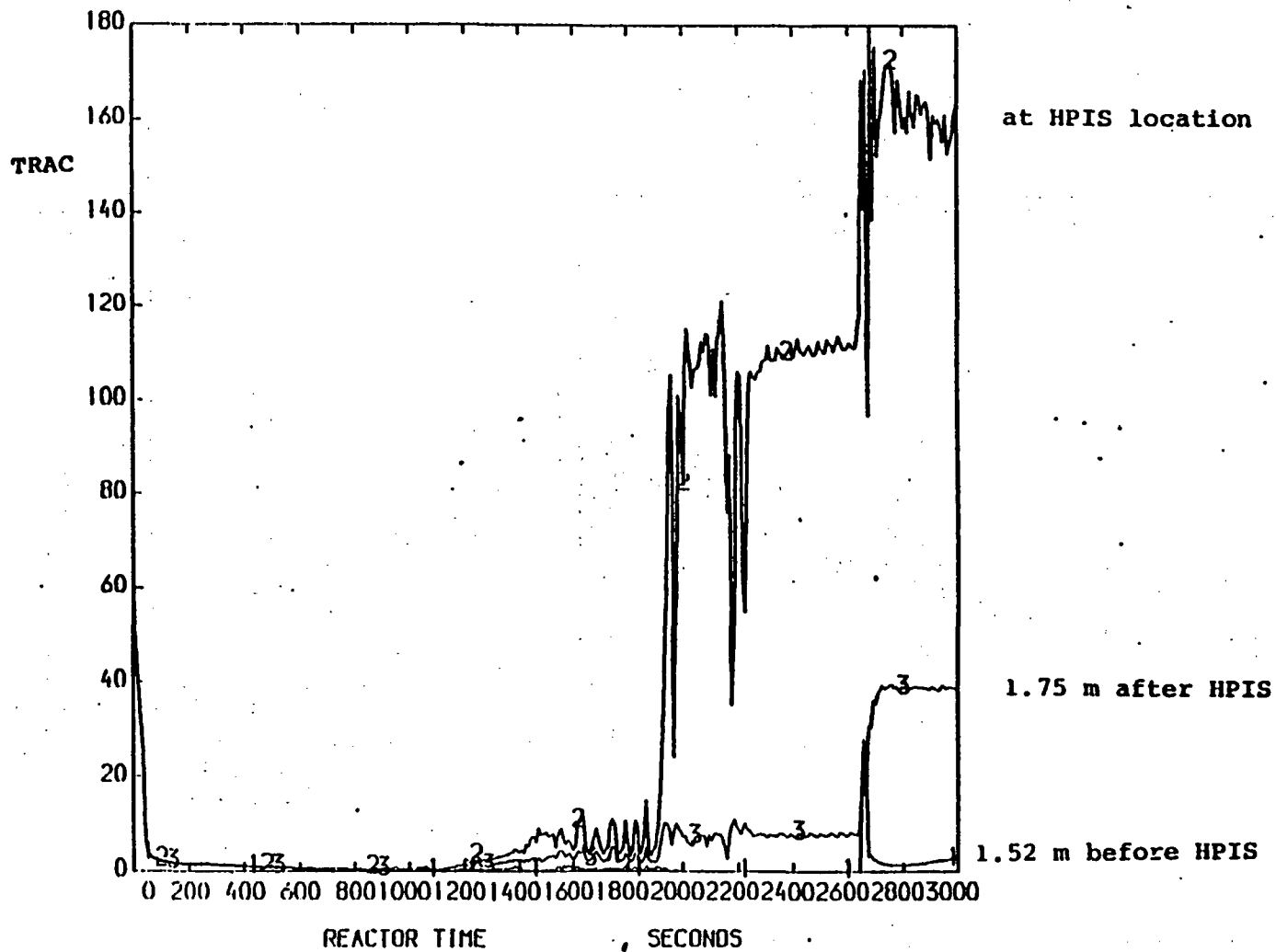
AEEW - R 2202

.66

THE FOLLOWING ARE PLOTTED AGAINST REACTOR TIME
FUNCTION

Winfrith

KEY		
SYN BN.	NAME	UNITS
-1-	FUNCTION	.
-2-	FUNCTION	
-3-	FUNCTION	



34

COLD LEG TEM SAT - TEM LIQ

++PLUS++

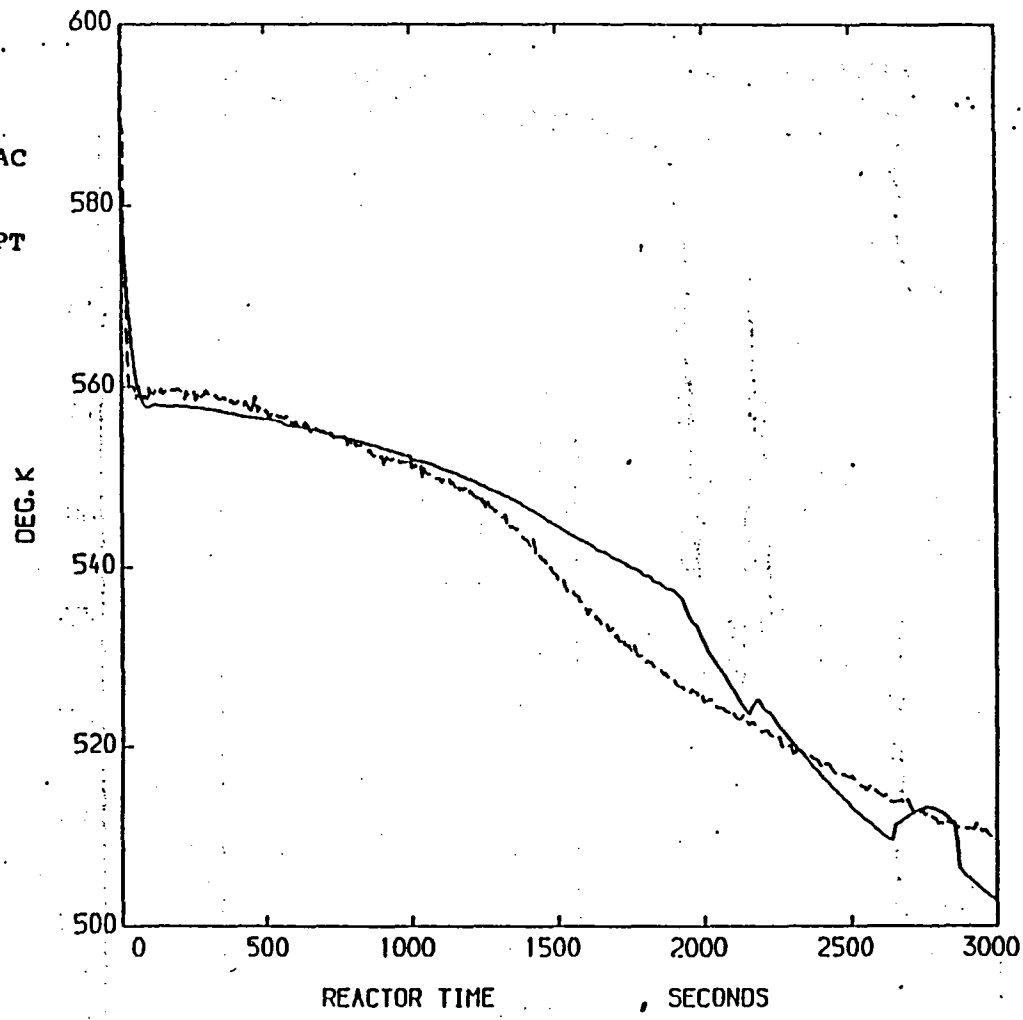
PLOTTING UTILITY SYSTEM

AEEW

THE FOLLOWING ARE PLOTTED AGAINST REACTOR TIME
 CLADDING TEMP -FINE, TE-5H07-058

KEY		
SYM BOL	NAME	UNITS
—	CLADDING TEMP -FINE, DEG. K	
LOC= 88/ 1/ 6	HNEH=THCL INF=1	
--	TE-5H07-058 , DEG. K	
LOC= 272/ 0/ 0	HNEH=THCL INF=2	

TRAC
 EXPT



35 CLADDING TEMPERATURE NEAR TOP OF THE CORE
 LP-SB-2 - TRAC PF1-MOD1 AND EXPERIMENT COMPARISON

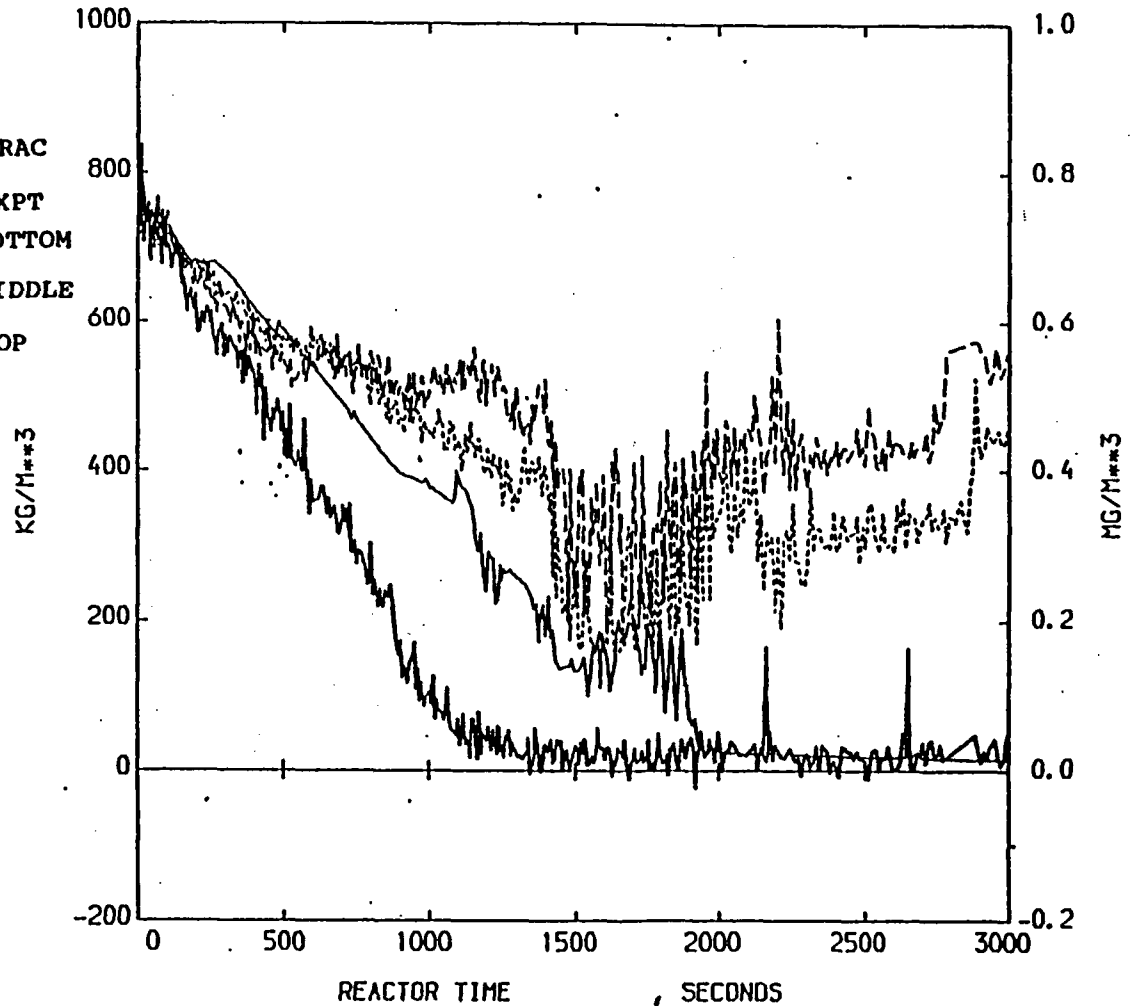
Winfrith

THE FOLLOWING ARE PLOTTED AGAINST REACTOR TIME

MIXTURE DENSITY ,DE-PC-002A ,DE-PC-002B
 DE-PC-002C

KEY		
SYN BOL	NAME	UNITS
—	MIXTURE DENSITY	,KG/M**3
LOC= 99/ 0/ 2	MHEM-DENM INF=1	
--	DE-PC-002A	,MG/M**3
LOC= 8/ 0/ 0	MHEM-DENM INF=2	
----	DE-PC-002B	,MG/M**3
LOC= 9/ 0/ 0	MHEM-DENM INF=2	
—	DE-PC-002C	,MG/M**3
LOC= 10/ 0/ 0	MHEM-DENM INF=2	

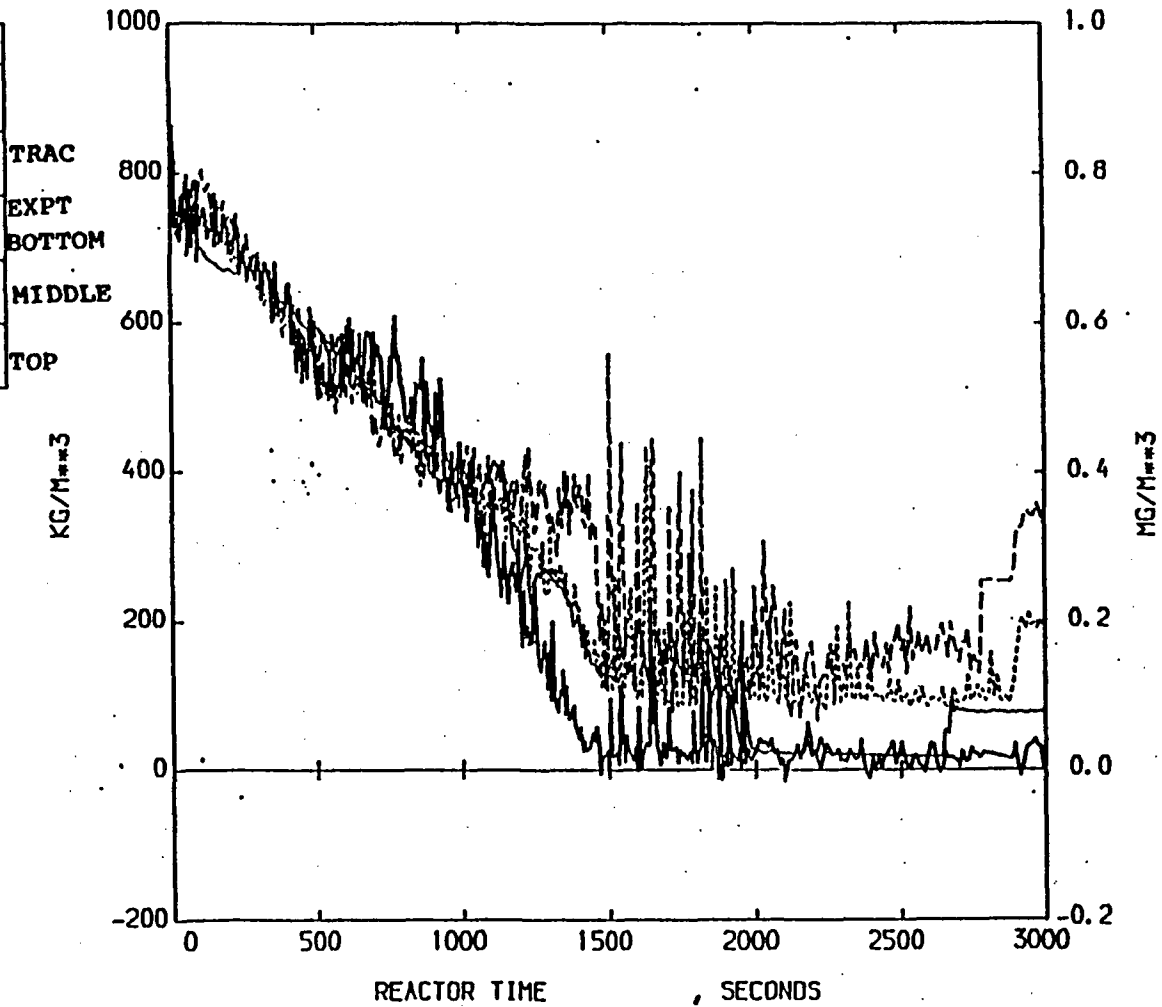
TRAC
 EXPT
 BOTTOM
 MIDDLE
 TOP



36 DENSITY IN THE HOT LEG INTACT LOOP
 LP-SB-2 - TRAC PF1-MOD1 AND EXPERIMENT COMPARISON

THE FOLLOWING ARE PLOTTED AGAINST REACTOR TIME
 MIXTURE DENSITY ,DE-PC-001A ,DE-PC-001B
 DE-PC-001C

KEY		
SYN BOL	NAME	UNITS
—	MIXTURE DENSITY	,KG/M ³
LOC= 7/ 0/ 4	MNEH-DENM INF=1	
--	DE-PC-001A	,HG/M ³
LOC= 5/ 0/ 0	MNEH-DENM INF=2	
----	DE-PC-001B	,HG/M ³
LOC= 6/ 0/ 0	MNEH-DENM INF=2	
—	DE-PC-001C	,HG/M ³
LOC= 7/ 0/ 0	MNEH-DENM INF=2	



37 DENSITY IN THE COLD LEG OF THE INTACT LOOP
 LP-SB-2 - TRAC PF1-MOD1 AND EXPERIMENT COMPARISON

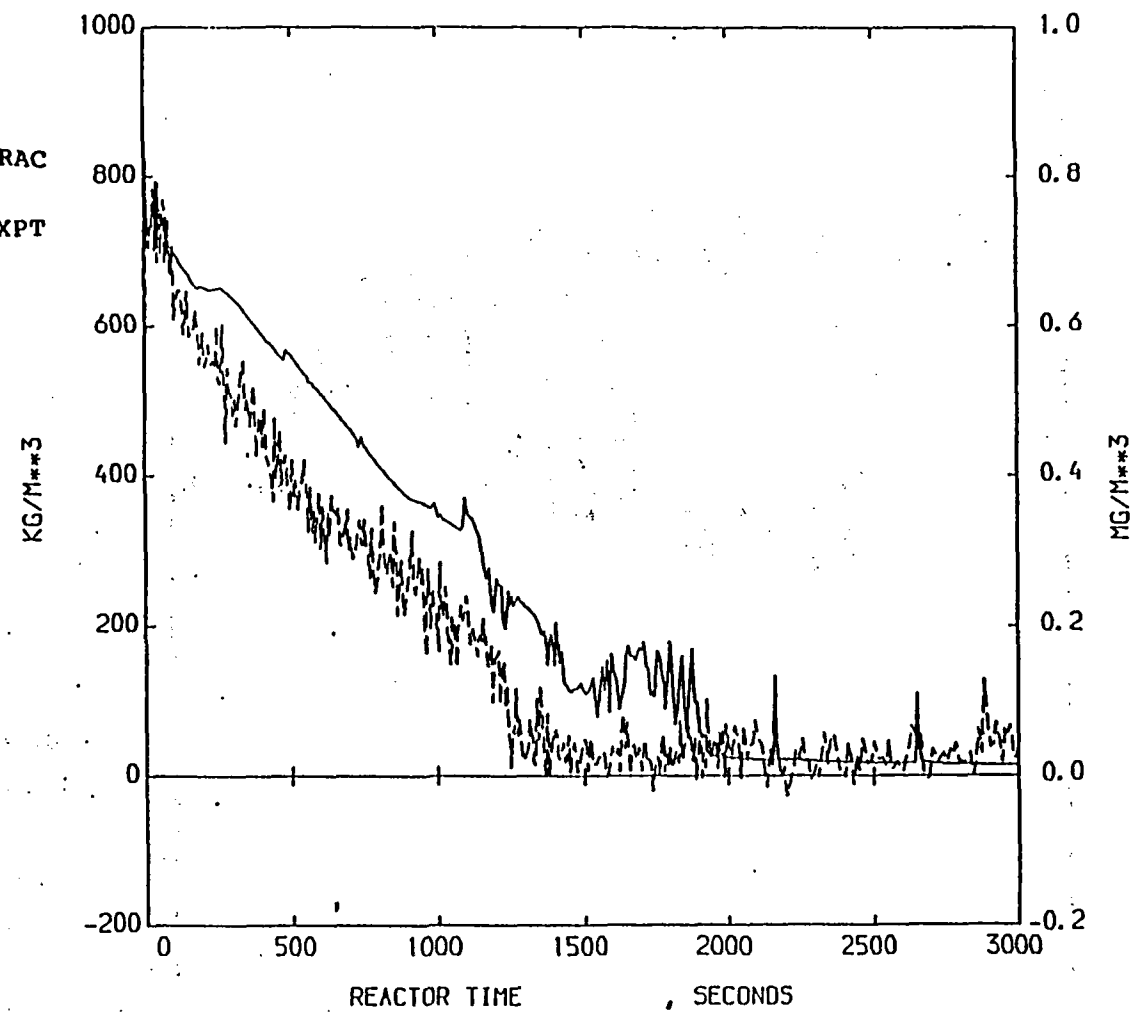
Winfrith

THE FOLLOWING ARE PLOTTED AGAINST REACTOR TIME
 MIXTURE DENSITY , DE-PC-S04B

KEY		
SYM BOL	NAME	UNITS
—	MIXTURE DENSITY	,KG/M**3
LOC= 99/ 0/ 8	MNEM=DENM	INF=1
- -	DE-PC-S04B	,MG/M**3
LOC= 4/ 0/ 0	MNEM=DENM	INF=2

TRAC

EXPT

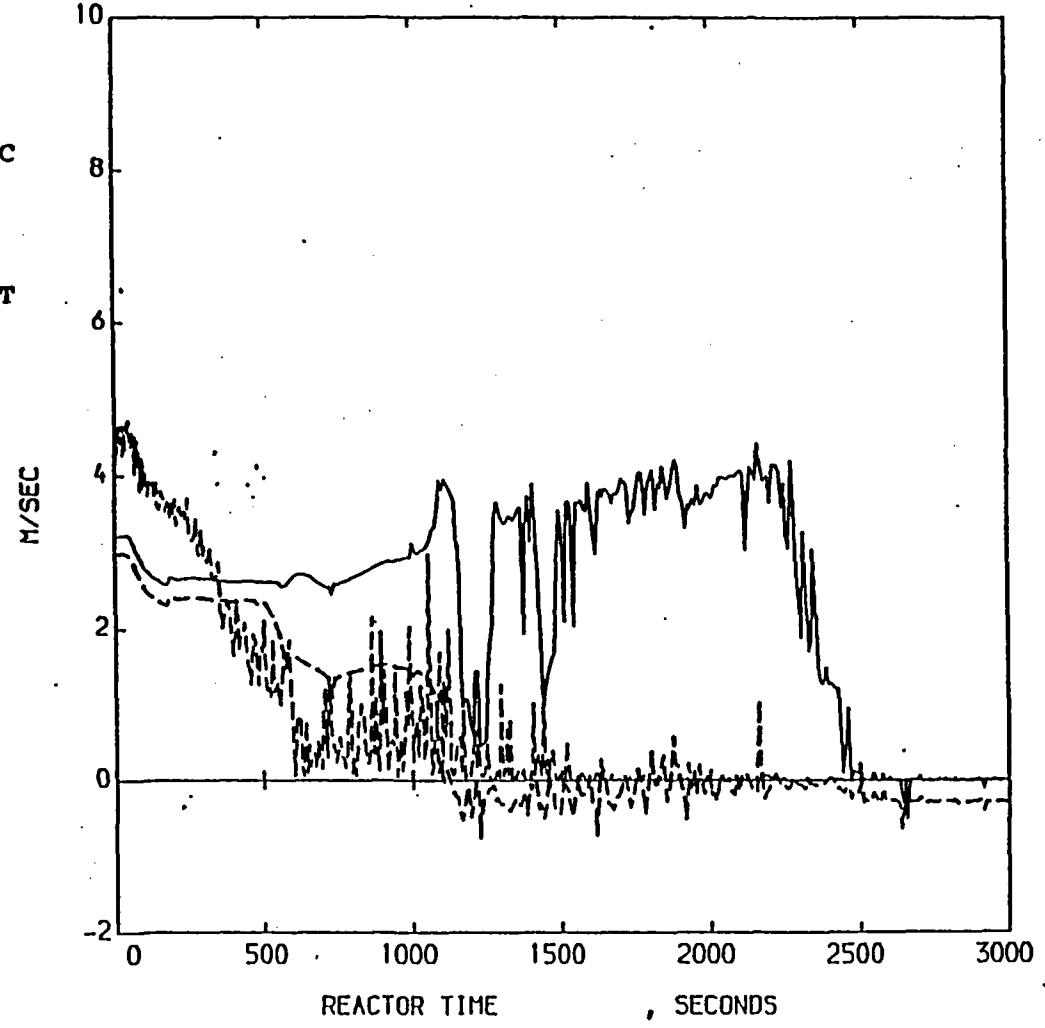


38 DENSITY IN THE BREAK LINE
 LP-SB-2 - TRAC PF1-MOD1 AND EXPERIMENT COMPARISON

THE FOLLOWING ARE PLOTTED AGAINST REACTOR TIME
 LIQUID VELOCITY , VAPOR VELOCITY , FE-1ST-001

KEY		
SYN BOL	NAME	UNITS
—	LIQUID VELOCITY	,M/SEC
LOC= B6/ 0/ 8	MNEM=VLIO	INF=1
- -	VAPOR VELOCITY	,M/SEC
LOC= B6/ 0/ 8	MNEM=VVAP	INF=1
- -	FE-1ST-001	,M/SEC
LOC= 18/ 0/ 0	MNEM=FE	INF=2

TRAC
 EXPT



39 LIQ AND VAP VELOCITY IN THE DOWNCOMER OF THE REACTOR VESSEL
 LP-SB-2 - TRAC PF1-MOD1 AND EXPERIMENT COMPARISON

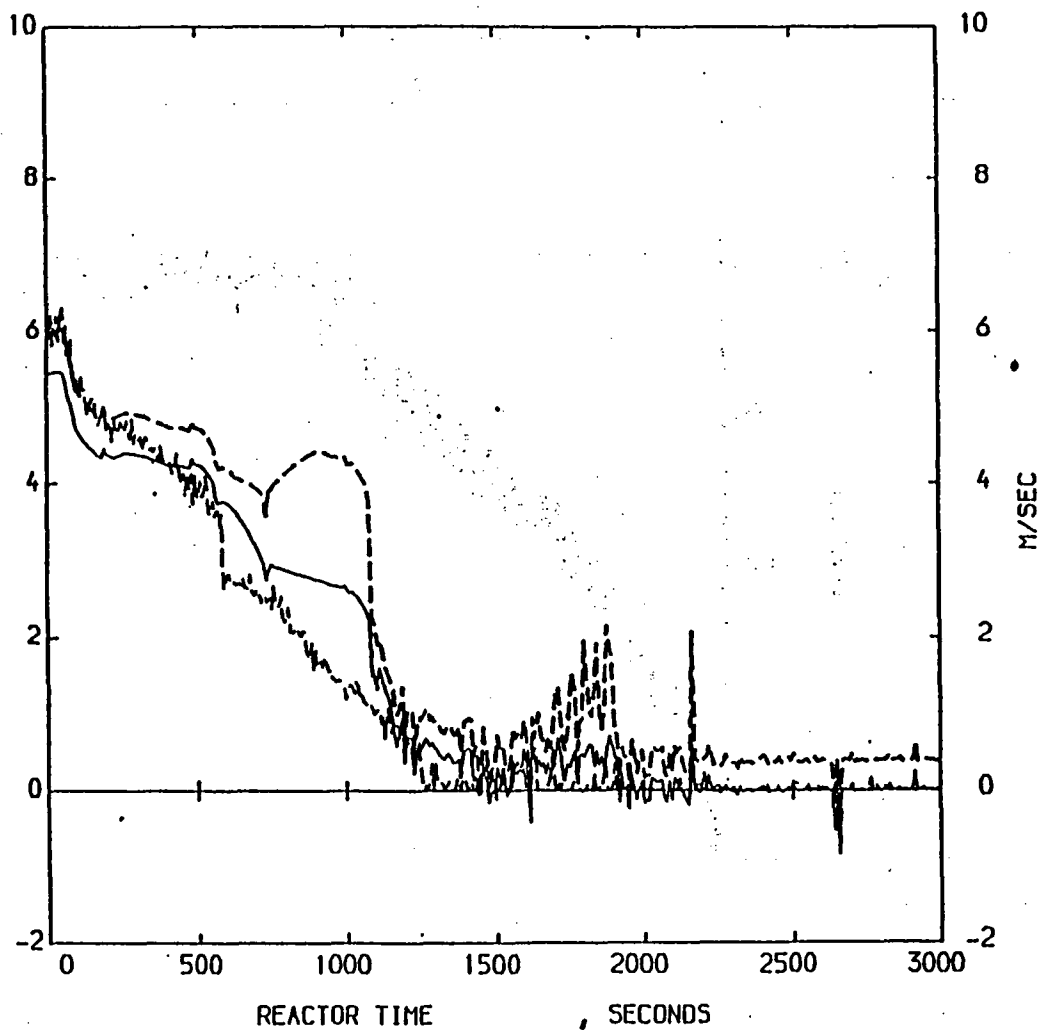
Winfrith

THE FOLLOWING ARE PLOTTED AGAINST REACTOR TIME

FUNCTION ,FE-SLP-001

KEY		
SYMBOL	NAME	UNITS
—	FUNCTION VLIO	,
- -	FUNCTION VVAP	,
- -	FE-SLP-001	,M/SEC
LOC= 20/ 0/ 0	MNEM=FE	INF=2

TRAC
EXPT

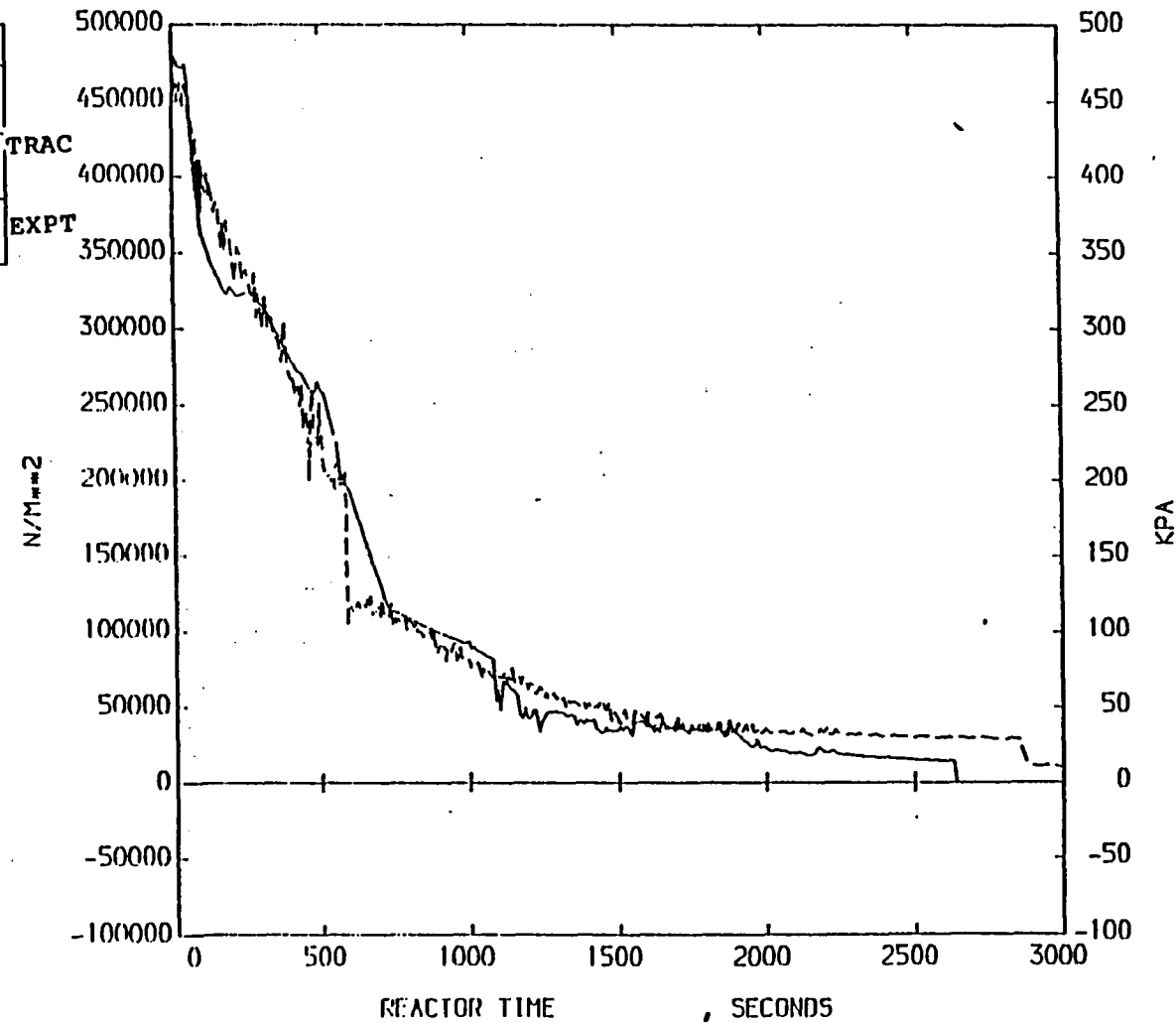


40 LIQ AND VAP VELOCITY AT CORE INLET
LP-SB-2 - TRAC PF1-MOD1 AND EXPERIMENT COMPARISON

THE FOLLOWING ARE PLOTTED AGAINST REACTOR TIME
 PUMP DELTA-P ,PDE-PC-001

Winfrith

KEY		
SYN BOL	NAME	UNITS
---	PUMP DELTA-P	N/M**2
LOC= 4/ 0/ 1	HNEH-DELP	INF=1
---	PDE-PC-001	KPA
LOC= 65/ 0/ 0	HNEH-PD	INF=2



41 PRESSURE DIFFERENCE OVER THE MAIN COOLANT PUMPS
 LP-SB-2 - TRAC PFI-M001 AND EXPERIMENT COMPARISON

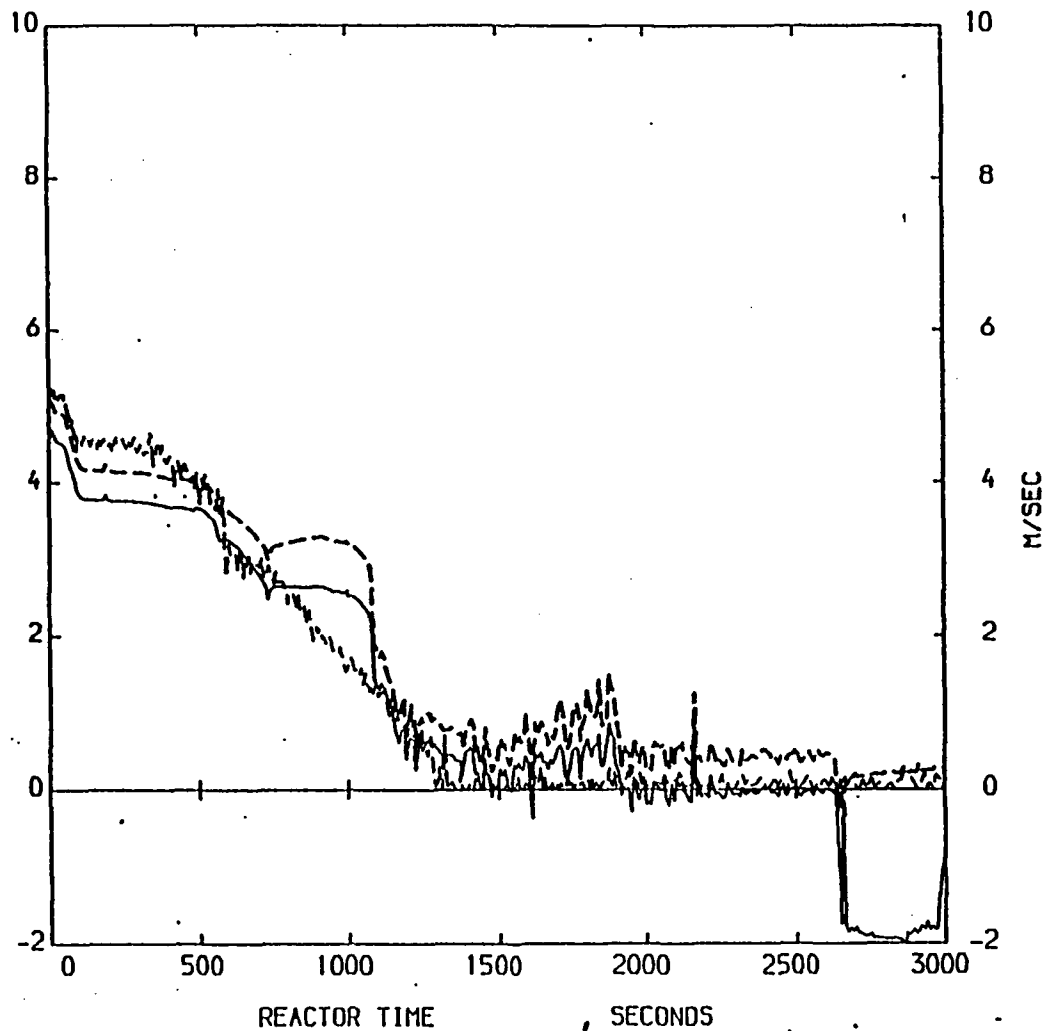
Winfrith

THE FOLLOWING ARE PLOTTED AGAINST REACTOR TIME
 FUNCTION , FE-SUP-001

KEY		
SYMBOL	NAME	UNITS
---	FUNCTION VLIO	M/SEC
---	FUNCTION VVAP	M/SEC
---	FE-SUP-001	M/SEC
LOC= 22/ 0/ 0	MNEM=FE	INF=2

TRAC

EXPT



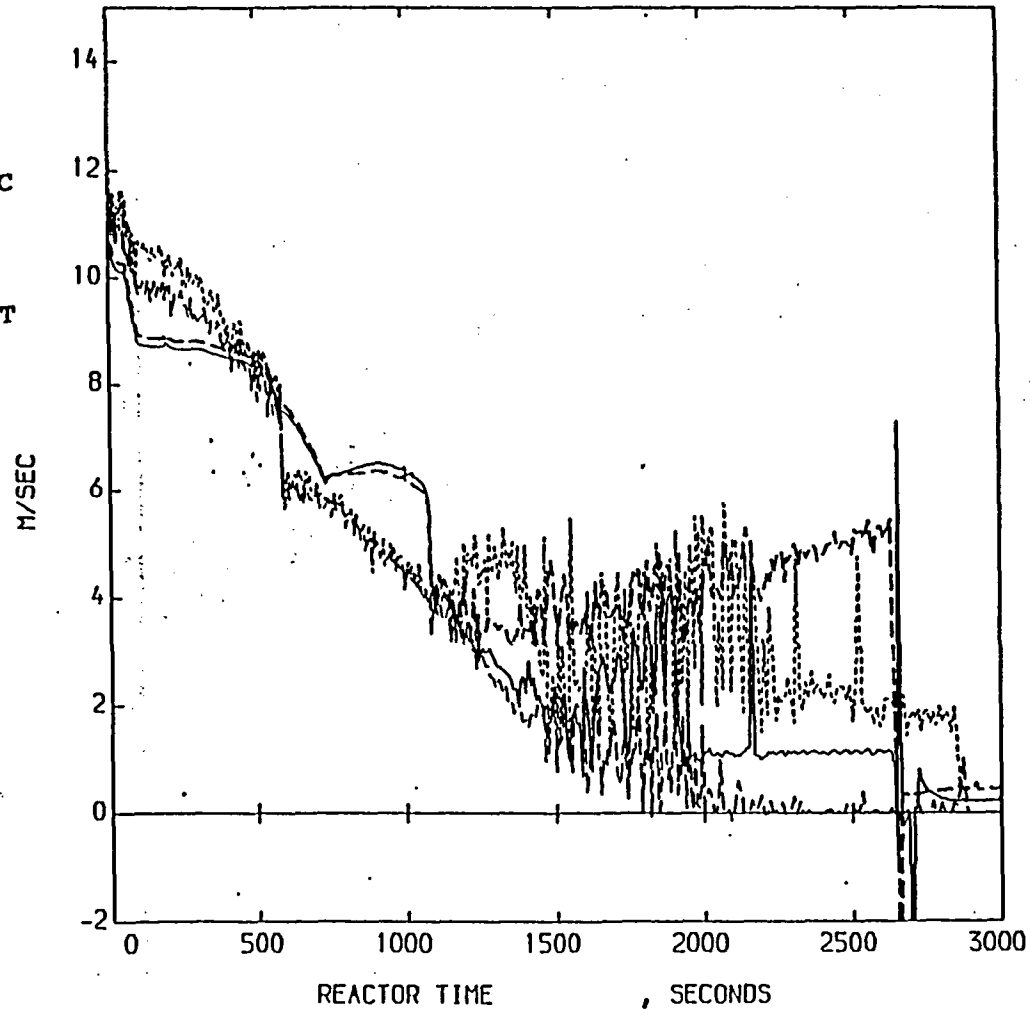
42 LIQ AND VAP VELOCITY AT CORE OUTLET
 LP-SB-2 - TRAC PF1-MOD1 AND EXPERIMENT COMPARISON

THE FOLLOWING ARE PLOTTED AGAINST REACTOR TIME

LIQUID VELOCITY , VAPOR VELOCITY , FE-PC-002A
 FE-PC-002C

KEY		
SYN BOL	NAME	UNITS
---	LIQUID VELOCITY	,H/SEC
LOC= 99/ 0/ 2	MNEH-VLIQ	INF=1
---	VAPOR VELOCITY	,H/SEC
LOC= 99/ 0/ 2	MNEH-VVAP	INF=1
---	FE-PC-002A	,H/SEC
LOC= 16/ 0/ 0	MNEH-FE	INF=2
----	FE-PC-002C	,H/SEC
LOC= 17/ 0/ 0	MNEH-FE	INF=2

TRAC
 EXPT



43

LIQ AND VAP VELOCITY IN THE HOT LEG
 LP-SB-2 - TRAC PF1-MOD1 AND EXPERIMENT COMPARISON

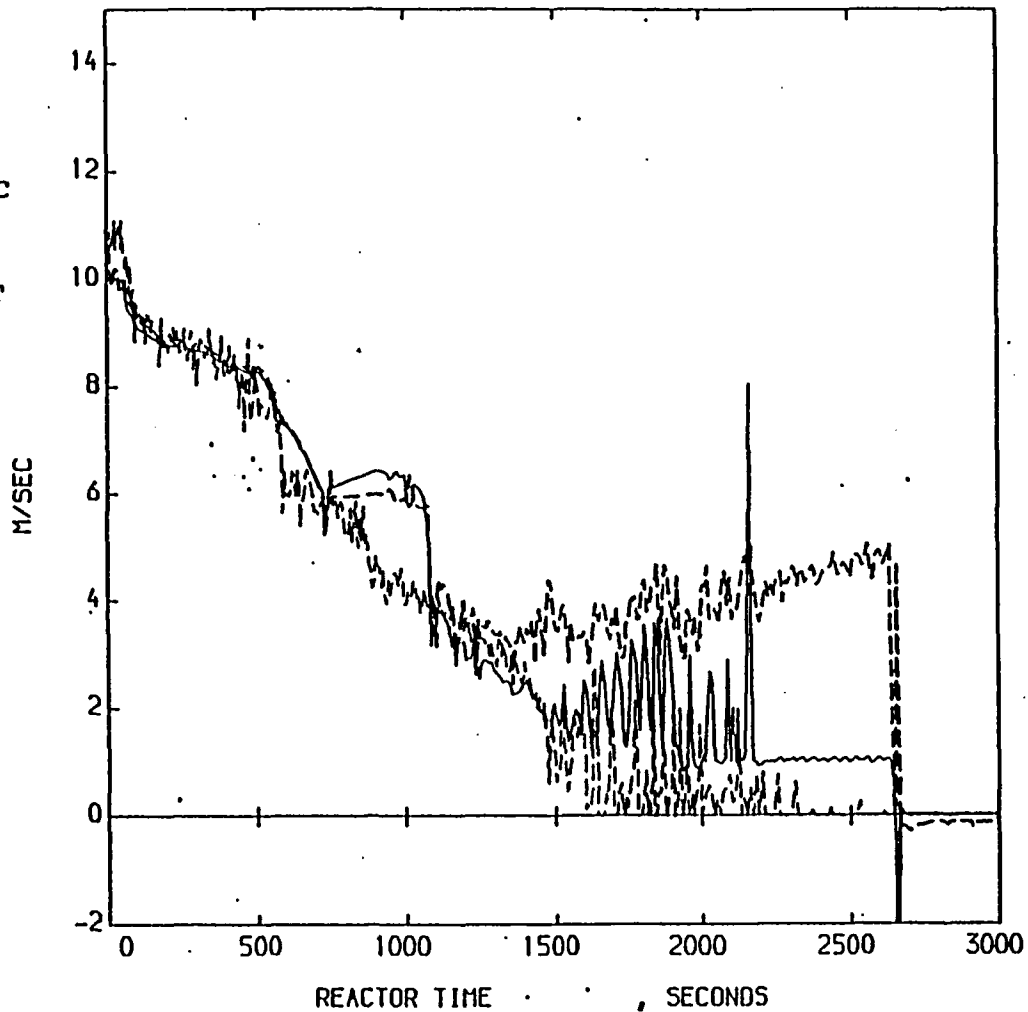
THE FOLLOWING ARE PLOTTED AGAINST REACTOR TIME

· LIQUID VELOCITY · VAPOR VELOCITY · FE-PC-001C

KEY		
SYN BOL	NAME	UNITS
—	LIQUID VELOCITY	M/SEC
LOC= 7/ 0/ 4	MNEM=VLIO	INF=1
- -	VAPOR VELOCITY	M/SEC
LOC= 7/ 0/ 4	MNEM=VVAP	INF=1
- -	FE-PC-001C	M/SEC
LOC= 15/ 0/ 0	MNEM=FE	INF=2

TRAC

EXPT



44

LIQ AND VAP VELOCITY IN THE COLD LEG
 LP-SB-2 - TRAC PF1-MOD1 AND EXPERIMENT COMPARISON

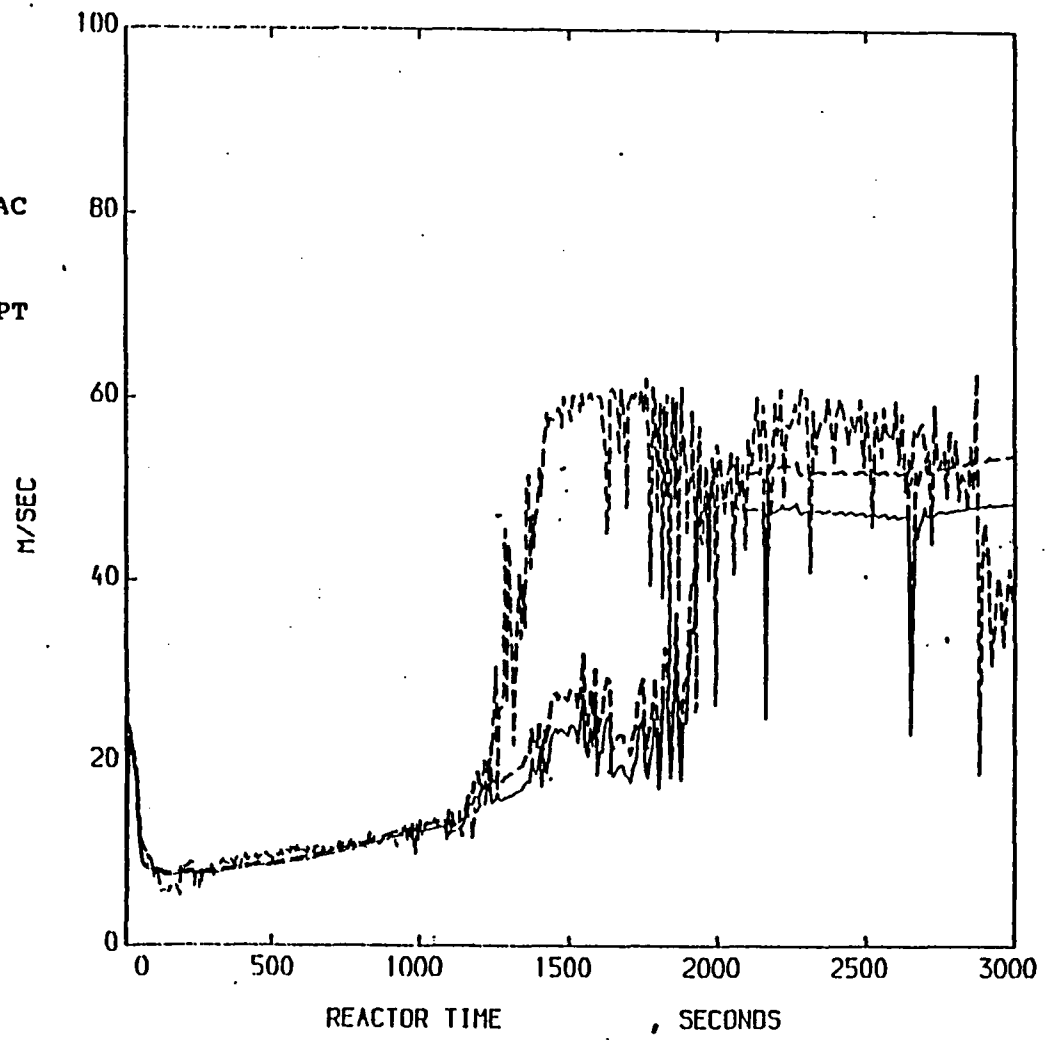
THE FOLLOWING ARE PLOTTED AGAINST REACTOR TIME.
 LIQUID VELOCITY , VAPOR VELOCITY , FE-PC-S03

AEW - R 2202

77

KEY		
SYM BOL	NAME	UNITS
—	LIQUID VELOCITY	,M/SEC
LOC= 99/ 0/ 8	MNEH=VLIO	INF=1
- -	VAPOR VELOCITY	,M/SEC
LOC= 99/ 0/ 8	MNEH=VAP	INF=1
- -	FE-PC-S03	,M/SEC
LOC= 14/ 0/ 0	MNEH=FE	INF=2

TRAC
EXPT

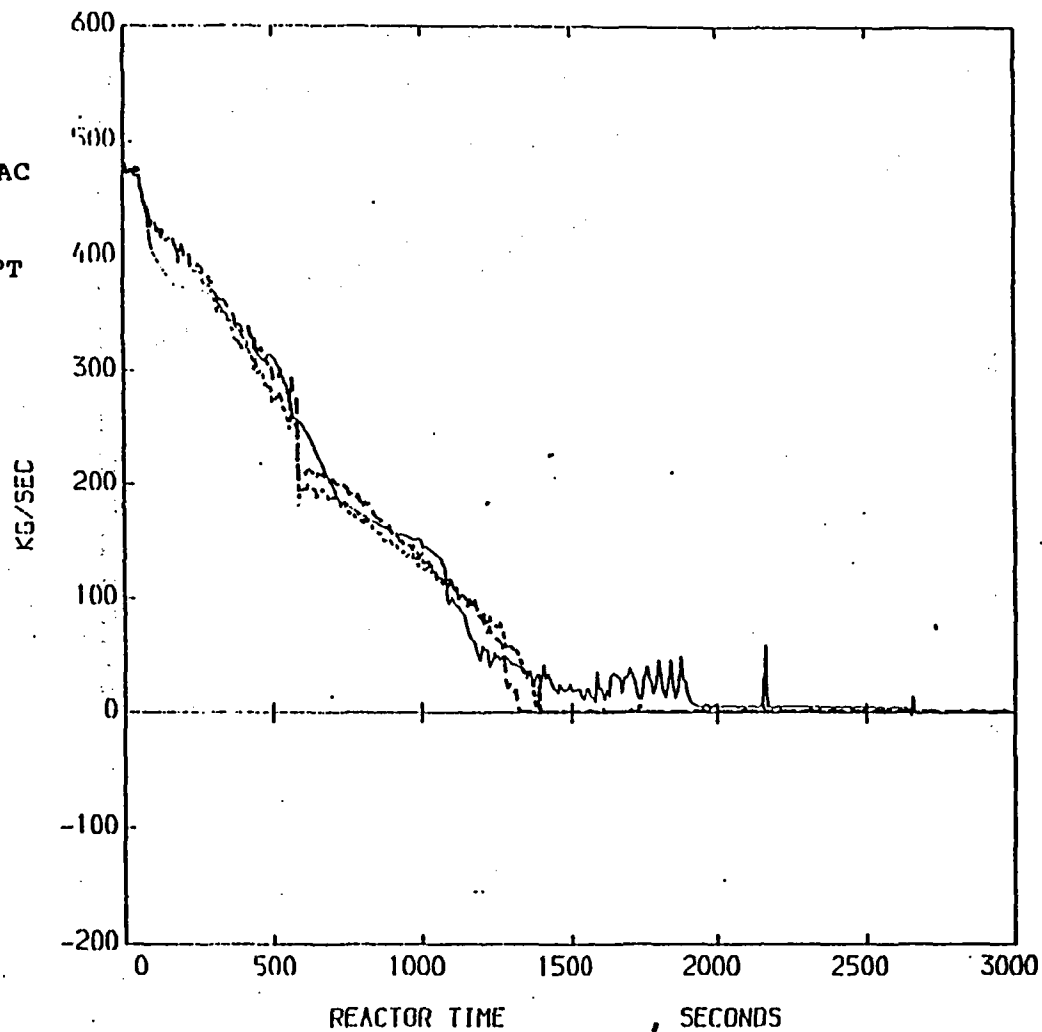


45 LIO AND VAP VELOCITY IN THE BREAK LINE
 LP-SB-2 - TRAC PFI-MOD1 AND EXPERIMENT COMPARISON

THE FOLLOWING ARE PLOTTED AGAINST REACTOR TIME
 MASS FLOW RATE ,FT-P139-27-1 ,FT-P139-27-2

KEY		
SYN BOL	NAME	UNITS
—	MASS FLOW RATE	,KG/SEC
LOC= 1/ 0/ 3	MNEM=FLOW INF=1	
--	FT-P139-27-1	,KG/SEC
LOC= 30/ 0/ 0	MNEM=FLOW INF=2	
----	FT-P139-27-2	,KG/SEC
LOC= 31/ 0/ 0	MNEM=FLOW INF=2	

TRAC
 EXPT



46 HOT LEG MASS FLOW RATE AT VENTURI LOCATION
 LP-SB-2 - TRAC PF1-MOD1 AND EXPERIMENT COMPARISON

AEEW - R 2202

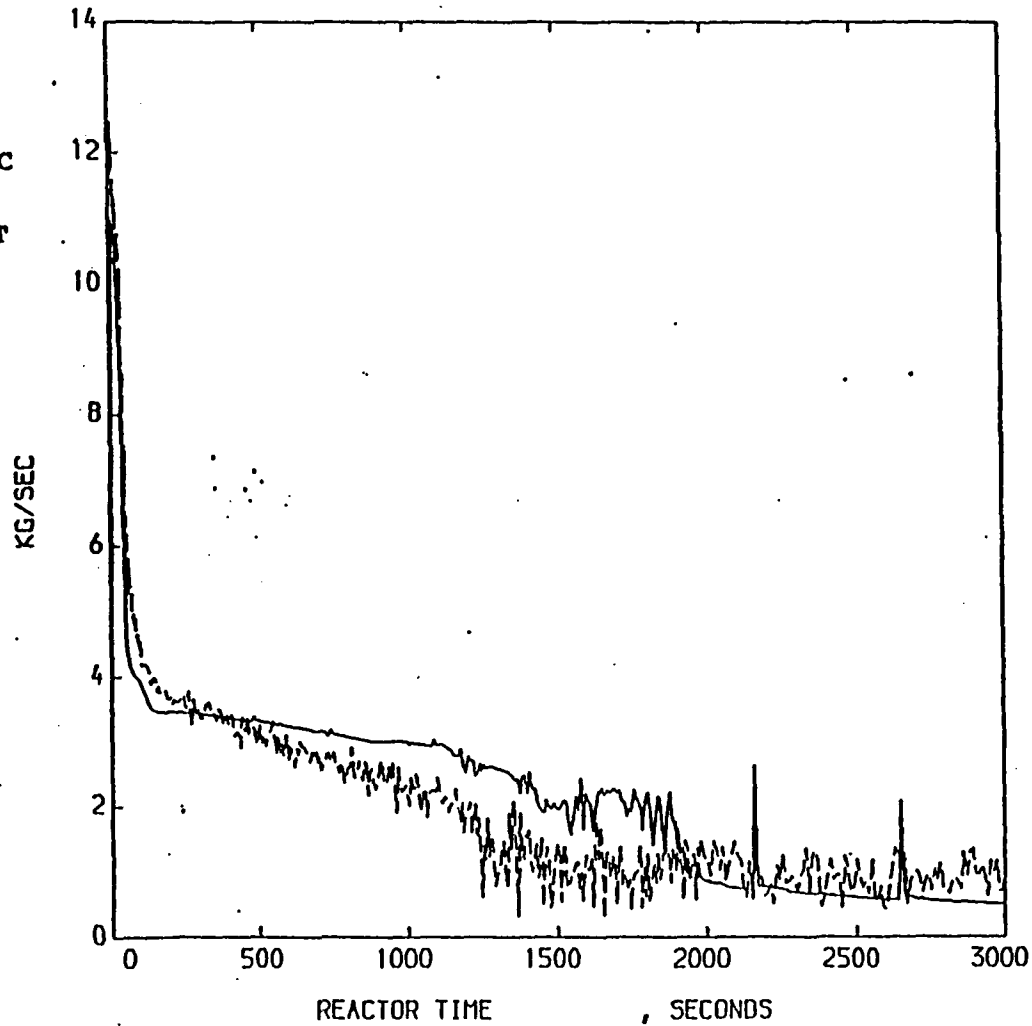
79

Winfrith

THE FOLLOWING ARE PLOTTED AGAINST REACTOR TIME
MASS FLOW RATE ,FR-PC-S03

KEY		
SYH BOL	NAME	UNITS
---	MASS FLOW RATE	,KG/SEC
LOC= 98/ 0/ 1	MNEH=FLOW INF=1	
---	FR-PC-S03	,KG/SEC
LOC= 23/ 0/ 0	MNEH=FLOW INF=2	

TRAC
EXPT

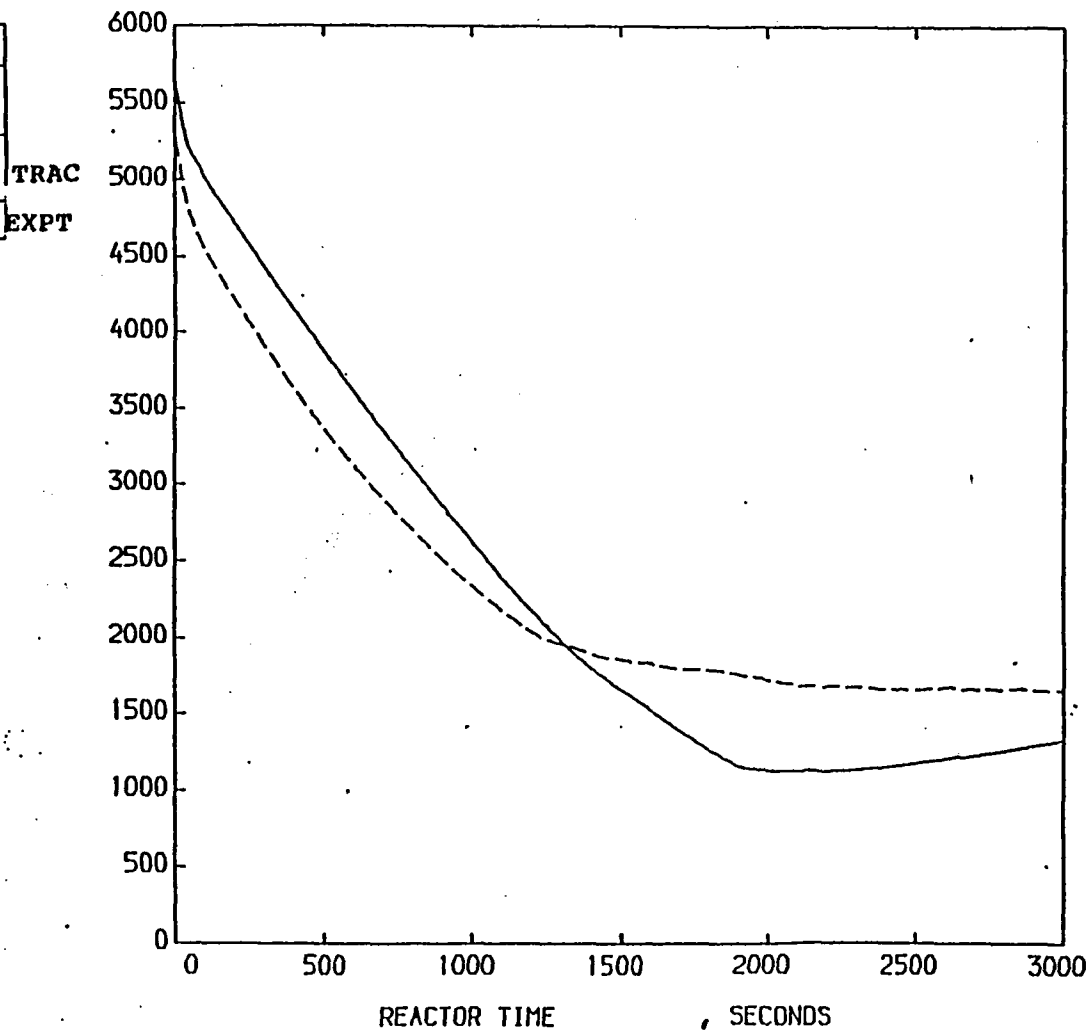


47 BREAK MASS FLOW RATE
LP-SB-2 - TRAC PF1-MOD1 AND EXPERIMENT COMPARISON

Winfrith

THE FOLLOWING ARE PLOTTED AGAINST REACTOR TIME
CONTROL BLK ID -81,FUNCTION

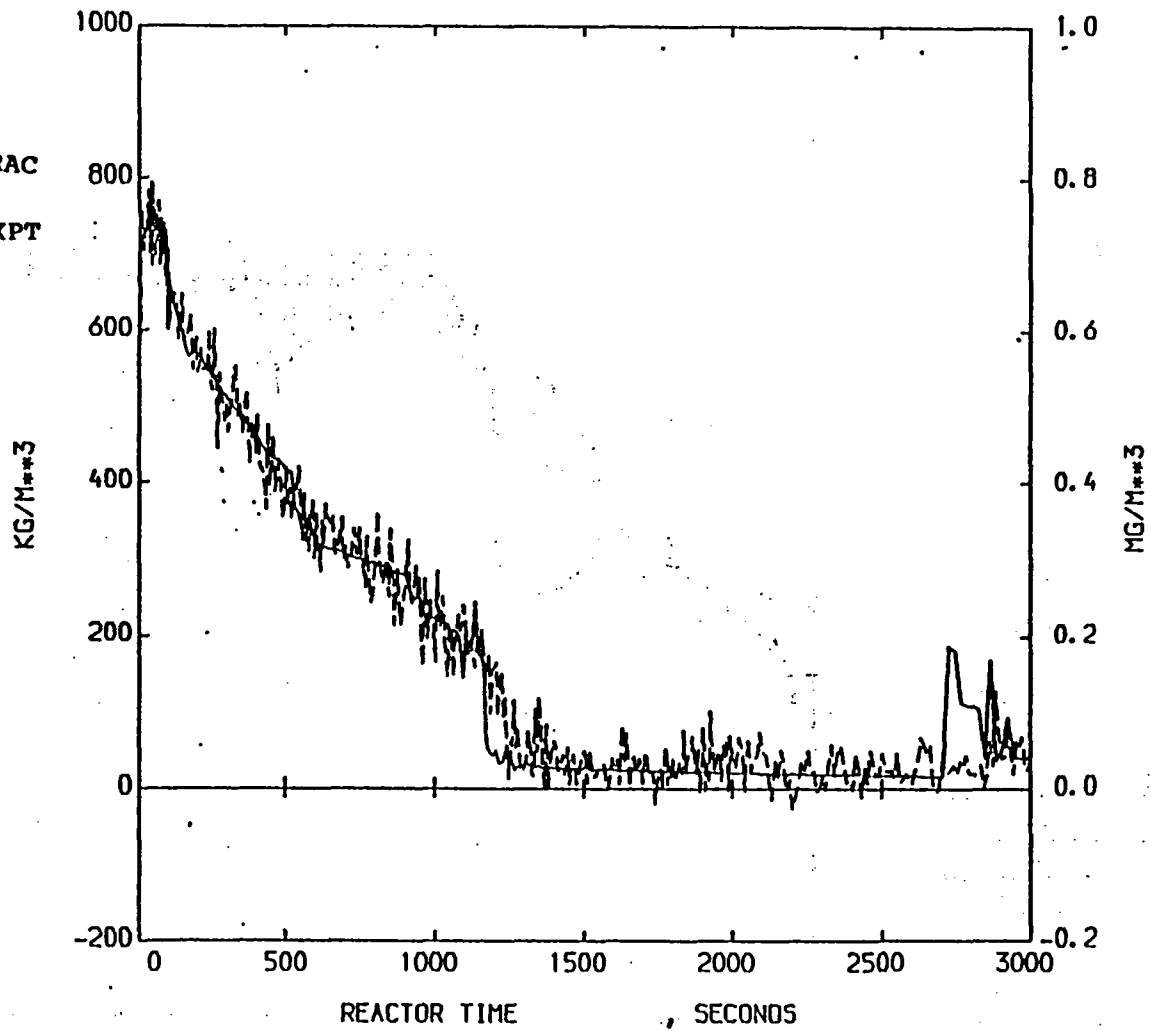
KEY		
SYM BOL	NAME	UNITS
—	CONTROL BLK ID -81, LOC= 0/ 0/ 1 MNEM=C-81 INF=1	TRAC
- -	FUNCTION	EXPT



THE FOLLOWING ARE PLOTTED AGAINST REACTOR TIME
 MIXTURE DENSITY ,DE-PC-S04B

KEY		
SYN BOL	NAME	UNITS
—	MIXTURE DENSITY	,KG/M**3
LOC= 95/ 0/ 4	MNEH=DENH INF=1	
--	DE-PC-S04B	,MG/M**3
LOC= 4/ 0/ 0	MNEH=DENH INF=2	

TRAC
 EXPT

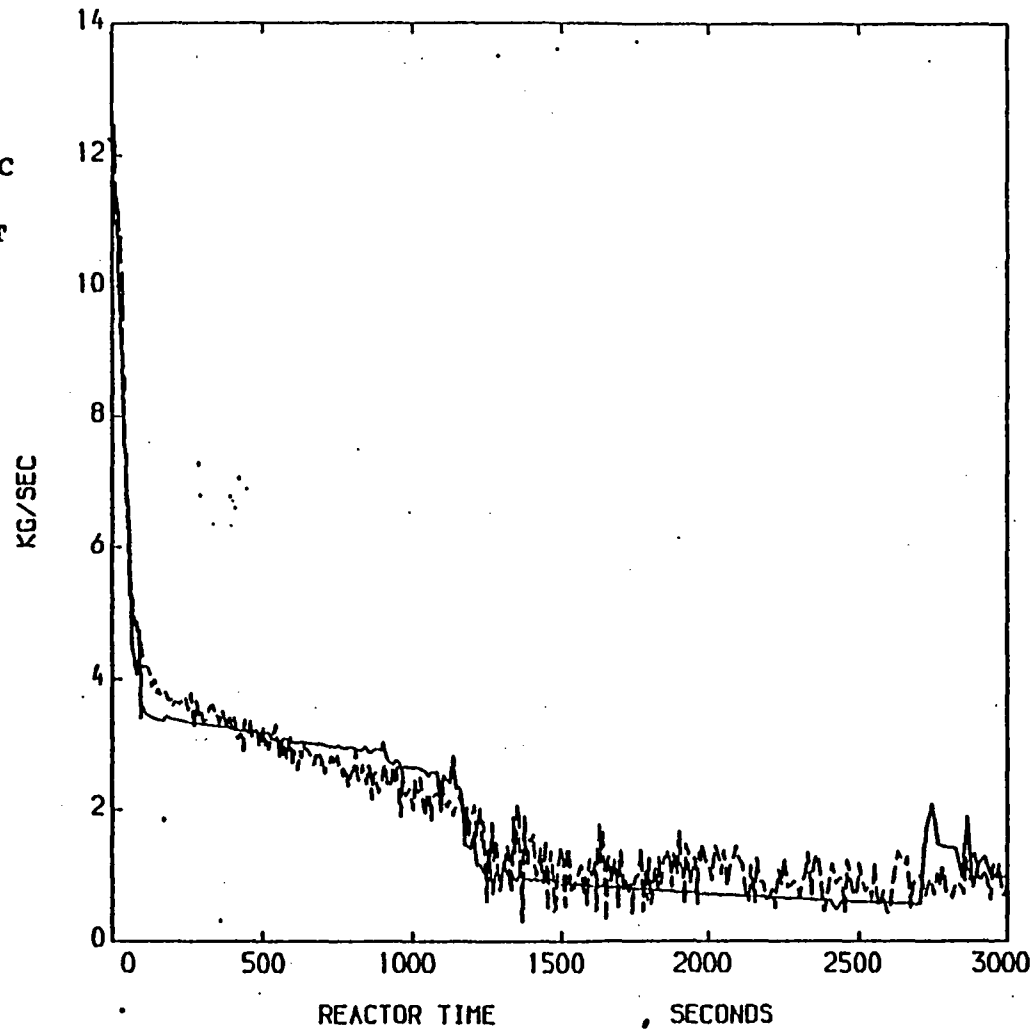


49 DENSITY IN THE BREAK LINE
 LP-SB-2 - TRAC PF1-MOD1 AND EXPERIMENT COMPARISON

THE FOLLOWING ARE PLOTTED AGAINST REACTOR TIME
 MASS FLOW RATE ,FR-PC-503

KEY		
SYM BOL	NAME	UNITS
—	MASS FLOW RATE	,KG/SEC
LOC- 98/ 0/ 1	MNEM-FLOW INF-1	
---	FR-PC-503	,KG/SEC
LOC- 23/ 0/ 0	MNEM-FLOW INF-2	

TRAC
 EXPT



50 BREAK MASS FLOW RATE
 LP-SB-2 - TRAC PF1-MOD1 AND EXPERIMENT COMPARISON

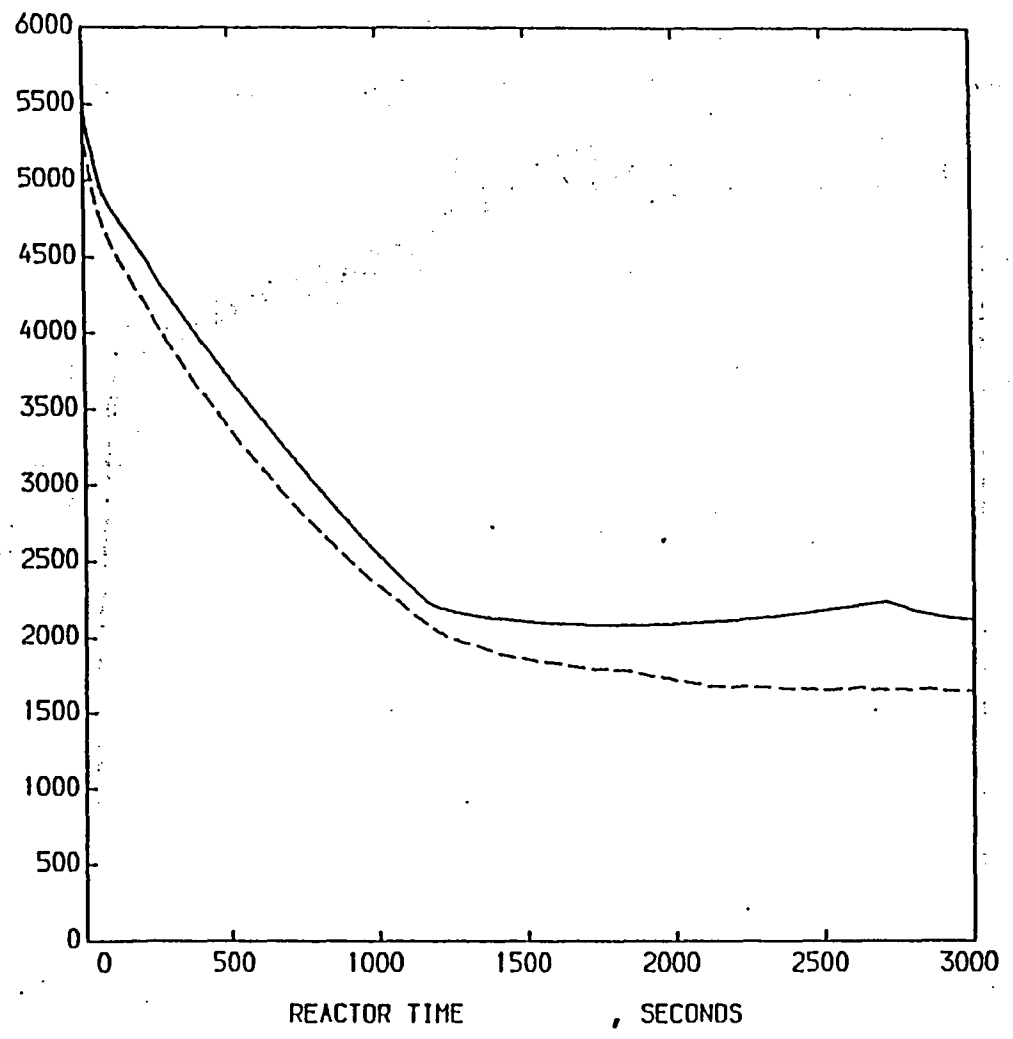
THE FOLLOWING ARE PLOTTED AGAINST REACTOR TIME
CONTROL BLK ID -81,FUNCTION

AEEW - R 2202

83

KEY		
SYH BOL	NAME	UNITS
—	CONTROL BLK ID -81, LOC= 0/ 0/ 1 MNEH=C-81 INF=1	TRAC
- -	FUNCTION	EXPT

TRAC
EXPT



51 TRANSIENT MASS INVENTORY
++PLUS++ PLOTTING UTILITY SYSTEM

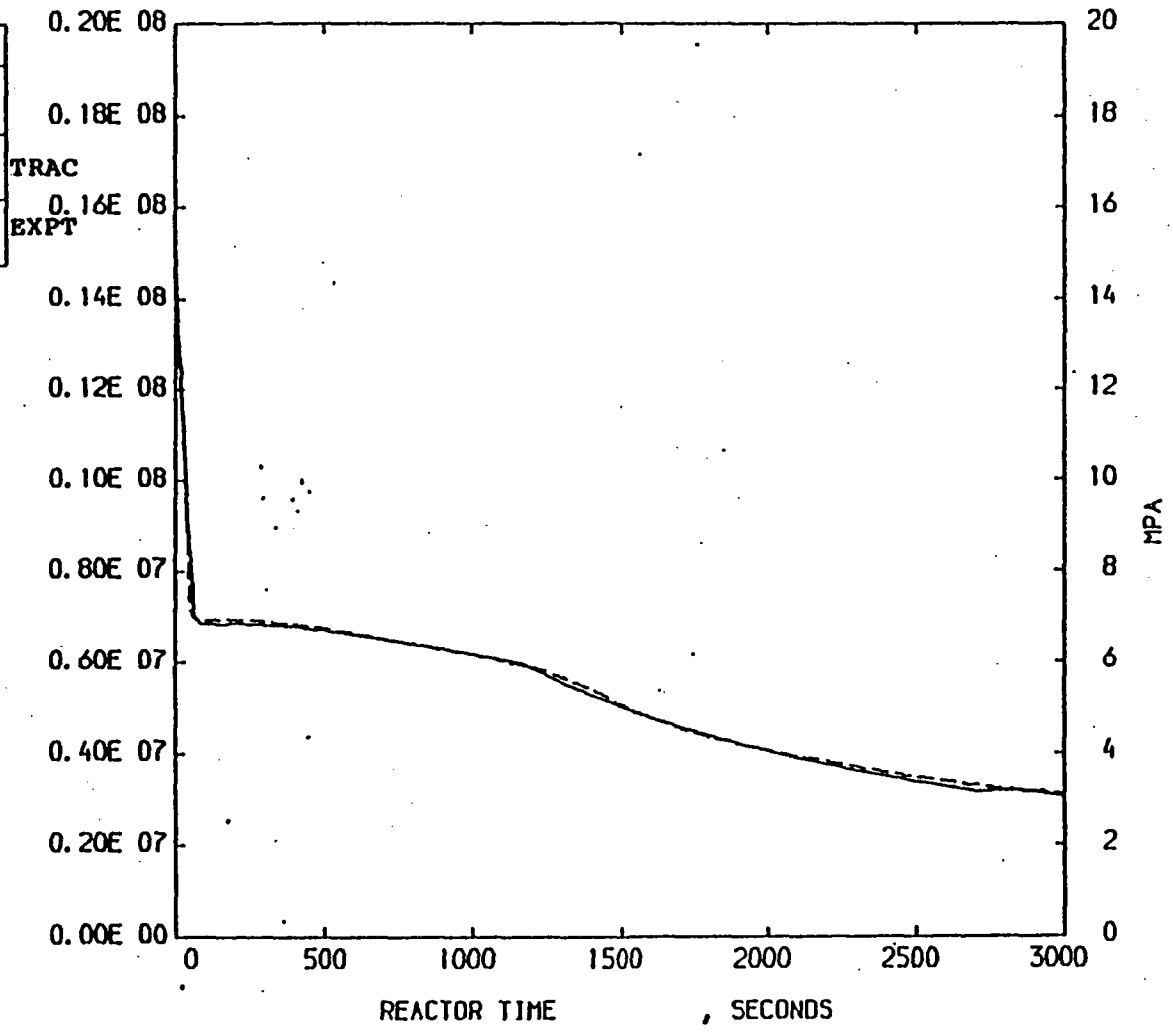
AEEW

AEW - R 2202

Winfrith

THE FOLLOWING ARE PLOTTED AGAINST REACTOR TIME
SIGNAL VAR. NO. 2, PE-PC-002

KEY		
SYM BOL	NAME	UNITS
—	SIGNAL VAR. NO. 2, LOC= 0/ 0/ 1 MNEM-S 2 INF=1	
- -	PE-PC-002 LOC= 77/ 0/ 0 MNEM-PRES INF=2	,MPA



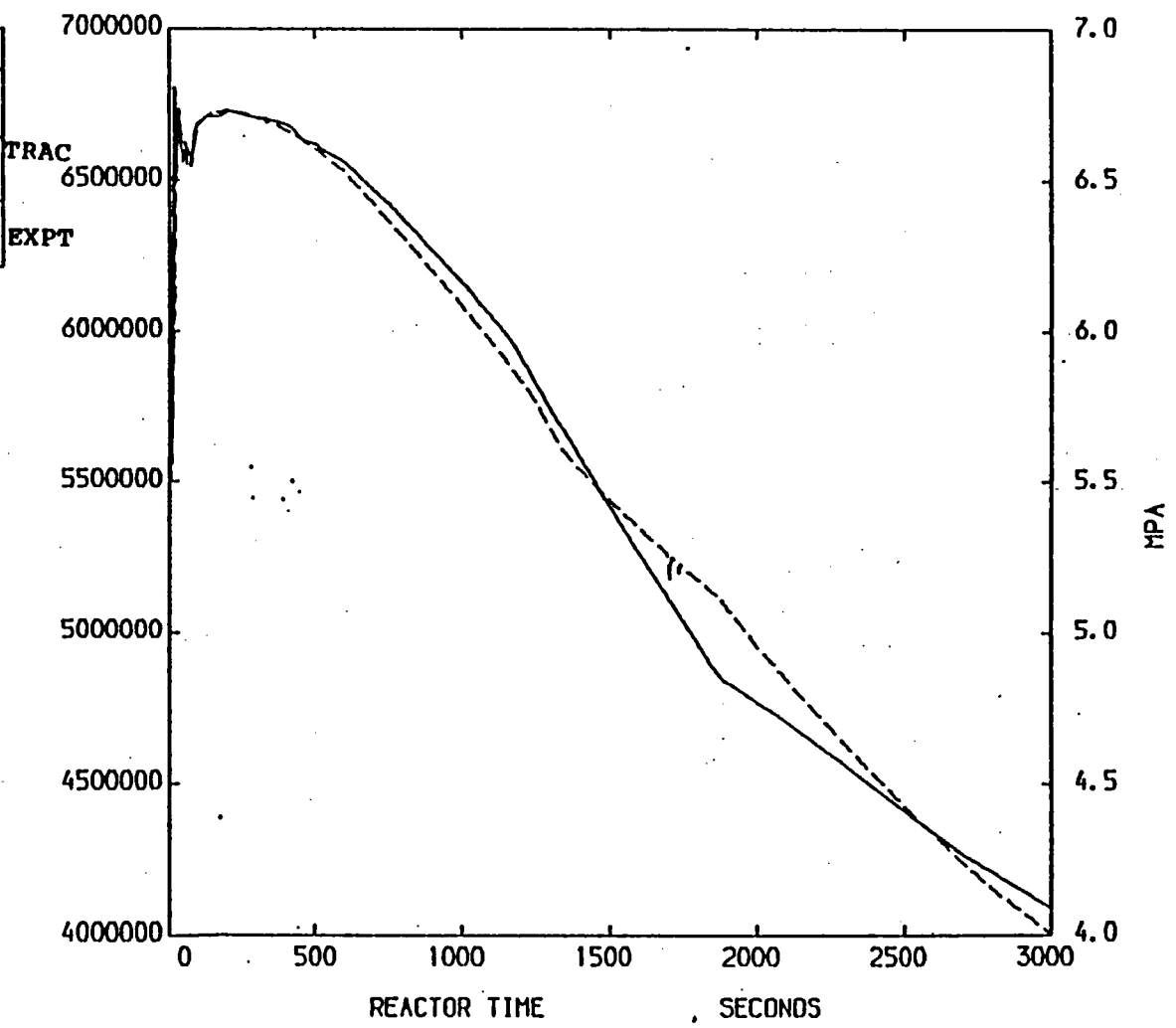
84

52 INTACT LOOP HOT LEG PRESSURE
LP-SB-2 - TRAC PF1-MOD1 AND EXPERIMENT COMPARISON

THE FOLLOWING ARE PLOTTED AGAINST REACTOR TIME
 SIGNAL VAR. NO. 6, PE-SGS-001

Winfrith

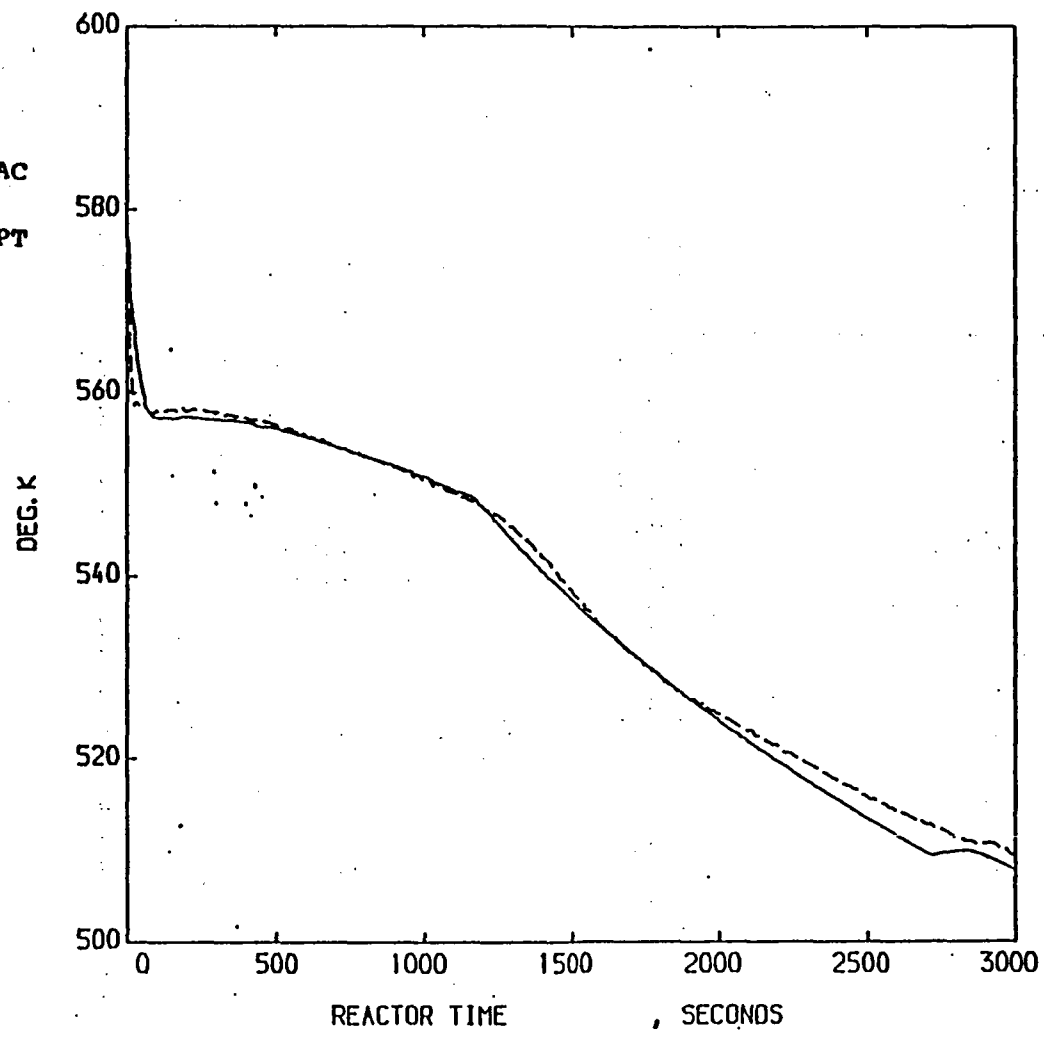
KEY		
SYM BOL	NAME	UNITS
—	SIGNAL VAR. NO. 6,	
	LOC= 0/ 0/ 1 MNEH=S 6 INF=1	
- - -	PE-SGS-001	, MPA
	LOC= 81/ 0/ 0 MNEH-PRES INF=2	



53 SECONDARY SIDE PRESSURE
 LP-SB-2 - TRAC PF1-MOD1 AND EXPERIMENT COMPARISON

THE FOLLOWING ARE PLOTTED AGAINST REACTOR TIME
LIQUID TEMPERATURE ,TE-PC-002B

KEY		
SYM BOL	NAME	UNITS
—	LIQUID TEMPERATURE	,DEG.K
LOC= 99/ 0/ 2	MNEM=TEHL	INF=1
---	TE-PC-002B	,DEG.K
LOC= 130/ 0/ 0	MNEM=TMCL	INF=2

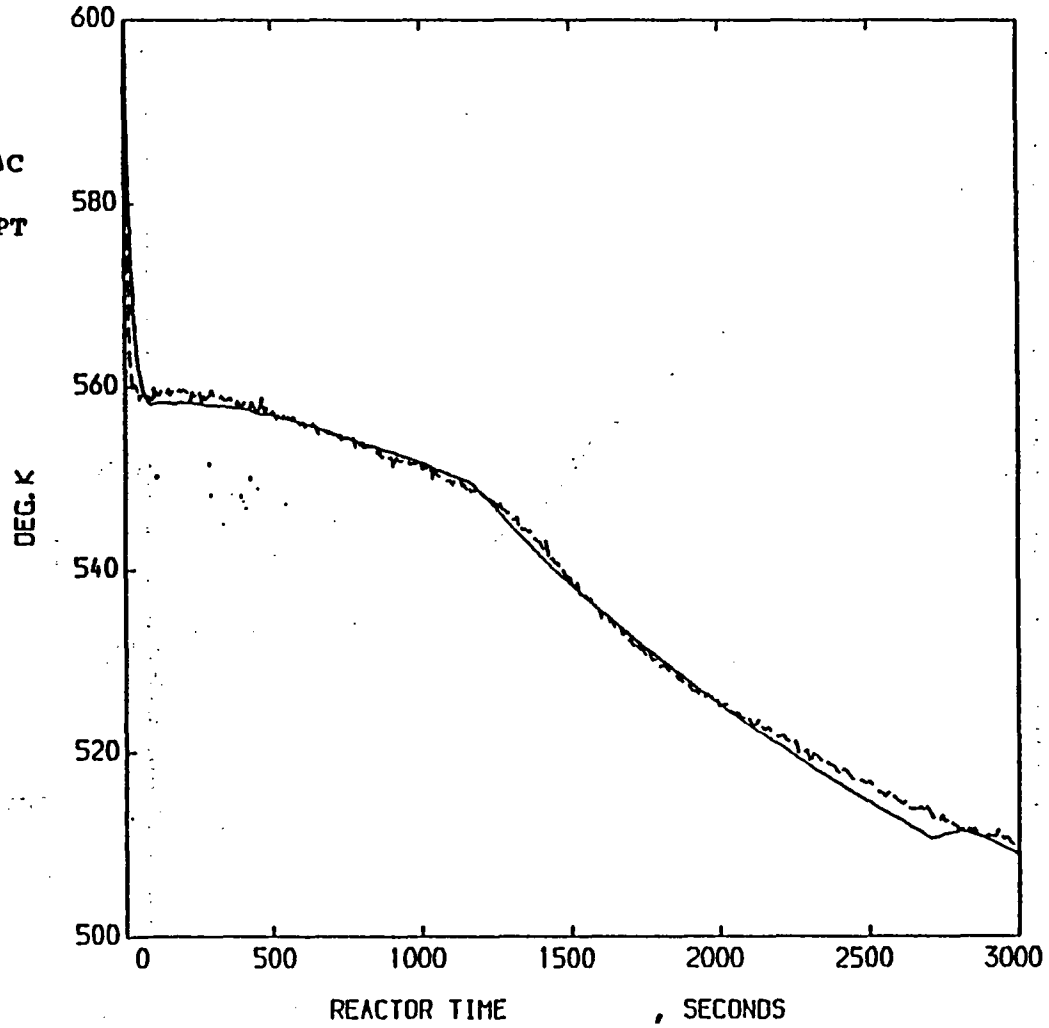


54 LIQ TEMPERATURE IN THE HOT LEG OF THE INTACT LOOP
LP-SB-2 - TRAC PF1-MOD1 AND EXPERIMENT COMPARISON

THE FOLLOWING ARE PLOTTED AGAINST REACTOR TIME
 CLADDING TEMP -FINE, TE-SH07-058

KEY		
SYMBOL	NAME	UNITS
—	CLADDING TEMP -FINE, DEG. K	
LOC= 88/ 1/ 5	MNEM=TMCL INF=1	
---	TE-SH07-058 , DEG. K	
LOC= 272/ 0/ 0	MNEM=TMCL INF=2	

TRAC
 EXPT



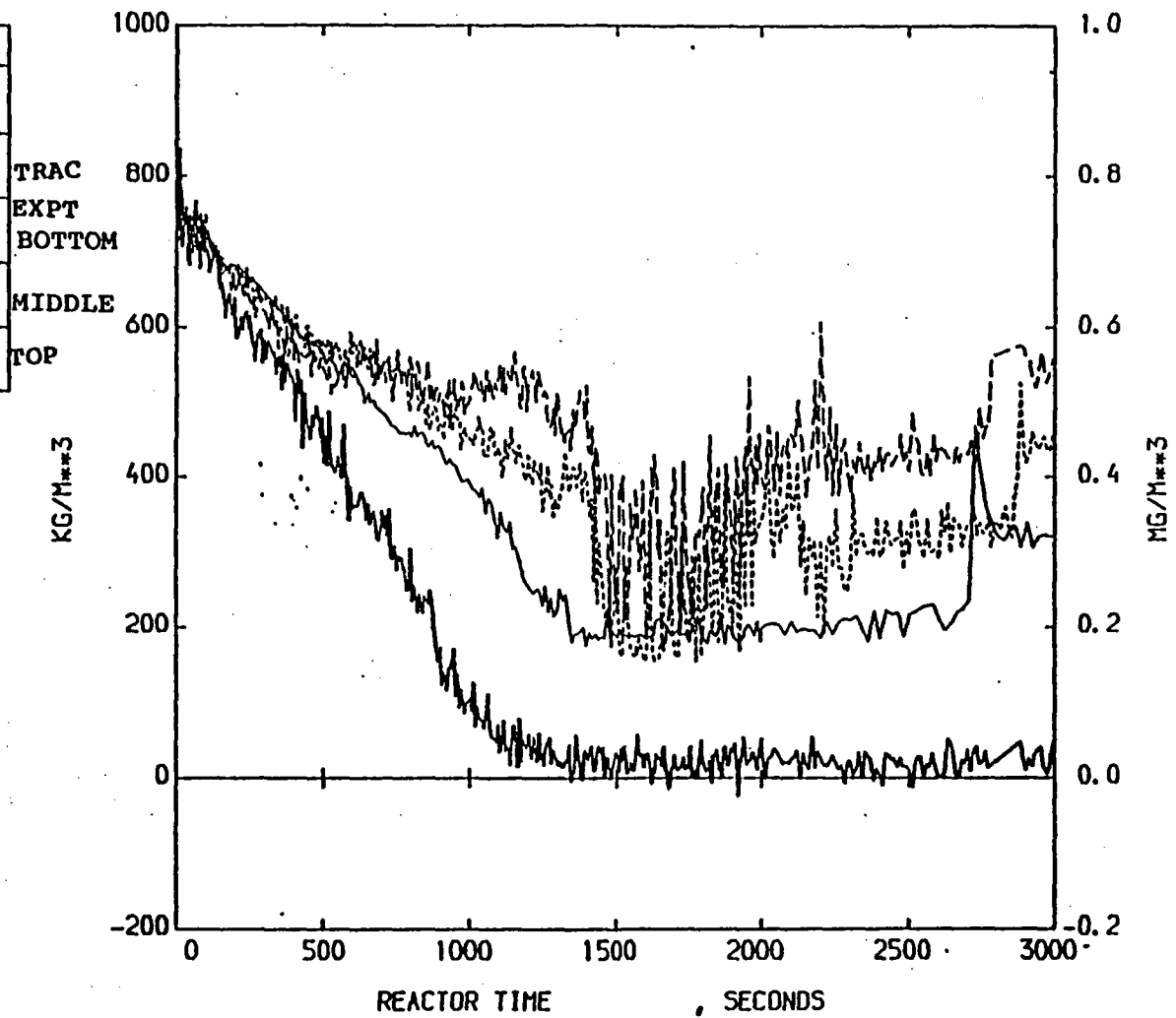
55 CLADDING TEMPERATURE NEAR TOP OF THE CORE
 LP-SB-2 - TRAC PF1-MODI AND EXPERIMENT COMPARISON

Winfrith

THE FOLLOWING ARE PLOTTED AGAINST REACTOR TIME

MIXTURE DENSITY , DE-PC-002A , DE-PC-002B
 DE-PC-002C

KEY		
SYH BOL	NAME	UNITS
—	MIXTURE DENSITY	,KG/M ³
LOC= 99/ 0/ 2	MNEH-DENH INF=1	
- -	DE-PC-002A	,MG/M ³
LOC= 8/ 0/ 0	MNEH-DENH INF=2	
----	DE-PC-002B	,MG/M ³
LOC= 9/ 0/ 0	MNEH-DENH INF=2	
—	DE-PC-002C	,MG/M ³
LOC= 10/ 0/ 0	MNEH-DENH INF=2	



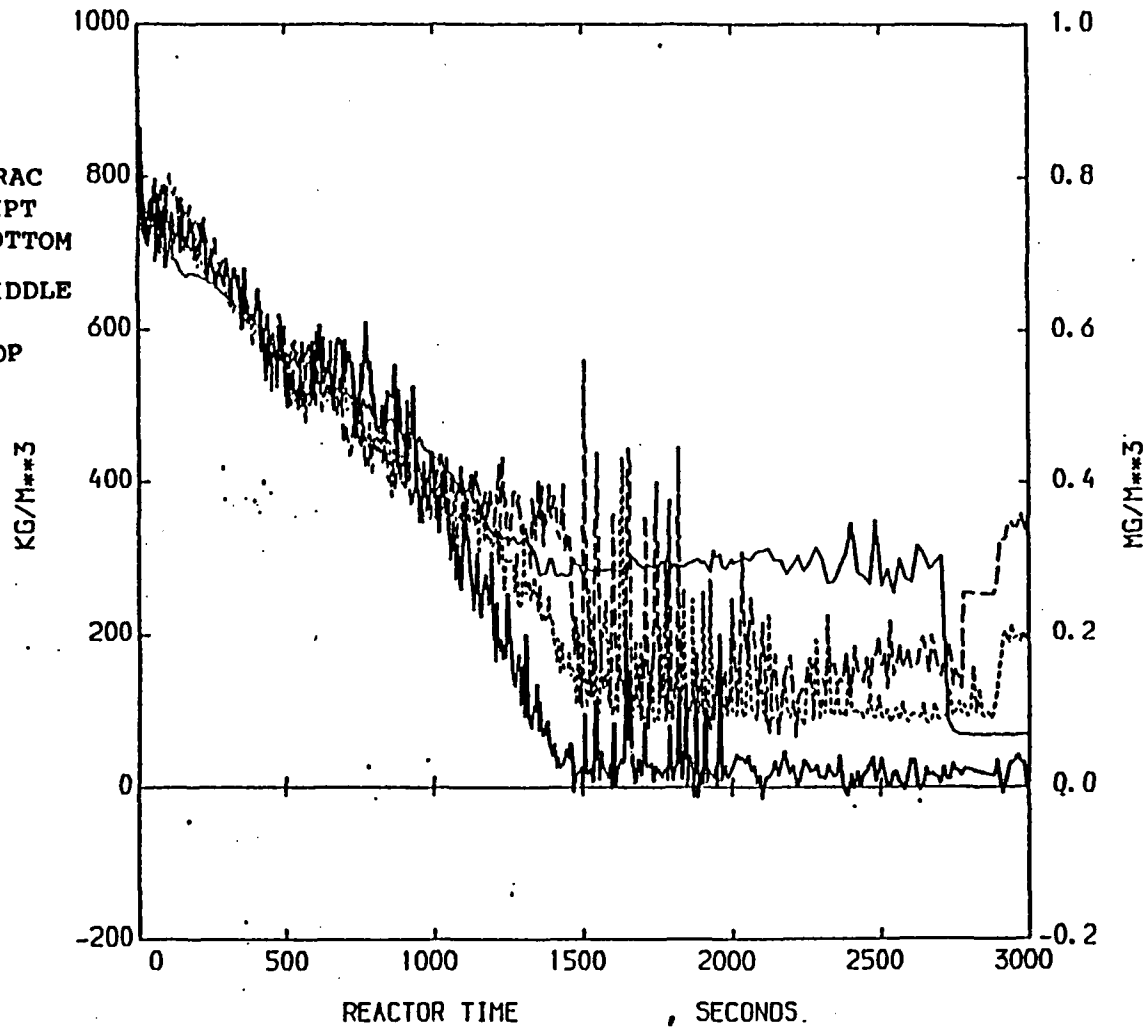
56 DENSITY IN THE HOT LEG INTACT LOOP
 LP-SB-2 - TRAC PF1-MOD1 AND EXPERIMENT COMPARISON

THE FOLLOWING ARE PLOTTED AGAINST REACTOR TIME

MIXTURE DENSITY ,DE-PC-001A ,DE-PC-001B
 DE-PC-001C

KEY		
SYM BOL	NAME	UNITS
—	MIXTURE DENSITY	,KG/M**3
LOC= 7/ 0/ 4	MNEH-DENH INF=1	
---	DE-PC-001A	,HG/M**3
LOC= 5/ 0/ 0	MNEH-DENH INF=2	
----	DE-PC-001B	,HG/M**3
LOC= 6/ 0/ 0	MNEH-DENH INF=2	
---	DE-PC-001C	,HG/M**3
LOC= 7/ 0/ 0	MNEH-DENH INF=2	

TRAC
 EXPT
 BOTTOM
 MIDDLE
 TOP

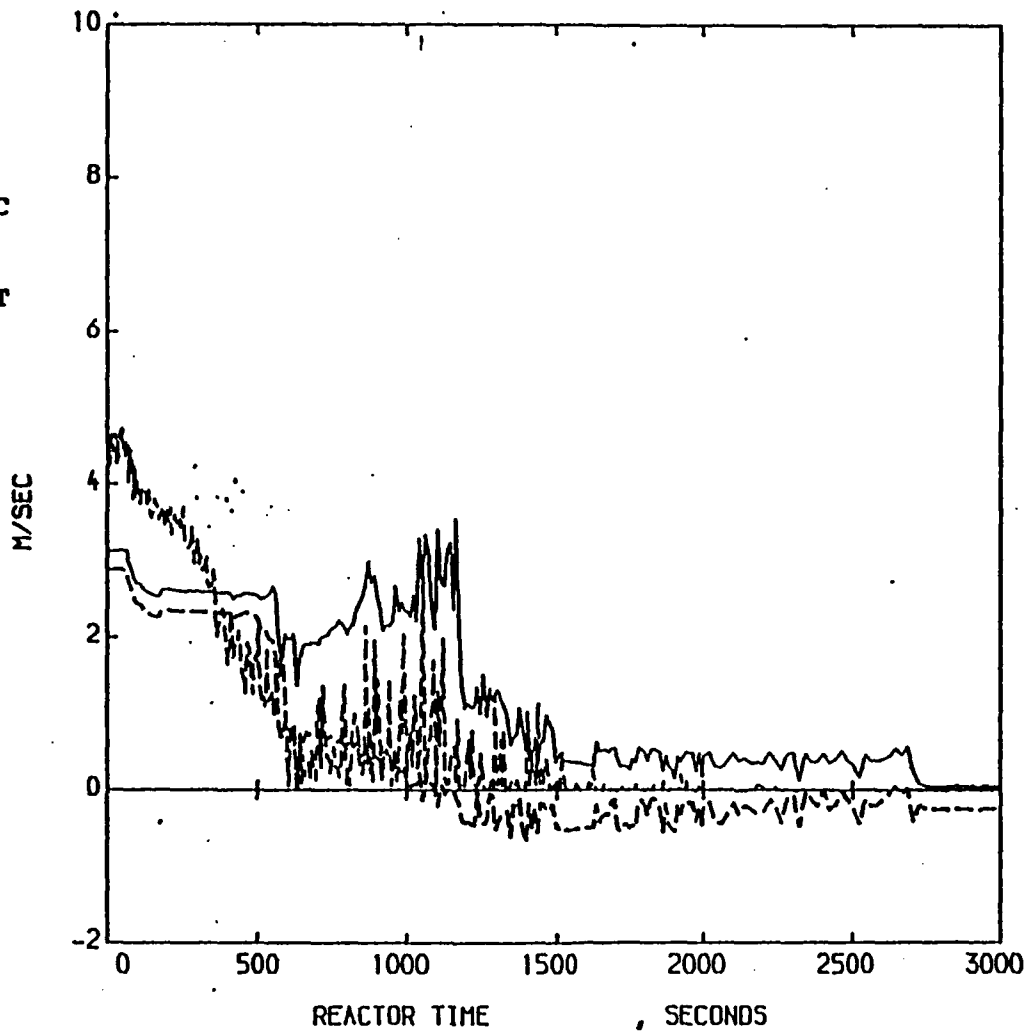


57 DENSITY IN THE COLD LEG OF THE INTACT LOOP
 LP-SB-2 - TRAC PF1-MOD1 AND EXPERIMENT COMPARISON

THE FOLLOWING ARE PLOTTED AGAINST REACTOR TIME
 LIQUID VELOCITY , VAPOR VELOCITY , FE-1ST-001

KEY		
SYM BOL	NAME	UNITS
—	LIQUID VELOCITY	,M/SEC
LOC= 86/ 0/ 8	MNEM=VLIQ	INF=1
- - -	VAPOR VELOCITY	,M/SEC
LOC= 86/ 0/ 8	MNEM=VAP	INF=1
- - -	FE-1ST-001	,M/SEC
LOC= 18/ 0/ 0	MNEM=FE	INF=2

TRAC
 EXPT



58 LIQ AND VAP VELOCITY IN THE DOWNCOMER OF THE REACTOR VESSEL
 LP-SB-2 - TRAC PF1-MOD1 AND EXPERIMENT COMPARISON

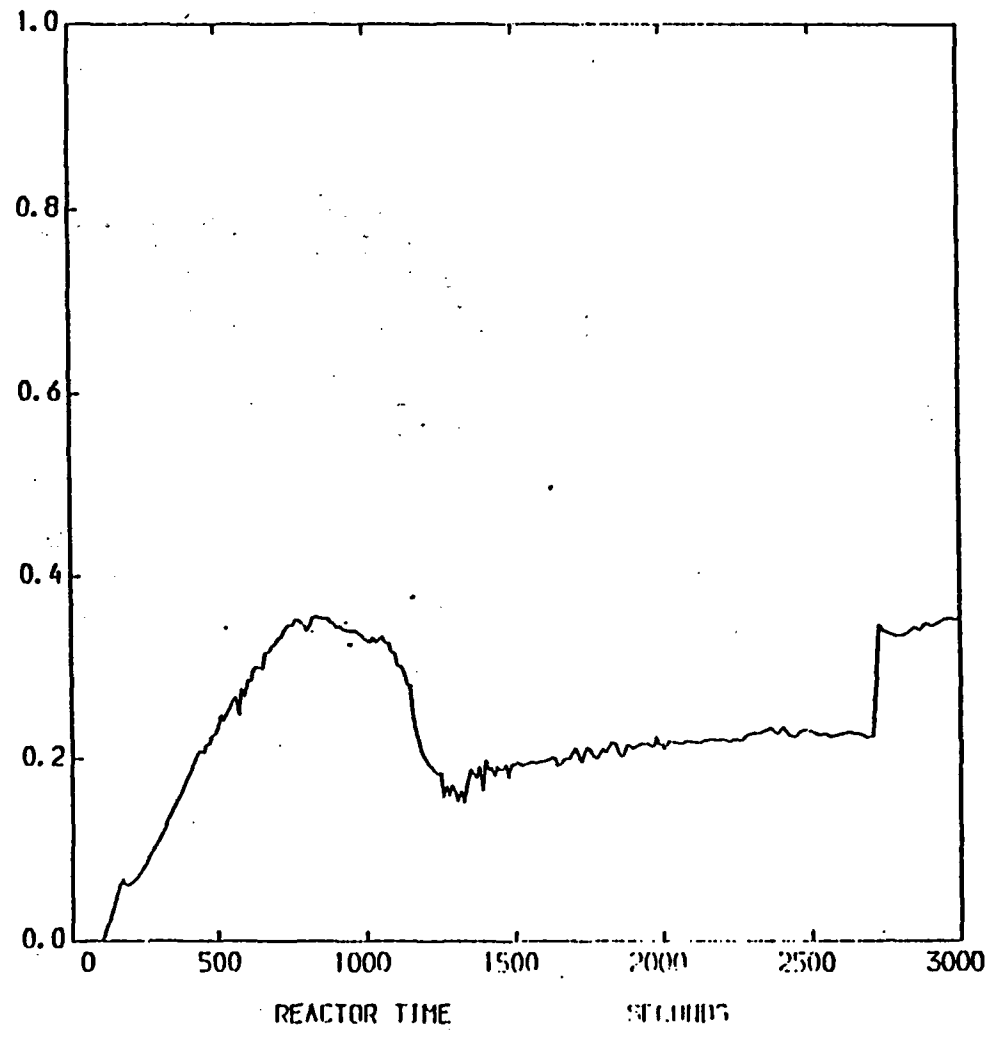
Winfrith

THE FOLLOWING ARE PLOTTED AGAINST REACTOR TIME

VAPOR FRACTION

KEY		
SYM BOL	NAME	UNITS
—	VAPOR FRACTION	
LOC= 08/ 0/ 5	WNEH=VOID	IF=1

TRAC



59 VOID FRACTION TOP FUEL REGION
LP-SB-2 - TRAC PF1-NOD1

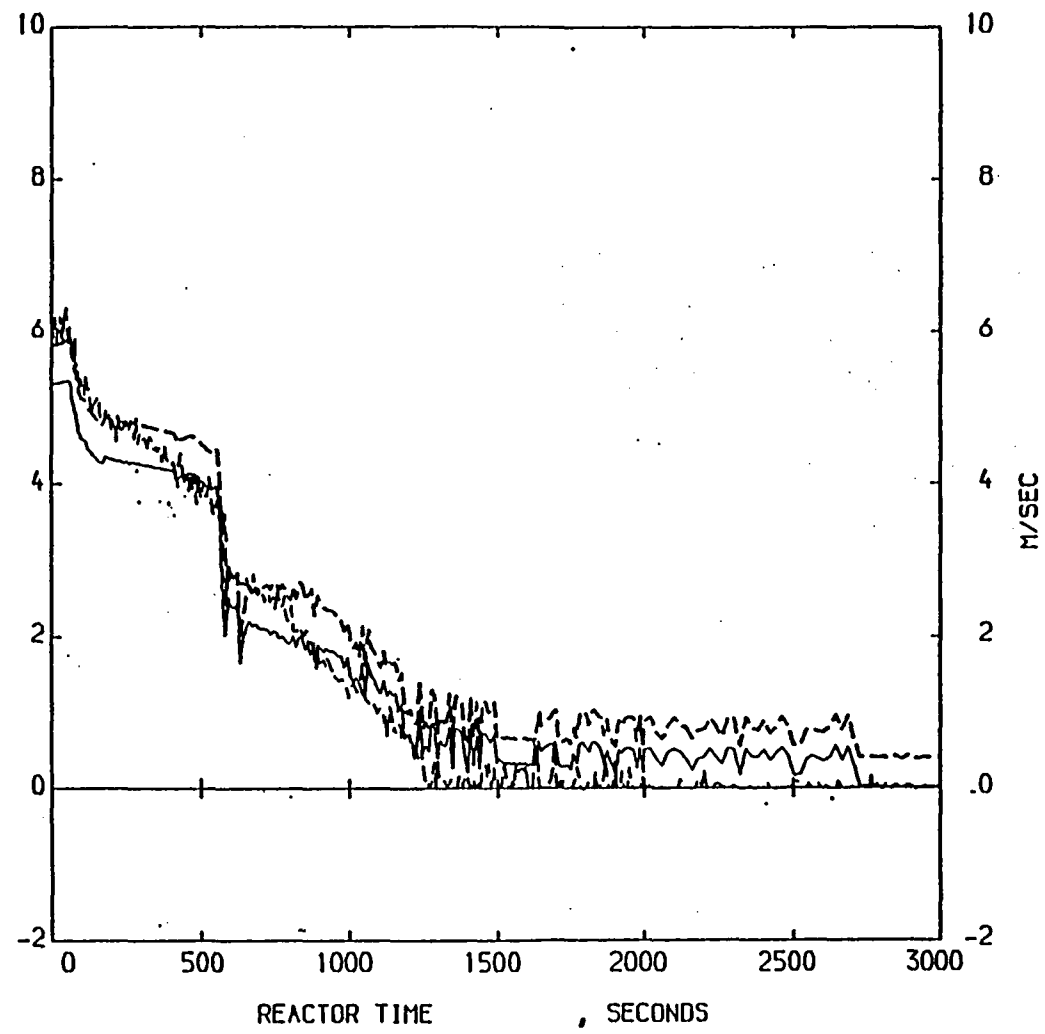
Winfrith

THE FOLLOWING ARE PLOTTED AGAINST REACTOR TIME

FUNCTION , FE-SLP-001

KEY		
SYM BOL	NAME	UNITS
---	FUNCTION VLIO ,	
---	FUNCTION VVAP ,	
---	FE-SLP-001	M/SEC
---	LOC= 20/ 0/ 0 MHEM-FE	INF-2

TRAC
EXPT



60 LIQ AND VAP VELOCITY AT CORE INLET
LP-SB-2 - TRAC PF1-MOD1 AND EXPERIMENT COMPARISON

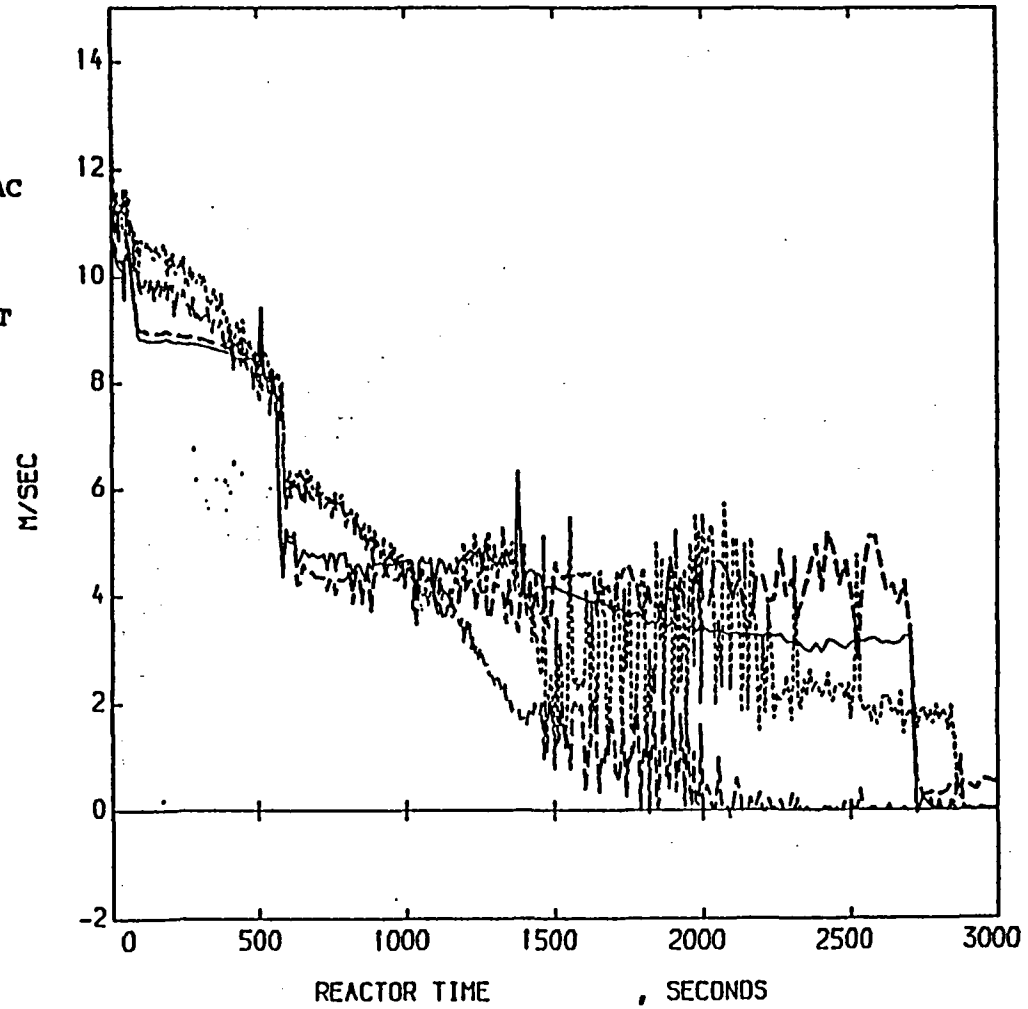
THE FOLLOWING ARE PLOTTED AGAINST REACTOR TIME

LIQUID VELOCITY , VAPOR VELOCITY , FE-PC-002A
 FE-PC-002C

KEY		
SYN BOL	NAME	UNITS
—	LIQUID VELOCITY	,H/SEC
LOC= 99/ 0/ 2	MNEH=VLIO	INF=1
- -	VAPOR VELOCITY	,H/SEC
LOC= 99/ 0/ 2	MNEH=VVAP	INF=1
- -	FE-PC-002A	,H/SEC
LOC= 16/ 0/ 0	MNEH=FE	INF=2
- - - -	FE-PC-002C	,H/SEC
LOC= 17/ 0/ 0	MNEH=FE	INF=2

TRAC

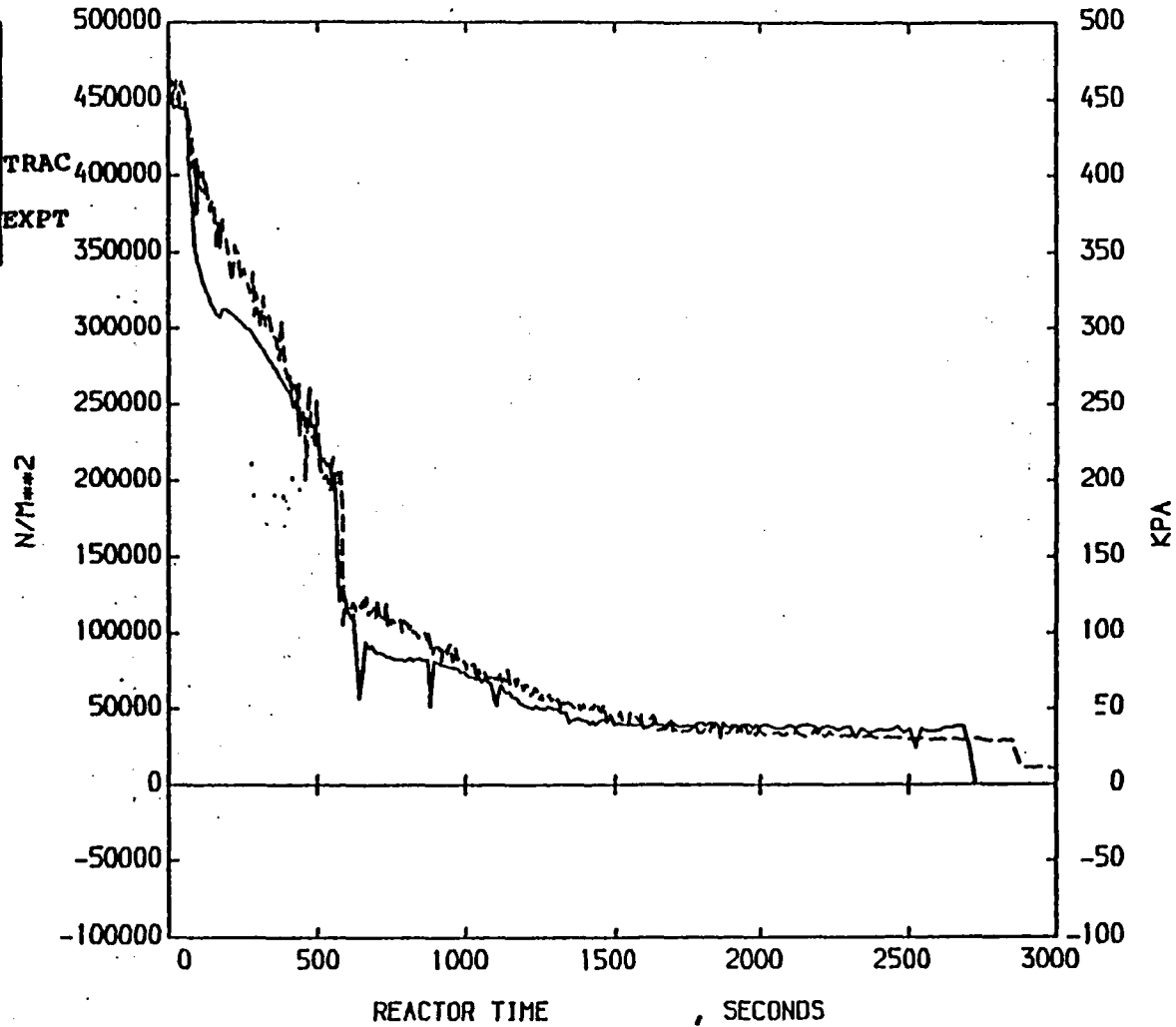
EXPT



61 LIO AND VAP VELOCITY IN THE HOT LEG
 LP-SB-2 - TRAC PF1-MOD1 AND EXPERIMENT COMPARISON

THE FOLLOWING ARE PLOTTED AGAINST REACTOR TIME
 PUMP DELTA-P , PDE-PC-001

KEY		
SYN BOL	NAME	UNITS
—	PUMP DELTA-P	, N/M ²
LOC= 4/ 0/ 1	MNEM=DELP	INF=1
- - -	PDE-PC-001	, KPA
LOC= 65/ 0/ 0	MNEM=PD	INF=2



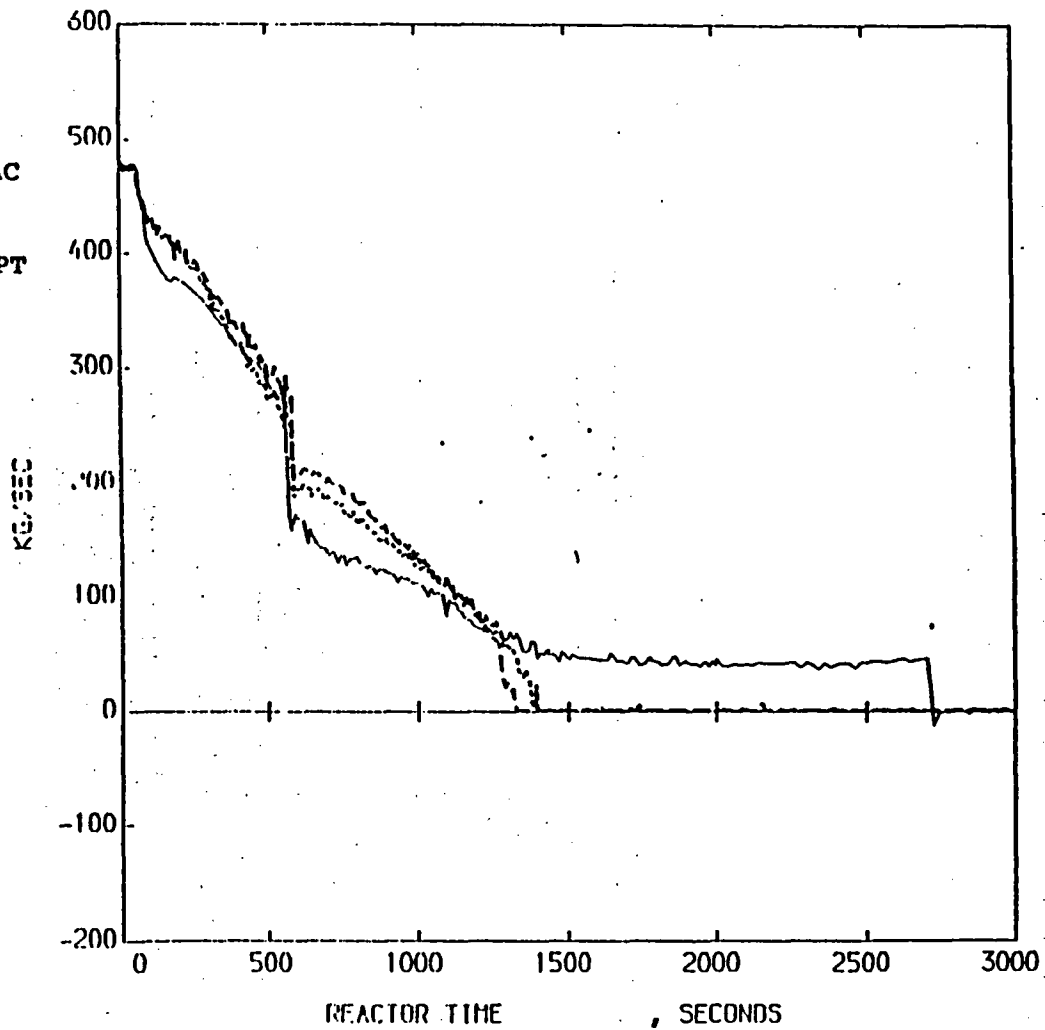
62 PRESSURE DIFFERENCE OVER THE MAIN COOLANT PUMPS
 LP-SB-2 - TRAC PF1-MOD1 AND EXPERIMENT COMPARISON

THE FOLLOWING ARE PLOTTED AGAINST REACTOR TIME
 MASS FLOW RATE , FT-P139-27-1 , FT-P139-27-2

KEY		
SYN BOL	NAME	UNITS
---	MASS FLOW RATE	,KG/SEC
LOC= 1/ 0/ 3	MNEM=FLOV INF=1	
---	FT-P139-27-1	,KG/SEC
LOC= 30/ 0/ 0	MNEM=FLOV INF=2	
----	FT-P139-27-2	,KG/SEC
LOC= 31/ 0/ 0	MNEM=FLOV INF=2	

TRAC

EXPT



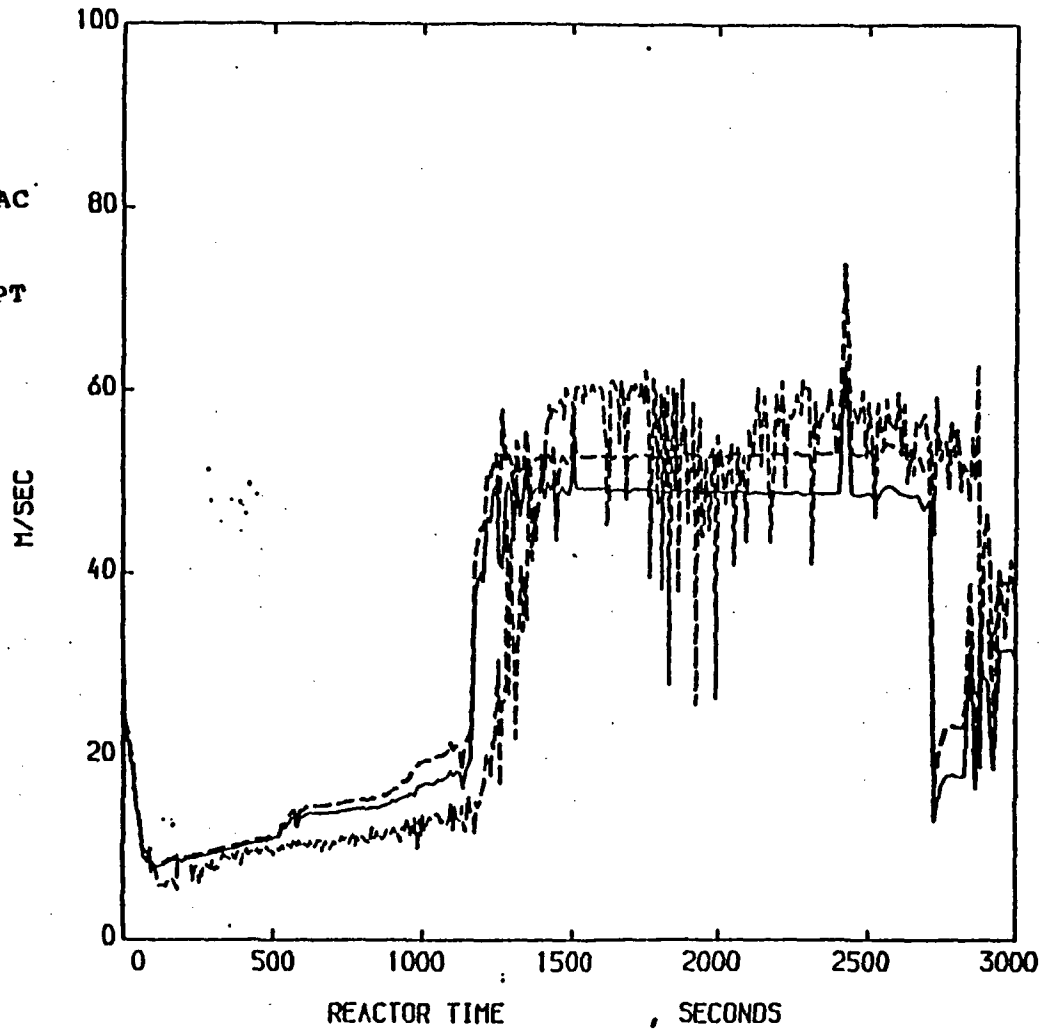
63 HOT LEG MASS FLOW RATE AT VENTURI LOCATION
 LP-SB-2 - TRAC PF1-MOD1 AND EXPERIMENT COMPARISON

THE FOLLOWING ARE PLOTTED AGAINST REACTOR TIME
 LIQUID VELOCITY , VAPOR VELOCITY , FE-PC-503

AEEM - R 2202

KEY		
SYM BOL	NAME	UNITS
—	LIQUID VELOCITY	,M/SEC
LOC= 95/ 0/ 4	MNEM=VLID	INF=1
- -	VAPOR VELOCITY	,M/SEC
LOC= 95/ 0/ 4	MNEM=VVAP	INF=1
- -	FE-PC-503	,M/SEC
LOC= 14/ 0/ 0	MNEM=FE	INF=2

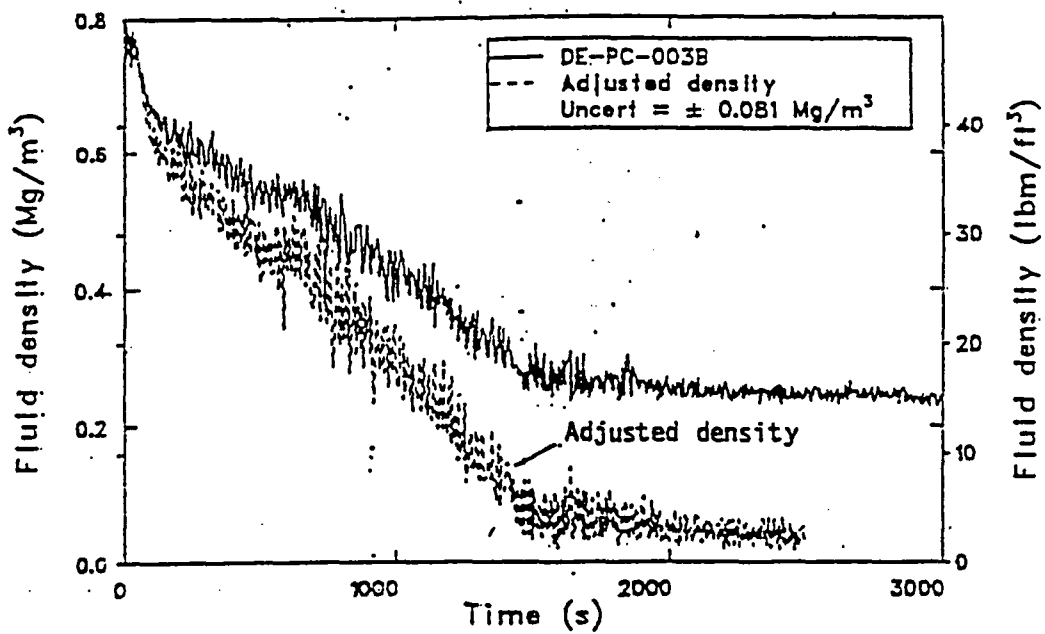
TRAC
 EXPT



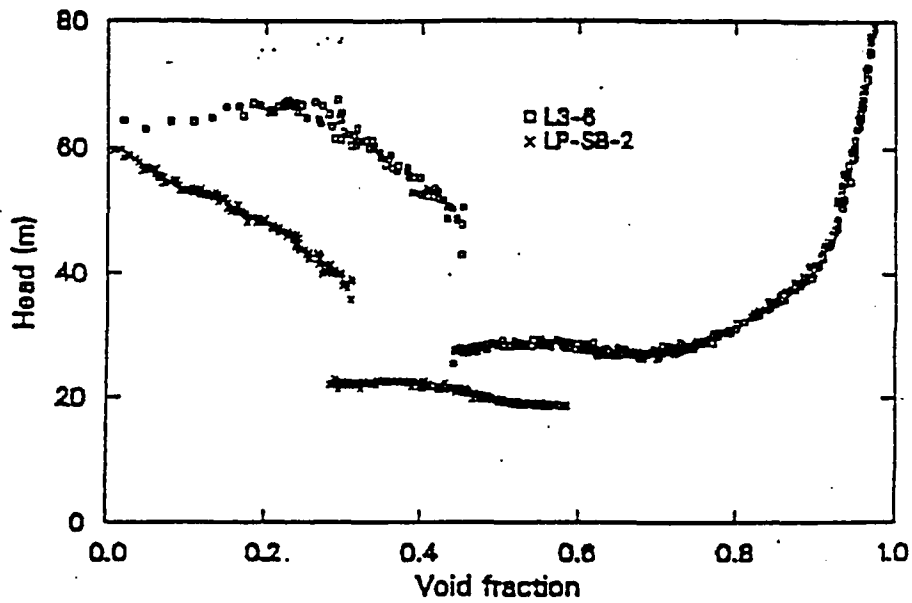
96

64 LIQ AND VAP VELOCITY IN THE BREAK LINE
 LP-SB-2 - TRAC PF1-MOD1 AND EXPERIMENT COMPARISON

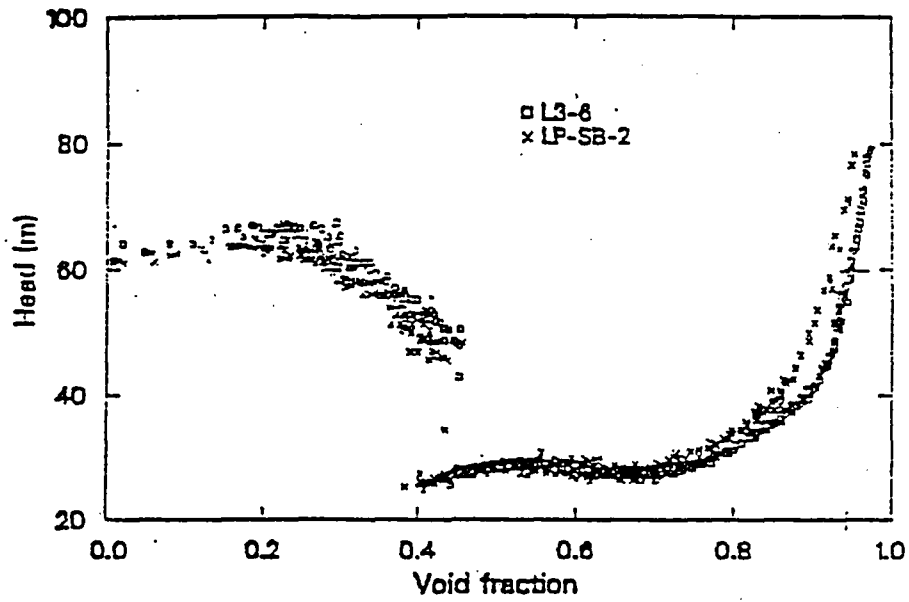
EXPERIMENT LP-SB-2



A1 Measured and adjusted cold leg densities at the steam generator outlet. From Reference 4



A2 Pump head as a function of void fraction for Experiments LP-SB-2 and L3-6. From Reference 4

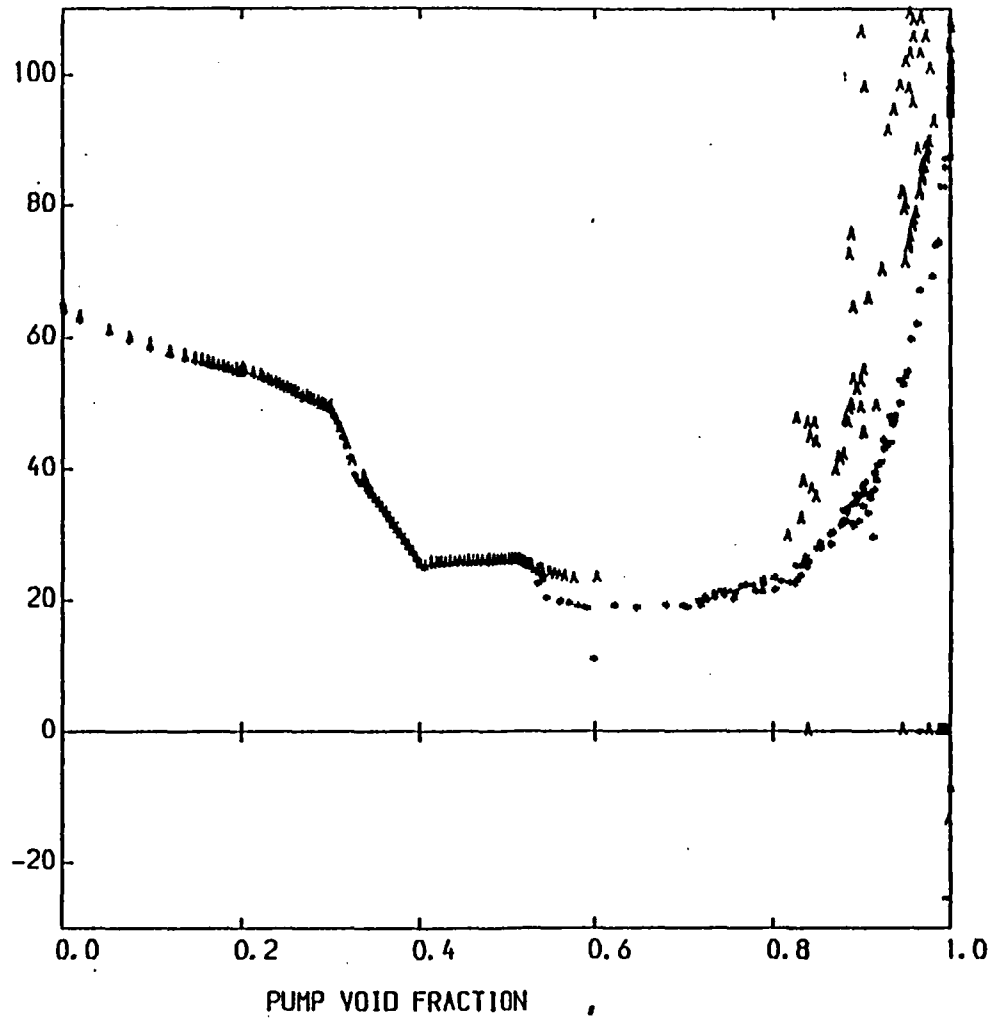


A3 Pump head as a function of void fraction obtained using the adjusted density at the steam generator outlet for Experiment LP-SB-2. From Reference 4

THE FOLLOWING ARE PLOTTED AGAINST PUMP VOID FRACTION
FUNCTION

KEY		
SYM BOL	NAME	UNITS
.	FUNCTION PUMP 2 ,	
A	FUNCTION PUMP 1 ,	

TRAC



A4 PUMP HEAD VS VOID FRACTION IN RUN A

++PLUS++

PLOTTING UTILITY SYSTEM

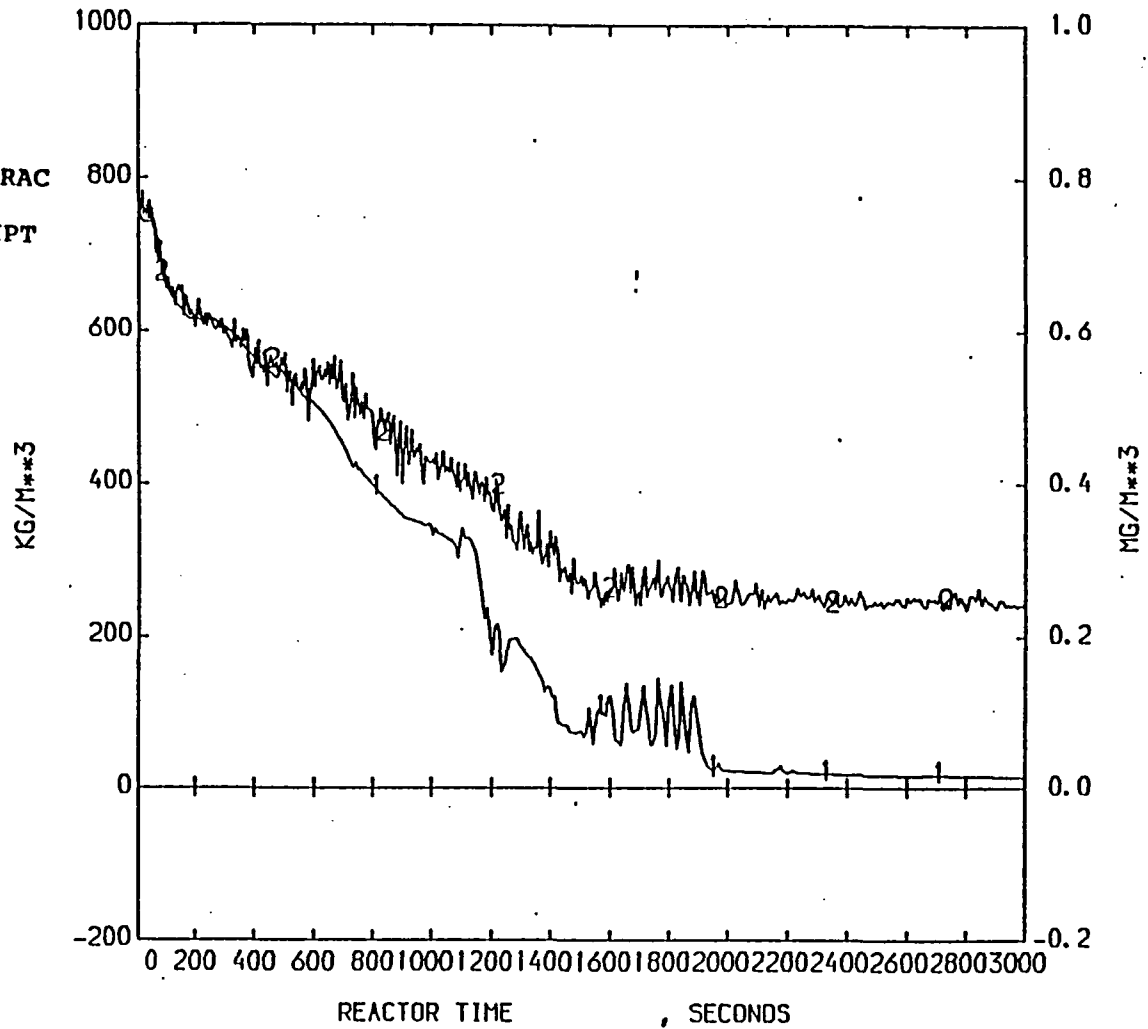
AEW

THE FOLLOWING ARE PLOTTED AGAINST REACTOR TIME
 MIXTURE DENSITY , DE-PC-003B

Winfrith

KEY		
SYM BOL	NAME	UNITS
1	MIXTURE DENSITY	,KG/M**3
LOC= 3/ 0/ 7 MNEH-DENH INF=1		
2	DE-PC-003B	,MG/M**3
LOC= 11/ 0/ 0 MNEH-DENH INF=2		

TRAC
 EXPT



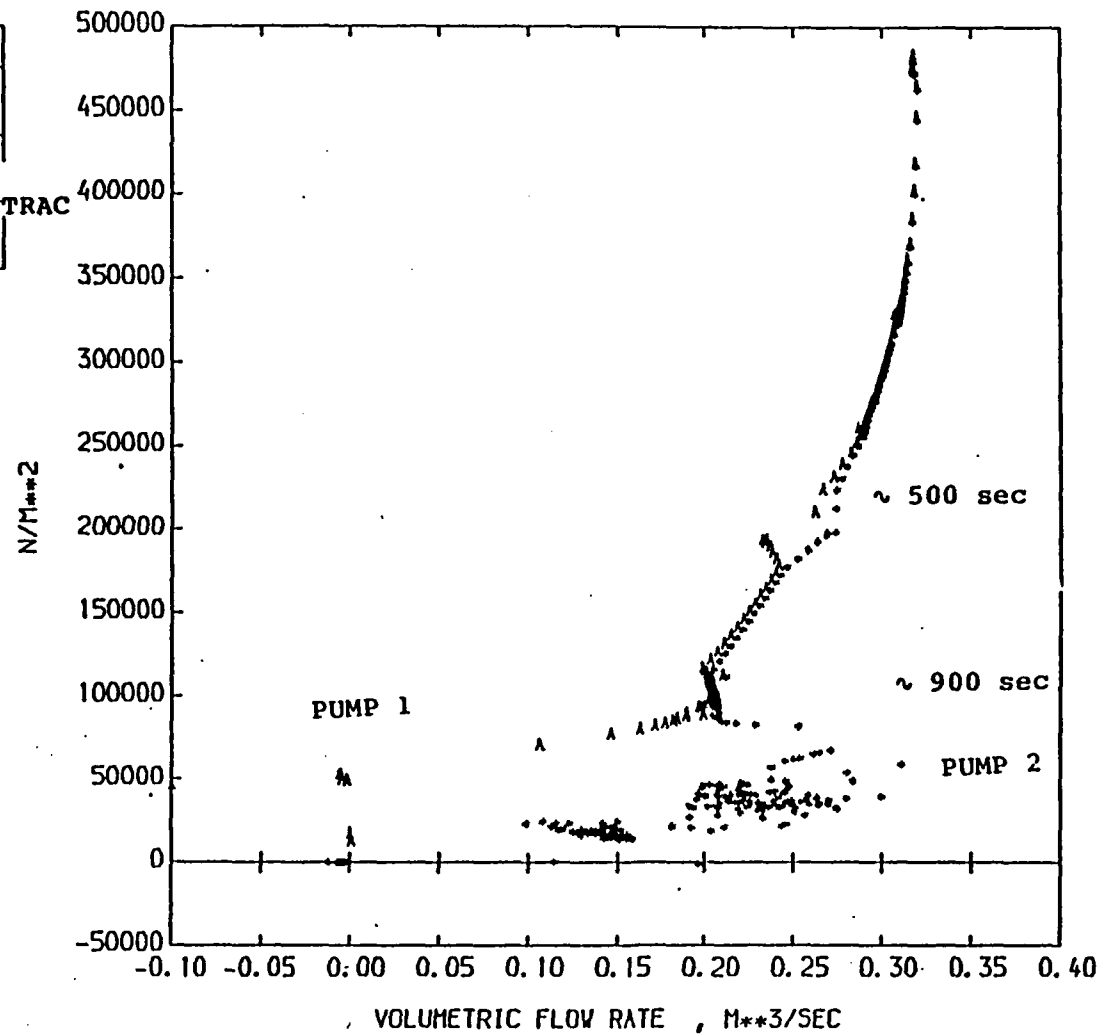
A5
 ++PLUS++

LOOP SEAL DENSITY IN RUN A
 PLOTTING UTILITY SYSTEM

AEEM

THE FOLLOWING ARE PLOTTED AGAINST VOLUMETRIC FLOW RATE
PUMP DELTA-P

KEY		
SYM BOL	NAME	UNITS
•	PUMP DELTA-P	,N/M**2
LOC= 4/ 0/ 1 MNEM=DELP INF=1		
▲	PUMP DELTA-P	,N/M**2
LOC= 5/ 0/ 1 MNEM=DELP INF=1		



A6 PUMPS PRESSURE INCREASE VS VOLUMETRIC FLOW RATE IN RUN A

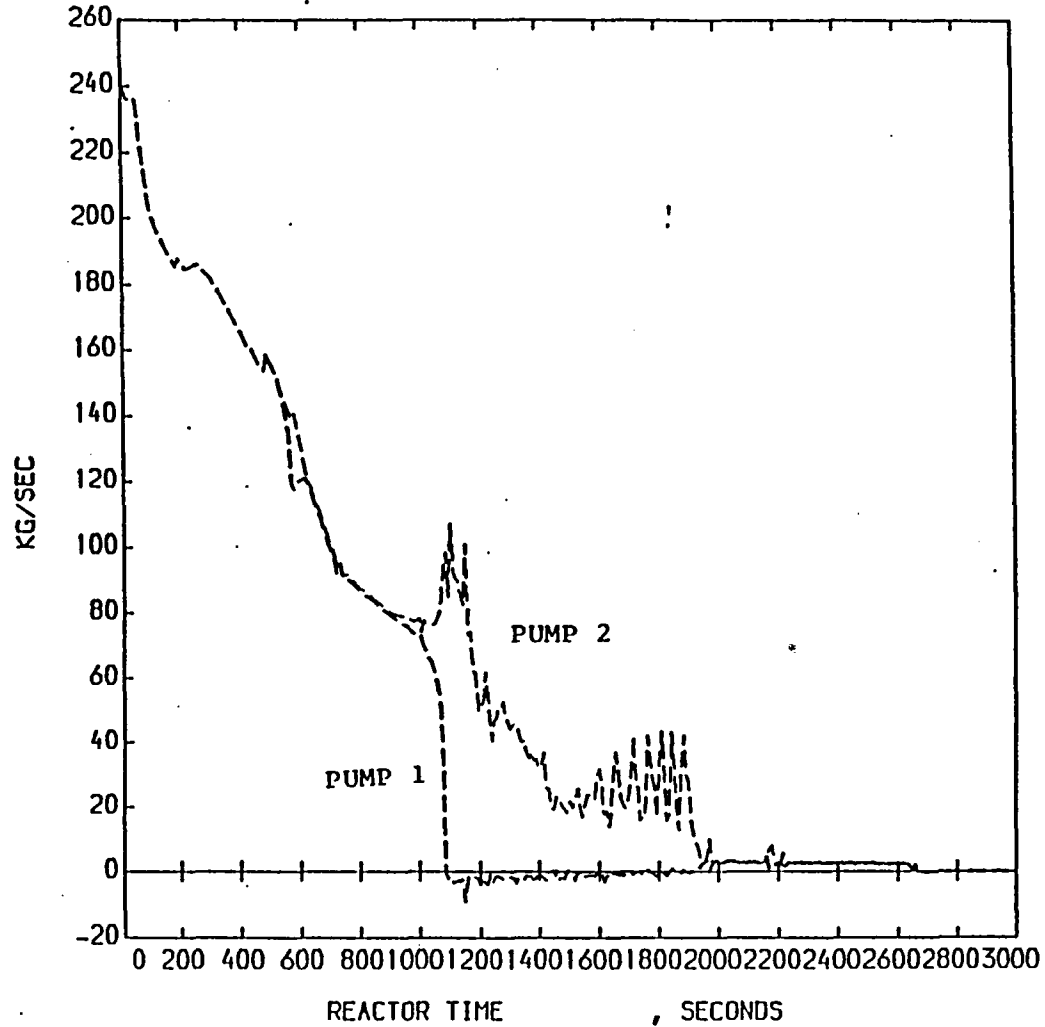
++PLUS++

PLOTTING UTILITY SYSTEM

AEEW

THE FOLLOWING ARE PLOTTED AGAINST REACTOR TIME
 MASS FLOW RATE

KEY		
SYN BOL	NAME	UNITS
--	HASS FLOW RATE	,KG/SEC
LOC= 4/ 0/ 1	MNEH-FLOW INF=1	
--	HASS FLOW RATE	,KG/SEC
LOC= 5/ 0/ 1	MNEH-FLOW INF=1	



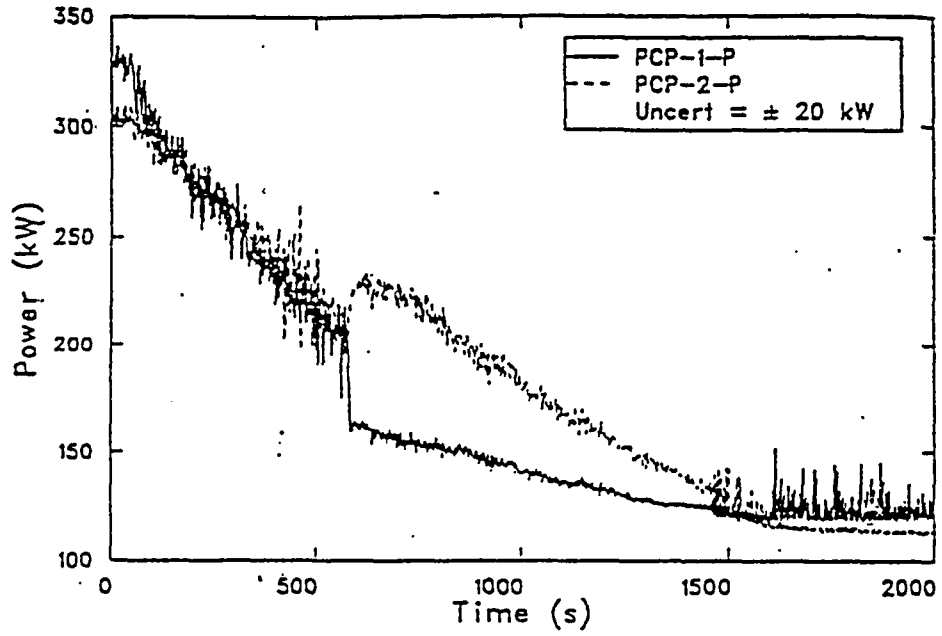
A7 PUMPS MASS FLOW RATE IN RUN A

++PLUS++

PLOTTING UTILITY SYSTEM

AEEW

EXPERIMENT LP-SB-2



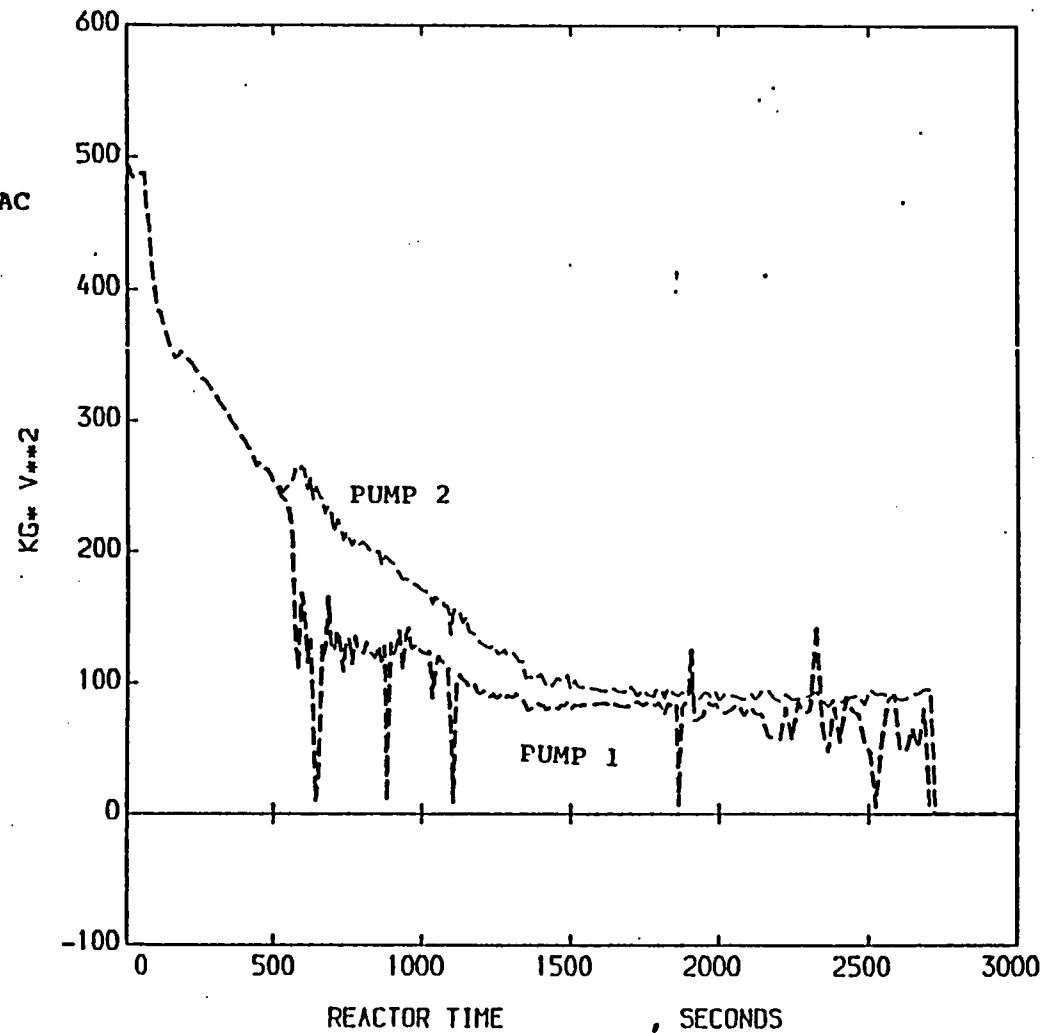
A8 Primary coolant pump power.
From Reference 4

THE FOLLOWING ARE PLOTTED AGAINST REACTOR TIME
PUMP TORQUE

AEW - R 2202

KEY		
SYH BOL	NAME	UNITS.
--	PUMP TORQUE	,KG* V**2
LOC= 4/ 0/ 1	MNEH-TORD INF=1	
--	PUMP TORQUE	,KG* V**2
LOC= 5/ 0/ 1	MNEH-TORD INF=1	

TRAC



105

A9 PUMPS TORQUES IN RUN B

++PLUS++

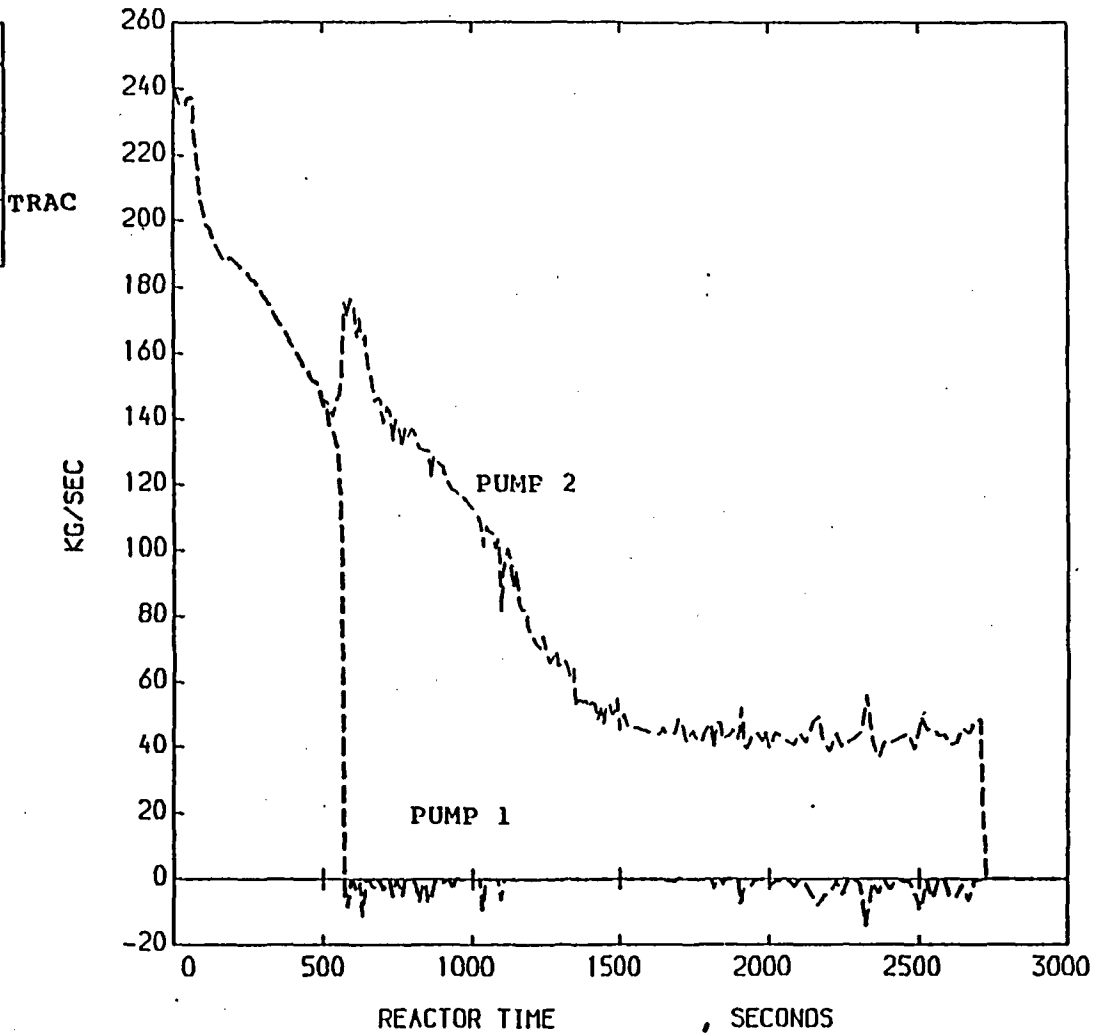
PLOTTING UTILITY SYSTEM

AEW

Winfrith

THE FOLLOWING ARE PLOTTED AGAINST REACTOR TIME
MASS FLOW RATE

KEY		
SYMBOL	NAME	UNITS
--	MASS FLOW RATE	,KG/SEC
LOC= 4/ 0/ 1	MNEM=FLOW INF=1	
--	MASS FLOW RATE	,KG/SEC
LOC= 5/ 0/ 1	MNEM=FLOW INF=1	



A10 PUMPS MASS FLOWS IN RUN B

++PLUS++

PLOTTING UTILITY SYSTEM

AEEM

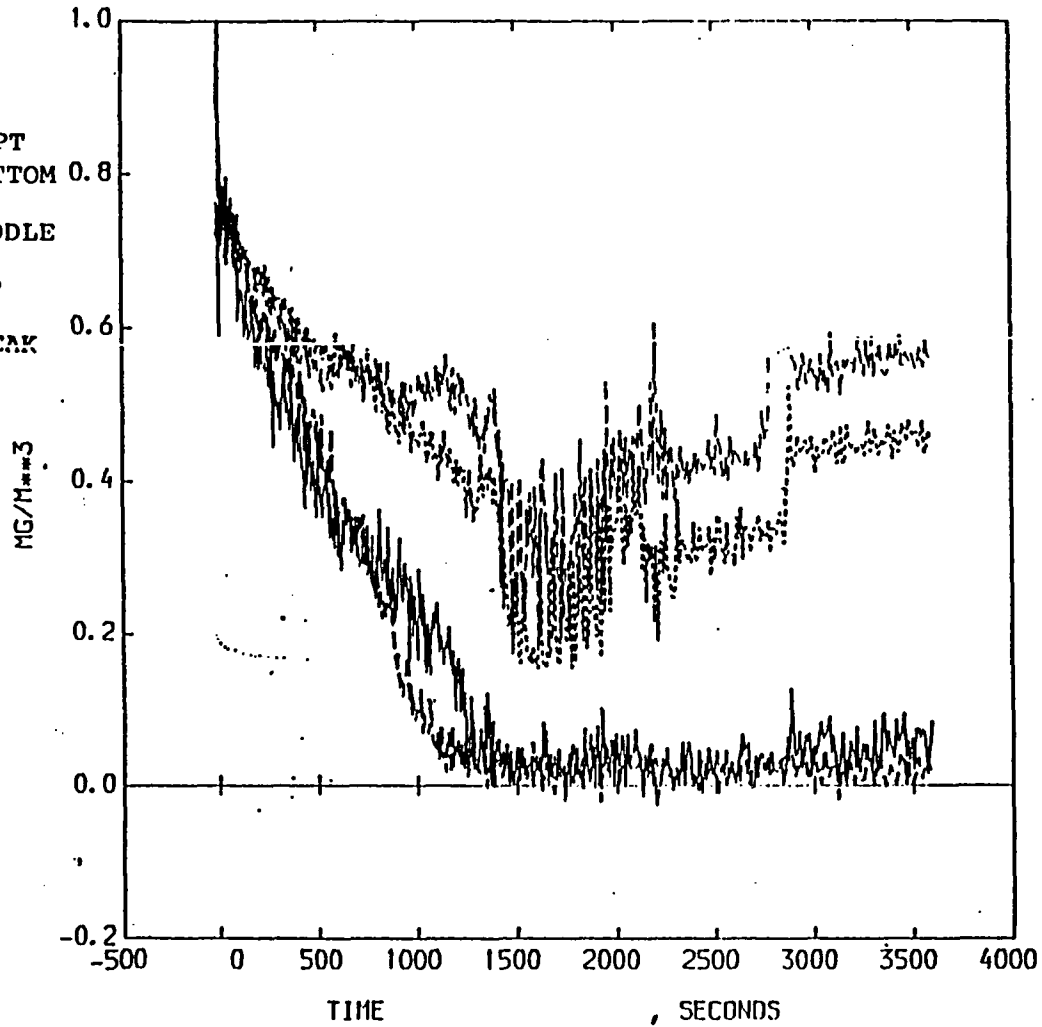
THE FOLLOWING ARE PLOTTED AGAINST TIME

DE-PC-002A
DE-PC-S04B

,DE-PC-002B

,DE-PC-002C

KEY		
SYMBOL	NAME	UNITS
---	DE-PC-002A	,MG/M**3
LOC=	8/ 0/ 0	MNEM=DENH INF=2
----	DE-PC-002B	,MG/M**3
LOC=	9/ 0/ 0	MNEM=DENH INF=2
---	DE-PC-002C	,MG/M**3
LOC=	10/ 0/ 0	MNEM=DENH INF=2
---	DE-PC-S04B	,MG/M**3
LOC=	4/ 0/ 0	MNEM=DENH INF=2

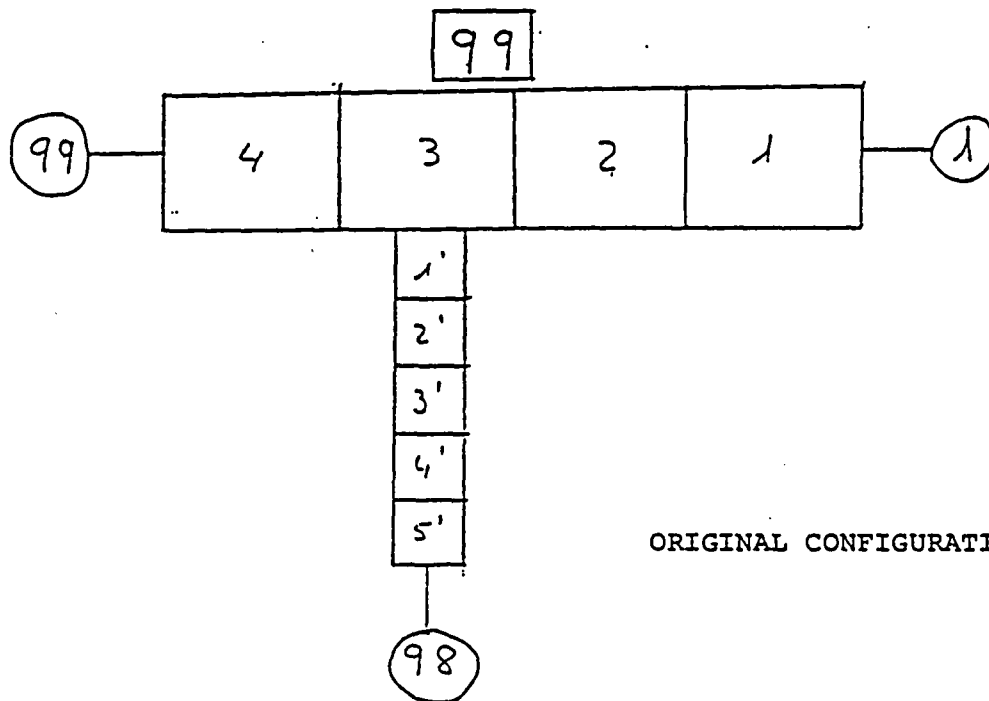


B1 EXPERIMENTAL HOT LEG DENSITY AND BREAK LINE DENSITY

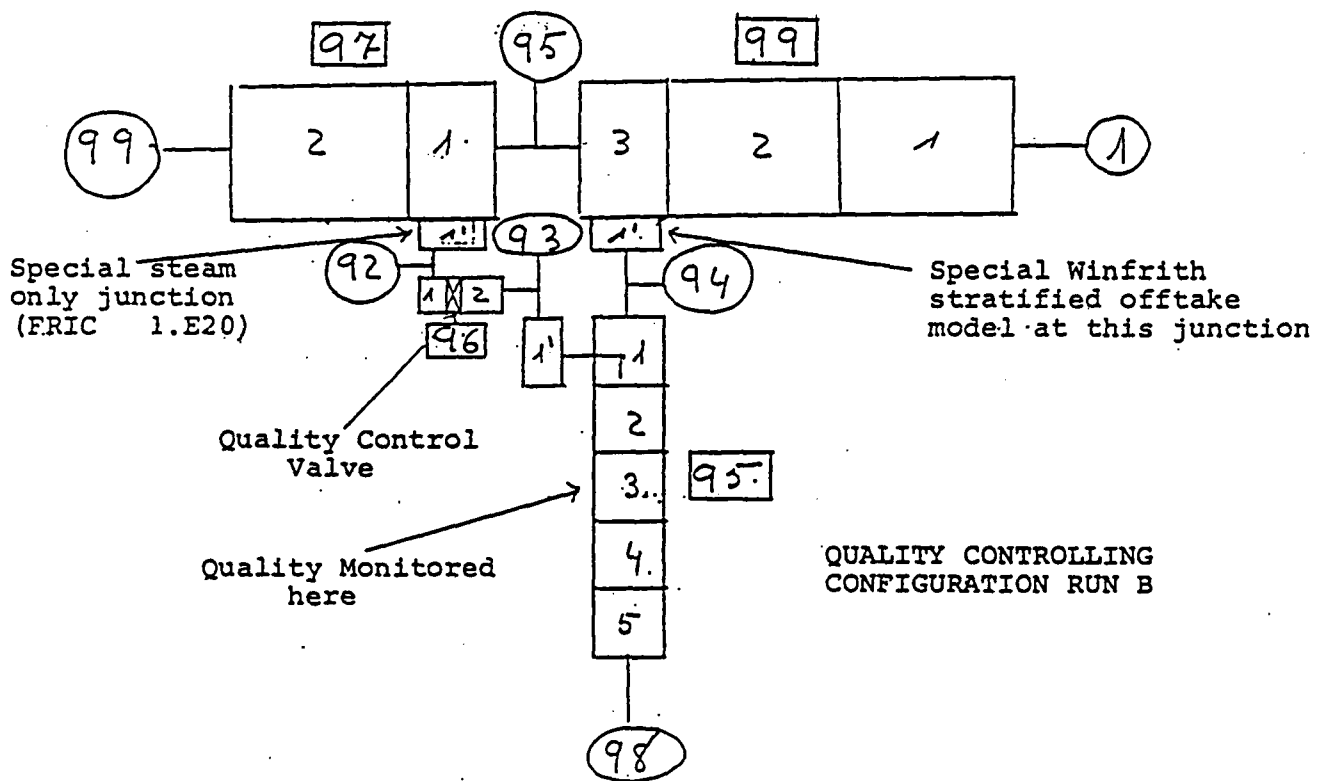
++PLUS++

PLOTTING UTILITY SYSTEM

AEEM

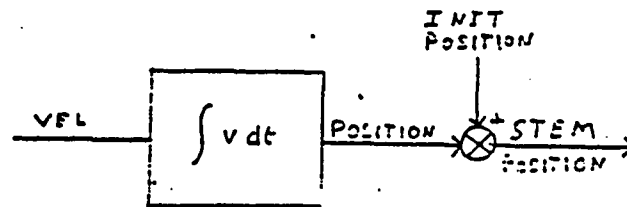
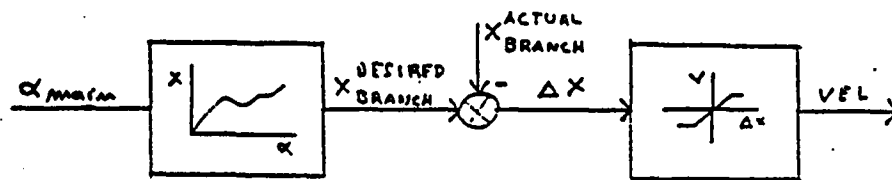


ORIGINAL CONFIGURATION RUN A



QUALITY CONTROLLING CONFIGURATION RUN B

B2 NODING MODIFICATIONS IN THE BREAK LINE

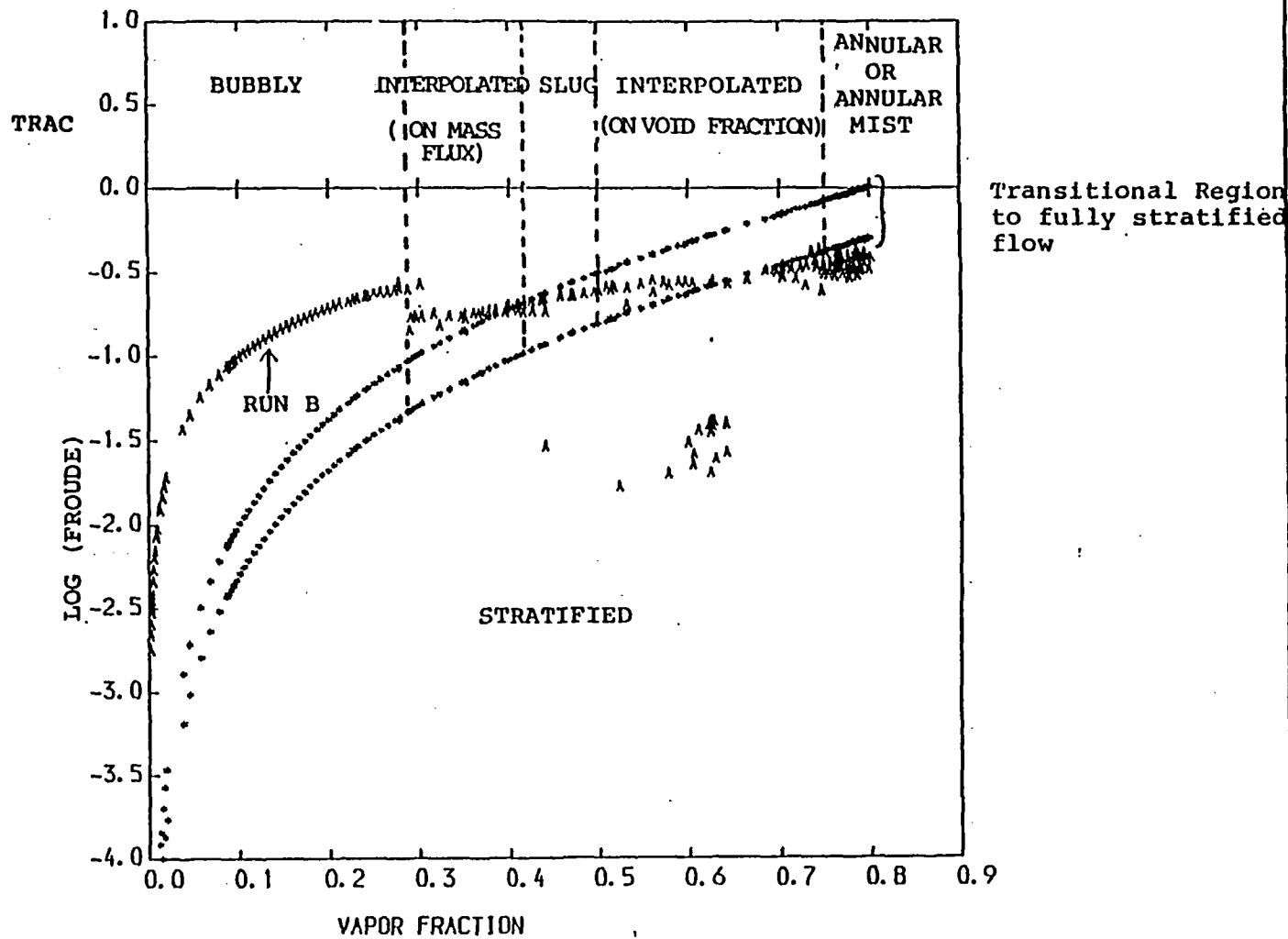


B3 QUALITY CONTROL VALVE CONTROL LOGIC

Winfrith

THE FOLLOWING ARE PLOTTED AGAINST VAPOR FRACTION
FUNCTION

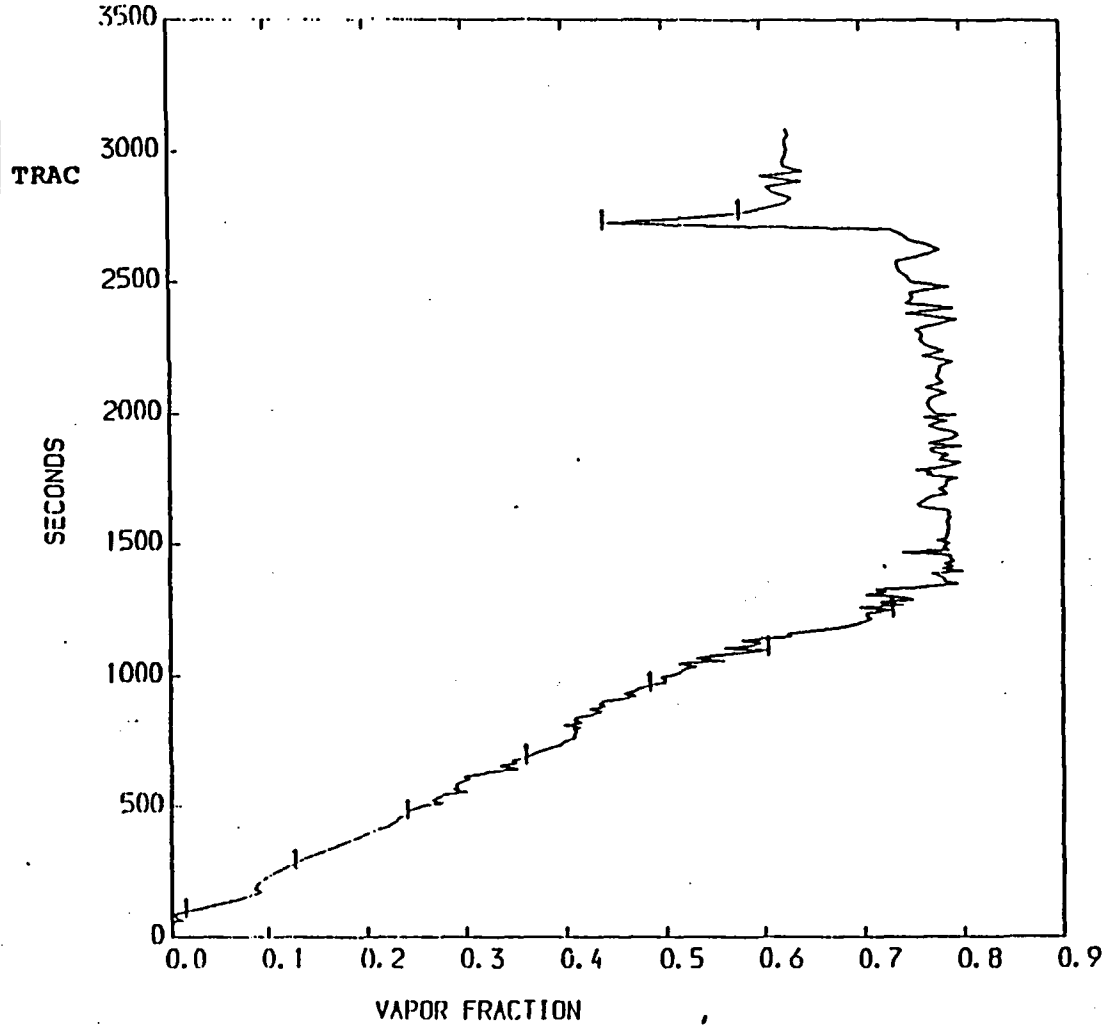
KEY		
SYM BOL	NAME	UNITS
•	FUNCTION	,
•	FUNCTION	,
A	FUNCTION	,



c1 TRAC FLOW REGIME MAP FOR LOFT LP-SB-2 HOT LEG CONDITIONS RUN B

THE FOLLOWING ARE PLOTTED AGAINST VAPOR FRACTION
REACTOR TIME

KEY		
SYM BOL	NAME	UNITS
+	REACTOR TIME	,SECONDS
LUC= 99/ 0/ 2 NNEH=TIME INF=1		



C2 TIME VS HOT LEG VOID FRACTION IN RUN B

AEEM - R 2202

111

TABLES

TABLE 1**INITIAL CONDITION FOR EXPERIMENT LP-SB-2 - RUN A**

Parameter	TRAC	Plant
Core ΔT	19.1	18.6 \pm 1.7 °K
Hot leg press	15.11	14.95 \pm 0.11 MPa
Cold leg temp	558.2	557.2 \pm 1.5 °K
Mass flow rate	480.0	480.0 \pm 3.2 kg/sec
Power level	49.1	49.1 \pm 1.2 Mw
Steam Generator Secondary Side		
Liquid level	3.13	3.13 \pm 0.01 m
Pressure	5.60	5.60 \pm 0.09 MPa
Steam mass flow	25.8	26.7 \pm 0.8 Kg
Pressurizer		
Liquid volume	0.6462	0.6462 \pm 0.002 m ³
Water temp	615.3	615.8 \pm 8.2 °K
Pressure	15.09	15.08 \pm 0.16 MPa

TABLE 2

OPERATION SET POINTS FOR EXPERIMENT LP-SB-2

Action	Reference	Plant	TRAC
Small break valve opened	time	0.0	0.0 secs
Reactor scrammed	intact loop hot leg pressure	14.28	14.28 MPa
Main feed water shutoff	intact loop hot leg pressure	14.28	14.28 MPa
HPIS flow initiated	intact loop hot leg pressure	8.07	8.07 MPa
Auxiliary feedwater initiated	time after reactor scram	62.0	62.0 secs
Auxiliary feedwater terminated	time after reactor scram	1800.2	1800.2 secs
Primary coolant pump tripped off	intact loop hot leg pressure	3.161	3.161 MPa

TABLE 3

CHRONOLOGY OF EVENTS FOR EXPERIMENT LP-SB-2 - RUN A

EVENT	time after initiation (seconds)	
	PLANT	TRAC
Small break valve opened	0.0	0.0
Reactor scrammed	1.8 ± 0.05	2.31
Main feedwater shutoff	1.8 ± 0.2	2.31
Main steam control valve started to close	2.8 ± 0.2	3.4
Main feedwater isolated	4.30 ± 0.05	4.14
Main steam control valve fully closed	14.8 ± 0.2	80. (a)
HPIS initiated	42.4 ± 0.2	41.3
Subcooled blowdown ended	50.2 ± 1	53.3 (b)
Auxiliary feedwater initiated	63.8	64.3
Pump two phase degradation	582.2 ± 0.2	590.0 (c)
Indications of stratified flow in the hot leg	~ 600.	1200.0
Collapsed level reaches break level	~ 1000. (d)	804.0
Break started to uncover	1192.5 ± 2.5	~ 1920.
Primary system pressure became less than secondary system pressure	1290.0 ± 45	1307.
Auxiliary feedwater shutoff	1864.0 ± 0.2	1864.
Inlet flow exceeded outlet flow	2284.0 ± 200.	2059.
Primary coolant pumps tripped (3.16 MPa in primary system)	2852.8 ± 0.2	2635.

- a) In the TRAC input deck the main steam control valve assumed the function of the steam bypass control valve. Thus it kept on moving up to 80 seconds when it was latched closed.
- b) That value is such that $100 \frac{T_{SAT} - T_2}{T_{SAT}} = 0.1$
- c) A smooth rather than a sharp degradation was obtained
- d) From Reference 9

TABLE 4

INSTRUMENT LOCATIONS FLOW AREAS

INSTRUMENT	LOFT Flow Area (M ²)	TRAC Flow Area (M ²)
FE-1ST-1 and -2 ME-1ST-1 and -2	0.141	0.142
FE-5LP-1 and -2 ME-5LP-1 and -2	0.106	0.139
FE-5UP-1 ME-3UP-1 and -5UP-1	0.125	0.164
FE-PC-S03 ME-PC-S03	0.0007	
FE-PC-1A, -1B, and -1C ME-PC-1A, -1B, and -1C FE-PC-2A, -2B, and -2C ME-PC-2A, -2B, and -2C	0.0634	0.0634

TABLE 5

INITIAL CONDITIONS FOR EXPERIMENT LP-SB-2 RUN B

PARAMETER	TRAC	PLANT
Core ΔT	19.1	18.6 \pm 1.7°K
Hot Leg Pressure	15.11	14.95 \pm 0.11 MPa
Cold Leg Temperature	558.1	557.2 \pm 1.5°K
Mass Flow Rate	480.0	480.0 \pm 3.2 kg/s
Power Level	49.1	49.1 Mw
Steam Generator Secondary Side		
Liquid Level	3.13	3.13 \pm 0.01 m
Pressure	5.60	5.60 \pm 0.05 MPa
Steam Mass Flow	25.8	26.7 \pm 0.8 kg/s
Pressurizer		
Liquid Volume	0.6462	0.6462 \pm 0.0002 m ³
Water Temperature	615.3	615.8 \pm 8.2°K
Pressure	15.09	15.08 \pm 0.16 MPa

TABLE 6

CHRONOLOGY OF EVENTS FOR EXPERIMENT LP-SB-2 RUN B

EVENT	PLANT	TRAC
Small Break Valve opened	0.0	0.0
Reactor scrammed	1.8 ± 0.05	1.93
Main Feedwater shutoff	1.8 ± 0.2	1.93
Main Steam control valve started to close	2.8 ± 0.2	2.92
Main feedwater isolated	4.3 ± 0.05	3.7
Main steam control valve fully closed	14.8 ± 0.2	80 (a)
HPIS initiated	42.4 ± 0.2	54.51
Subcooled blowdown ended	50.2 ± 1	70 (b)
Auxiliary feedwater initiated	63.8	69.3
Pumps two-phase degradation	582.2 ± 0.2	522
Indicators of stratified flow in hot leg	~ 600	~ 700
Stratified flow fully developed	~ 1200	~ 1150
Break started to uncover	1192.5 ± 2.5	1175 (c)
Primary system pressure became less than secondary system pressure	1290.0 ± 4.5	1175
Auxiliary feedwater shutoff	1864.0 ± 0.2	1864
Inlet flow exceeded outlet flow	2284 ± 200	1783
Primary coolant pumps tripped (3.16 MPa in primary system)	2852.8 ± 0.2	2706

(a) In the TRAC input deck the main steam control valve assumed the function of the steam bypass control valve. Thus it kept on moving up to 80 seconds when it was latched closed.

(b) That value is such that $100 \frac{T_{SAT} - T_l}{T_{SAT}} = 0.1$

(c) Sudden change in depressurisation rate.

TABLE A.1

PUMP HEAD MULTIPLIERS RUN A

<u>α</u>	<u>$M(\alpha)$</u>
0.0	0.0
0.15	0.14
0.2125	0.202
0.3	0.346
0.33	0.519
0.4	0.712
0.5125	0.702
0.5825	0.769
0.712	0.769
0.8125	0.731
0.9125	0.558
0.9625	0.25
1.0	0.0

The characteristic curves were those implemented in TRAC for LOFT with the exception of the first quadrant of the fully degraded curve that was made equal to zero.

TABLE A.2

PUMP HEAD MULTIPLIERS RUN B

PUMP 1

<u>α</u>	<u>$M(\alpha)$</u>
0.0	0.0
0.15	0.14
0.2125	0.202
0.3	0.346
0.34	0.519
0.35	0.9
0.5125	0.9
0.5825	0.9
0.712	0.9
0.8125	0.9
0.9125	0.558
0.9625	0.25
1.0	0.0

PUMP 2

<u>α</u>	<u>$M(\alpha)$</u>
0.0	0.0
0.15	0.14
0.2125	0.202
0.3	0.346
0.34	0.519
0.35	0.712
0.5125	0.739
0.5875	0.769
0.712	0.769
0.8125	0.731
0.9125	0.558
0.9625	0.25
1.0	0.0

The characteristic curves were those implemented in TRAC for LOFT with the exception of the first quadrant of the fully degraded curve that was made equal to zero.

TABLE B.1

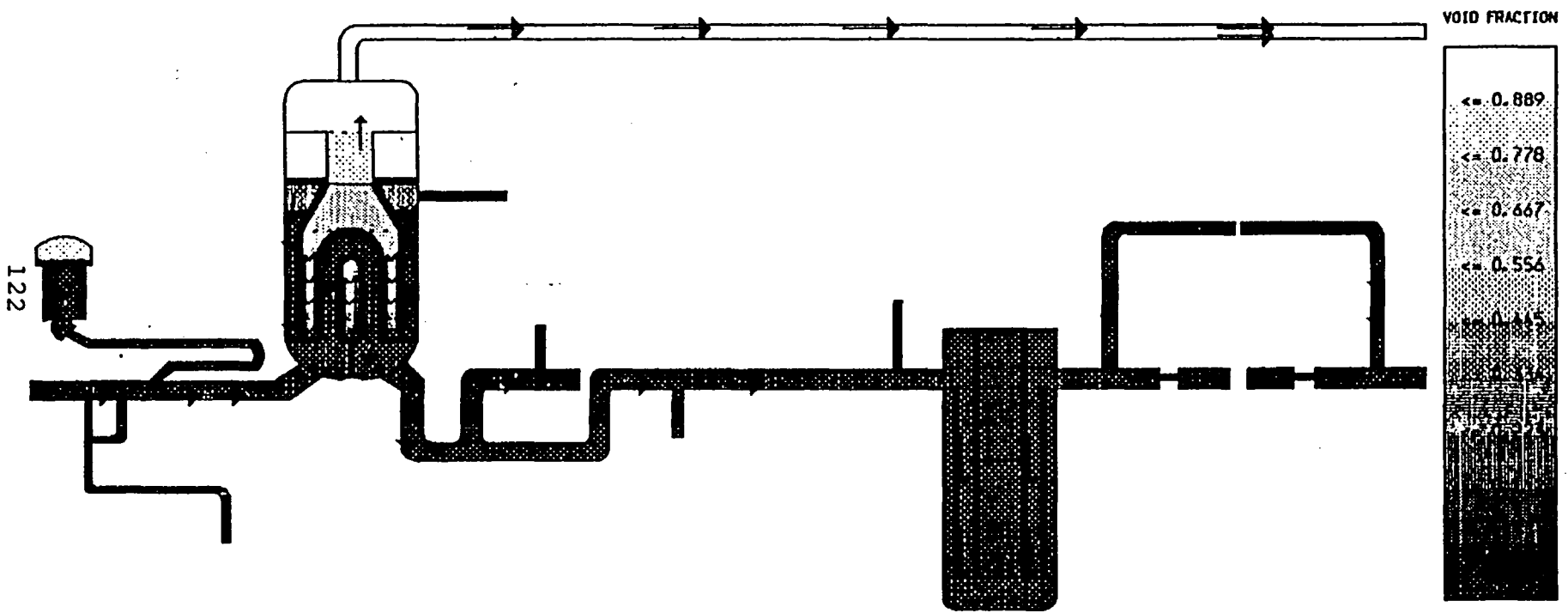
DESIRED BRANCH QUALITY VS VOID FRACTION
IN THE HOT LEG

<u>α</u>	<u>x</u>
0.0	0.0
0.0115	0.0048
0.0676	0.0113
0.1221	0.0194
0.1943	0.0275
0.2654	0.0378
0.2799	0.0508
0.3084	0.0638
0.3524	0.0639
0.4	0.0680
0.43	0.0750
0.45	0.08
0.47	0.09
0.48	0.1040
0.666	0.15
0.75	0.9

AEEW - R 2202

S.M.A.R.T. SYSTEM MIMIC FOR ANALYSIS OF REACTOR TRANSIENTS
TITLE OF FRAME: - LOFT SB-2 (RUN B) CORRELATED BREAK LINE QUALITY

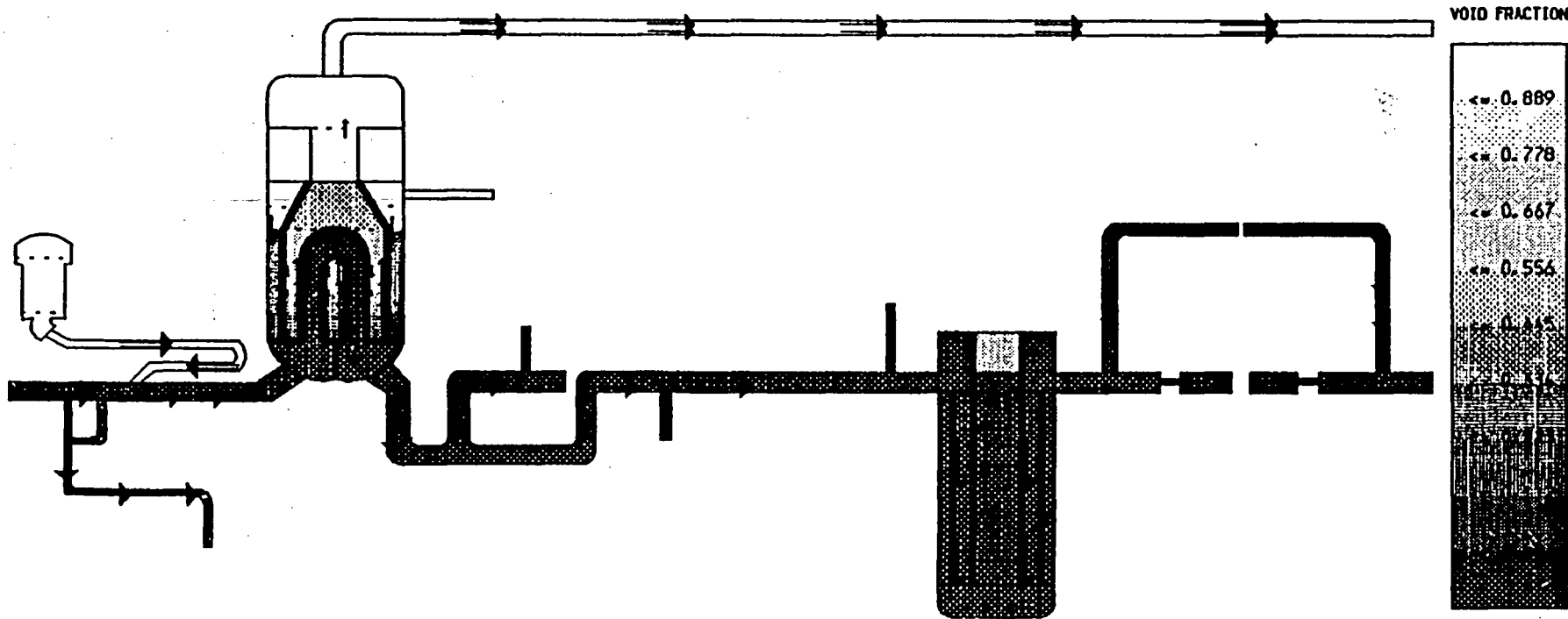
T1 0.0
VL10 →
(10.00)
VVAP →
(10.00)



122

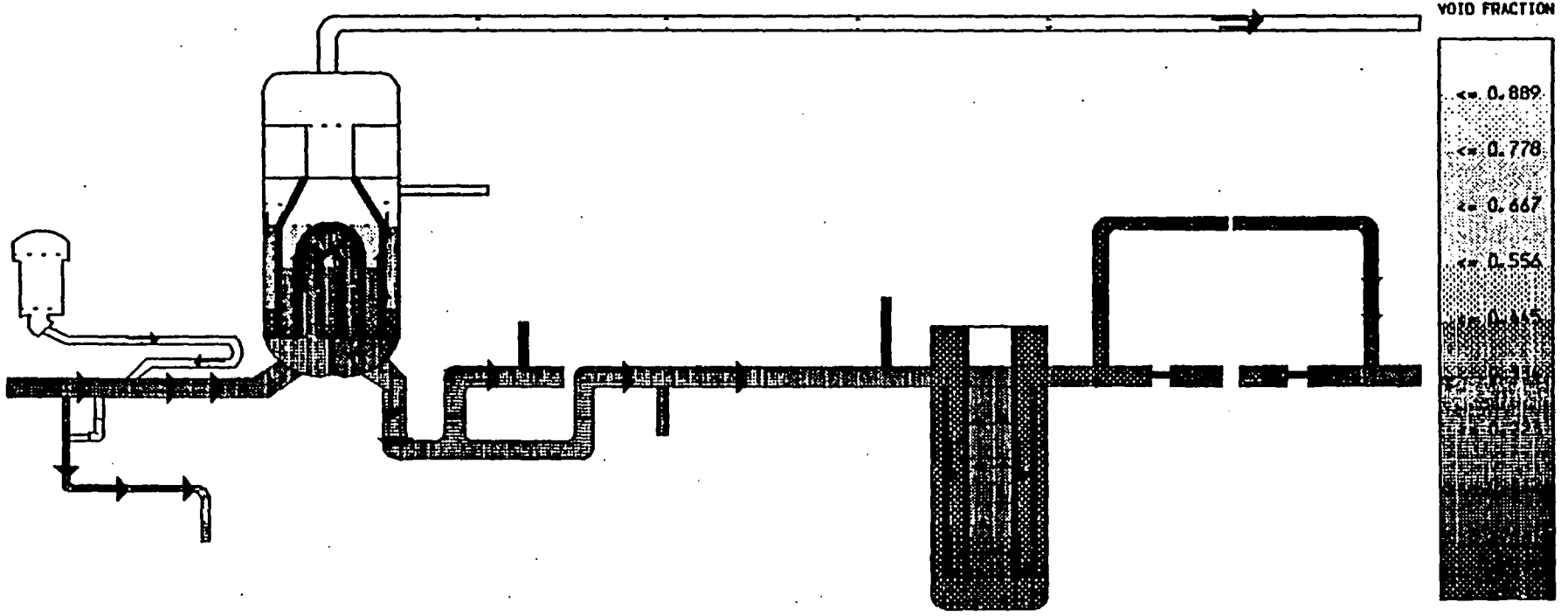
S. M. A. R. T. SYSTEM MIMIC FOR ANALYSIS OF REACTOR TRANSIENTS
TITLE OF FRAME: - LOFT SB-2 (RUN B) CORRELATED BREAK LINE QUALITY

T1	52.3
VL10	→
	(10.00)
VVAP	→
	(10.00)



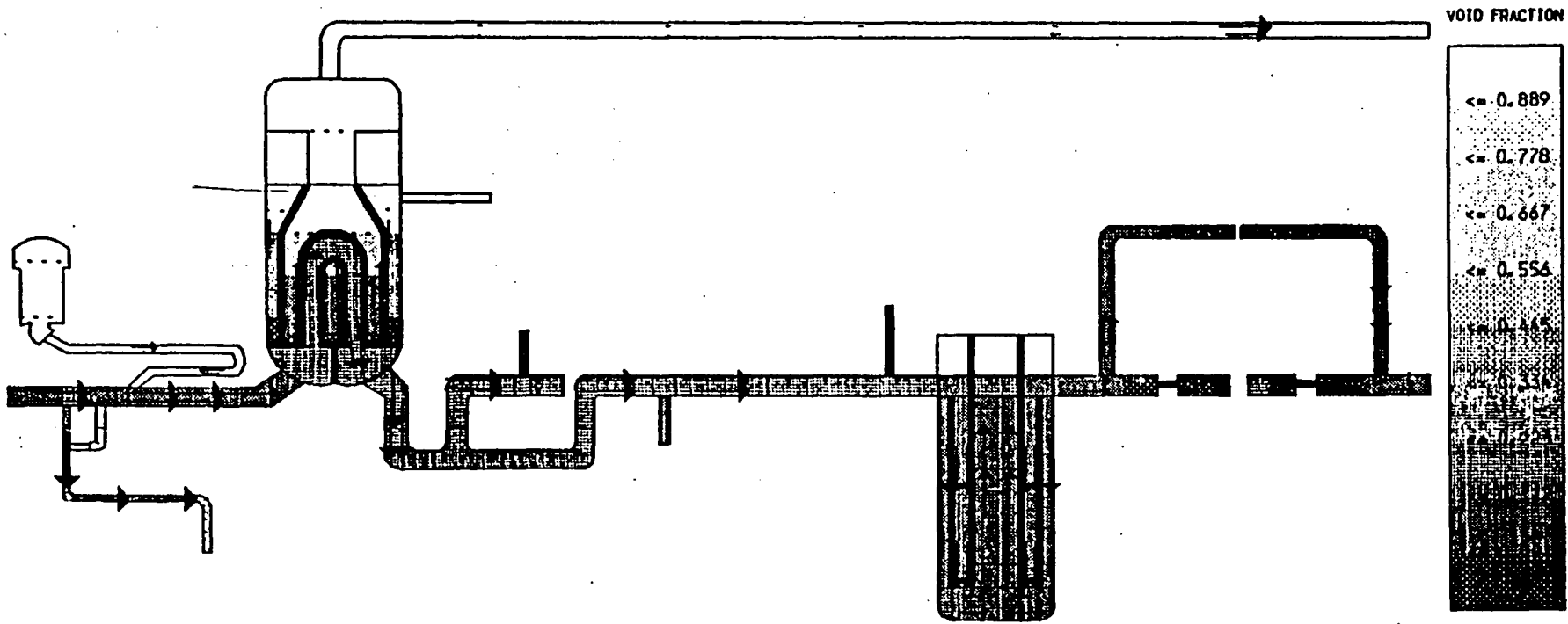
S.M.A.R.T. SYSTEM MIMIC FOR ANALYSIS OF REACTOR TRANSIENTS
TITLE OF FRAME: - LOFT SB-2 (RUN B) CORRELATED BREAK LINE QUALITY

Ti 150.7
VLIQ →
(10.00)
VVAP →
(10.00)



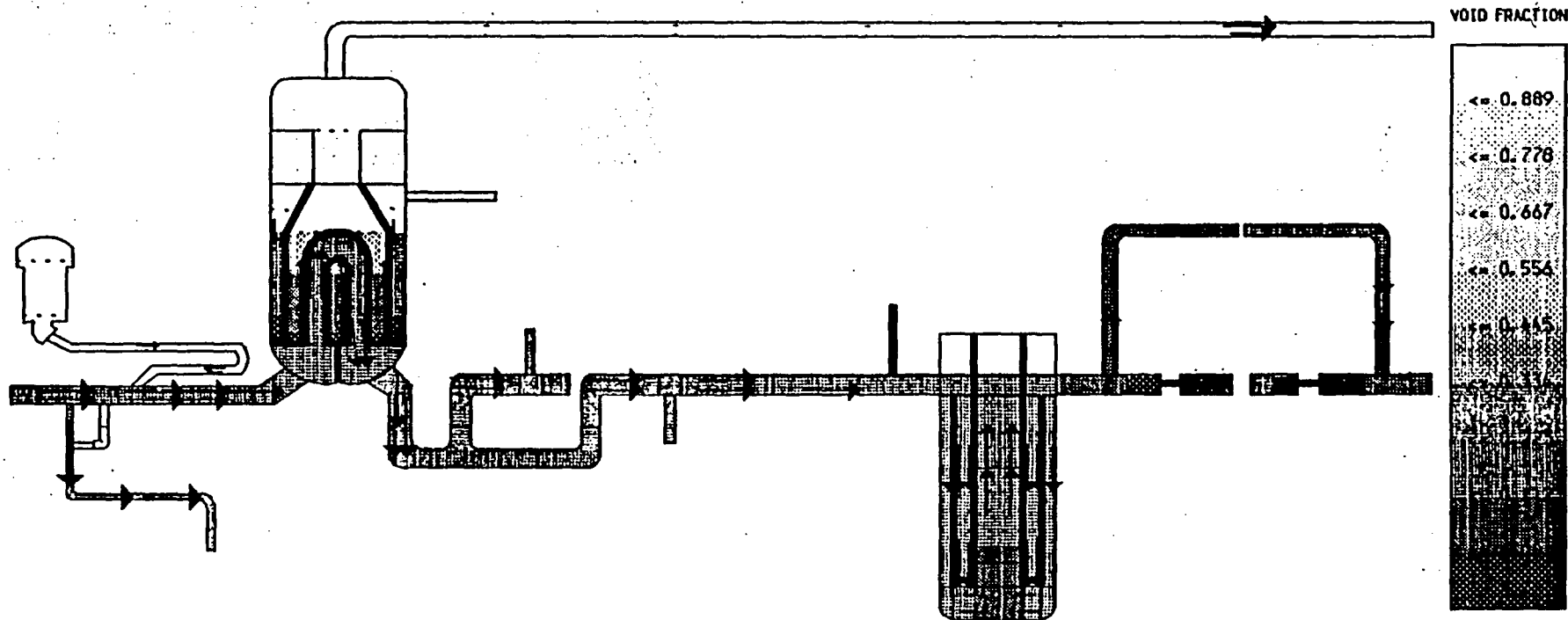
S. M. A. R. T. SYSTEM MIMIC FOR ANALYSIS OF REACTOR TRANSIENTS
TITLE OF FRAME: - LOFT SB-2 (RUN 8) CORRELATED BREAK LINE QUALITY

T: 250.7
VL10 →
(10.00)
VVAP →
(10.00)



S. M. A. R. T. SYSTEM MIMIC FOR ANALYSIS OF REACTOR TRANSIENTS
TITLE OF FRAME: - LOFT SB-2 (RUN B) CORRELATED BREAK LINE QUALITY

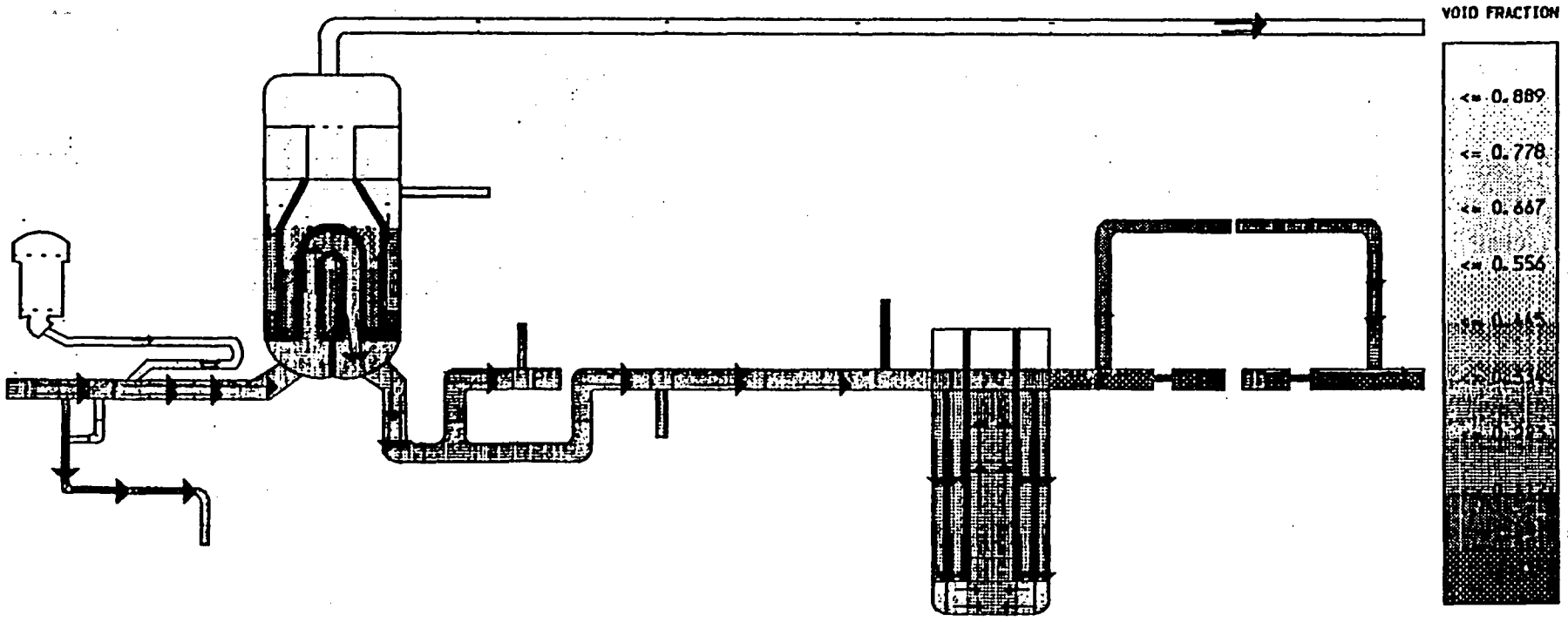
T: 350.7
VLIO →
(10.00)
VVAP →
(10.00)



S. M. A. R. T. SYSTEM MIMIC FOR ANALYSIS OF REACTOR TRANSIENTS

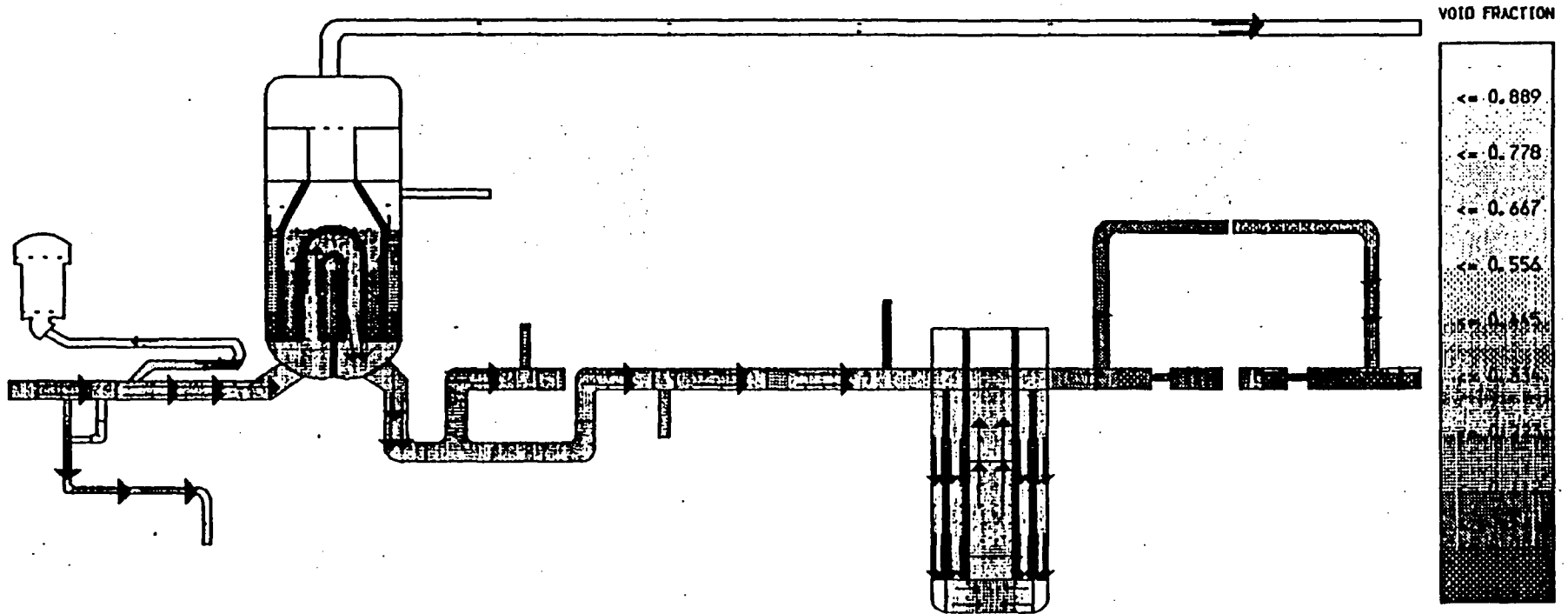
TITLE OF FRAME: - LOFT SB-2 (RUN B) CORRELATED BREAK LINE QUALITY

T1 451.0
VL10 →
(10.00)
VVAP →
(10.00)



S.M.A.R.T. SYSTEM MIMIC FOR ANALYSIS OF REACTOR TRANSIENTS
TITLE OF FRAME: - LOFT SB-2 (RUN B) CORRELATED BREAK LINE QUALITY

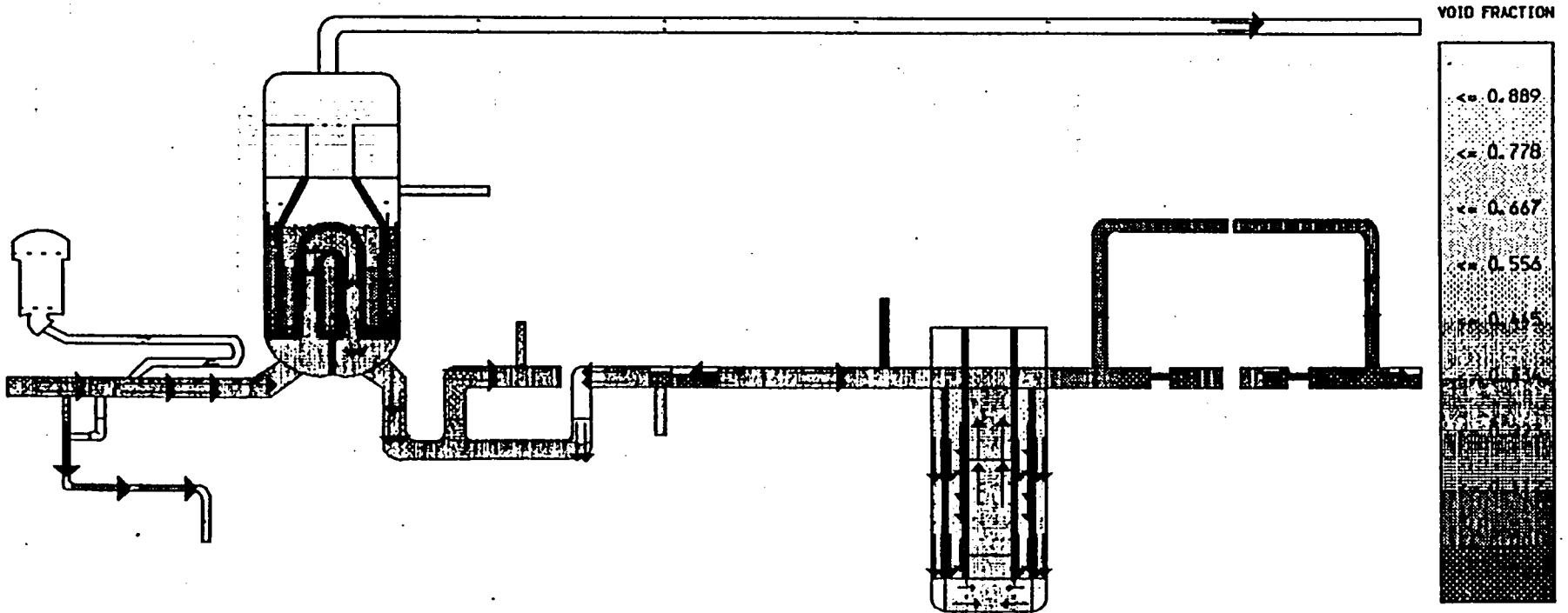
T1 551.7
VL10 →
(10.00)
VVAP →
(10.00)



VOID FRACTION
←= 0.889
←= 0.778
←= 0.667
←= 0.554

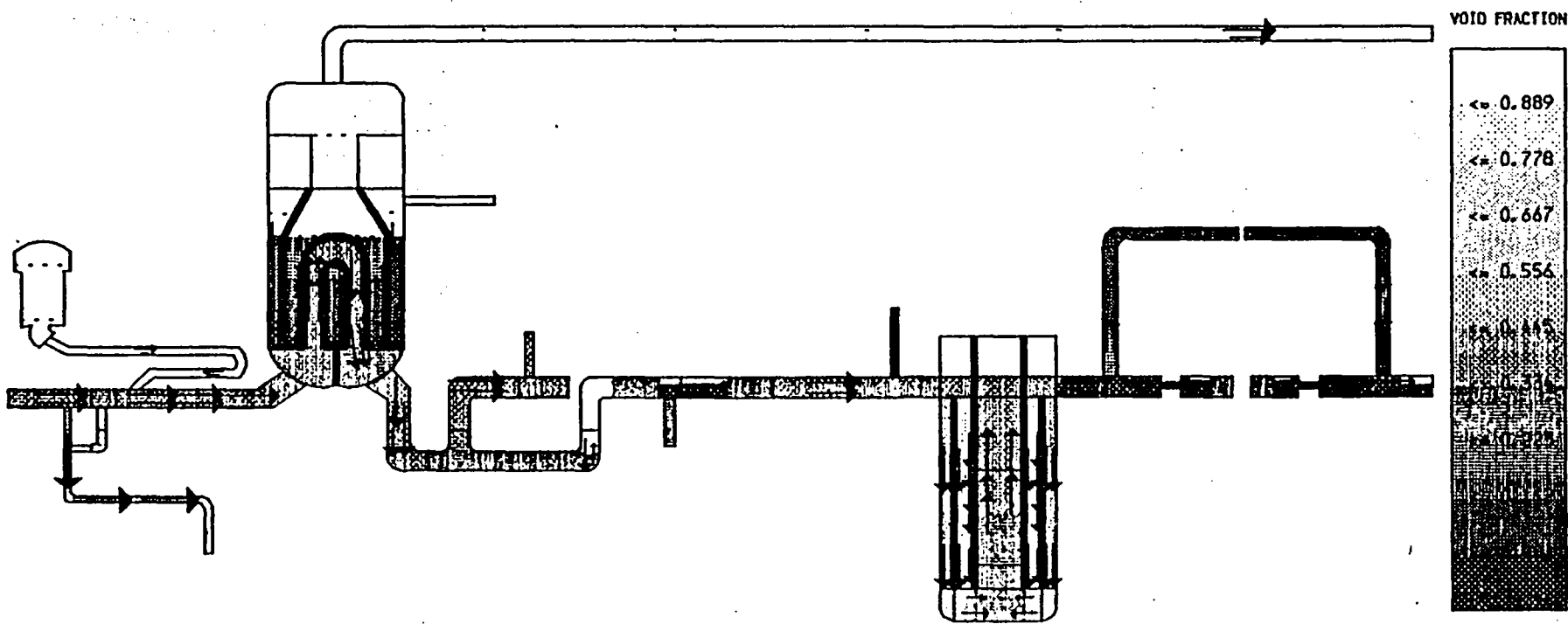
S. M. A. R. T. SYSTEM MIMIC FOR ANALYSIS OF REACTOR TRANSIENTS
TITLE OF FRAME, - LOFT SB-2 (RUN B) CORRELATED BREAK LINE QUALITY

T1 652.1
VL10 →
(10.00)
VVAP →
(10.00)



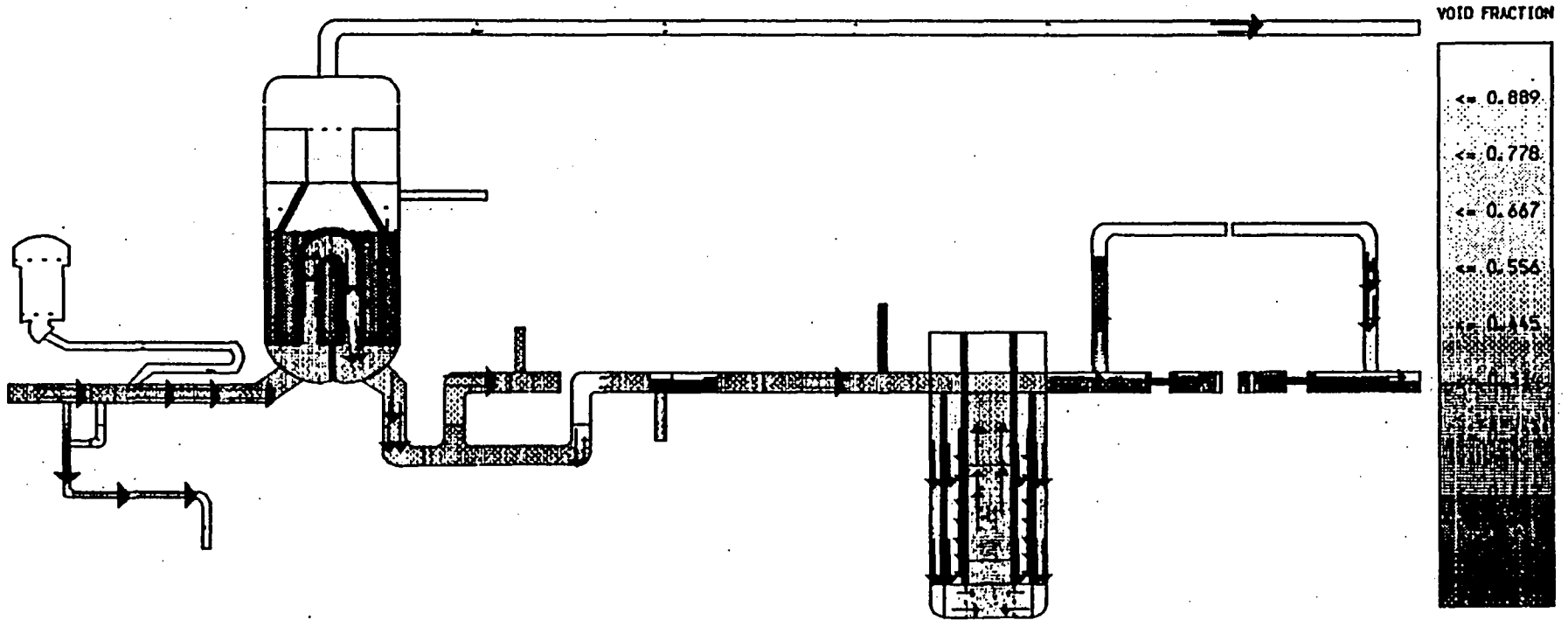
S.M.A.R.T. SYSTEM MIMIC FOR ANALYSIS OF REACTOR TRANSIENTS
 TITLE OF FRAME: - LOFT SB-2 (RUN B) CORRELATED BREAK LINE QUALITY

T1 752.8
 VL10 →
 (10.00)
 VVAP →
 (10.00)



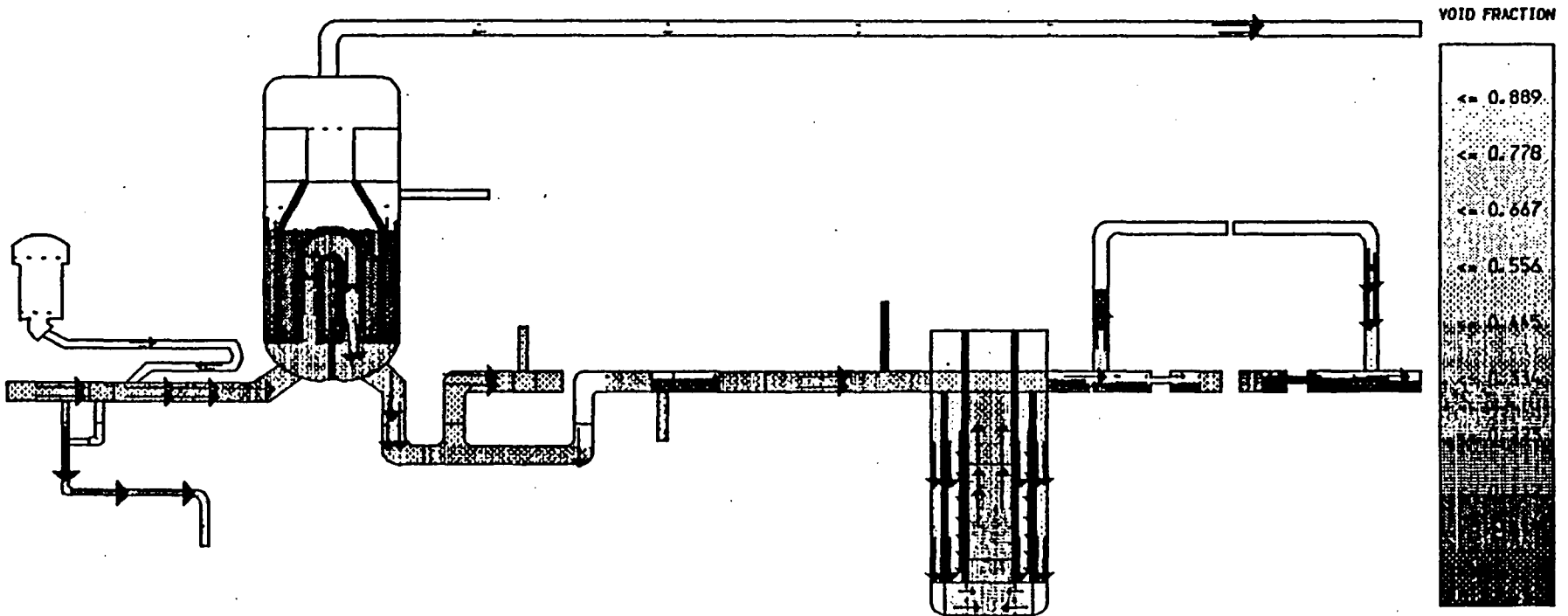
S.M.A.R.T. SYSTEM MIMIC FOR ANALYSIS OF REACTOR TRANSIENTS
TITLE OF FRAME: - LOFT SB-2 (RUN B) CORRELATED BREAK LINE QUALITY

T1 860.8
VL10 →
(10.00)
VVAP →
(10.00)



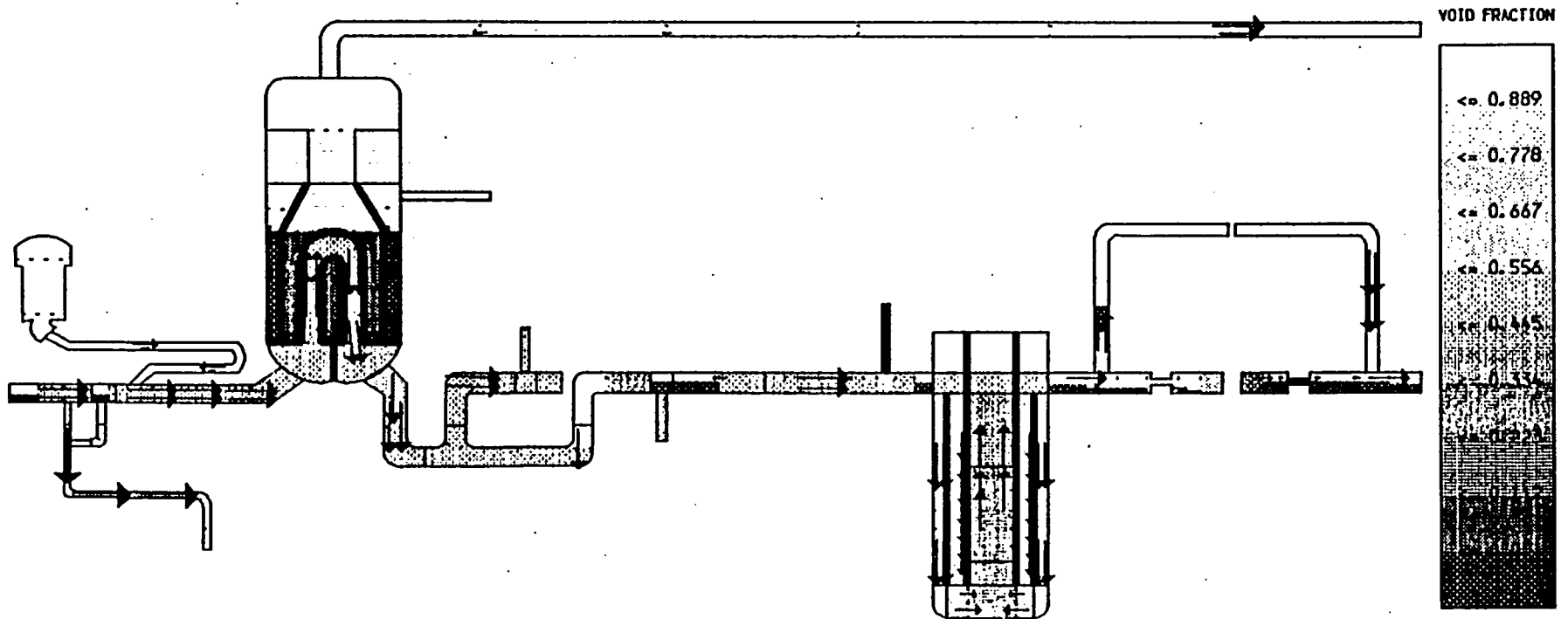
S.M.A.R.T. SYSTEM MIMIC FOR ANALYSIS OF REACTOR TRANSIENTS
TITLE OF FRAME, - LOFT SB-2 (RUN B) CORRELATED BREAK LINE QUALITY

T1 961.7
VL10 →
(10.00)
VVAP →
(10.00)



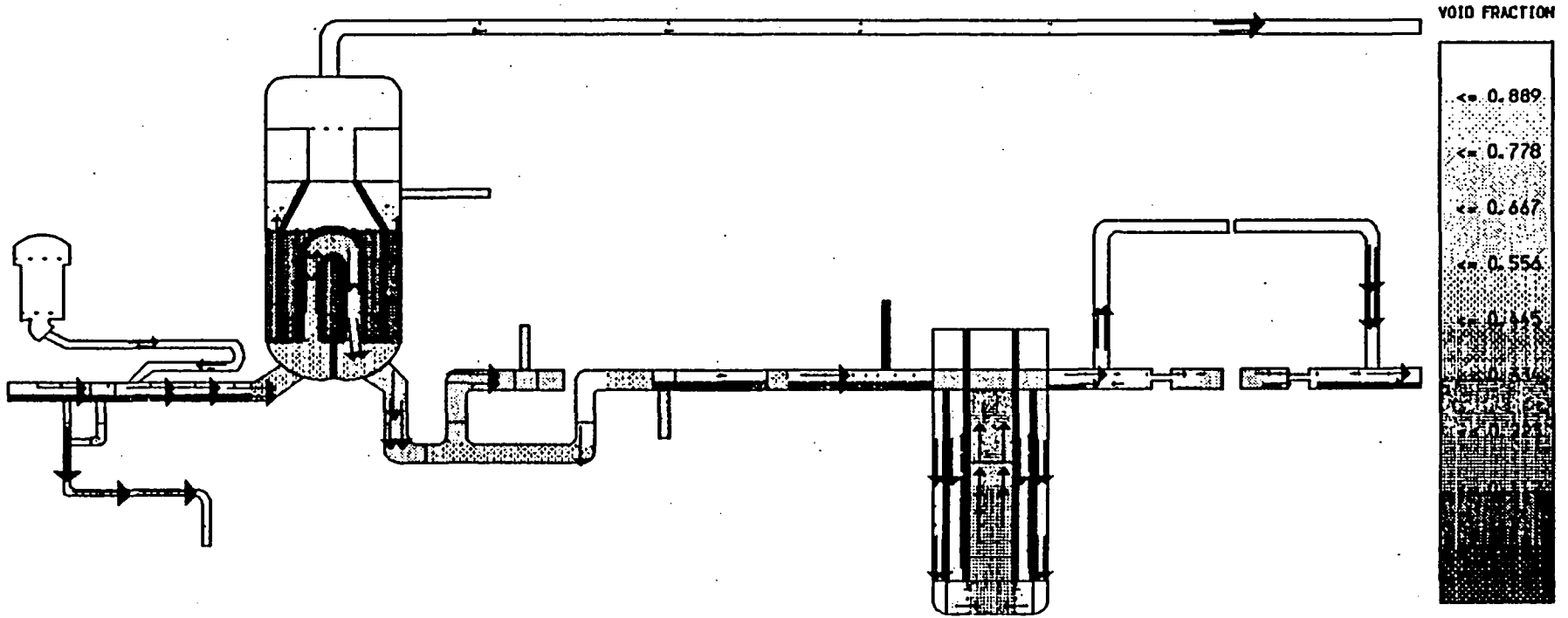
S. M. A. R. T. SYSTEM MIMIC FOR ANALYSIS OF REACTOR TRANSIENTS
TITLE OF FRAME: - LOFT SB-2 (RUN B) CORRELATED BREAK LINE QUALITY

T1 1063.2
VL10 →
(10.00)
VVAP →
(10.00)



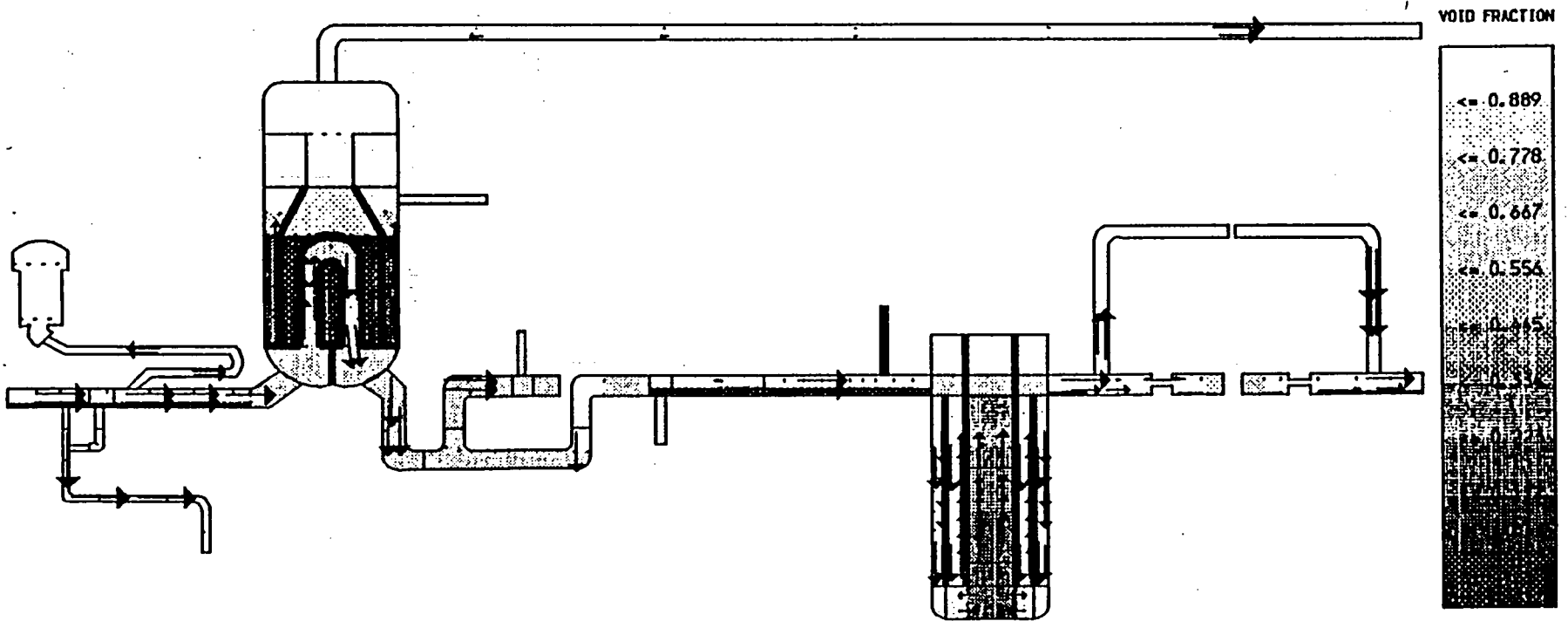
S. M. A. R. T. SYSTEM MIMIC FOR ANALYSIS OF REACTOR TRANSIENTS
 TITLE OF FRAME, - LOFT SB-2 (RUN B) CORRELATED BREAK LINE QUALITY

T1 1164.4
 VL10 →
 (10.00)
 VVAP →
 (10.00)



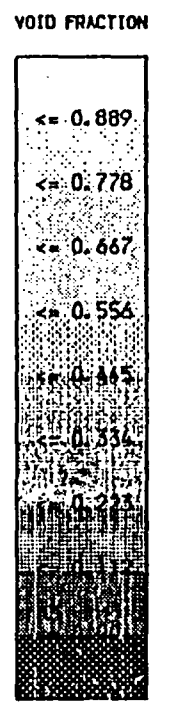
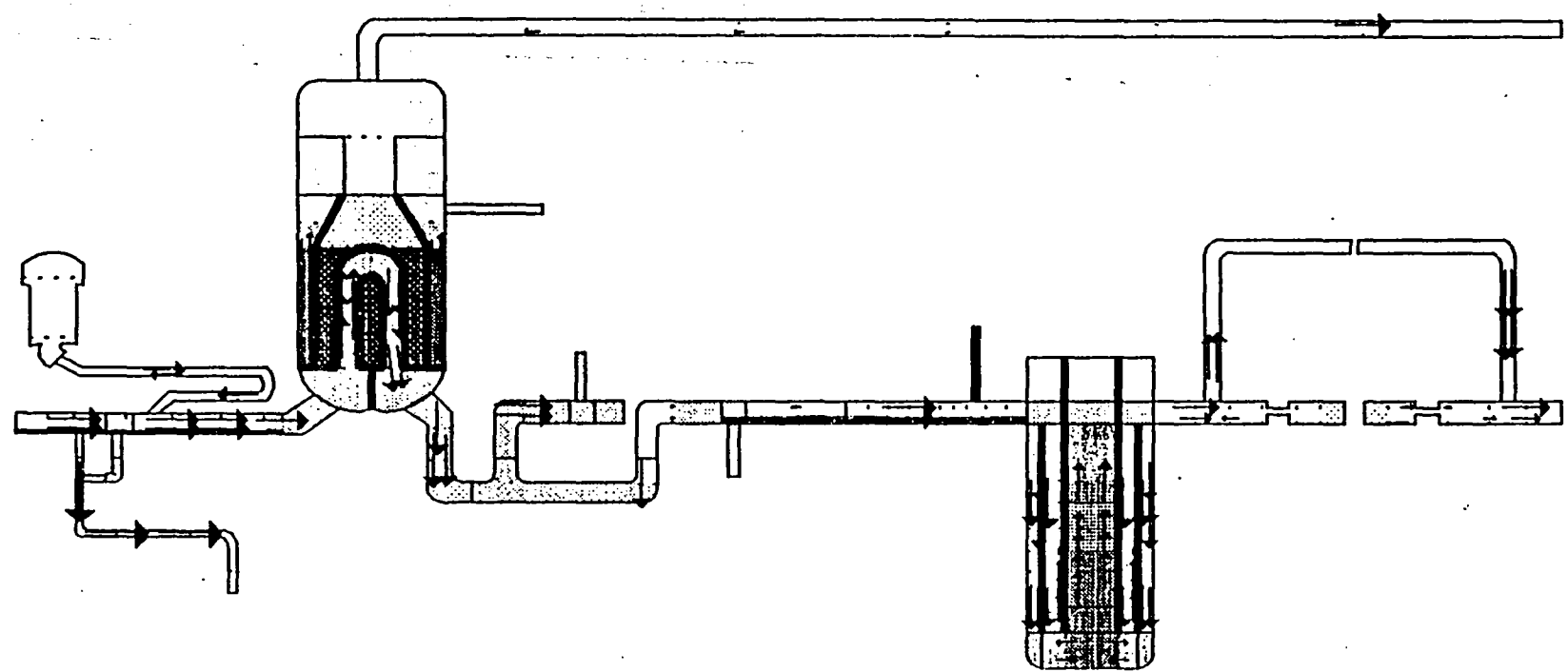
S.M.A.R.T. SYSTEM MIMIC FOR ANALYSIS OF REACTOR TRANSIENTS
TITLE OF FRAME: - LOFT SB-2 (RUN B) CORRELATED BREAK LINE QUALITY

T1 1265.3
VLIQ →
(10.00)
VVAP →
(10.00)



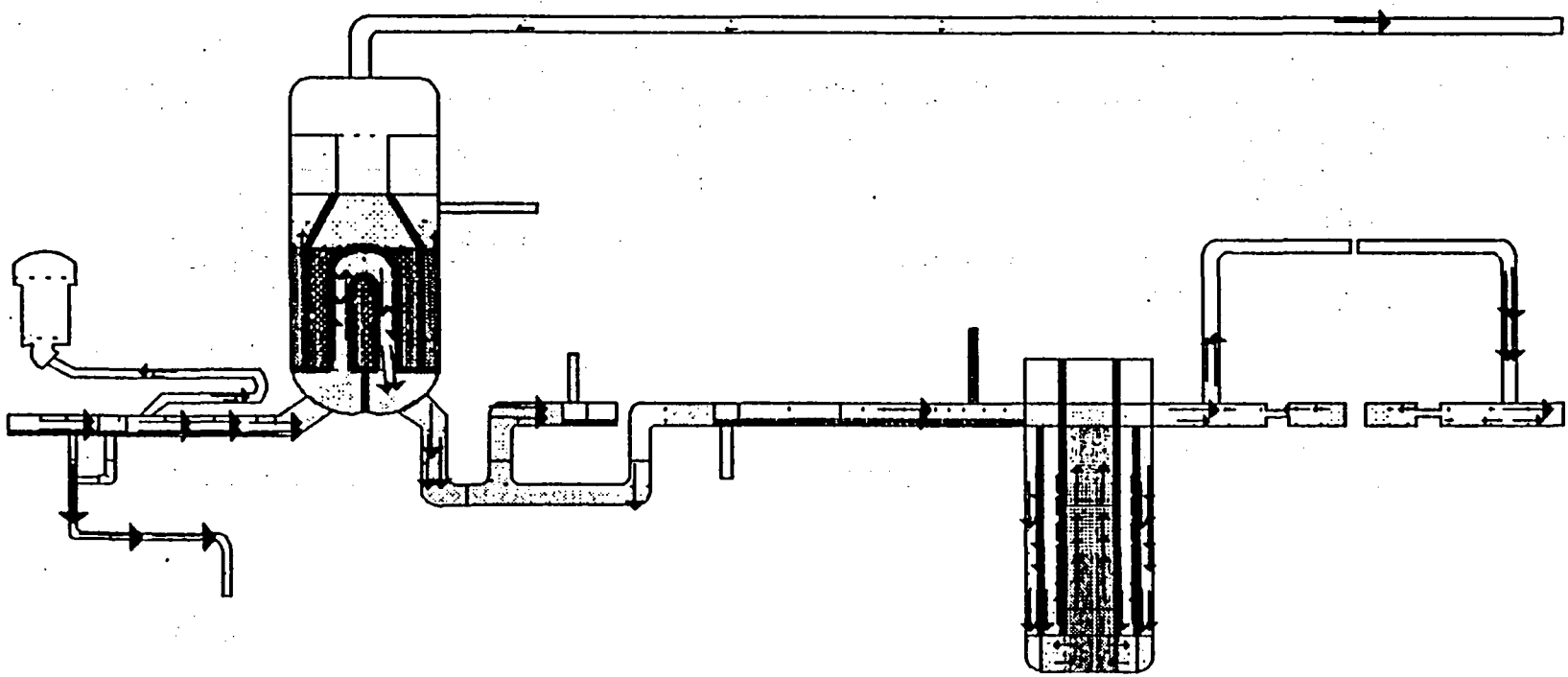
S. M. A. R. T. SYSTEM MIMIC FOR ANALYSIS OF REACTOR TRANSIENTS
TITLE OF FRAME: - LOFT SB-2 (RUN B) CORRELATED BREAK LINE QUALITY

Ti 1366.6
VLIO →
(10.00)
VVAP →
(10.00)

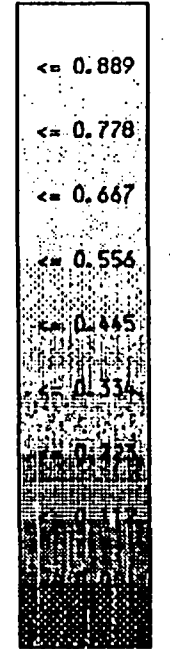


S.M.A.R.T. SYSTEM MIMIC FOR ANALYSIS OF REACTOR TRANSIENTS
TITLE OF FRAME, - LOFT SB-2 (RUN B) CORRELATED BREAK LINE QUALITY

T1 1467.8
VLIQ →
(10.00)
VVAP →
(10.00)

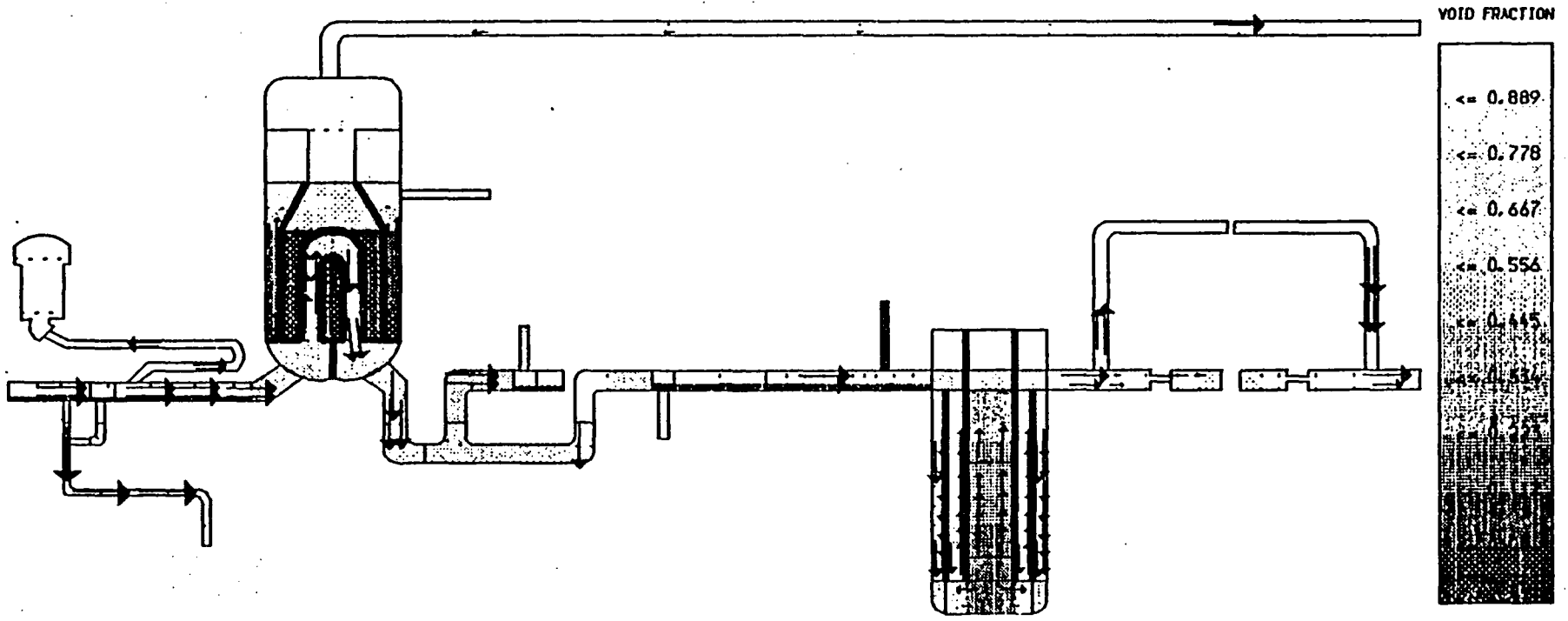


VOID FRACTION

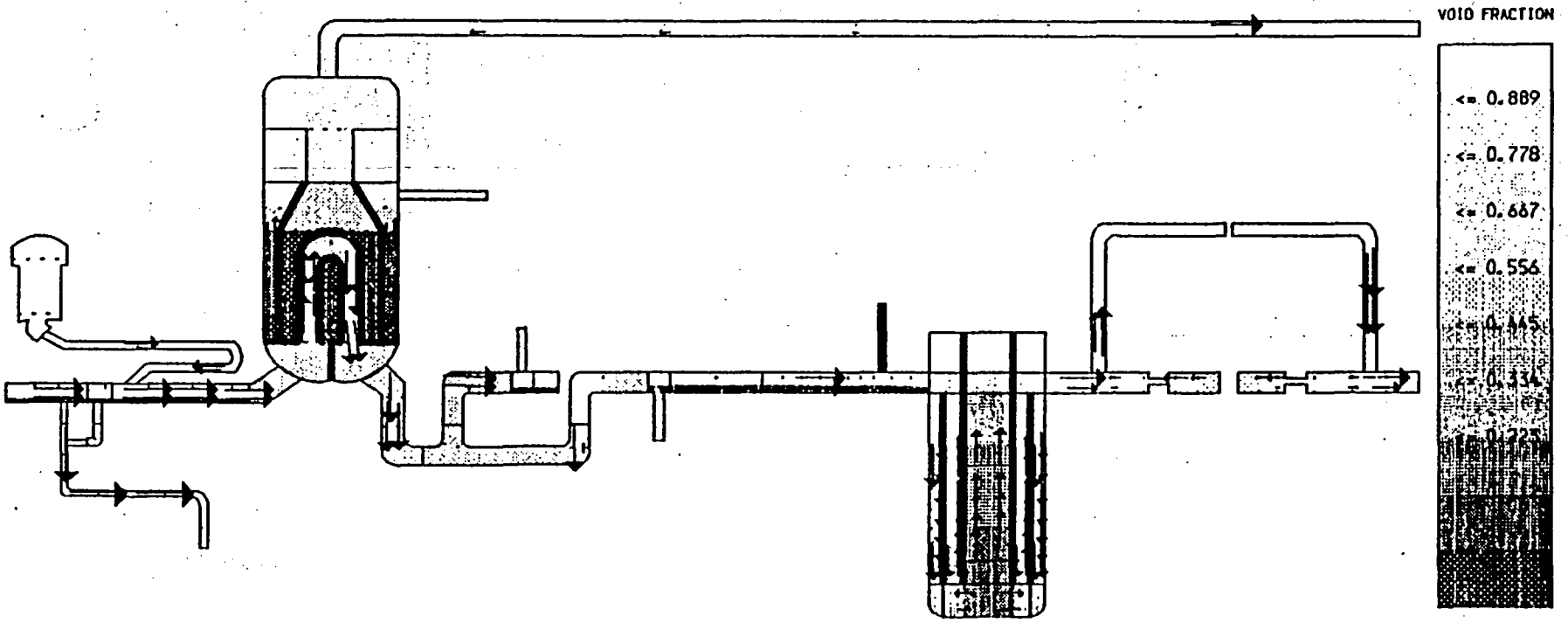


S.M.A.R.T. SYSTEM MIMIC FOR ANALYSIS OF REACTOR TRANSIENTS
TITLE OF FRAME, - LOFT SB-2 (RUN B) CORRELATED BREAK LINE QUALITY

T: 1562.2
VL10 →
(10.00)
VVAP →
(10.00)



S. M. A. R. T. SYSTEM MIMIC FOR ANALYSIS OF REACTOR TRANSIENTS
TITLE OF FRAME: - LOFT SB-2 (RUN B) CORRELATED BREAK LINE QUALITY

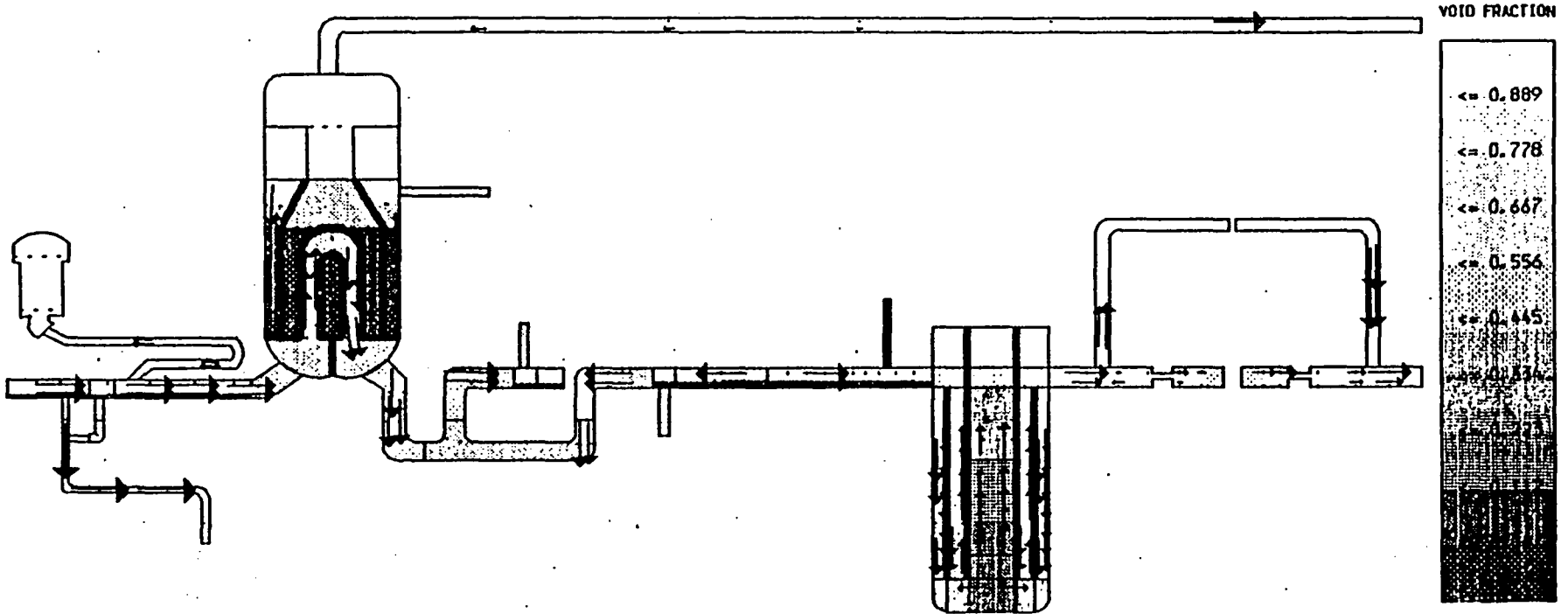


T1 1662.3
VL10 →
(10.00)
VVAP →
(10.00)

VOID FRACTION
← 0.889
← 0.778
← 0.667
← 0.556
← 0.445
← 0.334
← 0.223

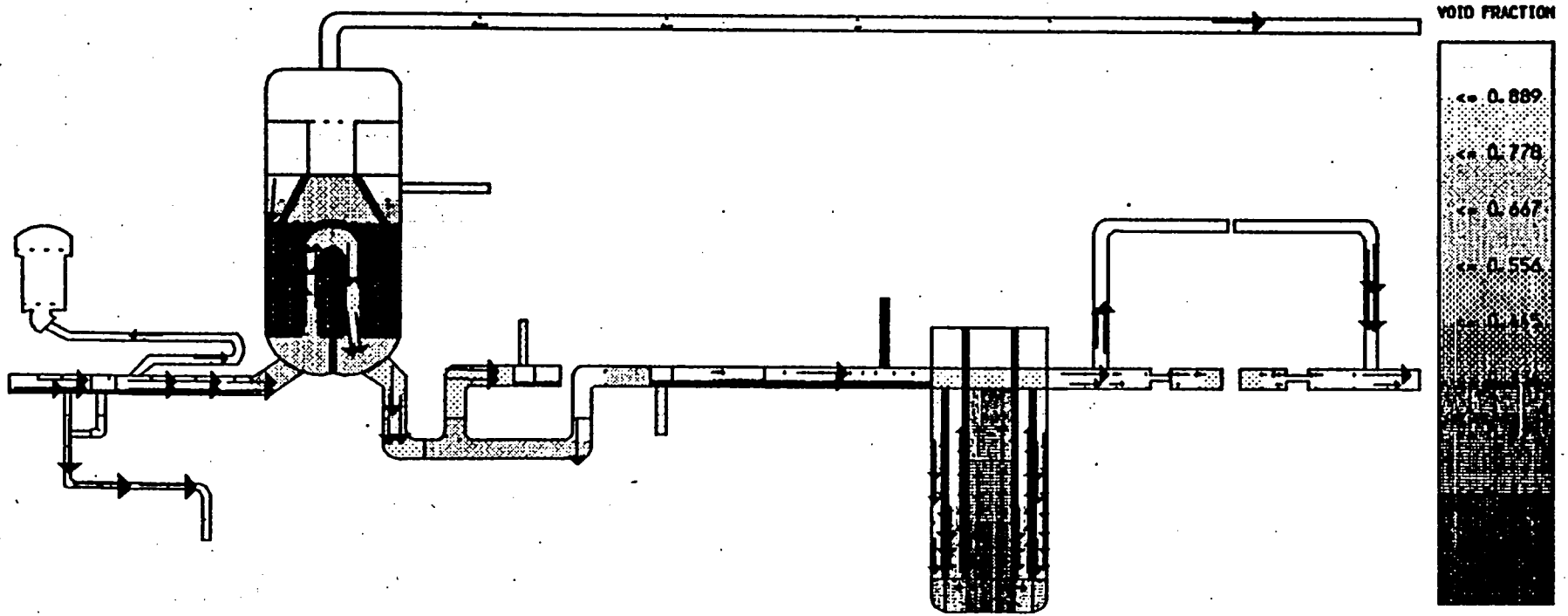
S.M.A.R.T. SYSTEM MIMIC FOR ANALYSIS OF REACTOR TRANSIENTS
TITLE OF FRAME: - LOFT SB-2 (RUN B) CORRELATED BREAK LINE QUALITY

T1 1863.9
VL10 →
(10.00)
VVAP →
(10.00)



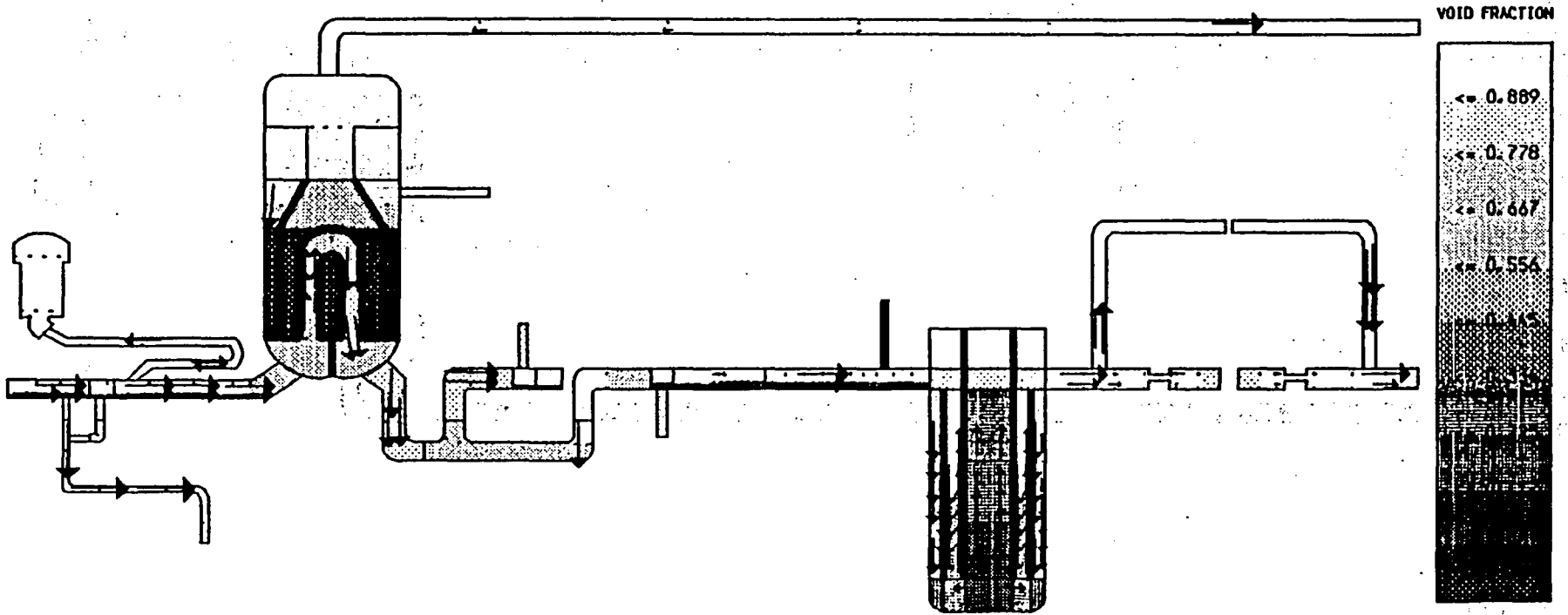
S. M. A. R. T. SYSTEM MIMIC FOR ANALYSIS OF REACTOR TRANSIENTS
TITLE OF FRAME: - LOFT SB-2 (RUN B) CORRELATED BREAK LINE QUALITY

T1 2060.4
VL10 →
(10.00)
VVAP →
(10.00)



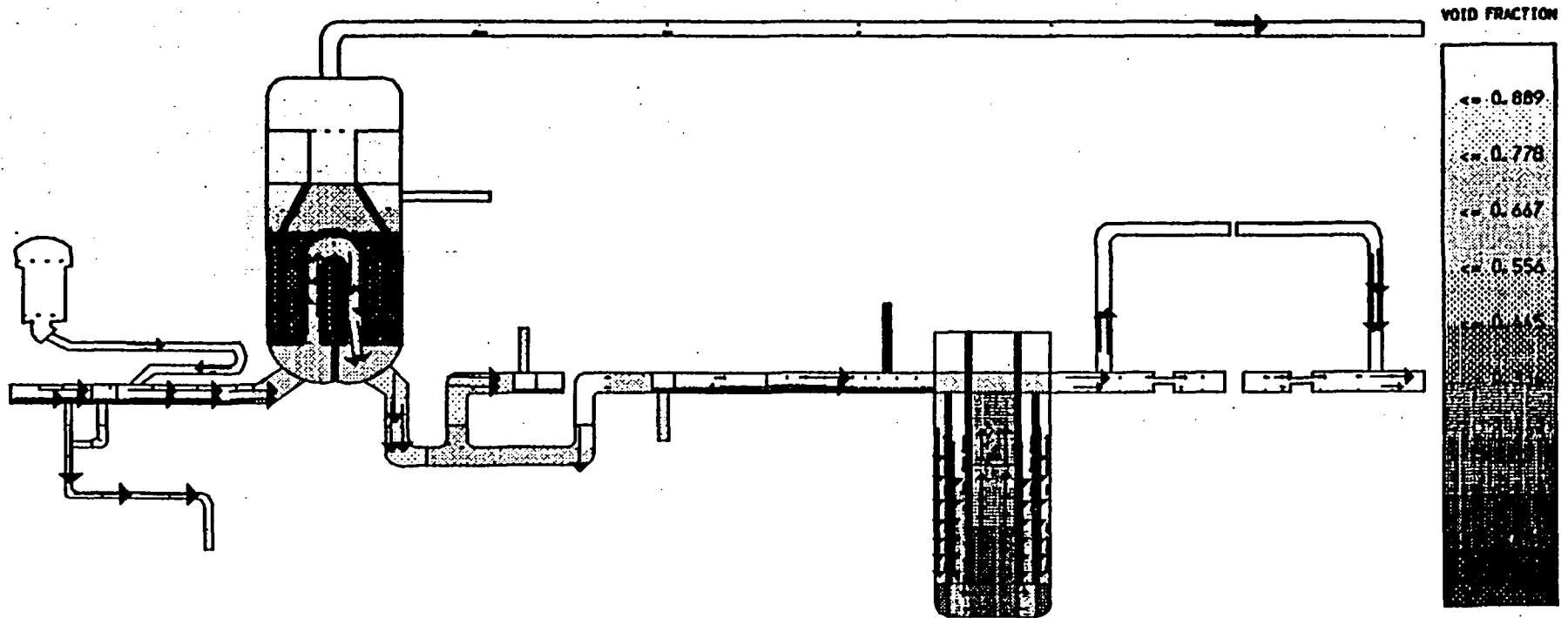
S.M.A.R.T. SYSTEM MIMIC FOR ANALYSIS OF REACTOR TRANSIENTS
TITLE OF FRAME, - LOFT SB-2 (RUN B) CORRELATED BREAK LINE QUALITY

T1 2261.4
VL10 →
(10.00)
VVAP →
(10.00)



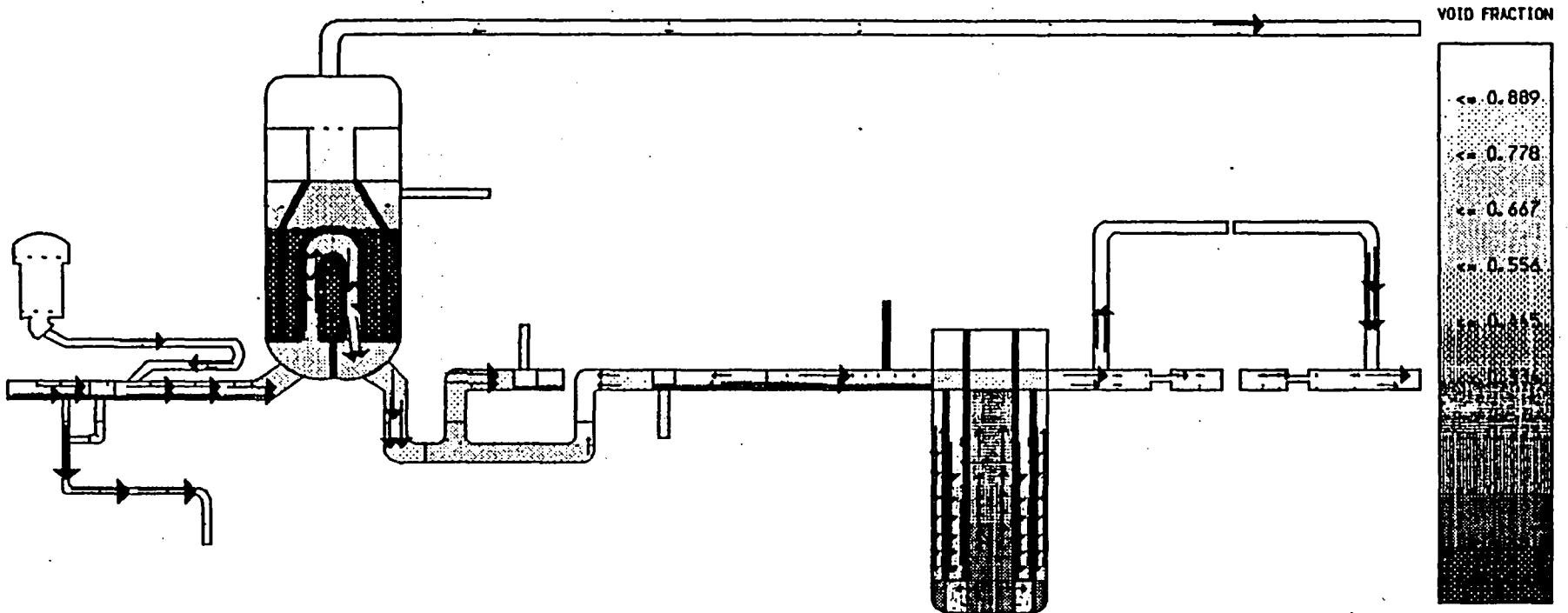
S. M. A. R. T. SYSTEM MIMIC FOR ANALYSIS OF REACTOR TRANSIENTS
TITLE OF FRAME: - LOFT SB-2 (RUN B) CORRELATED BREAK LINE QUALITY

T1 2462.7
VL10 →
(10.00)
VVAP →
(10.00)



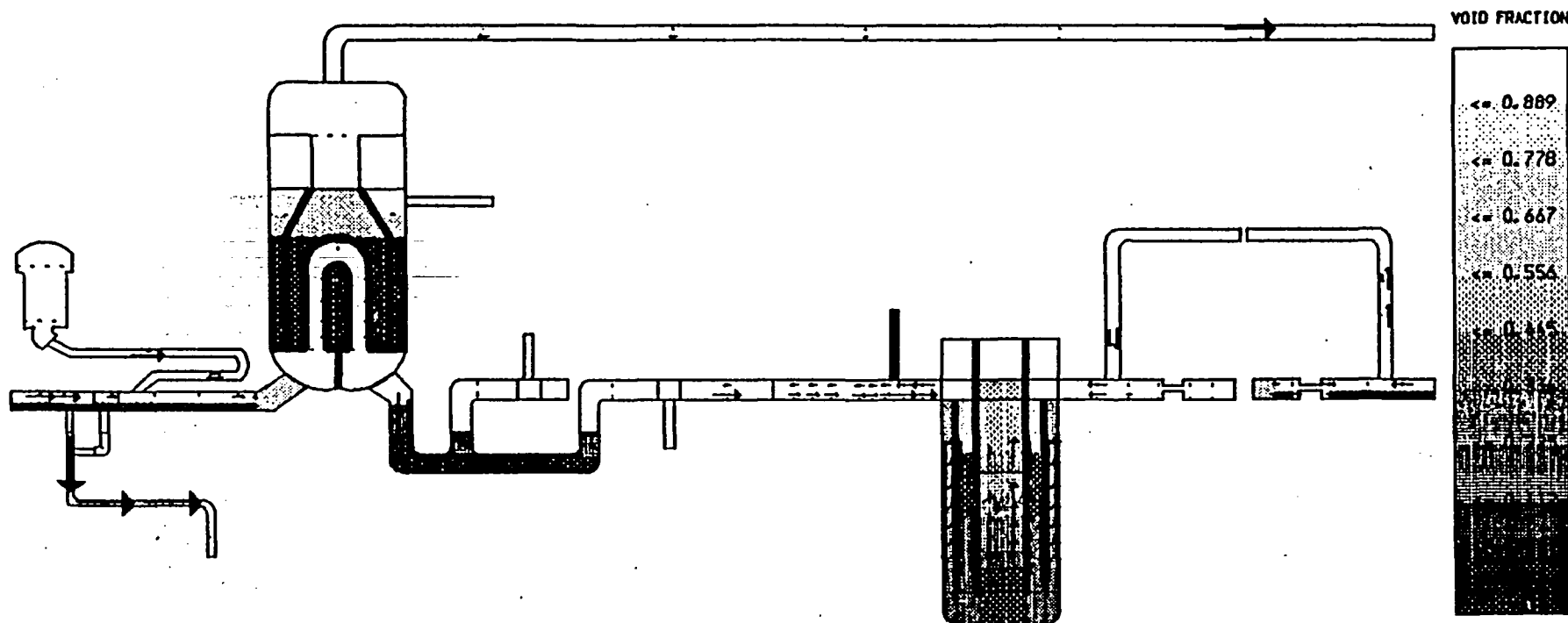
S. M. A. R. T. SYSTEM MIMIC FOR ANALYSIS OF REACTOR TRANSIENTS
TITLE OF FRAME: - LOFT SB-2 (RUN B) CORRELATED BREAK LINE QUALITY

T1 2663.7
VL10 →
(10.00)
VVAP →
(10.00)



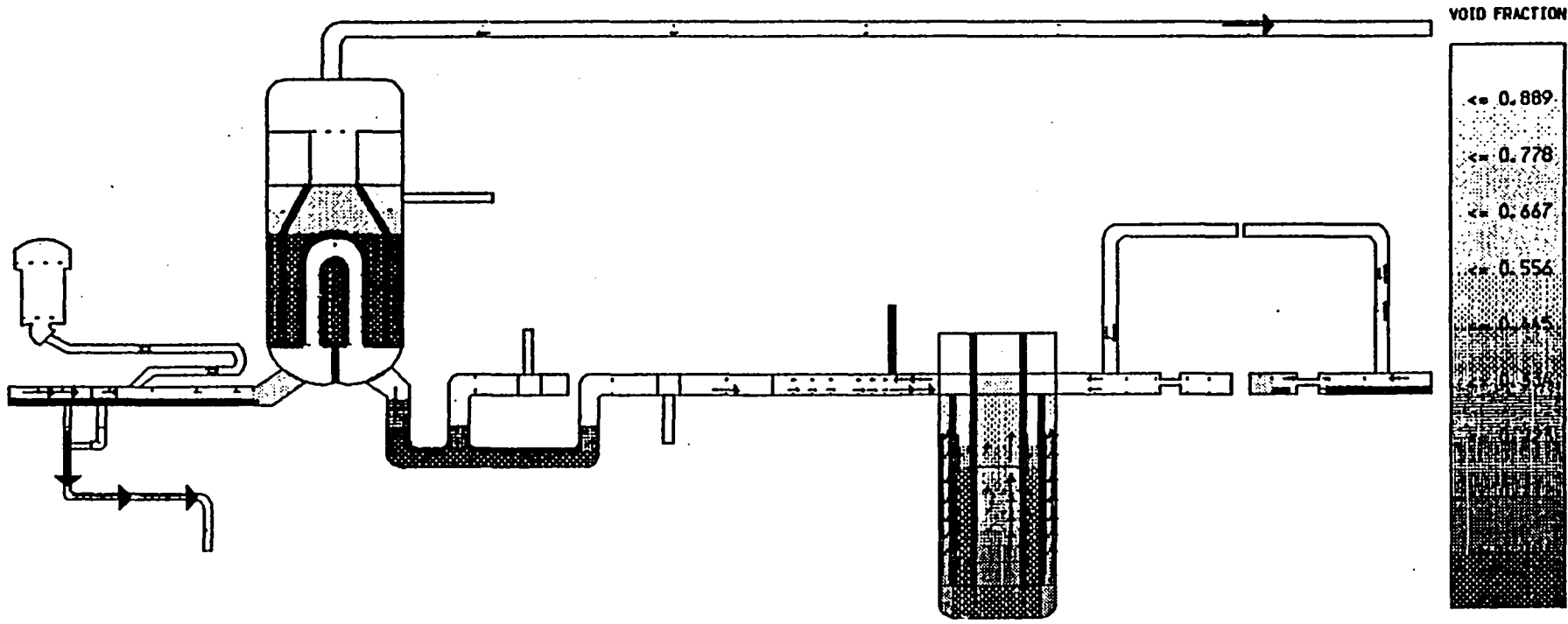
S.M.A.R.T. SYSTEM MIMIC FOR ANALYSIS OF REACTOR TRANSIENTS
TITLE OF FRAME: - LOFT SB-2 (RUN B) CORRELATED BREAK LINE QUALITY

T1 2764.2
VL10 →
(10.00)
VVAP →
(10.00)



S. M. A. R. T. SYSTEM MIMIC FOR ANALYSIS OF REACTOR TRANSIENTS
TITLE OF FRAME, - LOFT SB-2 (RUN B) CORRELATED BREAK LINE QUALITY

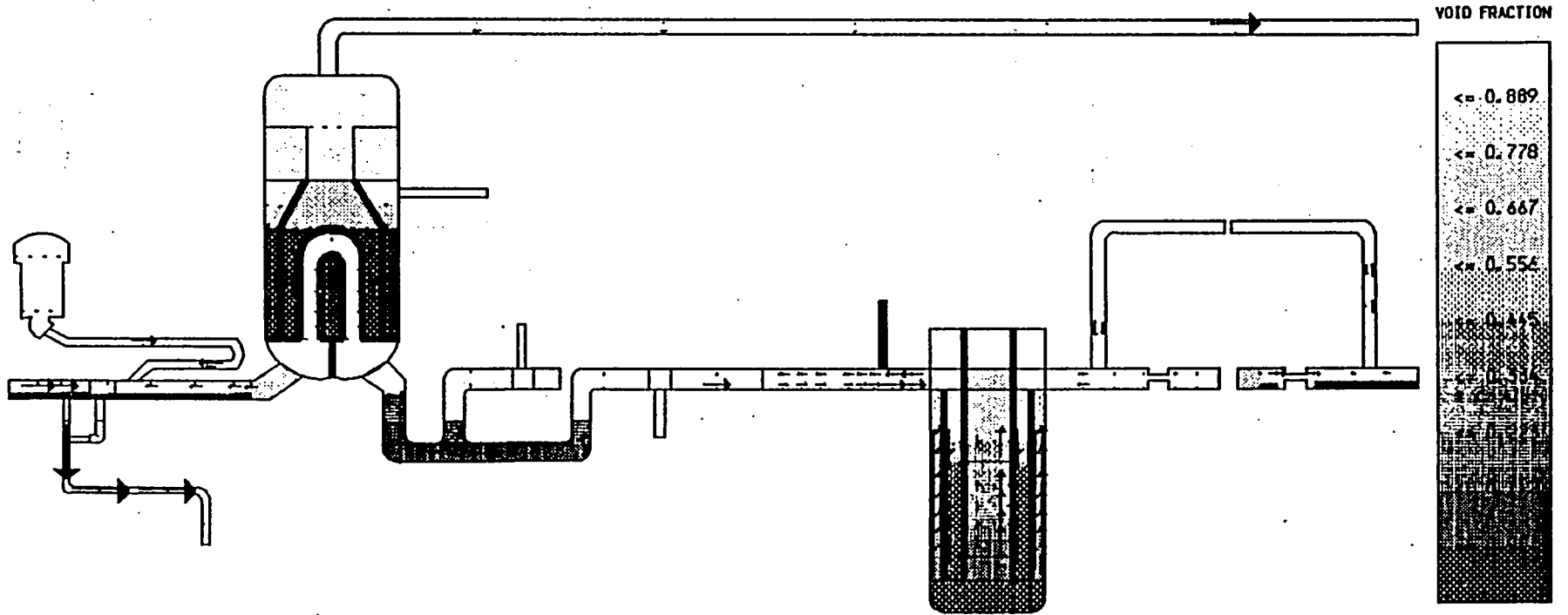
T1 2864.5
VL10 →
(10.00)
VVAP →
(10.00)



S. M. A. R. T. SYSTEM MIMIC FOR ANALYSIS OF REACTOR TRANSIENTS

TITLE OF FRAME: - LOFT SB-2 (RUN B) CORRELATED BREAK LINE QUALITY

T1 3085.3
VL10 →
(10.00)
VVAP →
(10.00)



APPENDIX A

RUN B SNAPSHOTS AT SELECTED TIMES

A set of 26 snapshots describing the evolution of liquid and steam velocities, fluid density and stratified flow conditions for Run B is shown.

The nodalization can be compared with that used for Run A (Fig 3). In the breakline the quality control valve has been attached. Components 79 and 83 (vessel) are not included in the snapshots frame.

APPENDIX B

MODIFICATIONS IMPLEMENTED IN TRAC-PF1/MOD1 WINFRITH
VERSIONS B02A AND B02C

IDE B001

Identify Version. Change this ident for each change in a version.

IDE B002

Correct core treatment in vessel.

Insert return in bits suite of subroutines.

IDE B003 B02C only

Reset limit on stratified flow to 30 degrees
(ie ARCSIN(0.5))

COM WINF

This com deck contains the new Winfrith namelist variable triggers

COM WINC

This com deck contains the stratified volume flag and variables for the condensation heat transfer mod

IDE W003

Option to bypass interface sharpener routines while leaving the fine mesh switched on. See also W007 for changes to namelist option.

IDE W004

Plug weighting in interphase condensation heat transfer no longer applied in stratified flow.

IDE W005

Allow wall condensation heat transfer in horizontal pipes

IDE W006

Allows negative friction factors.

IDE W007

Namelist extensions for W003 mods and printing diagnostic triggers.

IDE W008

Add stratified flow regime indicators for graphics. Add simple stratified offtake model option for tee components.* Add pointers for condensation heat transfer mod (W009).

* (Option not selected for calculation A).

IDE W009

Make liquid velocity used in interface condensation heat transfer continuous with changing void fraction. (Option not selected for these calculations).

IDE W010

Alternative form of void fraction for flow regime selection. (Option not selected for these calculations).

IDE W011

Mod to cure convergence problems in CHF use of secant method.

IDE W012

Correct error in evaluation of Forslund and Rohsenow liquid heat transfer coefficient.

IDE W013

Correction to stratified flow head term.

IDE W014

Correction to upper guess in subroutine CHF.

IDE W016

Corrects error for inflow from break when IVDV=0.

IDE W017

Correct unset value of joining cell flag in steam gen comp.

IDE W018

Attempt to make SS restart with pressurizer more smooth.

IDE W019 B02C only

Insert missing square root of pi in Taitel-Dukler stratified flow test in subroutine FEMON.



BIBLIOGRAPHIC DATA SHEET

(See instructions on the reverse)

1. REPORT NUMBER
(Assigned by NRC. Add Vol., Supp., Rev.,
and Addendum Numbers, if any.)

NUREG/IA-0019
AEEW-R-2202

2. TITLE AND SUBTITLE

TRAC-PF1/MOD1 Post-Test Calculations of the OECD
Loft Experiment LP-SB-2

3. DATE REPORT PUBLISHED

MONTH YEAR

December 1990

4. FIN OR GRANT NUMBER

5. AUTHOR(S)

F. Pelayo

6. TYPE OF REPORT

Technical

7. PERIOD COVERED (Inclusive Dates)

8. PERFORMING ORGANIZATION - NAME AND ADDRESS (If NRC, provide Division, Office or Region, U.S. Nuclear Regulatory Commission, and mailing address; if contractor, provide name and mailing address.)

United Kingdom Atomic Energy Authority
Atomic Energy Establishment, Winfrith
Dorchester Dorset DT2 BDH
United Kingdom

9. SPONSORING ORGANIZATION - NAME AND ADDRESS (If NRC, type "Same as above"; if contractor, provide NRC Division, Office or Region, U.S. Nuclear Regulatory Commission, and mailing address.)

Office of Nuclear Regulatory Research
U. S. Nuclear Regulatory Commission
Washington, DC 20555

10. SUPPLEMENTARY NOTES

11. ABSTRACT (200 words or less)

An analysis of the OECD-LOFT-LP-SB-2 experiment making use of TRAC-PF1/MOD1 is described in the report. LP-SB2 experiment studies the effect of a delayed pump trip in a small break LOCA scenario with a 3 inches equivalent diameter break in the hot leg of a commercial PWR operating at full power. The experiment was performed on 14 July 1983 in the LOFT facility at the Idaho National Engineering Laboratory under the auspices of the Organisation for Economic Co-operation and Development (OECD). This analysis presents an evaluation of the code capability in reproducing the complex phenomena which determined the LP-SB-2 transient evolution. The analysis comprises the results obtained from two different runs. The first run is described in detail analysing the main variables over two time spans: short and longer term. Several conclusions are drawn and then a second run testing some of these conclusions is shown.

12. KEY WORDS/DESCRIPTORS (List words or phrases that will assist researchers in locating the report.)

TRAC-PF1, OECD LOFT, Small break

13. AVAILABILITY STATEMENT

Unlimited

14. SECURITY CLASSIFICATION

(This Page)

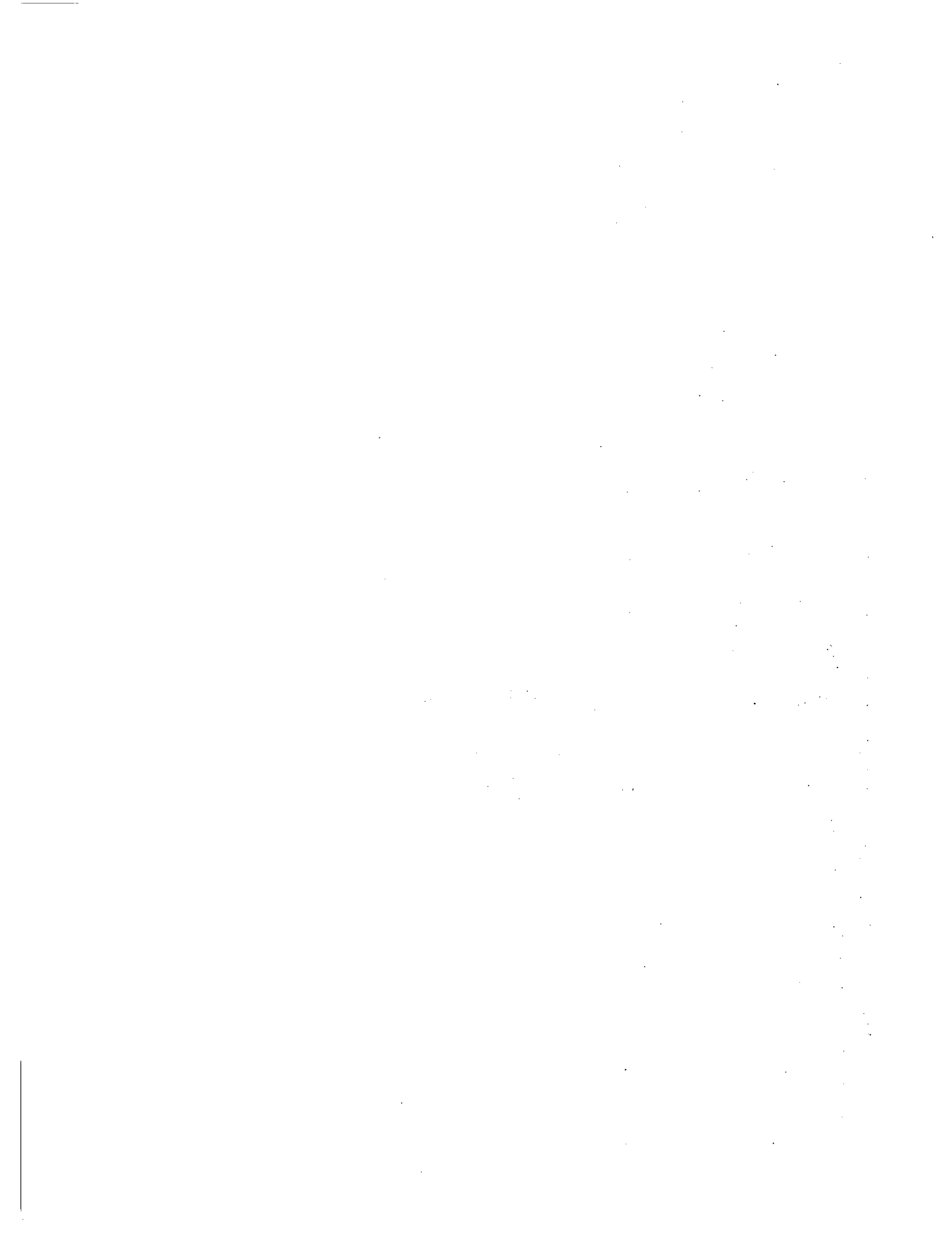
Unclassified

(This Report)

Unclassified

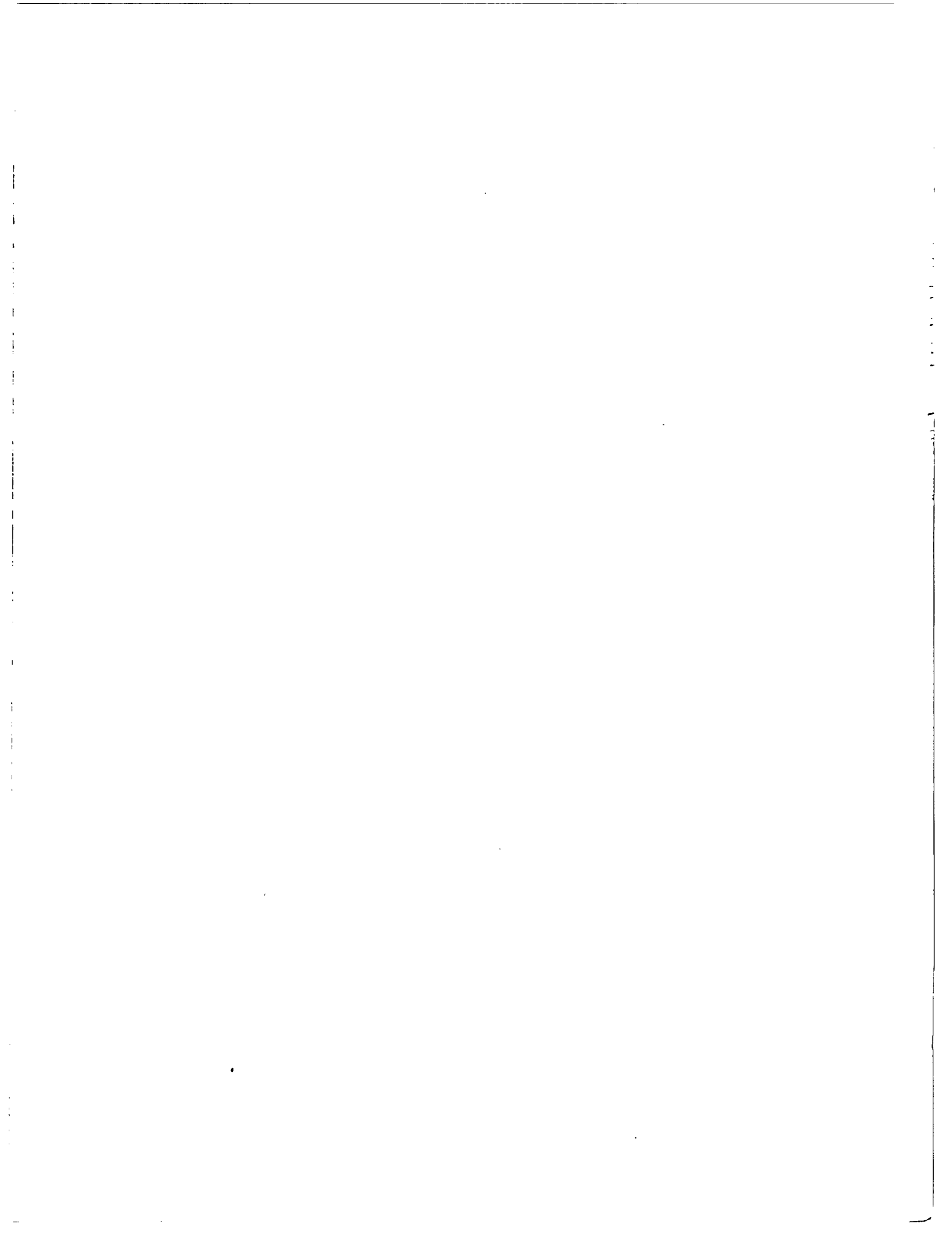
15. NUMBER OF PAGES

16. PRICE





THIS DOCUMENT WAS PRINTED USING RECYCLED PAPER.



**UNITED STATES
NUCLEAR REGULATORY COMMISSION
WASHINGTON, D.C. 20555**

**OFFICIAL BUSINESS
PENALTY FOR PRIVATE USE, \$300**

**SPECIAL FOURTH-CLASS RATE
POSTAGE & FEES PAID
USNRC
PERMIT No. G-67**

Gene Rhee (4)
NLN-337